IMMUNOBIOLOGY OF OSTEOARTICULAR DISEASES

EDITED BY: Erminia Mariani, Mariagrazia Uguccioni and Daniela Frasca
PUBLISHED IN: Frontiers in Immunology

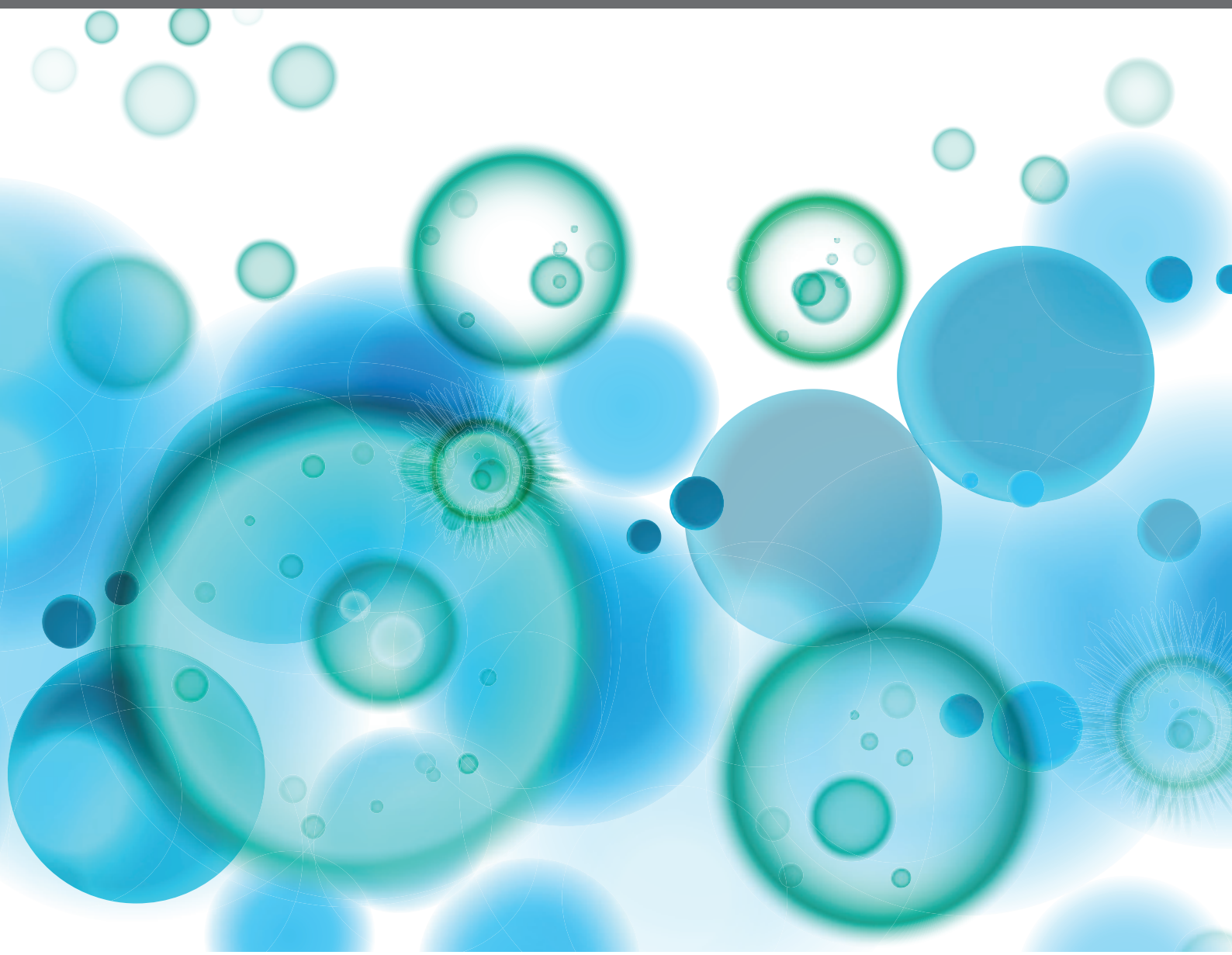

frontiers Research Topics

Frontiers eBook Copyright Statement

The copyright in the text of individual articles in this eBook is the property of their respective authors or their respective institutions or funders. The copyright in graphics and images within each article may be subject to copyright of other parties. In both cases this is subject to a license granted to Frontiers.

The compilation of articles constituting this eBook is the property of Frontiers.

Each article within this eBook, and the eBook itself, are published under the most recent version of the Creative Commons CC-BY licence. The version current at the date of publication of this eBook is CC-BY 4.0. If the CC-BY licence is updated, the licence granted by Frontiers is automatically updated to the new version.

When exercising any right under the CC-BY licence, Frontiers must be attributed as the original publisher of the article or eBook, as applicable.

Authors have the responsibility of ensuring that any graphics or other materials which are the property of others may be included in the CC-BY licence, but this should be checked before relying on the CC-BY licence to reproduce those materials. Any copyright notices relating to those materials must be complied with.

Copyright and source acknowledgement notices may not be removed and must be displayed in any copy, derivative work or partial copy which includes the elements in question.

All copyright, and all rights therein, are protected by national and international copyright laws. The above represents a summary only. For further information please read Frontiers' Conditions for Website Use and Copyright Statement, and the applicable CC-BY licence.

ISSN 1664-8714
ISBN 978-2-88966-969-1
DOI 10.3389/978-2-88966-969-1

About Frontiers

Frontiers is more than just an open-access publisher of scholarly articles: it is a pioneering approach to the world of academia, radically improving the way scholarly research is managed. The grand vision of Frontiers is a world where all people have an equal opportunity to seek, share and generate knowledge. Frontiers provides immediate and permanent online open access to all its publications, but this alone is not enough to realize our grand goals.

Frontiers Journal Series

The Frontiers Journal Series is a multi-tier and interdisciplinary set of open-access, online journals, promising a paradigm shift from the current review, selection and dissemination processes in academic publishing. All Frontiers journals are driven by researchers for researchers; therefore, they constitute a service to the scholarly community. At the same time, the Frontiers Journal Series operates on a revolutionary invention, the tiered publishing system, initially addressing specific communities of scholars, and gradually climbing up to broader public understanding, thus serving the interests of the lay society, too.

Dedication to Quality

Each Frontiers article is a landmark of the highest quality, thanks to genuinely collaborative interactions between authors and review editors, who include some of the world's best academicians. Research must be certified by peers before entering a stream of knowledge that may eventually reach the public - and shape society; therefore, Frontiers only applies the most rigorous and unbiased reviews.
Frontiers revolutionizes research publishing by freely delivering the most outstanding research, evaluated with no bias from both the academic and social point of view. By applying the most advanced information technologies, Frontiers is catapulting scholarly publishing into a new generation.

What are Frontiers Research Topics?

Frontiers Research Topics are very popular trademarks of the Frontiers Journals Series: they are collections of at least ten articles, all centered on a particular subject. With their unique mix of varied contributions from Original Research to Review Articles, Frontiers Research Topics unify the most influential researchers, the latest key findings and historical advances in a hot research area! Find out more on how to host your own Frontiers Research Topic or contribute to one as an author by contacting the Frontiers Editorial Office: frontiersin.org/about/contact

IMMUNOBIOLOGY OF OSTEOARTICULAR DISEASES

Topic Editors:
Erminia Mariani, University of Bologna, Italy
Mariagrazia Uguccioni, Institute for Research in Biomedicine (IRB), Switzerland
Daniela Frasca, University of Miami, United States

Citation: Mariani, E., Uguccioni, M., Frasca, D., eds. (2021). Immunobiology of Osteoarticular Diseases. Lausanne: Frontiers Media SA.
doi: 10.3389/978-2-88966-969-1

Table of Contents

frontiers in Immunology

EDITORIAL
published: 13 May 2021
doi: 10.3389/fimmu.2021.698992

Editorial: Immunobiology of Osteoarticular Diseases

Erminia Mariani[1,2*] *and Daniela Frasca*[3,4]

[1] Laboratory of Immunorheumatology and Tissue Regeneration, Istituto di Ricovero e Cura a Carattere Scientifico (IRCCS) IstitutoOrtopedico Rizzoli, Bologna, Italy, [2] Department of Medical and Surgical Sciences, Alma Mater Studiorum – University of Bologna, Bologna, Italy, [3] Department of Microbiology and Immunology, University of Miami Miller School of Medicine, Miami, FL, United States, [4] Sylvester Comprehensive Cancer Center, University of Miami Miller School of Medicine, Miami, FL, United States

Keywords: rheumatic diseases, osteoarticular diseases, osteoarthritis, rheumatoid anhritis, osteoporosis, Inflammation, immunological mechanisms, diagnosis

Editorial on the Research Topic

Immunobiology of Osteoarticular Diseases

Rheumatic and osteoarticular diseases, that include Osteoarthritis (OA), Rheumatoid Arthritis (RA) and Osteoporosis, represent the most diffuse chronic conditions in the elderly. These diseases affect the individual's working abilities and autonomy, as well as life expectancy. These chronic inflammatory diseases share similar patho-physiological pathways including increased bone remodeling/resorption, a senescence-associated phenotype, and accumulation of activated immune cells and soluble factors in the joints and skeletal tissue.

Despite the awareness of the importance of inflammatory dysregulation, the increasing knowledge that joint tissues contribute to damage in various osteoarticular diseases and that the disease progression can develop over a long period of time, many questions remain unanswered. Moreover, it is not surprising that treatments, either pharmacological or surgical, only partially address the clinical issue. Therefore, a more in-depth understanding of the mechanisms underlying the development of these disorders could lead to earlier intervention and to the identification of alternative, more appropriate, and less invasive therapeutic approaches.

This Research Topic includes 12 contributions from a number of prominent scientists in the field and addresses specific aspects in the field of Immunobiology of Osteoarticular Diseases. Here is a summary of the single contributions.

Paladini et al. review the evolution of the aminopeptidases Endoplasmic Reticulum Aminopeptidases 1 and 2, (ERAP1 and 2) and LNPEP (Leucyl and Cystinyl Aminopeptidase) in the zoological scale, their functions and associations with immune-mediated diseases. These peptidases play a role in the control of the vascular inflammatory response. Later on during evolution they acquired a role in antigen presentation, diversifying between those residing in the ER, (ERAP1 and 2), whose role is to refine the MHC-I peptidomes, and LNPEP, mostly present in the endosomal vesicles contributing to antigen cross-presentation or in the cell membrane as receptor for angiotensin IV. Therefore, their role in autoinflammatory/autoimmune diseases can be as "contributors" to the shaping of the immune-peptidomes as well as "regulators" of the vascular response.

Xu et al. summarize possible roles of PKM2, an isoform of Pyruvate Kinase in the pathogenesis of RA. PKM2, which is increased in the synovial tissue of RA patients, likely regulates the metabolic requirements of activated immune cells and sinoviocytes, needed to infiltrate the tissue, secrete

OPEN ACCESS

Edited and reviewed by:
Betty Diamond, Feinstein Institute for Medical Research, United States

***Correspondence:**
Erminia Mariani
erminia.mariani@unibo.it

Specialty section:
This article was submitted to Autoimmune and Autoinflammatory Disorders, a section of the journal Frontiers in Immunology

Received: *22 April 2021*
Accepted: *26 April 2021*
Published: *13 May 2021*

Citation:
Mariani E and Frasca D (2021) Editorial: Immunobiology of Osteoarticular Diseases. Front. Immunol. 12:698992. doi: 10.3389/fimmu.2021.698992

inflammatory mediators and regulate local inflammation. These results have suggested the possibility to block metabolic pathways to reduce synovial inflammation in RA patients.

Rolph and Das highlight the emerging role of KLF (Krüppel-like factor, a family of DNA-binding zinc finger proteins)-2 in regulation of osteoclastic differentiation. KLF2 overexpression inhibits intracellular pathways that depend on IL-1β signaling. More specifically in the context of RA, global deletion of KLF2 attenuates expression of MMP9 and inflammatory cytokines, contributing to elevated osteoclastogenesis and more aggressive disease progression. Overall data demonstrate that this factor may play a protective role in bones and surrounding tissue by attenuating inflammation in arthritic joints.

Möller et al. review how infectious agents present in the mouth or in the gut of RA patients, may have unique citrullinating capacity, and may also be involved in the establishment of local and systemic inflammation. The data presented in the review strongly indicate the potential role of different microbial taxa in the development of the disease.

Dong et al. demonstrate the pathological role of global and specific cell-free (cf) DNA molecules in RA and OA patients. These molecules are released in large amounts in body fluids of patients, more in RA as compared to OA patients, and induce apoptosis, pyroptosis and necrosis. These molecules in RA patients are highly inflammatory, induce the secretion of pro-inflammatory cytokines and are pathogenic for RA patients, suggesting that they can be potential targets of therapeutic intervention.

Nerviani et al. show that the histological analysis of the synovial tissue of RA patients may help to identify patients with lower probability of response to TNF-α blockade. Interestingly, the high baseline presence of inflammatory cell types predict the (better) response to TNF-α blockade.

Miao et al. show that CD147, a T cell activation marker, negatively regulates Th17 responses in RA patients, as well as in a mouse model of collagen-induces arthritis, by limiting their exuberant proliferation, AKT/mTORC1/STAT3 signaling as well as their interaction with inflammatory monocytes. These results have suggested the possible use of anti-CD147 antibodies as therapeutic options for RA patients.

Jiang et al. investigate the function of miR-146a, and its association with levels of regenerating islet-derived protein 3-alpha (REG3A), in regulating macrophage migration in Polymyositis and Dermatomyositis (PM/DM) patients. PM/DM, classified as typical idiopathic inflammatory myopathies, affect mainly proximal muscles and present some overlap with other disorders such as rheumatoid arthritis, supported by the persistent monocytes/macrophages markers in these disease processes. Reduced miR-146a expression in these myopathies leads to increased REG3A expression that increases inflammatory macrophage migration, which may be a possible underlying mechanism of DM/PM pathogenesis.

Assirelli et al. demonstrate that the different joint tissues (cartilage, synovium and bone) release the complements factors C3, C4 and CFB, and IL-1β pro-inflammatory stimulus enhance CFB. Cartilage and synovium tissues, as well as isolated chondrocytes and synoviocytes, were all able to spontaneously secrete complement activating factors (C3a, C5a, CFBa). Conversely, C5b-9 complex release was only detectable in cartilage and synovium tissue supernatants. An association between some C alternative pathway component and joint inflammation is suggested.

Warner et al. has evaluated the role of IL-15, and of genetic variants of the IL-15R gene, in the pathogenesis of cartilage degeneration in OA patients. Results have shown an association between pain and genetic variants of the IL-15R gene, suggesting that IL-15 signaling may be a target for pain. No associations however were found with cartilage matrix loss and radiographic severity.

Lorenzin et al. presented the results of the Italian arm of the SPACE study on Spondyloarthritis (on-going observational prospective cohort multi-center study II level evidence). Spondyloarthritis, a group of chronic inflammatory rheumatic diseases, can be divided into axial (axSpA) and peripheral forms. The first, mainly affecting the spine and sacroiliac joints and beginning at young age, can be further divided between non-radiographic and radiographic axSpA (also known as ankylosing spondylitis). At baseline, a significant prevalence of bone marrow edema lesions was observed both in sacroiliac joints and spine, with predominant involvement of thoracic district. Since positive MRI-spine images were observed in the absence of sacroiliitis, these findings seem to be relevant in the axSpA diagnosis. Early age of disease onset, long duration of low back pain, increased inflammatory biomarkers, higher use of NSAIDs, male gender, HLA-B27 positivity, Spondyloarthritis Research Consortium of Canada (SPARCC) sacroiliac joints score>2 appeared predictors of radiological damage and activity.

Toni et al. highlight the micro-topography of immune cells in the cancellous and cortical bone compartments in relation to the most consistent data on their action in bone remodeling, to offer an innovative space-related perspective of the action of immune cells involved in the osteoporotic process, and to understand how different osteoporotic lesions develop, thus prompting the design of experimental tools for *in vitro* modeling of early phases of the osteoporotic process and related innovative treatments.

AUTHOR CONTRIBUTIONS

All authors contributed to the article and approved the submitted version.

Conflict of Interest: The authors declare that the research was conducted in the absence of any commercial or financial relationships that could be construed as a potential conflict of interest.

Copyright © 2021 Mariani and Frasca. This is an open-access article distributed under the terms of the Creative Commons Attribution License (CC BY). The use, distribution or reproduction in other forums is permitted, provided the original author(s) and the copyright owner(s) are credited and that the original publication in this journal is cited, in accordance with accepted academic practice. No use, distribution or reproduction is permitted which does not comply with these terms.

frontiers in Immunology

MINI REVIEW
published: 18 December 2019
doi: 10.3389/fimmu.2019.02919

PKM2: A Potential Regulator of Rheumatoid Arthritis via Glycolytic and Non-Glycolytic Pathways

Danyi Xu[1†], *Junyu Liang*[1†], *Jin Lin*[1*] *and Chaohui Yu*[2*]

[1] *Department of Rheumatology, The First Affiliated Hospital, College of Medicine, Zhejiang University, Hangzhou, China,*
[2] *Department of Gastroenterology, The First Affiliated Hospital, College of Medicine, Zhejiang University, Hangzhou, China*

Immunometabolism provides a new perspective on the pathogenesis of rheumatoid arthritis (RA). In recent years, there have been investigations focusing on the role of intracellular glucose metabolism in the pathogenesis of RA. Previous studies have shown that glycolysis of synovial tissue is increased in RA patients, while glycolysis inhibitors can significantly inhibit synovitis. Pyruvate kinase (PK) is a key enzyme in glycolysis, catalyzing the final rate-limiting step in the process. An isoform of PK, PKM2, provides favorable conditions for the survival of tumor cells via its glycolytic or non-glycolytic functions and has become a potential therapeutic target in tumors. RA synovium has the characteristic of tumor-like growth, and, moreover, increased expression of PKM2 was identified in the synovial tissue of RA patients in recent studies, indicating the underlying role of PKM2 in RA. PKM2 has potential value as a new therapeutic target or biomarker for RA, but its exact role in RA remains unclear. In this review, the properties of PKM2 and existing research concerning PKM2 and RA are thoroughly reviewed and summarized, and the possible role and mechanism of PKM2 in RA are discussed.

Keywords: rheumatoid arthritis, PKM2, glycolysis, protein kinase, tumor

OPEN ACCESS

Edited by:
Erminia Mariani,
University of Bologna, Italy

Reviewed by:
David S. Gyori,
Semmelweis University, Hungary
Åsa Andersson,
Halmstad University, Sweden

***Correspondence:**
Jin Lin
linjinzju@zju.edu.cn
Chaohui Yu
zyyyych@zju.edu.cn

†These authors have contributed equally to this work

Specialty section:
This article was submitted to Autoimmune and Autoinflammatory Disorders, a section of the journal Frontiers in Immunology

Received: *01 August 2019*
Accepted: *27 November 2019*
Published: *18 December 2019*

Citation:
Xu D, Liang J, Lin J and Yu C (2019) PKM2: A Potential Regulator of Rheumatoid Arthritis via Glycolytic and Non-Glycolytic Pathways. Front. Immunol. 10:2919. doi: 10.3389/fimmu.2019.02919

INTRODUCTION

Rheumatoid arthritis (RA) is a common autoimmune disease with the pathological characteristics of invasive synovitis, pannus formation, and articular cartilage destruction. An imbalance between proliferation and apoptosis plays an important role in the pathogenesis of RA, and this tumor-like characteristic of the rheumatoid synovium has become a hot issue in RA research in recent years (1). However, its detailed pathogenesis remains unclear.

Currently, investigations on RA mainly focus on immunology, genetics, and cell biology, whereas studies on the pathogenesis of RA from the perspective of glucose metabolism have not been widely considered. However, glucose metabolism plays a pivotal role in the pathogenesis of RA. Previous studies found that the synovial tissues of RA patients were hypoxic and that this was accompanied by an increase in glycolytic enzyme gene expression and glycolytic activity (2). The key enzymes of glycolysis, such as glucose phosphate isomerase (GPI) (3), aldolase (ALD) (4), and triose phosphate isomerase (TPI) (5), can take part in autoimmune reaction in RA as antigens.

Pyruvate kinase (PK) is a key rate-limiting enzyme of glycolysis that irreversibly catalyzes the conversion of phosphoenolpyruvate (PEP) to pyruvate (6). PKM2, an isoform of PK, is highly expressed in tumor cells, leading to increased glucose uptake, a transition from oxidative phosphorylation to glycolysis, and accumulation of glucose metabolites. It thus provides favorable

and necessary conditions for the growth and survival of tumor cells (7). Alterations in energy metabolism are one of the most important differences between tumor cells and normal cells (8). PKM2 is a key factor leading to this effect, and it has become a potential target for the treatment of tumors. Synovial tissue in RA has been characterized as tumor-like proliferation. In recent years, a few studies have confirmed that the expression level of PKM2 in the synovial tissue of RA is significantly higher than that in patients with osteoarthritis (OA) (9), suggesting the potential role of PKM2 in RA, though further studies are still lacking. However, no summary has been made to help enhance our understanding in this area. Here, the characteristics of PKM2 and the existing evidence on PKM2 and RA are reviewed, and the potential role and mechanism of PKM2 in RA are discussed.

BIOLOGICAL CHARACTERISTICS OF PKM2

PK catalyzes the final rate-limiting and irreversible step in glycolysis, which produces pyruvate and ATP. In mammals, there are four PK isoforms: PKL, PKR, PKM1, and PKM2, expressing in different cells and tissues (10). PKM1 and PKM2 are encoded by the PKM gene and are generated through alternative splicing of two exons in PKM pre-mRNA (11). PKM1 is expressed in most well-differentiated tissues, whereas PKM2 is expressed in proliferative cells, such as embryonic cells, adult stem cells, and cancer cells, especially.

PKM2 can take dimer or tetramer forms with different functions, and these can be converted into each other (12). The tetramer form has a high affinity with its metabolic substrate PEP, while the dimer form has a low affinity with PEP, which means that the tetramer form has a high glycolytic enzyme activity under physiological conditions, while the dimer form has low enzyme activity (12). The tetramer form of PKM2 can efficiently promote glycolysis and energy production (13), while the presence of the low-activity PKM2 dimer stops the conversion from PEP to pyruvate, which leads to the accumulation of glucose metabolites in the upstream and the accumulation of a large number of precursor substances for the synthesis of macromolecules (7).

GLYCOLYTIC FUNCTION OF PKM2

It was found that although there is only one exon difference between the structures of PKM1 and PKM2, they have significant differences in function. Under physiological conditions, PKM1 constitutively exists in the form of a highly active tetramer, while PKM2 can exist in the dimer and tetramer forms (14). Small molecules and metabolites, such as fructose-1,6-bisphosphate (FBP) (15), Succinyl-5-aminoimidazole-4-carboxamide-1-ribose-50-phosphate (SAICAR) (16), serine (17), etc., can promote the tetramerization of PKM2. Meanwhile, PKM2 activity can be inhibited by posttranslational modification, such as phosphorylation (18), acetylation (19), and oxidation (20). The enzymatic activity of PKM2 can be regulated by endogenous mechanisms, so that proliferating cells may choose for PKM2 to allow PK enzyme activity to be turned on or off as the environment changes, thus providing metabolic flexibility.

The significant alteration in the energy metabolism of tumor cells is characterized by the increase of glucose consumption and the conversion of a large amount of glucose into lactate through glycolysis under aerobic conditions, namely aerobic glycolysis, also known as the Warburg effect (21). Another important feature of tumor cell metabolism is the rapid synthesis of large amounts of lipids, proteins, and nucleotides (8), which are necessary for the rapid growth of tumor cells. PKM2 is the major factor that leads to the change in tumor cell metabolism. The presence of the dimer and tetramer forms of PKM2 and their mutual conversion meets the large energy and anabolic substrate supply demands of tumor cells. Previous findings have confirmed that a dimer form PKM2 is commonly expressed in tumors (22). When tumor cells are short of energy, PKM2 transforms from a dimer structure to a tetramer structure and provides enough energy for the cells. When energy is sufficient, it can intercept the conversion of glucose to lactate in the form of a dimer, thus providing sufficient substrates for the anabolism of tumor cells. Therefore, PKM2 can optimize the supply of energy and synthetic substrates for tumor cells, contributing to tumor cell survival and proliferation in a complex microenvironment (23) (**Figure 1**).

NON-GLYCOLYTIC FUNCTION OF PKM2

Recent studies have shown that PKM2 has not only a glycolytic function but also has non-glycolytic function. Under various conditions, PKM2 can be depolymerized from a tetramer to a dimer and translocated to the nucleus, mitochondrial membrane, or outside the cell. PKM2 acts as a protein kinase by phosphorylating various protein substrates at both serine/threonine and tyrosine residues. PKM2 can use its metabolic substrate, PEP, as a phosphate donor for phosphorylation of a variety of target proteins, including STAT3, histone H3, myosin light chain 2 (MLC2), Bub3, and ERK1/2 (24). The translocated PKM2 dimer is involved in the regulation of gene transcription, metabolic reprogramming, mitosis, apoptosis, and other important life events by transcriptional activation, modulating signal transduction, or regulation of the phosphorylation of important proteins, endowing tumor cells with growth advantages (24).

Although protein kinase substrates of PKM2 are being continuously identified, PKM2-mediated gene expression has been challenged by other studies. A lack of a PKM2 gene in mouse models did not inhibit tumor growth (25), and

Abbreviations: ALD, aldolase; BCR, BTB–CUL3–RBX1; FBP, fructose-1,6-bisphosphate; FLS, fibroblast-like synoviocytes; FDG, fluorodeoxyglucose; GPI, glucose phosphate isomerase; GAPD, glyceraldehyde-3-phosphate dehydrogenase; GLUT-1, glucose transporter protein-1; HSP, heat shock protein; HIF-lα, hypoxia-inducible factor-1α; HK, hexokinase; LDH, lactic dehydrogenase; MLC2, myosin light chain 2; MMP, matrix metalloproteinase; NADPH, nicotinamide adenine dinucleotide phosphate; OA, osteoarthritis; PK, pyruvate kinase; PEP, phosphoenolpyruvate; PFK, phosphofructokinase; PGM, phosphoglycerate mutase; PPP, pentose phosphate pathway; RA, rheumatoid arthritis; SAICAR, succinyl-5-aminoimidazole-4-carboxamide-l-ribose-50-phosphate; TPI, triose phosphate isomerase; TCA, tricarboxylic acid; VEGF, vascular endothelial growth factor; 3PO, 3-(3-pyridiny1)-1-(4-pyridinyl)-2-propen-1-one.

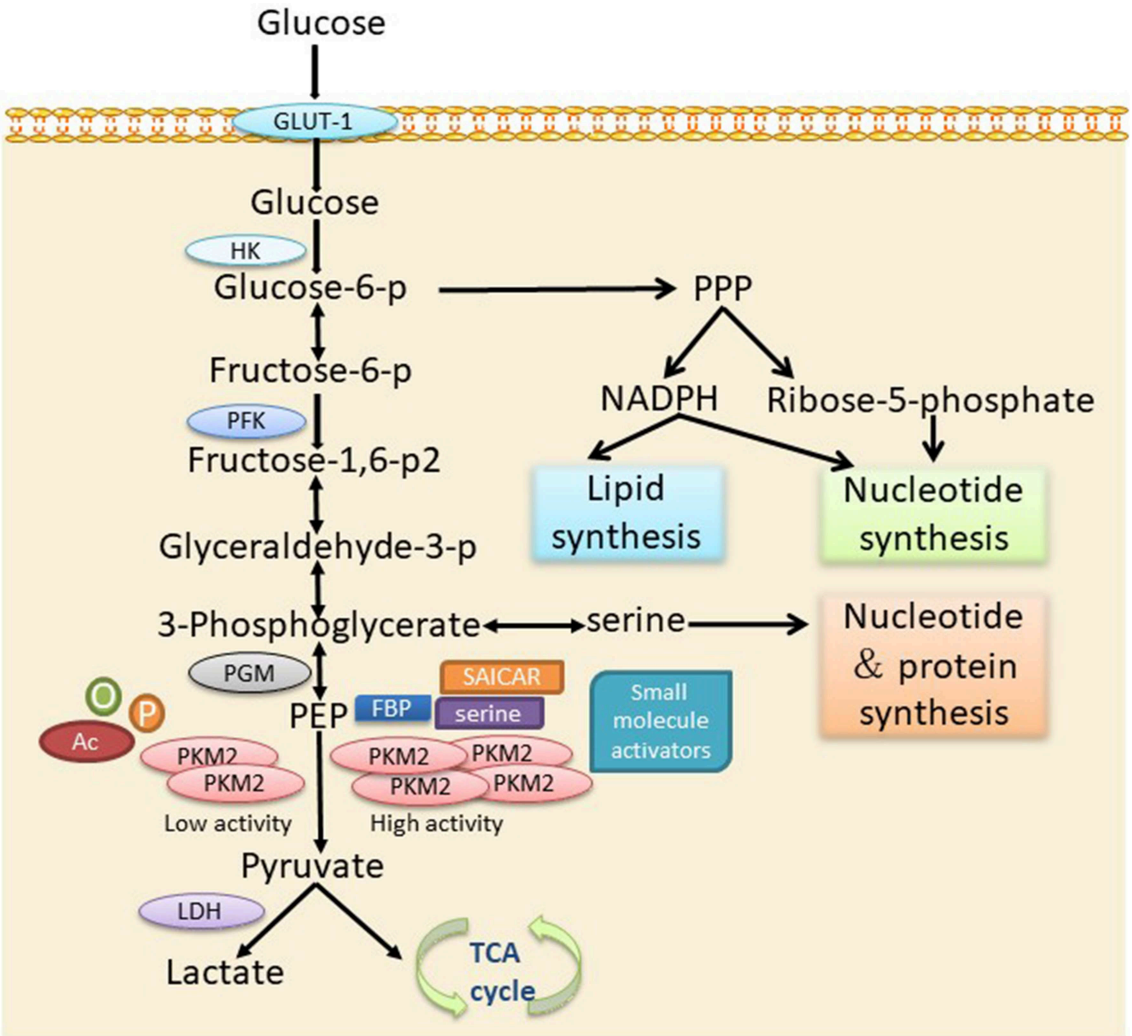

FIGURE 1 | The role of PKM2 in cellular metabolism via the glycolytic pathway. PKM2 is converted into an active tetramer under activation by serine, FBP, SAICAR, or small molecules, which promotes the conversion of PEP into pyruvate. Pyruvate enters the TCA cycle of the mitochondria and produces ATP through oxidative phosphorylation. In the absence of allosteric activators or post-transcriptional modifications, PKM2 presents mainly in an inactive dimer form, leading to the accumulation of glycolytic intermediates to meet the needs of the biosynthetic precursors of activated or proliferating cells. p, phosphorylation; Ac, acetylation; o, oxidation.

furthermore, PKM2 acting as a PEP-dependent protein kinase was not proved in a recent study (26). Therefore, PKM2 may be directly or indirectly involved in the transcriptional activation, signal transduction, or phosphorylation of some proteins. The specific mechanism demands further exploration.

EXISTING EVIDENCE CONCERNING PKM2 AND RA

Activated synovial cells have the biological behavior characteristics of excessive proliferation, migration, and invasion and form tumor-like pannus, which forms a low-oxygen microenvironment (27, 28). Hypoxia alters cellular bioenergetics by promoting a switch to glycolysis so as to efficiently produce enough ATP to support enhanced synovial proliferation and pannus formation. Compared to OA-fibroblast-like synoviocytes (FLS), the glycometabolism shifted toward glycolysis in RA-FLS (29). The increased fluorodeoxyglucose (FDG) uptake in swollen joints in patients with RA reported in several studies represents the up-regulation of glycolysis (30, 31). Further studies have confirmed that fibroblasts and activated macrophages contribute to the high level of FDG accumulation in the pannus (31). The finding of a marked increase in both glyceraldehyde-3-phosphate dehydrogenase (GAPD) and LDH activities in rheumatoid synoviocytes also suggests the up-regulation of glycolysis (32).

So far, our knowledge on PKM2 and RA is limited; however, several studies have demonstrated that PKM2 may be involved

in the pathogenesis of RA. As a key enzyme in the glycolytic pathway, the PKM2 expression of RA-FLS was significantly increased under hypoxic conditions, while inhibition of glycolytic activity by glycolytic inhibitor 3-(3-pyridinyl)-1-(4-pyridinyl)-2-propen-1-one(3PO) dramatically reverse pro-inflammatory mechanisms including invasion, migration, cytokine secretion, and the signaling pathways of hypoxia-inducible factor-1α(HIF-1α), pSTAT3, and Notch-1IC (33). Another study confirmed that PKM2 is more highly expressed in the lining layer, sublining layer, and vasculature of RA synovial tissue compared to OA (9). TLR2-activation can induce an increased glycolysis:respiration ratio in RA-FLS and enhanced PKM2 nuclear translocation. Similarly, 3PO inhibits TLR2-induced inflammation and signaling pathways (9). In a proteomic analysis of RA-FLS, a total of 1,633 and 1,603 protein spots were examined in RA patients and controls, respectively. Among them, 33 proteins were over-expressed by more than 3-fold, and 3 proteins, namely α-enolase, GRP75, and PKM2, were verified by Western blot (34). Therefore, PKM2 may be involved in the occurrence and development of RA, and further explorations to clarify its exact role and mechanism in RA will be of great significance.

POTENTIAL ROLE AND MECHANISM OF PKM2 IN RA

PKM2 has become a hotspot in the field of tumor research. However, there have been few studies on PKM2 and RA, and its function and mechanism in the development of RA remain unclear. Based on the tumor-like invasion characteristics of synovial tissue, we refer to studies on tumor and PKM2 and try to discuss the possible mechanism in terms of the following aspects so as to clarify the areas worthy of research interest in the future (**Figure 2**).

Glycolytic Regulation in RA

Increased glycolysis provides sufficient energy to maintain rapid cell proliferation for synovial tissue in RA (29). On the other hand, many intermediate metabolic products produced during glycolysis are necessary substrates for the synthesis of cellular macromolecules for synoviocyte proliferation. PKM2 may thereby optimize the supply of energy and synthetic substrates for synoviocytes to maintain the tumor-like proliferation.

The local acid microenvironment caused by increased glycolytic activity (32) can further aggravate the pathological process of RA. The acid environment is favorable for synoviocyte survival, as it is for tumor cells. It was found that lactate, as the end product of glycolysis, could trigger invasiveness of FLS (33). The large amount of lactate leaves tissues in an acid environment, capable of destroying the extracellular matrix either directly or by activating metalloproteinases (35). Lactate and pyruvic acid can stimulate the expression of vascular endothelial growth factor (VEGF) and HIF-1α, which are critical for angiogenesis (36). On the other hand, acidosis itself can cause mutations and aberrations that prevent DNA repair, as well as mutations in normal cells (37). Therefore, PKM2 may regulate glycolysis to make synovial tissues in an acid environment that is conducive to their proliferation and invasion.

The inflammatory response is an energy-intensive process that requires a transition from resting to a highly active metabolic state. Under inflammatory conditions, metabolic reprogramming is guided by the efficient generation of ATP and the synthesis of macromolecules for the activation and proliferation of immune cells. As with tumor cells, highly active immune cells also show metabolic changes from oxidative phosphorylation to glycolysis. Immune cell metabolism regulation has become an attractive potential therapeutic target for inflammatory and immune diseases. Studies have shown that glycolysis is associated with T cell differentiation (38, 39) and the production of IFNγ-1 (40). In RA synovial tissues and plasma, disorders of some glycolytic enzymes can induce the activation of immune cells (41, 42). Recent studies have shown that PKM2 is significantly increased in LPS-activated macrophages (43) and participates in regulating macrophage polarization (44). Hence, PKM2 may be a potential modulator of immune cell metabolism and function; this still needs to be further clarified.

Potential Protein Kinase Targets

It has been found that PKM2 can interact with a variety of proteins as a protein kinase. However, so far, no investigators have conducted relevant studies on PKM2 as a protein kinase in RA. Therefore, by referring to the findings of PKM2 in tumor studies, we discuss several possible targets of PKM2 as a protein kinase in RA.

STAT3

STAT is a family of cytoplasmic proteins that can trigger the transcription of corresponding target genes (45). It was found that PKM2 could phosphorylate STAT3 at Tyr705 and promote MEK5 transcriptional activity (46). Inhibition of PKM2 expression could effectively attenuate the neuropathic pain and inflammatory responses induced by CCI in rats, possibly by regulating ERK and STAT3 signaling pathways (47). LPS promoted PKM2 binding to the STAT3 promoter to enhance STAT3 expression and its subsequent nuclear translocation, inducing TNF-α and IL-1β production and cell proliferation in CRC cells (48). Targeting the JAK/STAT signaling pathway is a new way of treating RA, and further studies will be needed to confirm whether inhibiting PKM2 in RA can reduce cell proliferation and inflammatory cytokine secretion via the STAT pathway.

Bcl-2

Bcl-2 is a product of the B-lymphoma-2 gene, that regulates cell survival and inhibits apoptosis (49). Under oxidative stress, PKM2 translocates to the mitochondrial outer membrane, where heat shock protein (HSP)90α1 mediates conformational changes in PKM2 then interacts with and phosphorylates Bcl-2 at thr69. This phosphorylation prevents the binding of BTB–CUL3–RBX1 (BCR) E3 ligase to Bcl-2, thereby inhibiting the degradation of Bcl-2 and inhibiting the apoptosis of tumor cells (50). Knockdown of PKM2 induced apoptosis and autophagy in A549 cells, and this was dependent on decreased expression of Bcl-2

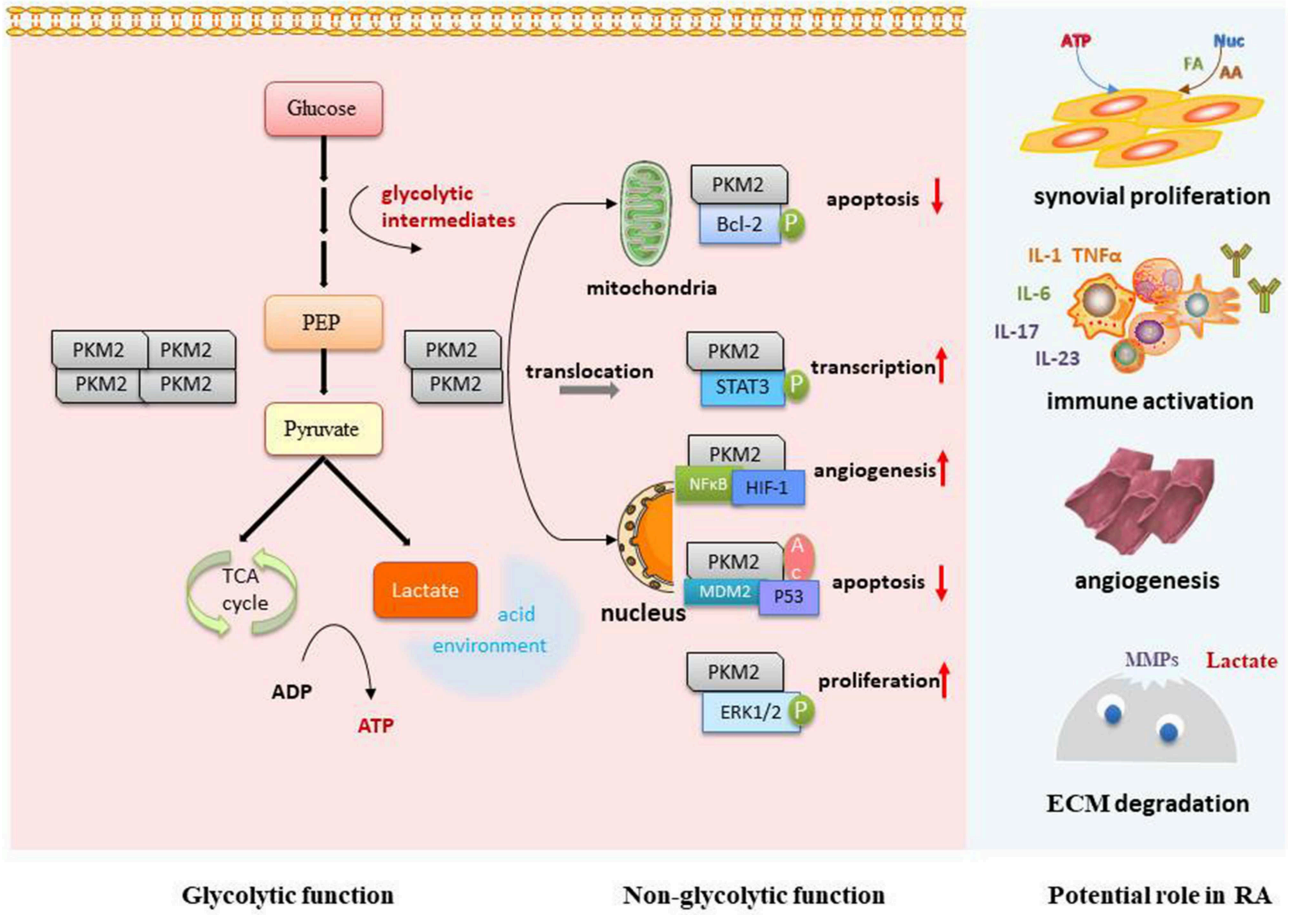

FIGURE 2 | Potential role and mechanism of PKM2 in RA. PKM2 can optimize the supply of energy and synthetic substrates for proliferative synoviocytes and activated immune cells via its glycolytic regulation function. The dimer form of PKM2 can interact with important RA transcription factors, such as STAT3, Bcl-2, HIF-1, and Erk1/2, so as to further regulate cell proliferation, apoptosis, angiogenesis, and immune activation. The local acidic microenvironment caused by increased glycolysis is favorable for synoviocyte invasion, MMP-1 activation, and angiogenesis. p, phosphorylation; Ac, acetylation; FA, fatty acid; AA, amino acid; Nuc, nucleotide; ECM, extracellular matrix.

(51). The IL-17/STAT3 pathway may promote the survival and proliferation of FLSs via upregulating the expression of Bcl-2 in RA (52). The overexpression of Bcl-2 may contribute to the reduced apoptosis of synoviocytes and peripheral B cells in RA patients (53). The relations between increased expression of Bcl-2 and PKM2 in synovial tissues deserve more investigation to clarify them further.

HIF-1α

HIF-1α is a major regulator of the transition from oxidative phosphorylation to anaerobic glycolysis (54). PKM2 was able to interact with NF-κB and HIF-1α in the nucleus and activate the expression of the target gene VEGF-A, thereby promoting tumor angiogenesis (55). Meanwhile, in macrophages, LPS-induced PKM2 could enter into a complex with HIF-1α, which directly bound to the IL-1β promoter, inhibiting LPS-induced HIF-1α and IL-1β, as well as the expression of a range of other HIF-1α-dependent genes (43). HIF-1α is highly expressed in the synovium of RA patients. HIF-1α can promote the migration of inflammatory cells to the RA synovium, and the expression of matrix metalloproteinase (MMP)-1 is up-regulated by HIF-1α under hypoxia (56). The "hypoxia-HIF-1α-VEGF" signaling pathway plays an important role in the formation of new blood vessels in RA, so targeting HIF-1α via PKM2 could make a lot of sense.

p53

p53 can work as a hub among a variety of intracellular signal transduction pathways, inhibiting cell proliferation, terminating cell processes, and inducing apoptosis (57). Recent studies have found that PKM2 may be involved in the regulation of p53 in tumor cells. In MCF7 cells exposed to DNA-damaging agent, PKM2 inhibited transactivation of the p21 gene by preventing p53 binding to the p21 promoter, leading to a nonstop G1 phase (58). Dimeric PKM2 has been found to bind directly with both p53 and MDM2 and to promote

MDM2-mediated p53 ubiquitination (59). PKM2 gene silencing suppresses proliferation and promotes apoptosis in LS-147T and SW620 cells, accompanied by increased p53 and p21 expression (60). Most studies suggest that p53 expression is decreased in RA-FLS and synovial tissue (61). Collagen-induced arthritis (CIA) was more severe and with more joint destruction in $p53^{-/-}$ mice than in wild type mice due to a reduction in synovial cell apoptosis (62). The future task is to clarify the regulation effect and molecular mechanism of PKM2 on p53 in synoviocytes.

ERK1/2

An ERK1/2 signaling pathway is an important intracellular pro-proliferation and anti-apoptosis pathway (63). In cancer cells, a PKM2-SAICAR complex phosphorylated and activated ERK1/2, which in turn sensitized PKM2 for SAICAR binding through phosphorylation (64). Additionally, PKM2-SAICAR was necessary to induce sustained ERK1/2 activation and mitogen-induced cell proliferation. In Panc-1 and Sw1990 pancreatic cancer cells, the expression levels of the p-ERK1/2 and p-p38 of the MAPK pathway in the PKM2 siRNA groups were markedly down-regulated (65). ERK1/2 is widely distributed in the synovial tissues of RA and is involved in the signal transduction process of synoviocytes (66). Clarifying the effect of PKM2 on ERK1/2 is helpful for exploring its role in the pathogenesis of RA.

CONCLUSION

In summary, glucose metabolism, especially increased glycolysis, plays a pivotal role in the pathogenesis of RA. Recent studies have confirmed the overexpression of PKM2 in RA synovium, suggesting a potential role for PKM2 in RA, though the exact role and mechanism have not been systematically studied. We infer that PKM2 may participate in RA pathogenesis through glycolytic or non-glycolytic pathways and that more investigations to are needed to clarify this further. PKM2 may be a potential therapeutic target due to its regulation of the immunometabolism and key signaling proteins in RA, and a small-molecule drug targeting the regulation of PKM2 activity or protein expression may be a novel approach for RA treatment.

AUTHOR CONTRIBUTIONS

DX and JLia wrote the review. CY and JLin edited the manuscript. All authors have read and approved the final manuscript.

FUNDING

This work was supported by the Medical and Health Research Program of Zhejiang Province (2018KY067).

REFERENCES

1. You S, Koh JH, Leng L, Kim WU, Bucala R. The tumor-like phenotype of rheumatoid synovium: molecular profiling and prospects for precision medicine. *Arthritis Rheumatol.* (2018) 70:637–52. doi: 10.1002/art.40406
2. Falconer J, Murphy AN, Young SP, Clark AR, Tiziani S, Guma M, et al. Review: synovial cell metabolism and chronic inflammation in rheumatoid arthritis. *Arthritis Rheumat.* (2018) 70:984–99. doi: 10.1002/art.40504
3. van Gaalen FA, Toes RE, Ditzel HJ, Schaller M, Breedveld FC, Verweij CL, et al. Association of autoantibodies to glucose-6-phosphate isomerase with extraarticular complications in rheumatoid arthritis. *Arthritis Rheum.* (2004) 50:395–9. doi: 10.1002/art.20028
4. Ukaji F, Kitajima I, Kubo T, Shimizu C, Nakajima T, Maruyama I. Serum samples of patients with rheumatoid arthritis contain a specific autoantibody to "denatured" aldolase A in the osteoblast-like cell line, MG-63. *Ann Rheum Dis.* (1999) 58:169–74. doi: 10.1136/ard.58.3.169
5. Xiang Y, Sekine T, Nakamura H, Imajoh-Ohmi S, Fukuda H, Nishioka K, et al. Proteomic surveillance of autoimmunity in osteoarthritis: identification of triosephosphate isomerase as an autoantigen in patients with osteoarthritis. *Arthritis Rheum.* (2004) 50:1511–21. doi: 10.1002/art.20189
6. Barnett JA. A history of research on yeasts 5: the fermentation pathway. *Yeast.* (2003) 20:509–43. doi: 10.1002/yea.986
7. Christofk HR, Vander Heiden MG, Harris MH, Ramanathan A, Gerszten RE, Wei R, et al. The M2 splice isoform of pyruvate kinase is important for cancer metabolism and tumour growth. *Nature.* (2008) 452:230–3. doi: 10.1038/nature06734
8. Hanahan D, Weinberg RA. Hallmarks of cancer: the next generation. *Cell.* (2011) 144:646–74. doi: 10.1016/j.cell.2011.02.013
9. McGarry T, Biniecka M, Gao W, Cluxton D, Canavan M, Wade S, et al. Resolution of TLR2-induced inflammation through manipulation of metabolic pathways in Rheumatoid Arthritis. *Sci Rep.* (2017) 7:43165. doi: 10.1038/srep43165
10. Takenaka M, Yamada K, Lu T, Kang R, Tanaka T, Noguchi T. Alternative splicing of the pyruvate kinase M gene in a minigene system. *Eur J Biochem.* (1996) 235:366–71. doi: 10.1111/j.1432-1033.1996.00366.x
11. Noguchi T, Inoue H, Tanaka T. The M1- and M2-type isozymes of rat pyruvate kinase are produced from the same gene by alternative RNA splicing. *J Biol Chem.* (1986) 261:13807–12.
12. Ikeda Y, Noguchi T. Allosteric regulation of pyruvate kinase M2 isozyme involves a cysteine residue in the intersubunit contact. *J Biol Chem.* (1998) 273:12227–33. doi: 10.1074/jbc.273.20.12227
13. Mazurek S, Zwerschke W, Jansen-Durr P, Eigenbrodt E. Effects of the human papilloma virus HPV-16 E7 oncoprotein on glycolysis and glutaminolysis: role of pyruvate kinase type M2 and the glycolytic-enzyme complex. *Biochem J.* (2001) 356(Pt 1):247–56. doi: 10.1042/bj3560247
14. Dombrauckas JD, Santarsiero BD, Mesecar AD. Structural basis for tumor pyruvate kinase M2 allosteric regulation and catalysis. *Biochemistry.* (2005) 44:9417–29. doi: 10.1021/bi0474923
15. Christofk HR, Vander Heiden MG, Wu N, Asara JM, Cantley LC. Pyruvate kinase M2 is a phosphotyrosine-binding protein. *Nature.* (2008) 452:181–6. doi: 10.1038/nature06667
16. Keller KE, Tan IS, Lee YS. SAICAR stimulates pyruvate kinase isoform M2 and promotes cancer cell survival in glucose-limited conditions. *Science.* (2012) 338:1069–72. doi: 10.1126/science.1224409
17. Morgan HP, O'Reilly FJ, Wear MA, O'Neill JR, Fothergill-Gilmore LA, Hupp T, et al. M2 pyruvate kinase provides a mechanism for nutrient sensing and regulation of cell proliferation. *Proc Natl Acad Sci USA.* (2013) 110:5881–6. doi: 10.1073/pnas.1217157110
18. Hitosugi T, Kang S, Vander Heiden MG, Chung TW, Elf S, Lythgoe K, et al. Tyrosine phosphorylation inhibits PKM2 to promote the Warburg effect and tumor growth. *Sci Signal.* (2009) 2:ra73. doi: 10.1126/scisignal.2000431
19. Lv L, Li D, Zhao D, Lin R, Chu Y, Zhang H, et al. Acetylation targets the M2 isoform of pyruvate kinase for degradation through chaperone-mediated autophagy and promotes tumor growth. *Mol Cell.* (2011) 42:719–30. doi: 10.1016/j.molcel.2011.04.025
20. Anastasiou D, Poulogiannis G, Asara JM, Boxer MB, Jiang JK, Shen M, et al. Inhibition of pyruvate kinase M2 by reactive oxygen species contributes to cellular antioxidant responses. *Science.* (2011) 334:1278–83. doi: 10.1126/science.1211485
21. Warburg O. On the origin of cancer cells. *Science.* (1956) 123:309–14. doi: 10.1126/science.123.3191.309

22. Altenberg B, Greulich KO. Genes of glycolysis are ubiquitously overexpressed in 24 cancer classes. *Genomics*. (2004) 84:1014–20. doi: 10.1016/j.ygeno.2004.08.010
23. Wong N, Ojo D, Yan J, Tang D. PKM2 contributes to cancer metabolism. *Cancer Lett*. (2015) 356(2 Pt A):184–91. doi: 10.1016/j.canlet.2014.01.031
24. Lu Z, Hunter T. Metabolic kinases moonlighting as protein kinases. *Trends Biochem Sci*. (2018) 43:301–10. doi: 10.1016/j.tibs.2018.01.006
25. Dayton TL, Gocheva V, Miller KM, Israelsen WJ, Bhutkar A, Clish CB, et al. Germline loss of PKM2 promotes metabolic distress and hepatocellular carcinoma. *Genes Dev*. (2016) 30:1020–33. doi: 10.1101/gad.278549.116
26. Hosios AM, Fiske BP, Gui DY, Vander Heiden MG. Lack of evidence for PKM2 protein kinase activity. *Mol Cell*. (2015) 59:850–7. doi: 10.1016/j.molcel.2015.07.013
27. Ng CT, Biniecka M, Kennedy A, McCormick J, Fitzgerald O, Bresnihan B, et al. Synovial tissue hypoxia and inflammation *in vivo*. *Ann Rheum Dis*. (2010) 69:1389–95. doi: 10.1136/ard.2009.119776
28. Hitchon CA, El-Gabalawy HS, Bezabeh T. Characterization of synovial tissue from arthritis patients: a proton magnetic resonance spectroscopic investigation. *Rheumatol Int*. (2009) 29:1205–11. doi: 10.1007/s00296-009-0865-z
29. Garcia-Carbonell R, Divakaruni AS, Lodi A, Vicente-Suarez I, Saha A, Cheroutre H, et al. Critical role of glucose metabolism in rheumatoid arthritis fibroblast-like synoviocytes. *Arthritis Rheumatol*. (2016) 68:1614–26. doi: 10.1002/art.39608
30. Kubota K, Ito K, Morooka M, Mitsumoto T, Kurihara K, Yamashita H, et al. Whole-body FDG-PET/CT on rheumatoid arthritis of large joints. *Ann Nucl Med*. (2009) 23:783–91. doi: 10.1007/s12149-009-0305-x
31. Matsui T, Nakata N, Nagai S, Nakatani A, Takahashi M, Momose T, et al. Inflammatory cytokines and hypoxia contribute to 18F-FDG uptake by cells involved in pannus formation in rheumatoid arthritis. *J Nucl Med*. (2009) 50:920–6. doi: 10.2967/jnumed.108.060103
32. Young SP, Kapoor SR, Viant MR, Byrne JJ, Filer A, Buckley CD, et al. The impact of inflammation on metabolomic profiles in patients with arthritis. *Arthritis Rheum*. (2013) 65:2015–23. doi: 10.1002/art.38021
33. Biniecka M, Canavan M, McGarry T, Gao W, McCormick J, Cregan S, et al. Dysregulated bioenergetics: a key regulator of joint inflammation. *Ann Rheum Dis*. (2016) 75:2192–200. doi: 10.1136/annrheumdis-2015-208476
34. Li XJ, Xu M, Zhao XQ, Zhao JN, Chen FF, Yu W, et al. Proteomic analysis of synovial fibroblast-like synoviocytes from rheumatoid arthritis. *Clin Exp Rheumatol*. (2013) 31:552–8.
35. Gillies RJ, Gatenby RA. Adaptive landscapes and emergent phenotypes: why do cancers have high glycolysis? *J Bioenerget Biomembr*. (2007) 39:251–7. doi: 10.1007/s10863-007-9085-y
36. Walenta S, Mueller-Klieser WF. Lactate: mirror and motor of tumor malignancy. *Semin Radiat Oncol*. (2004) 14:267–74. doi: 10.1016/j.semradonc.2004.04.004
37. Gatenby RA, Gillies RJ. Why do cancers have high aerobic glycolysis? *Nat Rev Cancer*. (2004) 4:891–9. doi: 10.1038/nrc1478
38. Chang CH, Curtis JD, Maggi LB Jr, Faubert B, Villarino AV, O'Sullivan D, et al. Posttranscriptional control of T cell effector function by aerobic glycolysis. *Cell*. (2013) 153:1239–51. doi: 10.1016/j.cell.2013.05.016
39. Shi LZ, Wang R, Huang G, Vogel P, Neale G, Green DR, et al. HIF1alpha-dependent glycolytic pathway orchestrates a metabolic checkpoint for the differentiation of TH17 and Treg cells. *J Exp Med*. (2011) 208:1367–76. doi: 10.1084/jem.20110278
40. De Bock K, Georgiadou M, Schoors S, Kuchnio A, Wong BW, Cantelmo AR, et al. Role of PFKFB3-driven glycolysis in vessel sprouting. *Cell*. (2013) 154:651–63. doi: 10.1016/j.cell.2013.06.037
41. Wang R, Dillon CP, Shi LZ, Milasta S, Carter R, Finkelstein D, et al. The transcription factor Myc controls metabolic reprogramming upon T lymphocyte activation. *Immunity*. (2011) 35:871–82. doi: 10.1016/j.immuni.2011.09.021
42. Macintyre AN, Gerriets VA, Nichols AG, Michalek RD, Rudolph MC, Deoliveira D, et al. The glucose transporter Glut1 is selectively essential for CD4 T cell activation and effector function. *Cell Metab*. (2014) 20:61–72. doi: 10.1016/j.cmet.2014.05.004
43. Palsson-McDermott EM, Curtis AM, Goel G, Lauterbach MA, Sheedy FJ, Gleeson LE, et al. Pyruvate kinase M2 regulates Hif-1alpha activity and IL-1beta induction and is a critical determinant of the warburg effect in LPS-activated macrophages. *Cell Metab*. (2015) 21:65–80. doi: 10.1016/j.cmet.2014.12.005
44. Kong Q, Li N, Cheng H, Zhang X, Cao X, Qi T, et al. HSPA12A Is a novel player in nonalcoholic steatohepatitis via promoting nuclear PKM2-mediated M1 macrophage polarization. *Diabetes*. (2019) 68:361–76. doi: 10.2337/db18-0035
45. Thomas SJ, Snowden JA, Zeidler MP, Danson SJ. The role of JAK/STAT signalling in the pathogenesis, prognosis and treatment of solid tumours. *Br J Cancer*. (2015) 113:365–71. doi: 10.1038/bjc.2015.233
46. Gao X, Wang H, Yang JJ, Liu X, Liu ZR. Pyruvate kinase M2 regulates gene transcription by acting as a protein kinase. *Mol Cell*. (2012) 45:598–609. doi: 10.1016/j.molcel.2012.01.001
47. Wang B, Liu S, Fan B, Xu X, Chen Y, Lu R, et al. PKM2 is involved in neuropathic pain by regulating ERK and STAT3 activation in rat spinal cord. *J Headache Pain*. (2018) 19:7. doi: 10.1186/s10194-018-0836-4
48. Yang P, Li Z, Li H, Lu Y, Wu H, Li Z. Pyruvate kinase M2 accelerates pro-inflammatory cytokine secretion and cell proliferation induced by lipopolysaccharide in colorectal cancer. *Cell Signal*. (2015) 27:1525–32. doi: 10.1016/j.cellsig.2015.02.032
49. Skommer J, Wlodkowic D, Deptala A. Larger than life: mitochondria and the Bcl-2 family. *Leukemia Res*. (2007) 31:277–86. doi: 10.1016/j.leukres.2006.06.027
50. Liang J, Cao R, Wang X, Zhang Y, Wang P, Gao H, et al. Mitochondrial PKM2 regulates oxidative stress-induced apoptosis by stabilizing Bcl2. *Cell Res*. (2017) 27:329–51. doi: 10.1038/cr.2016.159
51. Chen J, Xie J, Jiang Z, Wang B, Wang Y, Hu X. Shikonin and its analogs inhibit cancer cell glycolysis by targeting tumor pyruvate kinase-M2. *Oncogene*. (2011) 30:4297–306. doi: 10.1038/onc.2011.137
52. Lee SY, Kwok SK, Son HJ, Ryu JG, Kim EK, Oh HJ, et al. IL-17-mediated Bcl-2 expression regulates survival of fibroblast-like synoviocytes in rheumatoid arthritis through STAT3 activation. *Arthritis Res Ther*. (2013) 15:R31. doi: 10.1186/ar4179
53. Yang J, Zhao S, Yang X, Zhang H, Zheng P, Wu H. Inhibition of B-cell apoptosis is mediated through increased expression of Bcl-2 in patients with rheumatoid arthritis. *Int J Rheum Dis*. (2016) 19:134–40. doi: 10.1111/1756-185X.12706
54. Singh D, Arora R, Kaur P, Singh B, Mannan R, Arora S. Overexpression of hypoxia-inducible factor and metabolic pathways: possible targets of cancer. *Cell Biosci*. (2017) 7:62. doi: 10.1186/s13578-017-0190-2
55. Azoitei N, Becher A, Steinestel K, Rouhi A, Diepold K, Genze F, et al. PKM2 promotes tumor angiogenesis by regulating HIF-1alpha through NF-kappaB activation. *Mol Cancer*. (2016) 15:3. doi: 10.1186/s12943-015-0490-2
56. Lee YA, Choi HM, Lee SH, Hong SJ, Yang HI, Yoo MC, et al. Hypoxia differentially affects IL-1beta-stimulated MMP-1 and MMP-13 expression of fibroblast-like synoviocytes in an HIF-1alpha-dependent manner. *Rheumatology*. (2012) 51:443–50. doi: 10.1093/rheumatology/ker327
57. Kastenhuber ER, Lowe SW. Putting p53 in context. *Cell*. (2017) 170:1062–78. doi: 10.1016/j.cell.2017.08.028
58. Xia L, Wang XR, Wang XL, Liu SH, Ding XW, Chen GQ, et al. A novel role for pyruvate kinase M2 as a corepressor for P53 during the DNA damage response in human tumor cells. *J Biol Chem*. (2016) 291:26138–50. doi: 10.1074/jbc.M116.737056
59. Wu HL, Yang P, Hu WL, Wang YY, Lu YX, Zhang LC, et al. Overexpression of PKM2 promotes mitochondrial fusion through attenuated p53 stability. *Oncotarget*. (2016) 7:78069–82. doi: 10.18632/oncotarget.12942
60. Ao R, Guan L, Wang Y, Wang JN. Effects of PKM2 gene silencing on the proliferation and apoptosis of colorectal cancer LS-147T and SW620 cells. *Cell Physiol Biochem*. (2017) 42:1769–78. doi: 10.1159/000479456
61. Seemayer CA, Kuchen S, Neidhart M, Kuenzler P, Rihoskova V, Neumann E, et al. p53 in rheumatoid arthritis synovial fibroblasts at sites of invasion. *Ann Rheum Dis*. (2003) 62:1139–44. doi: 10.1136/ard.2003.007401
62. Simelyte E, Rosengren S, Boyle DL, Corr M, Green DR, Firestein GS. Regulation of arthritis by p53: critical role of adaptive immunity. *Arthritis Rheum*. (2005) 52:1876–84. doi: 10.1002/art.21099

63. Roskoski R Jr. ERK1/2 MAP kinases: structure, function, and regulation. *Pharmacol Res*. (2012) 66:105–43. doi: 10.1016/j.phrs.2012.04.005
64. Keller KE, Doctor ZM, Dwyer ZW, Lee YS. SAICAR induces protein kinase activity of PKM2 that is necessary for sustained proliferative signaling of cancer cells. *Mol Cell*. (2014) 53:700–9. doi: 10.1016/j.molcel.2014.02.015
65. Feng J, Ma T, Ge Z, Lin J, Ding W, Chen H, et al. PKM2 gene regulates the behavior of pancreatic cancer cells via mitogen-activated protein kinase pathways. *Mol Med Rep*. (2015) 11:2111–7. doi: 10.3892/mmr.2014.2990
66. Schett G, Tohidast-Akrad M, Smolen JS, Schmid BJ, Steiner CW, Bitzan P, et al. Activation, differential localization, and regulation of the stress-activated protein kinases, extracellular signal-regulated kinase, c-JUN N-terminalkinase, and p38 mitogen-activated protein kinase, in synovial tissue and cells in rheumatoid arthritis. *Arthritis Rheum*. (2000) 43:2501–12. doi: 10.1002/1529-0131(200011)43:11<2501::AID-ANR18>3.0.CO;2-K

Conflict of Interest: The authors declare that the research was conducted in the absence of any commercial or financial relationships that could be construed as a potential conflict of interest.

Copyright © 2019 Xu, Liang, Lin and Yu. This is an open-access article distributed under the terms of the Creative Commons Attribution License (CC BY). The use, distribution or reproduction in other forums is permitted, provided the original author(s) and the copyright owner(s) are credited and that the original publication in this journal is cited, in accordance with accepted academic practice. No use, distribution or reproduction is permitted which does not comply with these terms.

frontiers in Immunology

ORIGINAL RESEARCH
published: 21 February 2020
doi: 10.3389/fimmu.2020.00037

Reduced miR-146a Promotes REG3A Expression and Macrophage Migration in Polymyositis and Dermatomyositis

Tingwang Jiang[1,2†], Yuanlan Huang[3†], Haohao Liu[4], Qiangwei Xu[5], Yanping Gong[2], Yao Chen[4], Xiaowei Hu[4], Zhijun Han[4] and Mingzhu Gao[4,6*]*

[1] Key Laboratory, The Second People's Hospital of Changshu, Changshu, China, [2] Department of Clinical Immunology, Institution for Laboratory Medicine, Changshu, China, [3] Department of Laboratory Medicine, No. 455 Hospital of the Chinese People's Liberation Army, Shanghai, China, [4] Department of Laboratory Medicine, The Affiliated Wuxi No.2 People's Hospital of Nanjing Medical University, Wuxi, China, [5] Department of Rheumatology, The Affiliated Wuxi No.2 People's Hospital of Nanjing Medical University, Wuxi, China, [6] Affiliated Wuxi Clinical College of Nantong University, Wuxi, China

OPEN ACCESS

Edited by:
Erminia Mariani, University of Bologna, Italy

Reviewed by:
Janine Adele Lamb, University of Manchester, United Kingdom
Mrinal K. Sarkar, University of Michigan, United States

***Correspondence:**
Zhijun Han
zjhan1125@163.com
Mingzhu Gao
gaomingzhujewel@163.com

[†]These authors have contributed equally to this work

Specialty section:
This article was submitted to Autoimmune and Autoinflammatory Disorders, a section of the journal Frontiers in Immunology

Received: *13 August 2019*
Accepted: *08 January 2020*
Published: *21 February 2020*

Citation:
Jiang T, Huang Y, Liu H, Xu Q, Gong Y, Chen Y, Hu X, Han Z and Gao M (2020) Reduced miR-146a Promotes REG3A Expression and Macrophage Migration in Polymyositis and Dermatomyositis. Front. Immunol. 11:37. doi: 10.3389/fimmu.2020.00037

Background: Growing evidence from studies elsewhere have illustrated that microRNAs (miRNAs) play important roles in polymyositis and dermatomyositis (PM/DM). However, little has been reported on their relationship with regenerating islet-derived protein 3-alpha (REG3A) as well as their associative roles in macrophage migration. Therefore, this study sought to establish the association between miR-146a and REG3A as well as investigate their functional roles in macrophage migration and PM/DM pathogenesis.

Methods: Peripheral blood mononuclear cells (PBMCs) were isolated from PM/DM patients and healthy controls through density centrifugation. Macrophages were obtained from monocytes purified from PBMCs via differentiation before their transfection with miRNA or plasmids to investigate cell migration with transwell assay. An experimental autoimmune myositis murine model was used to investigate PM/DM. Real-time PCR and Western blot analysis were conducted to determine the expression levels of miR-146a, interferon gamma (IFN-γ), interleukin (IL)-17A, and REG3A.

Results: The messenger RNA (mRNA) expression level of miR-146a markedly decreased, while the mRNA level of REG3A, IFN-γ, and IL-17A expression increased substantially in PBMCs from PM/DM patients compared with the healthy controls. The levels of IFN-γ and IL-17A in serum from PM/DM patients was much higher than the healthy controls. Immunohistochemistry analysis showed that REG3A expression increased in muscle tissues from patients. Consistent with clinical data, the mRNA expression level of miR-146a also decreased, whereas the mRNA and protein level of REG3A, IFN-γ, and IL-17A significantly increased in the muscle tissues of experimental autoimmune myositis mice. Moreover, miR-146a inhibited monocyte-derived macrophage migration, and REG3A promoted macrophage migration. In addition, IL-17A induced REG3A expression, while miR146a inhibited expression of REG3A in monocyte-derived macrophages from the PBMCs of the healthy donors. Notably, inhibition of macrophage migration by miR-146a was via the reduction in REG3A expression.

Conclusions: Reduced miR-146a expression in PM/DM leads to increased REG3A expression that increases inflammatory macrophage migration, which may be a possible underlying mechanism of DM/PM pathogenesis.

Keywords: miR-146a, REG3A, macrophage migration, polymyositis and dermatomyositis, autoimmune disease

HIGHLIGHTS

- miR-146a is decreased and REG3A is increased in PM/DM patients.
- REG3A promotes macrophage migration, while miR-146a inhibits migratory capacity of macrophage.
- miR-146a inhibits macrophage migration via reduction in REG3A expression.

INTRODUCTION

Polymyositis and dermatomyositis (PM/DM), diseases of the connective tissues that are classified as typical idiopathic inflammatory myopathies, affect mainly proximal muscles and other body parts such as skin, lungs, esophagus, heart, and joints (1, 2). Although the clinical differentiation of DM from PM is difficult, the former discern from the latter based on classical cutaneous manifestations such as heliotrope rash, shawl sign, as well as Gottron's papules and signs (3). Usually, PM/DM are considered as separate autoimmune diseases, albeit some overlap with other disorders such as rheumatoid arthritis, systemic sclerosis, and systemic lupus erythematosus (1). To support this assertion, a previous report suggested the role of persistent monocytes/macrophages markers in these disease processes (4). Besides, DM is the most common form of classical inflammatory myopathy, while isolated PM is rare but frequent misdiagnosis (5). Therefore, detailed understanding of the exact pathological processes of PM/DM could be valuable for determining appropriate treatment options for patients suffering from the aforementioned conditions who are at 120% increased mortality risk (6, 7).

The pathogenic roles of microRNAs have been extensively investigated in malignant diseases as well as in autoimmune disorders. Although many microRNAs levels altered in PM/DM patients after treatment, little study reported the role of microRNA in PM/DM (8). So far, miR-21, miR-381, and miR-146a have been reported to regulate macrophage migration in PM/DM (9–11). However, the regulatory mechanism of these microRNAs in PM/DM remains unclear. miR-146a, a member of the microRNA precursors (family miR-146) found in mammals, is located on chromosome 5, which has been observed to play critical anti-inflammatory role by modulating nuclear factor kappa-light-chain-enhancer of activated B cells signal pathway activation as well as release of toll-like receptor 4-induced inflammatory factor (12). The modulation of the aforesaid physiological processes by miR-146a culminated in further downregulation of downstream inflammatory mediators such as interleukins (IL-1β, IL-6, and IL-8) coupled with tumor necrosis factor alpha, thereby preventing overreaction induced by negative immuno-inflammatory regulation (13–15). In this regard, Yin et al. reported the regulation of inflammatory macrophage infiltration in PM/DM by miR-146a via tumor necrosis factor receptor-associated factor 6 targeting and the IL-17/intercellular adhesion molecule 1 pathway dysregulation (11). It is described earlier that deficiency of miR-146a could result in increased expression of macrophages (M1) activation biomarkers with concomitant upregulation of proinflammatory cytokines in diabetic miR-146a$^{-/-}$ mice (16). Likewise, Peng et al. had previously established the involvement of muscle macrophage infiltration in PM/DM pathogenesis (17). In a related study, macrophage polarization in systemic juvenile idiopathic arthritis by miR-146a via the M1-associated gene, inhibin beta A subunit targeting (18).

Regenerating islet-derived protein 3-alpha (REG3A), also known as heptocarcinoma–intestine–pancreas or pancreatic-associated protein is a serum biomarker released from the gut upon injury to function as an antimicrobial protein by resisting bacterial proliferation at the injured site (19, 20). Beside the antimicrobial function, RegIIIγ expression, a mouse homolog of human REG3A, has been established to increase after a mucosal damage and hepatic injury with potential effect on tissue regeneration (21, 22). Likewise, it has been revealed that REG3A expression by skin keratinocyte was induced by IL-17 with possible mediation in epidermal hyperproliferation in psoriatic wound repair (23). Meanwhile, inhibition of REG3A expression in diabetic mice exacerbated toll-like receptor 3-mediated skin inflammation (21, 24). However, its role in inflammatory macrophage infiltration in PM/DM has not been elucidated. In this regard, the actual mechanistic role of miR-146a and its relationship with REG3A in the regulation of inflammatory macrophage migration to weakened muscle tissues in PM/DM pathophysiology awaits exploration.

Herein, this study aimed to investigate the function of miR-146a and its association with the level of REG3A in regulating macrophage migration in PM/DM patients vis-à-vis the healthy controls. The present study also sought to explore the role of IL-17A in the induction of REG3A expression.

MATERIALS AND METHODS

Recruitment of PM/DM Patients and the Healthy Controls

This study involved subjects (PM/DM patients and the healthy controls) recruited from inpatients at the Department of Laboratory Medicine, The Affiliated Wuxi NO.2 People's Hospital of Nanjing Medical University (Wuxi, Jiangsu Province, China) between 2016 and 2017. Peripheral blood was obtained from 20 healthy controls and 25 patients with PM/DM (6 PM,

19 DM; 8 male, 17 female; mean age, 37 ± 13 years). The PM/DM patients were age and gender matched with the healthy controls. The PM/DM patients were diagnosed via determination of their serum samples and muscle biopsy results according to the European Neuromuscular Center pathology diagnosis criteria as described elsewhere (25). The experimental protocol was approved by the Ethics Committee of The Affiliated Wuxi No. 2 People's Hospital of Nanjing Medical University. All patients provided written informed consent for the use of their tissues and data before the study.

Experimental Autoimmune Myositis Model

Adult (6–8 weeks old) Balb/c female mice were obtained from Jiangsu Synthgene Biotechnology Co., Ltd and maintained with free access to pellet foods and water under controlled conditions (22°C, 55% humidity, 12 h day/night). All animals received adequate care in compliance with laboratory practice guidelines, and the experimental protocol was approved by the Ethics Committee of The Affiliated Wuxi NO.2 People's Hospital of Nanjing Medical University. To induce an experimental autoimmune myositis (EAM) model, the mice were immunized subcutaneously with 100 μl of 50% complete Freund's adjuvant (Sigma-Aldrich, St. Louis, MS) containing 1.5 mg myosin and 5 mg/ml *Mycobacterium tuberculosis* (BD Biosciences, Franklin Lakes, NY) at the left hind limb and boosted at the tail base and flanks twice weekly as stated in earlier reports (26). The mice were injected intraperitoneally with 500 ng pertussis toxin (Sigma-Aldrich, St. Louis, MS) immediately after each immunization. The control group received saline/complete Freund's adjuvant and pertussis toxin twice. On day 14 after the first immunization, the serum and muscle tissues were collected for further assay.

PBMC Isolation and *in vitro* Macrophage Differentiation

Human peripheral blood was collected, and peripheral blood mononuclear cells (PBMCs) were isolated via density centrifugation (400 × *g*, 30 min) by human lymphocyte separation medium (Solarbio Life Sciences, China) according to the manufacturer's instruction. The mononuclear cells were washed with phosphate-buffered saline for 5 min at 400 × *g* and 4°C. For macrophage differentiation, PBMCs were cultured with Roswell Park Memorial Institute media and supplemented with glutamax, 20 ng/ml macrophage colony-stimulating factor and 10% fetal bovine serum for 7 days to cause differentiation into macrophages (Gibco Thermo Fischer, Waltham, MA).

Cell Transfection

Monocyte-derived macrophages were seeded into a six-well plate and transfected with microRNAs (miRNAs) (50 nM), small-interfering RNA (siRNA) (50 pmol), or plasmid (5 μg) using Lipofectamine 3000 (Invitrogen, Carlsbad, CA, USA) at 37°C according to the manufacturer's instruction. After 24 h, the cells underwent further experimentation. MiR-146a mimics, miR-146a inhibitor, and negative control miRNA were obtained from GenePharma (Shanghai, China). The negative control (NC) siRNA, REG3A siRNA, IL-17RA siRNA, pcDNA3.1-NC, and pcDNA3.1-hREG3A were synthesized by Invitrogen (Carlsbad, CA, USA).

Macrophage Migration Assay

The cells (2×10^5) were suspended in the free serum medium before they were added to the upper chamber of Transwell 96-Well. The medium containing 10% human serum was used as a chemoattractant in the lower chamber. After incubation for 24 h, the invaded cells into the lower chamber were stained with crystal violet. The migrated cells were counted, and photomicrographs were taken under an Olympus inverted microscope (IX71, Olympus, Japan).

Real-Time Quantitative PCR

Total RNA from muscle tissues and cells was prepared using Trizol reagent (Invitrogen, Carlsbad, CA) according to the manufacturer's instructions. Briefly, complementary DNA (cDNA) was synthesized from 1 μg RNA using SuperScript™ II Reverse Transcriptase (Invitrogen, Carlsbad, CA). Real-time PCR was performed with SYBR Green master Mix (Thermo Fisher Scientific, Waltham, MA) and ABI 7500 sequence detection system (Applied Biosystems, Foster City, CA). Data were analyzed by the $2^{(-\Delta\Delta Ct)}$ method. The primers for miR-146a (Qiagen, MS00001638) and RNU6-2 (Qiagen, MS00033740) were purchased from Qiagen. Each sample was measured in triplicate, and the relative messenger RNA (mRNA) expression was normalized using glyceraldehyde 3-phosphate dehydrogenase/U6. The quantitative PCR thermocycling conditions were as follows: 94°C for 5 min; followed by 40 cycles at 94°C for 30 s, and 60°C for 30 s. The sequences of the primers used for PCR amplification are listed in **Table 1**.

Enzyme-Linked Immunosorbent Assay

Briefly, the whole blood from mice was centrifuged at 8,000 × *g* for 15 min, and serum was collected. The levels of

TABLE 1 | The sequences of the primers used for PCR amplification.

Gene		Primer sequence
hIFN-γ	Sense	GCATCGTTTTGGGTTCTCTTG
	Antisense	AGTTCCATTATCCGCTACATCTG
hIL-17	Sense	AACCTGAACATCCATAACCGG
	Antisense	ACTTTGCCTCCCAGATCAC
hREG3A	Sense	CCTCAAGTCGCAGACACTATG
	Antisense	CTTTGGGACAGCGGATCC
mREG3A	Sense	AAGACATCTGGATTGGGCTC
	Antisense	CACGGTTGACAGTAGAGGAAG
mIL-17	Antisense	TCCAGAATGTGAAGGTCAACC
	Sense	TATCAGGGTCTTCATTGCGG
mIFN-γ	Antisense	TCCAGAATGTGAAGGTCAACC
	Sense	TATCAGGGTCTTCATTGCGG
GAPDH	Sense	GGAGCGAGATCCCTCCAAAAT
	Antisense	GGCTGTTGTCATACTTCTCATGG

The primers for miR-146a (Qiagen, MS00001638) and RNU6-2 (Qiagen, MS00033740) were purchased from Qiagen.

interferon gamma (IFN-γ) and IL-17A were quantified by ELISA commercial kits (R&D system, Minneapolis, MN).

Western Blot

Cells and muscle tissues were homogenized in RIPA buffer (25 mM Tris–HCl pH 7.6, 150 mM NaCl, 1% NP-40, 1% sodium deoxycholate, 0.1% sodium dodecyl sulfate) containing 1 mmol/L phenylmethylsulfonyl fluoride. After centrifugation for 10 min, the protein concentration in the supernatant was determined using Pierce™ BCA Protein Assay Kit (Thermo Fisher Scientific, Waltham, MA). The protein was separated by 10% sodium dodecyl sulfate polyacrylamide gel electrophoresis and transferred onto a polyvinylidene fluoride membrane. After blocking with 1.5% bovine serum albumin in Tris-buffered saline, the membrane was incubated with indicated primary antibodies and horseradish peroxidase-conjugated secondary antibody. The bands were detected by ECL reagent (Cell Signaling Technology, MA, United States) using Western blot detection system according to the specification of manufacturer's instructions.

Immunohistochemistry

Muscle tissue were fix in 10% formalin and embedded in paraffin. Slices (5 μm) of muscle tissues were deparaffinized in xylene and subjected to antigen retrieval. The sections were immunostained with primary REG3A antibody (Novus biologicals, #NBP2-24763) at room temperature for 1 h and secondary antibody for 30 min in a humidified chamber. The positive cells were detected by 3,3′-Diaminobenzidine solution according to manufacturer's instruction.

Statistical Analysis

Data were analyzed using SPSS 17.0 software package (SPSS Inc., IL, USA) and expressed as mean ± SEM. Statistical comparisons between two groups were performed using the Student's *t*-test. A $p < 0.05$ was considered statistically significant.

RESULTS

The mRNA Expression Levels of REG3A Increased and miR-146a Decreased in PM/DM Patients

PM/DM are considered as the two most prevalent inflammatory myopathies, which are characterized by the increasing levels of inflammatory cytokines such as IFN-γ and IL-17A. The mRNA expression levels in PBMCs isolated from patients and the healthy controls were detected by real-time PCR. As we expected in **Figure 1A**, the mRNA expression levels of IFN-γ and IL-17A were remarkably higher in PBMCs from PM/DM patients compared with healthy controls group ($p < 0.01$). Likewise, in comparison with the control group, mRNA expression levels of REG3A was significantly ($p < 0.01$) higher in PBMCs from PM/DM patients, while miR-146a expression was markedly downregulated ($p < 0.01$). Moreover, the levels of IFN-γ and IL-17A in serum from PM/DM patients were significantly increased compared with the healthy controls (**Figure 1B**). Immunohistochemistry analysis showed that REG3A expression level in the muscle tissue from PM/DM patients was much higher than the healthy controls (**Figure 1C**).

The mRNA Expression Levels of REG3A Increased and miR-146a Decreased in an EAM Murine Model

To confirm the levels of REG3A and miR-146a in PM/DM, an EAM murine model was established, and the mRNA levels of IFN-γ, IL-17A, REG3A, and miR-146a were determined by real-time PCR. The data showed that the mRNA expression of miR-146a was remarkably lower in muscle tissues, while significantly higher mRNA expression of REG3A, IFN-γ, and IL-17A in muscle samples were observed. Furthermore, the IFN-γ and IL-17A in serum were determined by ELISA assay. As shown in **Figure 2B**, the protein levels of IFN-γ and IL-17A in serum were significantly ($p < 0.01$) elevated in the model group compared with the control cohort, indicating that the model was well-established in mice. Consistently, Western blot analysis showed similar increase in the protein levels of REG3A in muscle tissues compared with the control group (**Figure 2C**). These results suggest the promotion of inflammatory infiltration in the mice muscle tissues with concomitant elevation of REG3A expression, while reduced levels of miR-146a expression was observed.

miR-146a and REG3A Regulate Macrophage Migration

Macrophage plays a key role in inflammatory response and the development of PM/DM. Therefore, we aimed to probe the effect of miR-146a and REG3A on macrophage migration. First, monocytes were isolated from the PBMCs of the healthy donors and differentiated into macrophages. Monocyte-derived macrophages of healthy donors were transfected with the NC miRNA, miR-146a mimics, and miR-146a inhibitors for 24 h. As shown in **Figure 3A**, the numbers of migrated cells as indicated by the transwell assay showed a substantial decrease ($p < 0.05$) in miR-146a mimics group compared with the NC group (**Figure 3A**). Conversely, a significant increase ($p < 0.01$) in migratory cell numbers was observed upon treatment with miR-146a inhibitors compared with the NC group (**Figure 3A**). Next, the macrophages were transfected with the NC-siRNA, REG3A-siRNA, pcDNA3.1-NC, and pcDNA3.1-REG3A plasmids for 24 h. As depicted in **Figure 3B**, the numbers of migrated cells were substantially decreased ($p < 0.05$) after transfection with REG3A-siRNA compared with the NC-siRNA group. Likewise, overexpression of REG3A with pcDNA3.1-REG3A plasmids in macrophage resulted in migratory cell numbers markedly increased ($p < 0.05$) compared with the pcDNA3.1-NC group. Taken together, these findings indicate that miR-146a and REG3A regulated macrophage migration.

IL-17A Induced REG3A Expression in Macrophage

IL-17-mediated inflammation is crucial for autoimmune diseases, which induce a set of gene expression through IL-17 receptor pathway. The relationship among IL-17A miR-146a and REG3A in macrophage remains unclear especially among

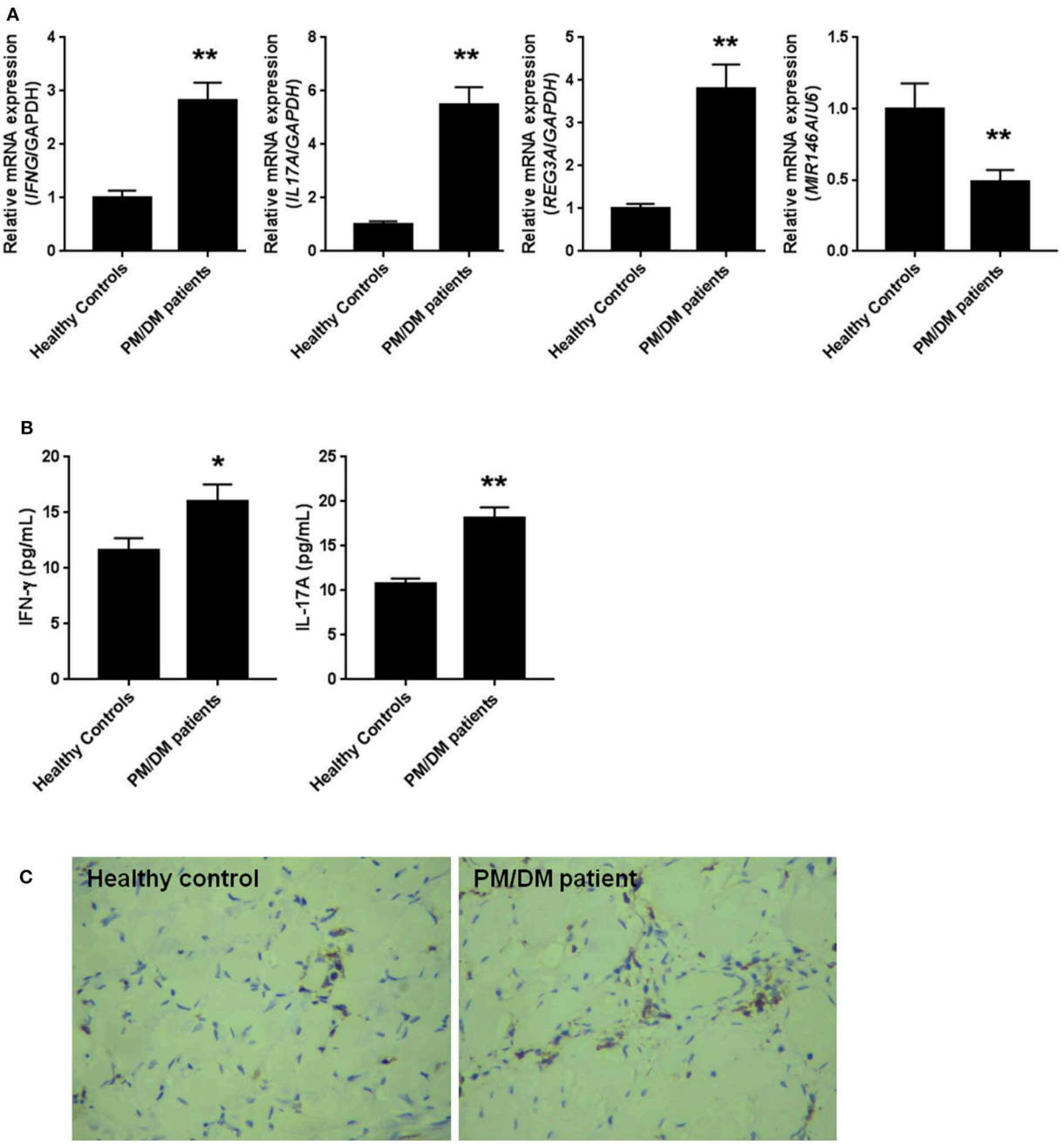

FIGURE 1 | The levels of regenerating islet-derived protein 3-alpha (REG3A) was increased and miR-146a was decreased in polymyositis and dermatomyositis (PM/DM) patients. **(A)** Peripheral blood mononuclear cells (PBMCs) were isolated from patients ($n = 25$) and the healthy controls ($n = 20$) and the messenger RNA (mRNA) levels of interferon gamma (IFN-γ), interleukin (IL)-17A, REG3A, and miRNA-146a were determined by real-time PCR. The relative mRNA expression was normalized using glyceraldehyde 3-phosphate dehydrogenase (GAPDH)/U6. **(B)** The levels of IFN-γ and IL-17A in serum from patients and the healthy controls were determined by ELISA assay. **(C)** The REG3A levels from patients and the healthy controls were determined by immunohistochemistry. Data are shown as means ± SEM. $^{*}p < 0.05$, $^{**}p < 0.01$ in comparison with the healthy controls. PBMCs were obtained from 20 healthy controls and 25 patients with PM/DM.

PM/DM patients. Monocyte-derived macrophages obtained from healthy donors were treated with different concentrations of IL-17A for 24 h. Notably, we found that the mRNA expression of REG3A significantly ($p < 0.01$) increased by IL-17A treatment in a dose-dependent manner (**Figure 4A**). Conversely, similar treatment with diverse concentrations of IL-17A did not affect mRNA expression of miR-146a (**Figure 4B**). Next, Western blot analysis confirmed the induction of REG3A expression by IL-17A in a dose-dependent manner (**Figure 4C**). Finally, we tested whether IL-17 induced REG3A expression through

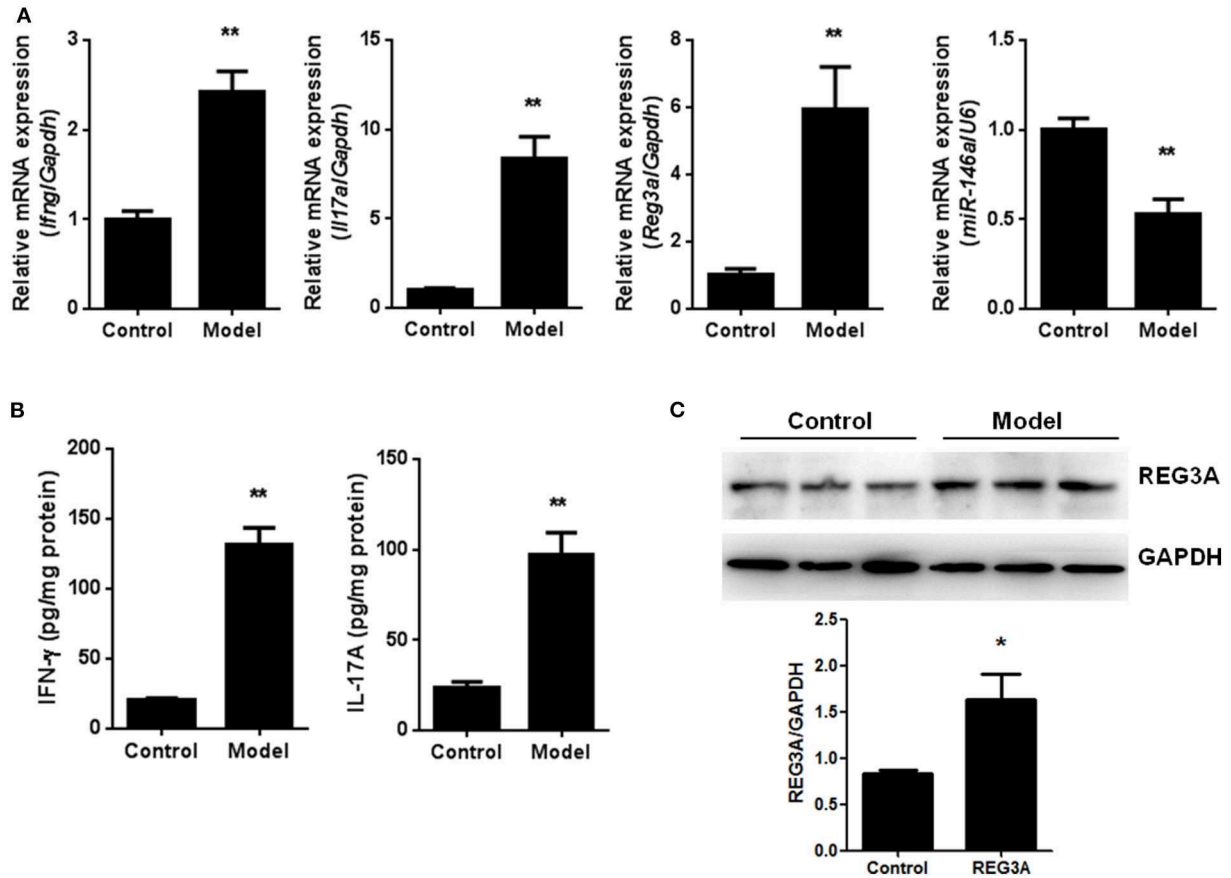

FIGURE 2 | The levels of regenerating islet-derived protein 3-alpha (REG3A) and miR-146a in an experimental autoimmune myositis (EAM) model. **(A)** The messenger RNA (mRNA) expression of interferon gamma (IFN-γ), interleukin (IL)-17A, REG3A, and miRNA-146a in muscle tissues were determined by real-time PCR. The relative mRNA expression was normalized using glyceraldehyde 3-phosphate dehydrogenase (GAPDH)/U6. ($n = 9$) **(B)**. The levels of IFN-γFand IL-17A in serum from the EAM mice were determined by ELISA assay ($n = 9$). **(C)** The protein levels of REG3A in muscle tissues were determined by Western blot ($n = 3$). GAPDH was used as the internal controls for Western blot analysis. Bands were quantified using ImageJ. Data are shown as means ± SEM. $^*p < 0.05$, $^{**}p < 0.01$ in comparison with the control group.

IL-17RA receptor. Western blot analysis showed that the IL-17A treatment significantly ($p < 0.05$) increased the expression of REG3A compared with the NC group. Treatment with IL-17A + NC siRNA significantly induced REG3A expression, while the inhibition of REG3A expression was observed upon treatment with IL-17A + IL-17RA siRNA (**Figure 4D**). Altogether, these results show that IL-17A can induce the expression of REG3A in macrophage through IL-17RA pathway.

miR-146a Regulates REG3A Expression in Macrophage

To understand the relationship between miR-146a and REG3A, the regulation of the expression of the latter by the former was established in monocyte-derived macrophages via transfection with NC miRNA, miR-146a mimics, or miR-146a inhibitor for 24 h. Consequently, the real-time PCR and Western blot results showed a significant ($p < 0.05$) increase in expression of REG3A in miR-146a inhibitor-treated group compared with the NC group. Conversely, transfection with miR-146a mimics resulted in the substantial ($p < 0.05$) downregulation of REG3A expression in relation to the NC group (**Figures 5A,B**). On the other hand, transfection with NC siRNA, REG3A siRNA, pcDNA3.1-NC, and pcDNA3.1-REG3A plasmids for 24 h could not alter the level of miR146a (**Figure 5C**). Notably, treatment of monocyte-derived macrophages with miR-146a mimics in the absence of IL-17A showed decreased mRNA and protein expression of REG3A in comparison with IL-17A treatment group (**Figures 5D,E**). These findings suggest that the increased expression of miR-146a might lead to the inhibition of REG3A expression irrespective of the presence of IL-17A.

miR-146a Inhibits Macrophage Migration via Suppression of REG3A Expression

To investigate whether suppression of REG3A by miR-146a has any effect on macrophage migration, we transfected monocyte-derived macrophages obtained from healthy donors with NC siRNA or REG3A siRNA in the absence or presence of miR-146a inhibitor for 24 h. Transwell assay showed that the number of

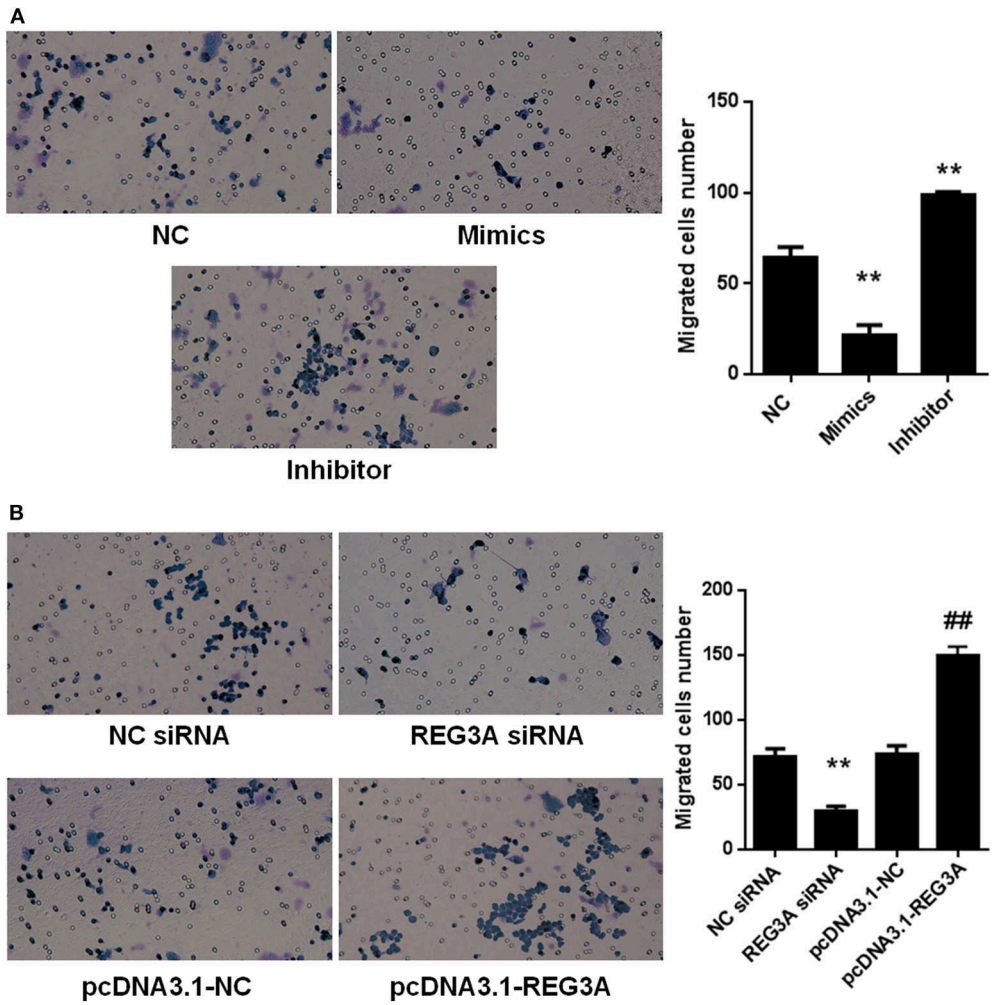

FIGURE 3 | The effects of miR-146a and regenerating islet-derived protein 3-alpha (REG3A) on macrophage migration. **(A)** Monocyte-derived macrophages from the PBMCs of the healthy donors ($n = 3$) were transfected with the negative control (NC) microRNA (miRNA) and miR-146a mimics, miR-146a inhibitors for 24 h. **(B)** Monocyte-derived macrophages from the peripheral blood mononuclear cells (PBMCs) of the healthy donors ($n = 3$) were transfected with the NC siRNA, REG3A siRNA, pcDNA3.1-NC, and pcDNA3.1-REG3A plasmids for 24 h. All treated cells (2×10^5) were suspended and added to the upper chamber of transwell. The medium containing 10% human serum was used as a chemoattractant in the lower chamber. After incubation for 24 h, the invaded cells into the lower chamber were stained with crystal violet. The migrated cells were counted, and photomicrographs were taken under an Olympus inverted microscope (IX71, Olympus, Japan). Data are shown as means ± SEM of three independent experiments. $^*p < 0.05$, $^{**}p < 0.01$ in comparison with the control group. $^{\#\#}p < 0.05$ in comparison with pcDNA3.1-NC group.

migrated cells significantly decreased ($p < 0.01$) after transfection with NC + REG3A siRNA compared with the NC + NC siRNA group. Contrarily, migratory cell numbers obviously increased upon treatment with inhibitor + NC siRNA ($p < 0.05$). However, treatment with inhibitor + REG3A siRNA resulted in the substantial decrease in migrated cell number compared with the inhibitor + NC siRNA and NC + NC siRNA group (**Figure 6A**), indicating that inhibition of miR-146a could not promote REG3A-silenced macrophage migration. In addition, we transfected monocyte-derived macrophages with the pcDNA3.1-NC or pcDNA3.1-REG3A plasmids in the absence or presence of miR-146a mimics for 24 h. As shown in **Figure 6B**, a substantial ($p < 0.01$) decreased number of migrated cells was observed in mimics + pcDNA3.1 group compared with the NC + pcDNA3.1 group. Consistent with results in **Figure 3B**, transfection of the macrophages with NC + pcDNA3.1-REG3A plasmids led to a significant increase ($p < 0.05$) in migrated cell numbers compared with the NC + pcDNA3.1 group (**Figure 6B**). However, treatment of the macrophage with mimics + pcDNA3.1-REG3A displayed a significant decrease in cell migration compared with the NC + pcDNA3.1-REG3A group, indicating that the overexpression of REG3A-induced macrophage migration was inhibited by miR-146a treatment. These data suggest that miR-146a may inhibit macrophage migration via suppression of REG3A expression.

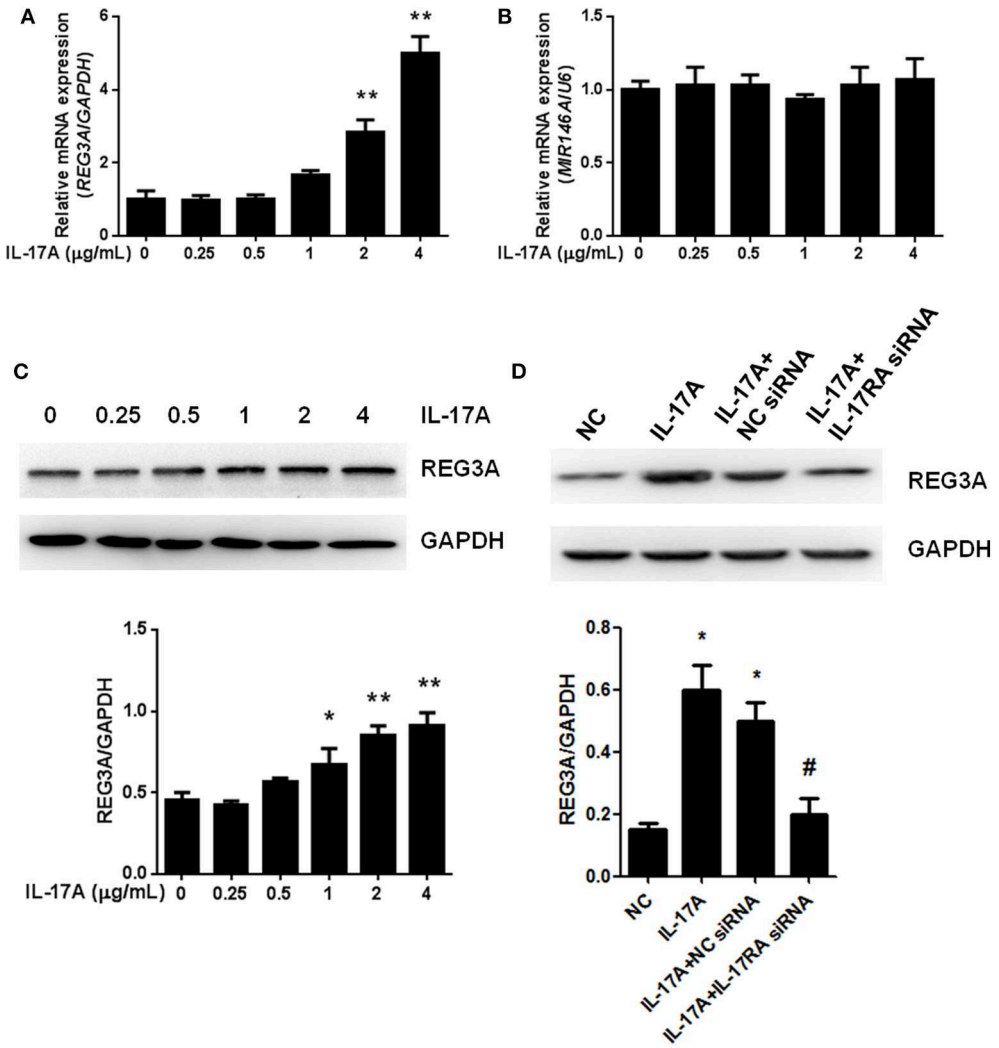

FIGURE 4 | Interleukin (IL)-17A induced regenerating islet-derived protein 3-alpha (REG3A) expression in macrophage. **(A)** Monocyte-derived macrophages from the peripheral blood mononuclear cells (PBMCs) of the healthy donors ($n = 3$) were treated with the different concentrations of IL-17A for 24 h. The messenger RNA (mRNA) expression of REG3A was determined by real-time PCR. Glyceraldehyde 3-phosphate dehydrogenase (GAPDH) was used as the internal controls. **(B)** Monocyte-derived macrophages from the PBMCs of the healthy donors ($n = 3$) were treated with the different concentrations of IL-17A for 24 h. The mRNA expression of miR-146a was determined by real-time PCR. U6 was used as the internal controls. **(C)** Monocyte-derived macrophages from the PBMCs of the healthy donors ($n = 3$) were treated with the different concentrations of IL-17A for 24 h. The protein levels of REG3A were determined by Western blot. GAPDH was used as the internal controls. **(D)** Monocyte-derived macrophages were transfected with the NC small-interfering RNA (siRNA) and IL-17RA siRNA in the absence or presence of IL-17A for 24 h. The protein levels of REG3A were determined by Western blot. GAPDH was used as the internal controls. Western blot bands were quantified using ImageJ and normalized to GAPDH. Data are shown as means ± SEM of three independent experiment. $^{*}p < 0.05$, $^{**}p < 0.01$ in comparison with the control group. $^{\#}p < 0.05$ in comparison with IL-17A + NC siRNA group.

DISCUSSION

This study was designed to test the possibility that miR-146a inhibits macrophage migration by downregulating REG3A expression, which might contribute to the development of PM/DM. The following observations emerged from the present study: the findings support the evidence that the mRNA expression levels are increased in IFN-γ, IL-17A, and REG3A, while miR-146a expression is reduced in PBMCs from PM/DM patients. An EAM murine model increased mRNA expression of REG3A as well as decreased miR-146a mRNA expression. miR-146a inhibited macrophage migration, while REG3A promoted PBMC-differentiated macrophage migration. IL-17A induced REG3A expression in macrophage in a dose-dependent manner *in vitro*. while miR146a inhibited expression of REG3A in macrophage. Notably, inhibition of macrophage migration by miR-146a was via the reduction in REG3A expression.

Most PM/DM patients experience muscle weakness, skin lesions, fatigue, and breathing difficulties, which majorly affect the quality of their daily life. An earlier study has observed

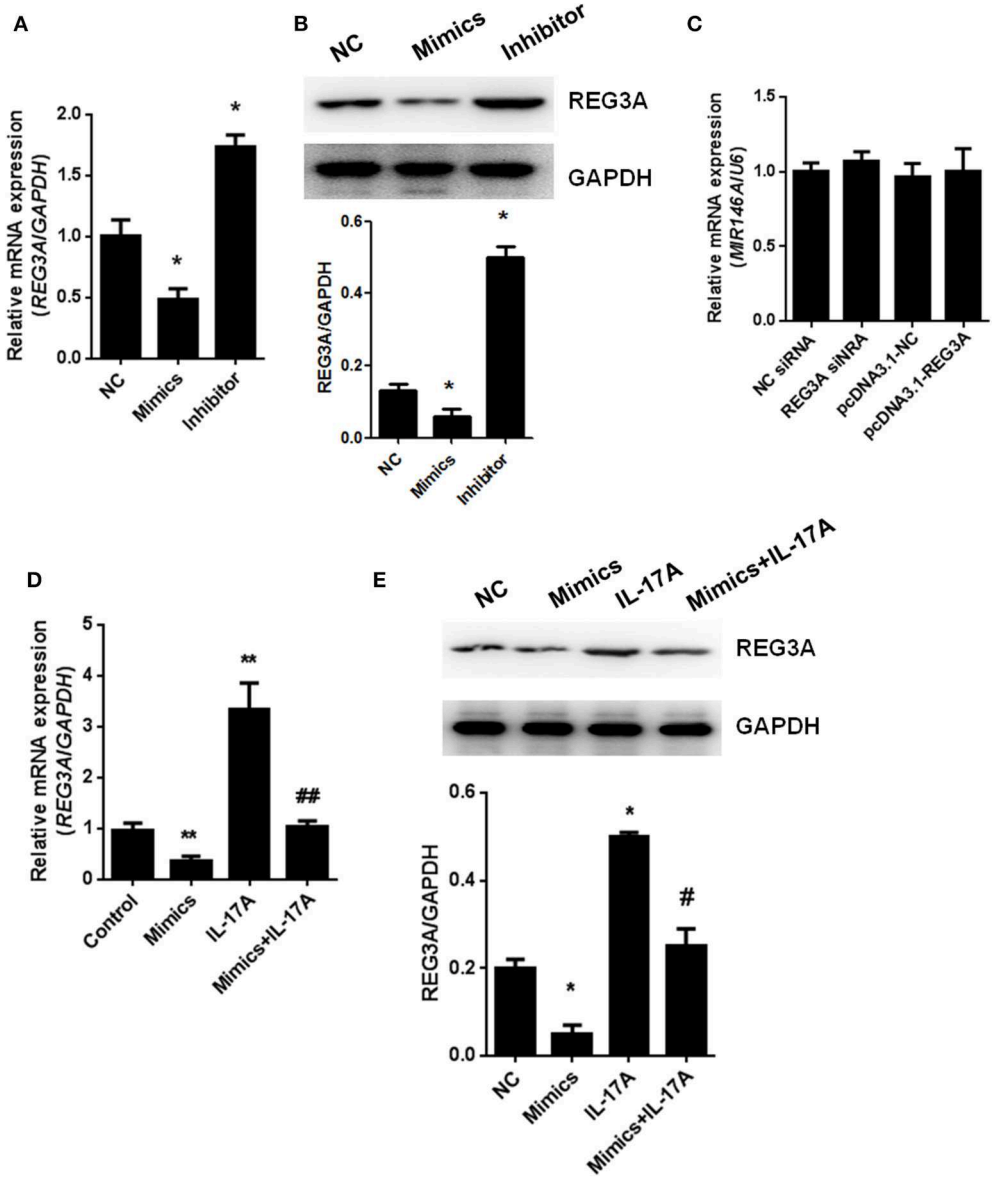

FIGURE 5 | miR-146a regulates regenerating islet-derived protein 3-alpha (REG3A) expression in macrophage. **(A,B)** Monocyte-derived macrophages from the peripheral blood mononuclear cells (PBMCs) of the healthy donors ($n = 3$) were transfected with negative control (NC) microRNA (miRNA), miR-146a mimics, or miR-146a inhibitor for 24 h. The messenger RNA (mRNA) and protein levels of REG3A were determined by real-time PCR and Western blot. Glyceraldehyde 3-phosphate dehydrogenase (GAPDH) was used as the internal controls. **(C)** The cells were transfected with NC small-interfering RNA (siRNA), REG3A siRNA, pcDNA3.1-NC, and pcDNA3.1-REG3A plasmids for 24 h. The mRNA levels of miR-146a were determined by real-time PCR. U6 was used as the internal controls. **(D,E)** The cells were transfected with NC miRNA or miR-146a mimics in the absence or presence of IL-17A for 24 h. The mRNA and protein levels of REG3A were determined by real-time PCR and Western blot. GAPDH was used as the internal controls. Data are shown as means ± SEM of three independent experiments. $^{*}p < 0.05$, $^{**}p < 0.01$ in comparison with the control group. $^{\#}p < 0.05$, $^{\#\#}p < 0.01$ in comparison with IL-17A treatment group.

lack of evidence-based theory to identify appropriate treatment options for PM/DM owing to unclear pathology underlying these conditions (7). However, as an idiopathic inflammatory myositis, it has been postulated that inflammation is the primarily underlying mechanism of the aforementioned symptoms of these diseases (27). Over the years, physician experience and empirical data have played key roles in selecting treatments for PM/DM, but difficulty in timely diagnosing PM/DM caused by similar symptoms of the disease to those of myositis has hampered this practice (28). Clinically, previous review showed that corticosteroids yielded only a modest benefit, while azathioprine and methotrexate were demonstrated to be effective in only 8 out of 35 trials (25, 26, 29, 30). Thus, understanding the detailed mechanism underlying the signs and symptoms of PM/DM will

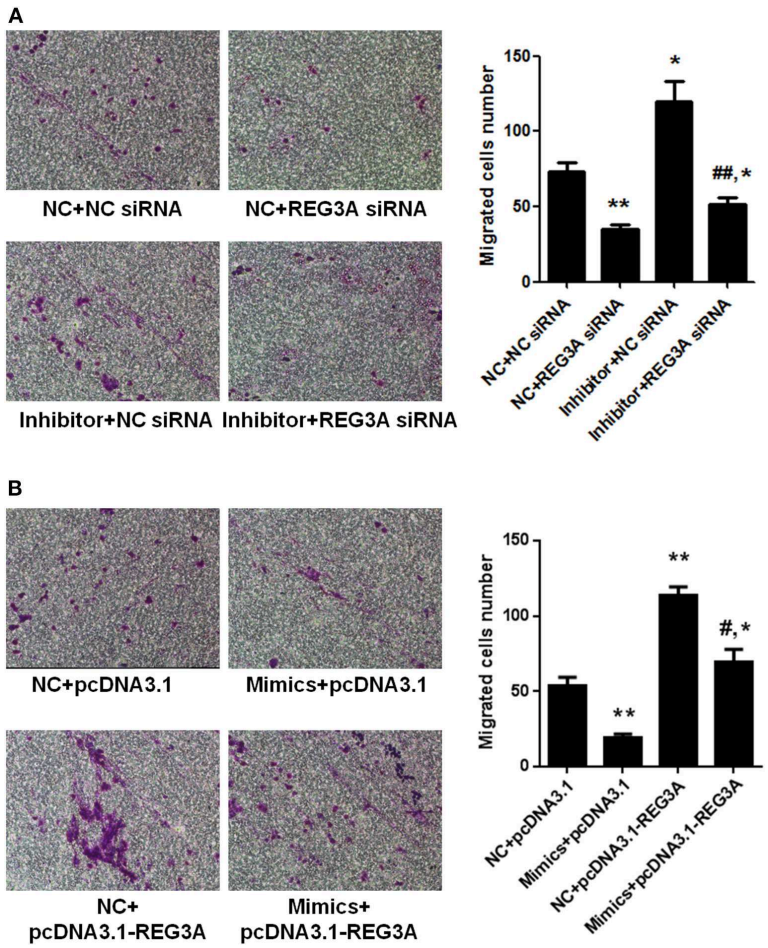

FIGURE 6 | miR-146a inhibited macrophage migration through suppression of regenerating islet-derived protein 3-alpha (REG3A) expression. **(A)** Monocyte-derived macrophages from the PBMCs of the healthy donors ($n = 3$) were transfected with the NC siRNA or REG3A siRNA in the absence or presence of miR-146a inhibitor for 24 h. **(B)** Monocyte-derived macrophages were transfected with the pcDNA3.1-NC or pcDNA3.1-REG3A plasmids in the absence or presence of miR-146a mimics for 24 h. All treated cells (2×10^5) were suspended and added to the upper chamber of transwell well. The medium containing 10% human serum was used as a chemoattractant in the lower chamber. After incubation for 24 h, the invaded cells into the lower chamber were stained with crystal violet. The migrated cells were counted, and photomicrographs were taken under an Olympus inverted microscope (IX71, Olympus, Japan). Data are shown as means ± SEM of three independent experiment. $^{*}p < 0.05$, $^{**}p < 0.01$ in comparison with NC + NC siRNA or NC + pcDNA3.1 group. $^{\#}p < 0.05$, $^{\#\#}p < 0.01$ in comparison with inhibitor + NC siRNA or NC + pcDNA3.1-REG3A group.

aid in the identification of pharmacological biomarkers and the development of effective therapeutic approaches for the cure of these diseases.

Emerging evidence suggests that miRNAs, particularly miR-146a, is reported to play a vital role in the pathological process of inflammatory diseases like PM/DM (31). Likewise, the activation of downstream IL-17A and IFN-γ signaling pathways has been observed to promote inflammation in several diseases (28, 32). Besides, it has been reported elsewhere that the antimicrobial protein REG3A expressed by keratinocytes is induced by IL-17 via activation of keratinocyte-encoded IL-17RA (23). These emerging pieces of evidence, therefore, support the concept that IL-17A, miR-146a, and REG3A are involved in the pathogenesis of inflammatory disease such as PM/DM. In the present study, it was shown that IL-17A and IFN-γ was highly expressed in PBMCs from PM/DM patients with higher mRNA expression of REG3A and lower miR-146a expression (**Figure 1**). This result corroborates earlier findings that higher levels of IL-17 and its proinflammatory counterparts IL-17RA are produced in PM/DM patients by T helper cells (33, 34). Consistently, the *in vivo* data obtained from mice model showed that autoimmune myositis resulted in increased mRNA expression of REG3A as well as decreased miR-146a expression (**Figure 2**). Thus, the associative effect of these biological molecules is relevant for the immune response-inflammatory processes in the PM/&DM pathophysiology. Inflammation is a necessary defensive reaction to several physiological conditions involving immune cells, blood vessels, and molecular mediators. Nevertheless, it contributes significantly to the pathogenesis of various diseases, including PM/DM (1). The primary pathological process in these disorders

occurs with inflammatory infiltrates in the muscles (5). Notably, macrophage-mediated inflammatory infiltrates are critical for a variety of human inflammatory muscle disorders as macrophages are key cell types involved in orchestration and modulation of the repair process (31, 35). In addition, unresolved inflammatory infiltration facilitated by macrophage may lead to persistent muscle tissue destruction by immune cells or collagen deposition (36). Therefore, therapeutic strategies targeting inflammatory response in PM/DM may be a promising approach to manage these conditions. A previous report has established the regulation of inflammation infiltration in PM/DM by macrophages via targeting tumor necrosis factor receptor-associated factor 6 and affecting IL-17/intercellular adhesion molecule 1 pathway (11). However, the mechanism underlying inflammatory macrophage infiltration in muscle tissue restoration among PM/DM patients is incompletely understood. Earlier studies have shown that IL-17 has strong influence on the pathogenesis of several other autoimmune diseases, such as rheumatoid arthritis, multiple sclerosis, and psoriasis (37–39). In addition, in muscle tissue, IL-17 coupled with other proinflammatory cytokines, such as IFN-γ produced by monocytes and innate immune responses, acts to potentiate immune responses, which might lead to destruction of muscle tissues (40). Consequently, the increased expression of REG3A induced by IL-17A (**Figure 4**) might exacerbate the PM/DM condition, thereby potentially heightening immune responses. On the other hand, REG3A is established to be highly expressed in skin cells in concert with IL-17 during psoriasis and wound healing (23), which might play a critical role in muscle tissue healing in PM/DM. Thus, future researches can explore the development of IL-17A/REG3A targeted antibody therapies and their prospect in treating PM/DM. Besides, since REG3A is reported to promote wound healing in skin injuries (41), its role in improving muscular cell growth and tissue restoration in PM/DM patients will be given the needed attention in our subsequent investigations.

Actually, miR-146a expression levels were observed to be markedly lower in either patients and mice models than healthy subjects or the control group, respectively (**Figures 1**, **2**). In addition, experimental treatment with mimics or inhibitors of miR-146a impacted on REG3A expression levels as well as macrophage migratory capacity (**Figures 3**, **5**, **6**). Based on these and other findings, we hypothesized that miR-146a and IL-17A regulate the expression of REG3A in PM/DM patients. Although earlier report has recognized the significance of miR-146a in PM/DM (38, 42), its relationship with REG3A has not been established yet. On the account of a previous investigation, which has suggested the abnormal expression of miR-146a and its negative regulatory role in inflammation (43), this study unearths possible mechanism underlying macrophage-mediated inflammatory infiltrates via REG3A (**Figure 3**). Specifically, increased miR-146a expression was observed to inhibit REG3A expression (**Figure 5**). Suppression of REG3A expression by miR-146a resulted in the inhibition of macrophage migratory capacity (**Figure 6**). In the present report, IL-17A and miR-146a inhibitors had positive influence on REG3A expression coupled with macrophage migration, which were counteracted via transfection with REG3A siRNA. Altogether, these findings suggest the relationship between miR-146a and REG3A as well as their involvement in PM/DM pathophysiology. MiR-146a is well established to inhibit cell migration and mediate suppression of inflammatory response in human adipocytes (44, 45). Conversely, REGs are reported to be highly expressed in diseases such as hepatic injury and inflammatory bowel disease-related colonic inflammation (22, 46). Preliminary, this report has evidenced that miR-146a and IL-17A can regulate the pathogenesis of PM/DM via targeting of REG3A, which, to the best of our knowledge, has not been established in other reports. However, the interplay between miR-146a, REG3A, and its related pathways such as defensins and innate immune systems in the pathogenesis of PM/DM will be investigated comprehensively in future studies.

In summary, the present study for the first time proves that reduced miR-146a in PM/DM promotes REG3A expression and inflammatory macrophage migration. We believe that this preliminary evidence will contribute to the understanding of the mechanism underlying PM/DM pathogenesis, which can possibly facilitate diagnosis of the disease. Nonetheless, future investigations are needed to further elucidate other REGs and targeting proteins involve in PM/DM pathogenesis to develop appropriate treatment approaches.

DATA AVAILABILITY STATEMENT

The raw data supporting the conclusions of this article will be made available by the authors, without undue reservation, to any qualified researcher.

ETHICS STATEMENT

The experimental protocol was approved by the Ethics Committee of The Affiliated Wuxi No. 2 People's Hospital of Nanjing Medical University. All patients provided written informed consent for the use of their tissues and data prior to the study. All animals received adequate care in compliance with laboratory practice guidelines and the experimental protocol was approved by the Ethics Committee of The Affiliated Wuxi No. 2 People's Hospital of Nanjing Medical University.

AUTHOR CONTRIBUTIONS

All authors listed have made a substantial, direct and intellectual contribution to the work, and approved it for publication.

FUNDING

This work was supported by grants from National Natural Science Foundation of China (No. 81601406), Natural Science Foundation of Jiangsu Province (No. BK20171147), The Science and Technology Projects of Wuxi City (Nos. WX18IIAN022, Z201804, and Q201701), The Key Technologies of Prevention and Control for Infectious Diseases of Suzhou (No. GWZX201604), and Jiangsu Youth Medical Talents Project (No. QNRC2016214).

REFERENCES

1. Mammen AL. Dermatomyositis and polymyositis: clinical presentation, autoantibodies, and pathogenesis. *Ann N Y Acad Sci*. (2010). 1184:134–53. doi: 10.1111/j.1749-6632.2009.05119.x
2. Danieli MG, Gambini S, Pettinari L, Logullo F, Veronesi G, Gabrielli A. Impact of treatment on survival in polymyositis and dermatomyositis. a single-centre long-term follow-up study. *Autoimmun Rev*. (2014). 13:1048–54. doi: 10.1016/j.autrev.2014.08.023
3. Marvi U, Chung L, Fiorentino DF. Clinical presentation and evaluation of dermatomyositis. *Indian J Dermatol*. (2012). 57:375–81. doi: 10.4103/0019-5154.100486
4. Rostasy KM, Piepkorn M, Goebel HH, Menck S, Hanefeld F, Schulz-Schaeffer WJ. Monocyte/macrophage differentiation in dermatomyositis and polymyositis. *Muscle Nerve*. (2004) 30:225–30. doi: 10.1002/mus.20088
5. Hilton-Jones D. Diagnosis and treatment of inflammatory muscle diseases. *J Neurol Neurosurg Psychiatry*. (2003). 74(Suppl. 2):ii25–31. doi: 10.1136/jnnp.74.suppl_2.ii25
6. Vermaak E, Shaddick G, McHugh NJ. Mortality in polymyositis and dermatomyositis: a single centre study. *Arthrit Rheum*. (2013) 65:S878.
7. Dalakas MC. Immunotherapy of myositis: issues, concerns and future prospects. *Nat Rev Rheumatol*. (2010) 6:129–37. doi: 10.1038/nrrheum.2010.2
8. Hirai T, Ikeda K, Tsushima H, Fujishiro M, Hayakawa K, Yoshida Y, et al. Circulating plasma microRNA profiling in patients with polymyositis/dermatomyositis before and after treatment: miRNA may be associated with polymyositis/dermatomyositis. *Inflamm Regen*. (2018) 38:1. doi: 10.1186/s41232-017-0058-1
9. Yan W, Chen C, Chen H. Estrogen downregulates miR-21 expression and induces inflammatory infiltration of macrophages in polymyositis: role of CXCL10. *Mol Neurobiol*. (2017) 54:1631–41. doi: 10.1007/s12035-016-9769-6
10. Liu Y, Gao Y, Yang J, Shi C, Wang Y, Xu Y. MicroRNA-381 reduces inflammation and infiltration of macrophages in polymyositis via downregulating HMGB1. *Int J Oncol*. (2018). 53:1332–42. doi: 10.3892/ijo.2018.4463
11. Yin Y, Li F, Shi J, Li S, Cai J, Jiang Y. MiR-146a regulates inflammatory infiltration by macrophages in polymyositis/dermatomyositis by targeting TRAF6 and affecting IL-17/ICAM-1 pathway. *Cell Physiol Biochem*. (2016). 40:486–98. doi: 10.1159/000452563
12. Zheng CZ, Shu YB, Luo YL, Luo J. The role of miR-146a in modulating TRAF6-induced inflammation during lupus nephritis. *Eur Rev Med Pharmacol Sci*. (2017). 21:1041–8.
13. Sharma N, Verma R, Kumawat KL, Basu A, Singh SK. miR-146a suppresses cellular immune response during Japanese encephalitis virus JaOArS982 strain infection in human microglial cells. *J Neuroinflam*. (2015). 12:30. doi: 10.1186/s12974-015-0249-0
14. Stickel N, Prinz G, Pfeifer D, Hasselblatt P, Schmitt-Graeff A, Follo M, et al. MiR-146a regulates the TRAF6/TNF-axis in donor T cells during GVHD. *Blood*. (2014) 124:2586–95. doi: 10.1182/blood-2014-04-569046
15. Li S, Yue Y, Xu W, Xiong S. MicroRNA-146a represses mycobacteria-induced inflammatory response and facilitates bacterial replication via targeting IRAK-1 and TRAF-6. *PLoS ONE*. (2013). 8:e81438. doi: 10.1371/journal.pone.0081438
16. Bhatt K, Lanting LL, Jia Y, Yadav S, Reddy MA, Magilnick N, et al. Anti-inflammatory role of MicroRNA-146a in the pathogenesis of diabetic nephropathy. *J Am Soc Nephrol*. (2016). 27:2277–88. doi: 10.1681/ASN.2015010111
17. Peng QL, Zhang YL, Shu XM, Yang HB, Zhang L, Chen F, et al. Elevated serum levels of soluble CD163 in polymyositis and dermatomyositis: associated with macrophage infiltration in muscle tissue. *J Rheumatol*. (2015) 42:979–87. doi: 10.3899/jrheum.141307
18. Li D, Duan M, Feng Y, Geng L, Li X, Zhang W. MiR-146a modulates macrophage polarization in systemic juvenile idiopathic arthritis by targeting INHBA. *Mol Immunol*. (2016) 77:205–12. doi: 10.1016/j.molimm.2016.08.007
19. Brandl K, Plitas G, Mihu CN, Ubeda C, Jia T, Fleisher M, et al. Vancomycin-resistant enterococci exploit antibiotic-induced innate immune deficits. *Nature*. (2008) 455:804–7. doi: 10.1038/nature07250
20. Vaishnava S, Yamamoto M, Severson KM, Ruhn KA, Yu X, Koren O, et al. The antibacterial lectin RegIIIgamma promotes the spatial segregation of microbiota and host in the intestine. *Science*. (2011) 334:255–8. doi: 10.1126/science.1209791
21. Pull SL, Doherty JM, Mills JC, Gordon JI, Stappenbeck TS. Activated macrophages are an adaptive element of the colonic epithelial progenitor niche necessary for regenerative responses to injury. *Proc Natl Acad Sci USA*. (2005) 102:99–104. doi: 10.1073/pnas.0405979102
22. Lieu HT, Batteux F, Simon MT, Cortes A, Nicco C, Zavala F, et al. HIP/PAP accelerates liver regeneration and protects against acetaminophen injury in mice. *Hepatology*. (2005) 42:618–26. doi: 10.1002/hep.20845
23. Lai Y, Li D, Li C, Muehleisen B, Radek KA, Park HJ, et al. The antimicrobial protein REG3Ah regulates keratinocyte proliferation and differentiation after skin injury. *Immunity*. (2012) 37:74–84. doi: 10.1016/j.immuni.2012.04.010
24. Wu Y, Quan Y, Liu Y, Liu K, Li H, Jiang Z, et al. Hyperglycaemia inhibits REG3A expression to exacerbate TLR3-mediated skin inflammation in diabetes. *Nat Commun*. (2016) 7:13393. doi: 10.1038/ncomms13393
25. Emery A, Rutgers M. European collaboration in research into rare diseases: experience of the European neuromuscular centre. *Clin Med*. (2001) 1:200–2. doi: 10.7861/clinmedicine.1-3-200
26. Kang J, Zhang HY, Feng GD, Feng DY, Jia HG. Development of an improved animal model of experimental autoimmune myositis. *Int J Clin Exp Pathol*. (2015) 8:14457–64.
27. Choy EH, Isenberg DA. Treatment of dermatomyositis and polymyositis. *Rheumatology*. (2002) 41:7–13. doi: 10.1093/rheumatology/41.1.7
28. Milisenda JC, Selva-O'Callaghan A, Grau JM. The diagnosis and classification of polymyositis. *J Autoimmun*. (2014) 48–49:118–21. doi: 10.1016/j.jaut.2014.01.025
29. Joffe MM, Love LA, Leff RL, Fraser DD, Targoff IN, Hicks JE, et al. Drug therapy of the idiopathic inflammatory myopathies: predictors of response to prednisone, azathioprine, and methotrexate and a comparison of their efficacy. *Am J Med*. (1993) 94:379–87. doi: 10.1016/0002-9343(93)90148-I
30. Leff RL, Miller FW, Hicks J, Fraser DD, Plotz PH. The treatment of inclusion body myositis: a retrospective review and a randomized, prospective trial of immunosuppressive therapy. *Medicine*. (1993). 72:225–35. doi: 10.1097/00005792-199307000-00002
31. Li J, Wan Y, Guo Q, Zou L, Zhang J, Fang Y, et al. Altered microRNA expression profile with miR-146a upregulation in CD4+ T cells from patients with rheumatoid arthritis. *Arthritis Res Ther*. (2010) 12:R81. doi: 10.1186/ar3006
32. Li L, Huang L, Vergis AL, Ye H, Bajwa A, Narayan V, et al. IL-17 produced by neutrophils regulates IFN-gamma-mediated neutrophil migration in mouse kidney ischemia-reperfusion injury. *J Clin Invest*. (2010). 120:331–42. doi: 10.1172/JCI38702
33. Mielnik P, Chwalinska-Sadowska H, Wiesik-Szewczyk E, Maslinski W, Olesinska M. Serum concentration of interleukin 15, interleukin 2 receptor and TNF receptor in patients with polymyositis and dermatomyositis: correlation to disease activity. *Rheumatol Int*. (2012) 32:639–43. doi: 10.1007/s00296-010-1692-y
34. Zong M, Loell I, Lindroos E, Nader GA, Alexanderson H, Hallengren CS, et al. Effects of immunosuppressive treatment on interleukin-15 and interleukin-15 receptor alpha expression in muscle tissue of patients with polymyositis or dermatomyositis. *Ann Rheum Dis*. (2012) 71:1055–63. doi: 10.1136/annrheumdis-2011-200495
35. Rybalko V, Hsieh PL, Merscham-Banda M, Suggs LJ, Farrar RP. The development of macrophage-mediated cell therapy to improve skeletal muscle function after injury. *PLoS ONE*. (2015) 10:e0145550. doi: 10.1371/journal.pone.0145550
36. Nathan C. Points of control in inflammation. *Nature*. (2002) 420:846–52. doi: 10.1038/nature01320
37. Kenna TJ, Brown MA. The role of IL-17-secreting mast cells in inflammatory joint disease. *Nat Rev Rheumatol*. (2013) 9:375–9. doi: 10.1038/nrrheum.2012.205
38. Miossec P. Interleukin-17 in fashion, at last: ten years after its description, its cellular source has been identified. *Arthritis Rheum*. (2007) 56:2111–5. doi: 10.1002/art.22733
39. Baeten DL, Kuchroo VK. How cytokine networks fuel inflammation: Interleukin-17 and a tale of two autoimmune diseases. *Nat Med*. (2013) 19:824–5. doi: 10.1038/nm.3268

40. Tournadre A, Miossec P. Interleukin-17 in inflammatory myopathies. *Curr Rheumatol Rep*. (2012) 14:252–6. doi: 10.1007/s11926-012-0242-x
41. Jiang Z, Liu Y, Li C, Chang L, Wang W, Wang Z, et al. IL-36gamma Induced by the TLR3-SLUG-VDR axis promotes wound healing via REG3A. *J Invest Dermatol*. (2017) 137:2620–9. doi: 10.1016/j.jid.2017.07.820
42. Okada Y, Jinnin M, Makino T, Kajihara I, Makino K, Honda N, et al. MIRSNP rs2910164 of miR-146a is associated with the muscle involvement in polymyositis/dermatomyositis. *Int J Dermatol*. (2014) 53:300–4. doi: 10.1111/j.1365-4632.2012.05739.x
43. Ammari M, Presumey J, Ponsolles C, Roussignol G, Roubert C, Escriou V, et al. Delivery of miR-146a to Ly6C (high) monocytes inhibits pathogenic bone erosion in inflammatory arthritis. *Theranostics*. (2018) 8:5972–85. doi: 10.7150/thno.29313
44. Chen G, Umelo IA, Lv S, Teugels E, Fostier K, Kronenberger P, et al. miR-146a inhibits cell growth, cell migration and induces apoptosis in non-small cell lung cancer cells. *PLoS ONE*. (2013). 8:e60317. doi: 10.1371/journal.pone.0060317
45. Roos J, Enlund E, Funcke JB, Tews D, Holzmann K, Debatin KM, et al. miR-146a-mediated suppression of the inflammatory response in human adipocytes. *Sci Rep*. (2016) 6:38339. doi: 10.1038/srep38339
46. van Beelen Granlund A, Ostvik AE, Brenna O, Torp SH, Gustafsson BI, Sandvik AK. REG gene expression in inflamed and healthy colon mucosa explored by in situ hybridisation. *Cell Tissue Res*. (2013) 352:639–46. doi: 10.1007/s00441-013-1592-z

Conflict of Interest: The authors declare that the research was conducted in the absence of any commercial or financial relationships that could be construed as a potential conflict of interest.

Copyright © 2020 Jiang, Huang, Liu, Xu, Gong, Chen, Hu, Han and Gao. This is an open-access article distributed under the terms of the Creative Commons Attribution License (CC BY). The use, distribution or reproduction in other forums is permitted, provided the original author(s) and the copyright owner(s) are credited and that the original publication in this journal is cited, in accordance with accepted academic practice. No use, distribution or reproduction is permitted which does not comply with these terms.

frontiers in Immunology

ORIGINAL RESEARCH
published: 28 April 2020
doi: 10.3389/fimmu.2020.00662

Identification of Specific Joint-Inflammatogenic Cell-Free DNA Molecules From Synovial Fluids of Patients With Rheumatoid Arthritis

Cong Dong[1], Yu Liu[2], Chengxin Sun[1], Huiyi Liang[1], Lie Dai[3], Jun Shen[3]*, Song Wei[4], Shixin Guo[2], Kam W. Leong[5], Yongming Chen[1], Lai Wei[2]* and Lixin Liu[1]**

[1] Key Laboratory for Polymeric Composite and Functional Materials of Ministry of Education, Center for Functional Biomaterials, School of Materials Science and Engineering, Sun Yat-sen University, Guangzhou, China, [2] State Key Laboratory of Ophthalmology, Zhongshan Ophthalmic Center, Sun Yat-sen University, Guangzhou, China, [3] Sun Yat-sen Memorial Hospital, Sun Yat-sen University, Guangzhou, China, [4] Department of Rheumatology, General Hospital of Guangzhou Military Command of PLA, Guangzhou, China, [5] Department of Biomedical Engineering, Columbia University, New York, NY, United States

OPEN ACCESS

Edited by:
Erminia Mariani,
University of Bologna, Italy

Reviewed by:
Erika H. Noss,
University of Washington, United States
Laura Mandik-Nayak,
Lankenau Institute for Medical Research, United States

***Correspondence:**
Lie Dai
liedai2004@163.com
Jun Shen
shenjun@mail.sysu.edu.cn
Lai Wei
weil9@mail.sysu.edu.cn
Lixin Liu
liulixin@mail.sysu.edu.cn

Specialty section:
This article was submitted to Autoimmune and Autoinflammatory Disorders, a section of the journal Frontiers in Immunology

Received: 15 January 2020
Accepted: 23 March 2020
Published: 28 April 2020

Citation:
Dong C, Liu Y, Sun C, Liang H, Dai L, Shen J, Wei S, Guo S, Leong KW, Chen Y, Wei L and Liu L (2020) Identification of Specific Joint-Inflammatogenic Cell-Free DNA Molecules From Synovial Fluids of Patients With Rheumatoid Arthritis. Front. Immunol. 11:662. doi: 10.3389/fimmu.2020.00662

Elevated cell-free DNA (cfDNA) levels in the plasma and synovial fluid of rheumatoid arthritis (RA) patients are proposed to be pathologically relevant. However, direct evidence to support this perception is lacking, and molecular feature of the cfDNA molecules with assumed pathological function is not well characterized. Here, we confirm remarkably increased levels of total synovial fluid and plasma cfDNAs in a large cohort of patients with rheumatoid arthritis compared to the counterparts in osteoarthritis, and demonstrate the potent inflammatogenic effects of RA synovial fluid cfDNA on both human monocyte cell line and primary cells related to RA. Massively parallel sequencing identifies distinct molecular pattern of cfDNA in RA, as characterized by enriching CpG-motif containing sequences. Importantly, these identified CpG-motif-rich sequences are hypomethylated in RA patients and induce severe inflammatory responses both *in vitro* and *in vivo*. Our data demonstrate the pathological role of global and specific cfDNA molecules in RA, thereby identifying novel therapeutic target candidate and potential biomarker for RA.

Keywords: autoimmunity, cell-free DNA, CpG-motif, inflammation, rheumatoid arthritis

INTRODUCTION

In pathological conditions, including cancers, inflammatory disorders and severe trauma (1–3), abnormal amounts of cfDNA are released into body fluids following exorbitant apoptosis, necrosis, NETosis, and pyroptosis (4). Some of previous studies of autoimmune diseases, especially in rheumatoid arthritis (RA) and systemic lupus erythematosus (SLE), have shown that increased level of cfDNA in plasma correlates with disease progression, and thus, cfDNA has been used as a marker to monitor therapeutic responses to certain autoimmune diseases (5, 6).

In addition to the application as a biomarker, prior studies have attempted to determine if cfDNA plays a role in inflammation associated with autoimmune diseases (7). Initially, it was shown that vertebrate cfDNA failed to induce an inflammatory response in autologous plasmacytoid dendritic cells, which are sensitive to bacterial nucleic acids. As a result, it was thought that because

cfDNAs are products of self-DNA, the host immune system has tolerance to this self-component. However, the development of improved technology led to the finding that cfDNA, especially derived from mitochondrial DNA, has a high degree of oxidative damage and is similar to bacterial DNA, and can bind with LL-37, HMGB, auto-Ig, and other proteins to form immunocomplexes. These immunocomplexes deliver various cfDNAs into cells, which are then recognized by pattern recognition receptors (PRRs), such as TLR-9 or STING, leading to downstream signaling cascade amplification and cytokine overexpression. Consequently, cfDNA contributes to the etiology of psoriatic arthritis, atherosclerosis, and SLE (8–10).

Like SLE, accumulating evidence suggests that cfDNA might play an important role in the pathogenesis of rheumatoid arthritis (RA). For example, intra-articular injection of CpG ODNs, the unmethylated CpG oligodeoxynucleotides prevalent in bacteria, triggers reactive arthritis in mice (11–13). Further, DNase knock-out mice spontaneously develop polyarthritis with symptoms resembling that of human RA (6, 14). Activation of TLR-9 by chromatin combined with IgG2a can stimulate B cells to produce autoantibodies, known as rheumatoid factors (15). Moreover, it is known that the concentration of cfDNA in plasma and synovial fluid (SF) of RA patients is significantly elevated (16–18). However, the direct evidence that endorses the pathological role of cfDNA in RA is not established, and the molecular nature of RA cfDNA potentially implicated in onset and development of RA is unknown.

In this study, we analyzed cfDNA isolated from the synovial fluid (SFcfDNA) of 113 RA and osteoarthritis (OA) patients via massively parallel sequencing and other *in vitro* and *in vivo* approaches. Our findings confirm the inflammatogenic property of cfDNA from RA patients, and the molecular characteristics of SFcfDNA identified in this study provide novel insights into the role of cfDNA in RA.

MATERIALS AND METHODS

Study Design

Plasma and synovial fluid were collected from 163 individuals, including 50 healthy donors (HDs) for plasma, 33 OA subjects for synovial fluid, 80 rheumatoid arthritis patients for plasma and synovial fluid, and the detailed information of the study population is illustrated in **Supplementary Table 1**. Primary synovial fluid mononuclear immune cells (SFMICs) and fibroblast-like synoviocytes (FLSs) were collected from RA synovial fluid and synovium tissue, respectively, which were stimulated with total cfDNA purified from the SF of the same patient. Intracellular TNF-α staining and cytokine bead assay (CBA)/ELISA were carried out for detection of cytokine expression. Then, the cfDNA size distribution frequency and the discrepancy sequence feature between RA and OA were analyzed. Specific CpG-motif-rich (CMR) sequences and CpG-motif-free (CMF) sequences were acquired by virtue of bioinformatics technique, which would be described in detail in the method of sequencing and analysis. Finally, pro-inflammation capability of high-frequency sequences was tested *in vitro* and *in vivo*.

Participants

All the plasma, synovial fluid, and synovium samples of RA patients were collected from Sun Yat-sen Memorial Hospital, General Hospital of Guangzhou Military Command of PLA after informed consent. RA patients who were selected for the study were confirmed with ACR 2010 standards, without bacterial and virus infection. SF of OA control was collected from patients who underwent arthroplasty surgeries in the First Affiliated Hospital, Sun Yat-sen University. Healthy plasma samples were obtained from volunteer donors. The average age of RA (n = 80), OA patients (33) or HDs (n = 50) was 56 ± 3, 58 ± 4, 48 ± 5, respectively. For the sequencing investigation, the subjects were female with the average age 48.5 (±12.7) years in the RA group and 51.0 (±6.2) years in the OA group. The detailed information of patients used in each experiment are displayed in **Supplementary Table 1**. Studies were approved by the ethics committee of the General Hospital of Guangzhou Military Command PLA, Sun Yat-sen Memorial Hospital and the First Affiliated Hospital of Sun Yat-sen University, respectively. The recruited patients gave written consent according to a protocol approved by the above Committees.

cfDNA Purification and Quantification

After synovial fluid was extracted from joints of patients, an equal volume of PBS was added to dilute the samples, followed by adding hyaluronidase (1 mg/ml, pH = 7.4) and incubated at 37°C for 0.5 h. Then Ficoll-Paque was used for mononuclear cell sorting, and supernatant was collected for cfDNA purification. cfDNA was purified with circulating cfDNA purification kit following the instructions of the manufacturer. The purified cfDNA concentration was quantified via Picogreen$^{@}$ dye.

Intracellular TNF-α Staining Assay

After diluting SF with PBS, the samples were incubated with hyaluronidase (1 mg/ml, pH = 7.4) at 37°C for 0.5 h. Then the samples were passed through a 70-μm filter, and the SFMICs were collected with Ficoll-Paque. Isolated SFMICs were plated in 24-well plates at a density of 5×10^5 cells/ml with RIPM-1640 (Gibco) completed medium and transfected with 500 ng of cfDNA or CpG 2006 for 24 h via Lipofectamine 2000 (Lipo2000; Invitrogen) following instructions of the manufacturer. The wells with equal volume of Lipo2000 were used as background controls. Monensin solution (1:1,000; BioLegend) was added to inhibit the cytokine secretion before sample staining. After the cells were blocked with Human TruStain FcX^{TM} kit (1:50; BioLegend), they were stained with AF700 Human CD45 (1:100; BioLegend) (**Supplementary Table 2**) for 30 min at room temperature. Viability was determined by Zombie Yellow^{TM} Fixable Viability kit (1:1,000; BioLegend). Cells were washed twice with PBS, fixed and permeabilized with Transcription Factor Fix/Perm Buffer (eBioscience). After the cells were washed by PBS with 2% FBS, they were stained with BV421 Human TNF-α (1:100; BioLegend) (**Supplementary Table 2**) for 30 min. Then the samples were analyzed by Attune CytoFlex analyzer (ThermoFisher). For TNF-α staining of THP-1 cell line, the same procedure was performed, except for CD45 staining. Briefly, a percentage of TNF-α-expressing cells was analyzed through flow

cytometry. Gating strategy was based on, first, viable cells gating via Live/Dead dye, followed by $CD45^+$ gating, then singlet cells of $CD45^+$ cells were gated according to FSC-A/FCS-H properties. Finally TNF-α positive cells were determined.

Cytokines Expression

FLS Isolation

Synovial samples were acquired from discarded arthroplasty tissue. After careful dissection, mincing, and digestion with Collagenase I (1 mg/ml; Sigma-Aldrich) in RIPM medium (Gibco) for 30 min with agitation, cells were passed through a 70-μm cell strainer. Then the cells were subjected to red cell lysis and were cultured with DMEM high-glucose completed medium. Three- to nine-passage primary FLS was used for functional assay. Primary FLS validation: Primary FLS used for the study was measured by flow cytometry. The percentage of double positive ratio of PE Anti-Human CD55 (1:100; BioLegend) and PerCP-Cy5.5 Anti-Human CD90 (Thy1; 1:100; BioLegend) (**Supplementary Table 2**) was more than 98%. For stimulation assay, 500 ng of SFcfDNA was transfected to FLS at a density of 5×10^3 cells per 300 μl in 48-well plates via Lipo2000 following manufacturer's instructions, and an equal volume of Lipo2000 (1 μl) was added into the control wells. After 4 h, the medium was changed, and after 24 h, the supernatant was collected for cytokine evaluation with human ELISA kit Ready-SET-Go! (eBioscience). The concentration of cfDNA for FLS stimulation assay without transfection was 15 μg/ml. For SFMIC stimulation assay, 1×10^5 cells were seeded into 96-well plates, and 500 ng of SFcfDNA was transfected to cells with Lipo2000. After 24 h, the supernatant was collected for cytokine evaluation with ELISA kit. High-frequency sequence PCR purification and amplification were obtained with Advantage® GC2 PCR kit (Takara Biomed), PrimeSTAR® Max (Takara Biomed) on Mastercycler nexus X2 PCR platform (Eppendorf), QIAquick Gel Extraction kit (Qiagen), and QIAquick PCR Purification kit (Qiagen). For CMRs and CMFs stimulation to THP-1 cell lines, the same process was performed as that of SFMIC.

Illumina Sequencing

Cell-free DNA was extracted from SF samples using the MasterPure Complete DNA and RNA Purification kit (Epicenter) according to the instructions of the manufacturer. Next, the sequencing library was prepared using the ND604-VAHTS Universal DNA Library Prep kit (Vazyme) based on the protocol. Then the DNA library was sequenced on Illumina HighSeq 2500 sequencer, and the initial image processing was done by CASAVA (v1.8.2, Illumina).

Sequencing Data Analysis

Sequencing reads were cleaned using Trimmomatic (version 0.36) (19) in order to (i) remove the primers and sequencing adapters; (ii) trim nucleotides with the average quality per base drops below 15 in a four-base-wide sliding window from the 3′ end; and (iii) drop read below the 30 bases long. Cleaned reads were subsequently aligned to the human genome (hg19) using BWA (version 0.7.15) (20). The reads that were uniquely mapped to the human genome were retained for analysis. To compare the genomic distribution of SFcfDNA between samples, two types of fragments were investigated and a normalized sequence density for each fragment, which is similar to the RPKM (Reads Per Kilobase Million) in RNA-seq analysis, was calculated as follows:

$$\text{Sequence density} = \frac{\text{number of reads mapped to a CpG sequence}}{\text{Sample} - \text{specific normalized factor} \times \text{CpG length (50 kilobase)}}$$

The first type of fragments was chromosome bins with 400-bp width, which provided genomic distribution of SFcfDNA molecules, and the other was the CpG islands across the human genome, which is epigenetically relevant. The sample-specific normalized factor is used for sequencing depth normalization. In detail, a sliding window of 50 kilobase was applied across each chromosome, and the number of sequences falling within each window was counted, and the median value was chosen to be the representative of the chromosome. Because the sex chromosome for each sample might be different, the median sequence representatives among autosomes were used as the normalized factor. Human genome sequence (hg19) and CpG positions from hg19 were downloaded from the UCSC website (http://genome.ucsc.edu/) on April 12, 2018. In total, 28,691 CpG sequences were computationally annotated. Because all the participants in the sequencing cohort were female, CpG islands in human chromosome 1–22 and X, which included 27,537 CpG positions, were involved in the analysis. All the read numbers were counted by featureCounts (version 1.5.2), and the normalized sequence densities were used for comparison among samples in the CpG-enrichment analysis (21).

Total cfDNA and CMR Methylation

For detection of the global SFcfDNA methylation levels of RA and OA, we applied the 5-mC DNA ELISA kit (Zymo Research) according to the manufacturer's instructions. In brief, 100 ng of DNA was coated on the wells of the plate. Then primary (specific for 5-methylcytosine) and secondary antibodies were added to the wells. The OD value was read out by a Bioteck microplate reader at a wavelength of 450 nm. The result was calculated via a standard curve generated by different percentages of methylation levels of standard 5-mC DNA. Specific CMR methylation in RA and OA SFcfDNA was determined with a OneStep qMethyl-Lite kit (Zymo Research). Briefly, 20 ng of global DNA was incubated in the presence (test reaction) or absence (reference reaction) of methyl-sensitive restriction enzymes (5 U each; BStUI, HpyCH4IV and HpaII, NEB) at 37°C for 2 h, followed by real-time reverse transcription PCR (RT-PCR) as described in the manufacturer's instructions. Percentage methylation was calculated using the formula $100 \times 2^{-\Delta Ct}$, where ΔCt is the average Ct value from the test reaction minus the average Ct value from the reference reaction. Percentage methylation is relative to each experiment.

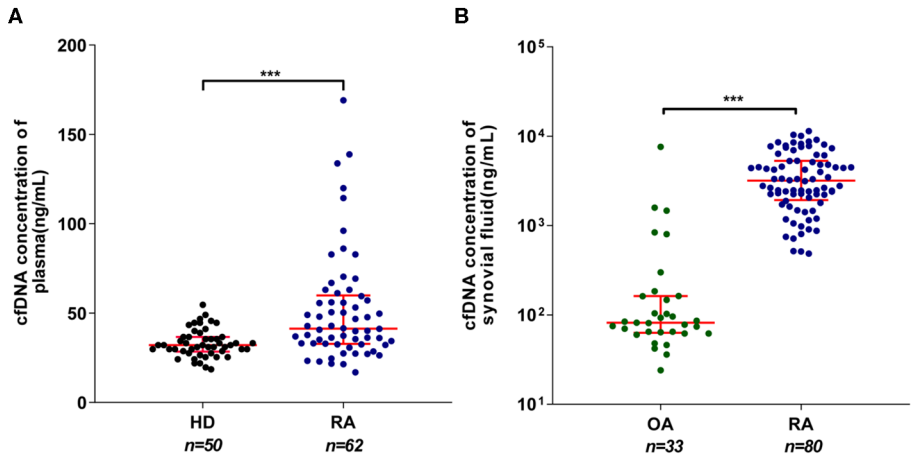

FIGURE 1 | Elevated cell-free DNA (cfDNA) isolated from the synovial fluid (SFcfDNA) concentrations in RA patients. **(A)** cfDNA concentrations in plasma of healthy donors (HDs) and rheumatoid arthritis (RA) patients. **(B)** cfDNA levels of synovial fluid in RA and osteoarthritis (OA) patients. Data was calculated by non-parametric Mann–Whitney test; $P < 0.05$ is recognized as statistically significant. $^{***}P < 0.001$. Data are presented as median with interquartile range.

SiRNA Knock Down Assay

Three different sequences of human TLR-9 and siRNA were designed and ordered from RiboBio Biotechnology, Guangzhou, China, and are listed in **Supplementary Table 3**. SiRNAs (200 nM) were transfected via Neon Transfection System (Life technology, Thermo Fisher) following the manufacturer's instruction. The down-regulation of target genes was evaluated by qPCR, with GAPDH as the internal control. After 24 h of stimulation, cell supernatants were collected for TNF-α and IFN-β detection.

Animal Assay

Female BALB/c mice (6–8 weeks) were purchased from Guangdong Medical Laboratory Animal Center. All mice were bred, housed, and used under specific pathogen-free conditions in the animal facility of the School of Life Science, Sun Yat-sen University. The animal studies were performed with the approval of the ethics committee of the School of Life Science, Sun Yat-sen University. At 1 day, 6 μg of CMR-3, CMR-7, CpG 1668 (positive control), CMF-4 in 20 μl of sterile PBS and the same volume of PBS were intra-articularly injected into mouse knees. The same dose of DNA was boosted at Day 4, respectively.

Joint Swelling Measurements and Clinical Scores

The diameter of mice articular joints was measured by a vernier caliper (Guanglu) from the first day of the onset of arthritis. The clinical scores were acquired according to the reported standard description (22): Score 0: no evidence of erythema and swelling occurred. Score 1: erythema and mild swelling appeared. Score 2: erythema and mild swelling extended from the ankle to the tarsals. Score 3: erythema and moderate swelling extended from the ankle to metatarsal joints. Score 4: erythema and severe swelling encompassed the ankle, paws, and digits or ankylosis of the limb.

Morphology Study

Photograph

After articular injection of DNA sequences at 3 days, the hindpaws of mice were photographed by a camera. Micro-CT imaging: At day 6, the mice were sacrificed, and the joints were fixed in 10% buffered formalin for a week, then scanned at 80 kV and 500 μA with the resolution of 19 μm in *ex vivo* micro-computed tomography (Siemens Inveon Micro-CT/PET) for 50 min. Three-dimensional images of joints were obtained by Inveon Research Workplace. Bone mineral density and the trabecular parameters including bone volume/total volume, bone surface area/bone volume, trabecular thickness, trabecular spacing, and trabecular pattern factor were measured by Inveon Research Workplace. MRI imaging: The mice were anesthetized by i.p. injection of 3.5% chloral hydrate, and then the Coronal fat-suppressed T2W TSE MRI (MRI; Achieva 3.0T; Philips Healthcare) of the inflammation articular joints were obtained with an eight-channel transversal animal coil. The parameter briefly: time of repeat/time of echo, 800/80 ms; field of view, 55 × 55 mm^2; slice thickness, 1 mm; slice number, 8; number of signal average, 1; matrix, 176 × 190. Spectral pre-saturation inversion recovery (SPIR) fat suppression technique was used. The total imaging time of this sequence was about 4 min 19 s. Readers scored synovitis, bone marrow edema, and bone erosions according to the Rheumatoid Arthritis MRI Scoring (RAMRIS) system (23). RAMRIS scores of mouse joints were obtained following a standard evaluation process. The scale of synovitis is 0–3. Score 0–4 is normal, mild, moderate, severe, respectively. The scale of bone marrow edema is 0–3. 0 = no osteitis; 1 = 1–33% of bone with osteitis; 2 = 34–66%; 3 = 67–100%. The scale of bone erosions is 0–10. 0 = no erosion; 1 = 1–10% of bone eroded;

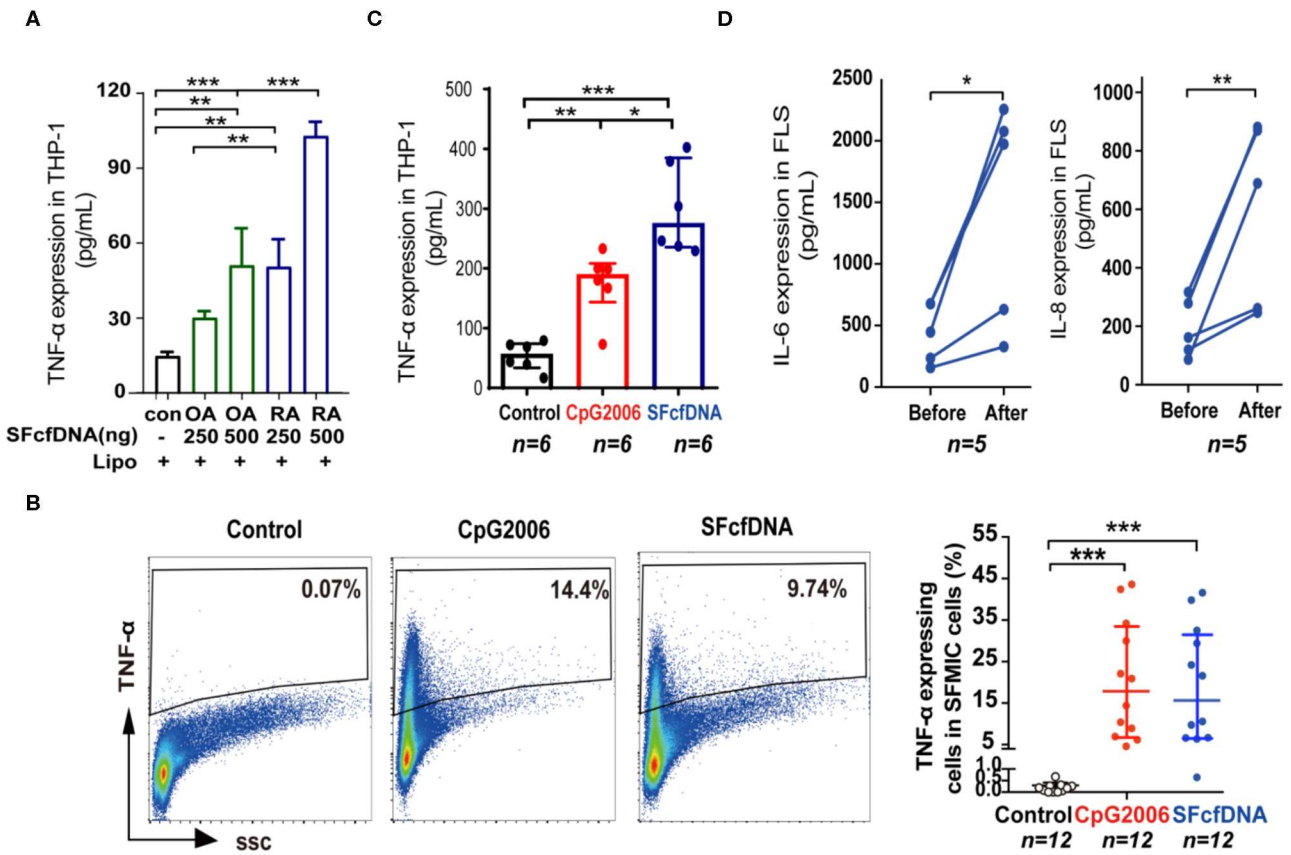

FIGURE 2 | Cellular stimulatory function of SFcfDNA from RA patients. **(A)** Expression of TNF-α by THP-1 cells stimulated with SFcfDNA from OA or RA patients at two concentrations. The data shown are representative of three independent experiments with the same tendency. **(B)** The percentage of primary SFMICs from RA patients expressing intracellular TNF-α upon stimulation with SFcfDNA or CpG 2006. The data on the left is a representative sample and on the right is the mean of 12 samples. **(C)** TNF-α secretion by SFMICs ($n = 6$) stimulated with CpG 2006 or SFcfDNA (0.5 μg/2 × 10^5 cells) using the same procedure. **(D)** IL-6 and IL-8 expression on primary FLSs from RA patients ($n = 5$) stimulated with SFcfDNA from RA patients. Statistical significance was calculated by one-way ANOVA **(A)**, Kruskal–Wallis Dunn's multiple comparison test **(B,C)**, two-tailed paired T testing **(D)**. *$0.01 < P < 0.05$, **$0.001 < P < 0.01$, ***$P < 0.001$. Data are presented as the mean with SD **(A)**, and **(B,C)** data are presented as the median with interquartile range.

2 = 11–20%; 3 = 21–30%, etc. The cumulative score of synovitis, bone marrow edema, and bone erosions on a scale of 0–16 served as a measure of the severity of inflammation and joint damage.

Histological Analysis and Immunohistochemical Staining

At day 6, the animals were sacrificed, then the ankle, knee, digital, and wrist joints were fixed with 10% buffered formalin. After, joints were incubated in decalcifying solution (4% hydrochloric acid in 4% formaldehyde) at room temperature for 7 days. The samples were paraffinized and cut into microtome (Leica) slices of 2 μm for histological examination. After staining the slices with hematoxylin and eosin, respectively, the inflammatory cell accumulation in synovial tissues, bone, and cartilage was evaluated by Vectra Automated Quantitative Pathology Imaging System (PerkinElmer).

To evaluate the histology scores of the knee and ankle joints of each mice, the histopathologic feature was graded using a scoring system as previously described (24): synovial cell lining hyperplasia (0–2); mononuclear cell infiltration (0–3); pannus formation (0–3); polymorphonuclear leukocyte infiltration in periarticular soft tissue (0–3); cellular infiltration and bone erosion at distal tibia (0–3); and cellular infiltration of cartilage (0–2). In addition, the sum of all the histopathologic feature scores was the histology score of each animal joint.

Real-Time PCR

At day 6, the mice were sacrificed, then the tissue just above the ankle joint with shinbones were removed and homogenized in TRIzol™ reagent with a homogenizer (T18 digital ULTRATURRAX, IKA) as described previously (6). Briefly, total RNA was extracted with Rneasy Universal Tissue kit (Qiagen); then, they were reverse-transcribed into cDNA using PrimeScript™ RT Reagent kit with gDNA Eraser and oligo (dT; Takara Biomed) and SYBR® Premix Ex Taq™ II kit (Takara Biomed). qPCR was carried to compare the cytokine expression, and glyceraldehyde-3-phosphate dehydrogenase (GAPDH) was the internal control. The relative mRNA levels of cytokines and

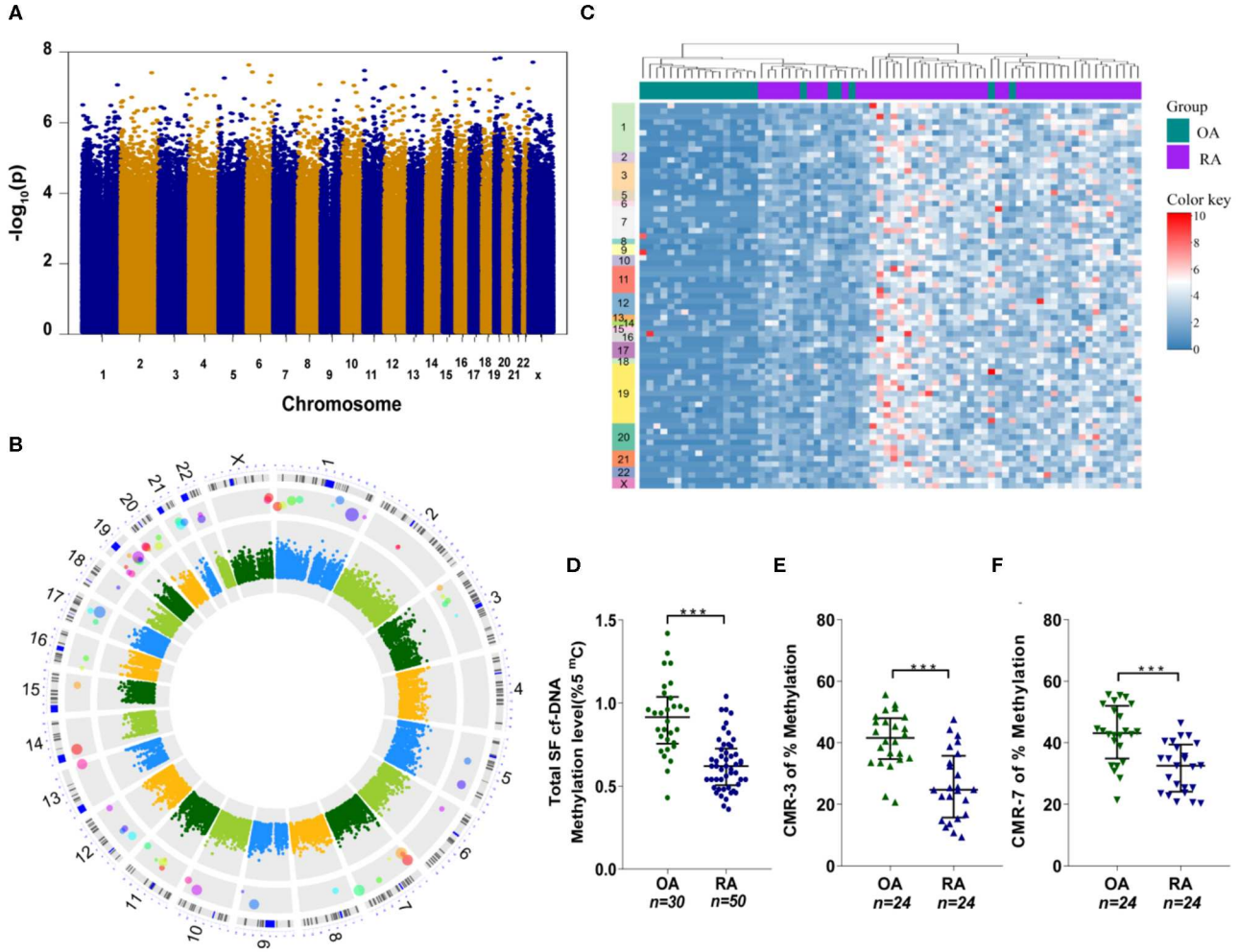

FIGURE 3 | SFcfDNA distribution and CpG-motif-rich (CMR) sequences in synovial fluid. **(A)** Distribution of total cfDNA density across chromosomes. Briefly, Manhattan plot with –logarithm *P*-values for the distribution comparison of total cfDNA density across chromosomes. Sequence density of 400-bp chromosome bins across the human genome was used for the measurement of overall genomic distribution of SFcfDNA molecules. Totally 7,590,771 chromosome bins were included and compared. **(B)** Circular Manhattan plot for the distribution comparison of SFcfDNA at CpG-motif regions. Features aligned onto the main chromosomes as concentric rings (from inner to outer) correspond to (1) Between-group difference (RA–OA) of sequence density of CpG-island regions. The values were coded by color, and the key legend was shown in the center. (2) Manhattan plot with –logarithm *P*-values for the comparison of sequence density of CpG regions. Totally 28,691 CpG sequences were compared, and the Bonferroni-corrected cut-off with minus logarithm scale is about 5.8. (3) CpG-rich locations identified by sequence density comparison at CpG regions. The larger the circle is, the higher significance it has. (4) The chromosome ideograms. (5) The number of chromosomes. **(C)** The average sequence density in every CpG location grouped by RA (purple) and OA (green), which clearly shows the presence of CMR sequences mainly in RA-cfDNA originated from RA patients. **(D)** Assessment of global cfDNA methylation levels in RA ($n = 50$) and OA ($n = 30$) patients through analysis of the percentage of 5-mC by ELISA. **(E,F)** Percentage of methylated **(E)** CMR-3 and **(F)** CMR-7 in SFcfDNA from RA and OA patients. **(D–F)** Statistical significance was calculated by non-parametric Mann–Whitney test, $^{***}P < 0.001$. Data are presented as median with interquartile range.

MMP-3 in the normal group were set as 1. The sequences of the primers are shown in **Supplementary Table 3**.

Statistical Analysis

Statistical differences were calculated with PRISM 5.0 software (GraphPad) using non-parametric Mann–Whitney test, two tailed-paired T test, one-way ANOVA, and Kruskal–Wallis Dunn's multiple comparison. Data were considered statistically significant when values were $P \leq 0.05$.

RESULTS

Increased cfDNA Levels in Large Cohort of RA Patients

A number of prior studies reported elevated cfDNA levels in circulation and SF of RA patients (16, 25). However, contradictory data were also emerged recently (26). To clarify this issue, we evaluated the concentrations of plasma and SF cfDNA in large control and RA patient population (80 RA cases) via Picogreen-based assay that only detects intact dsDNA. Our data

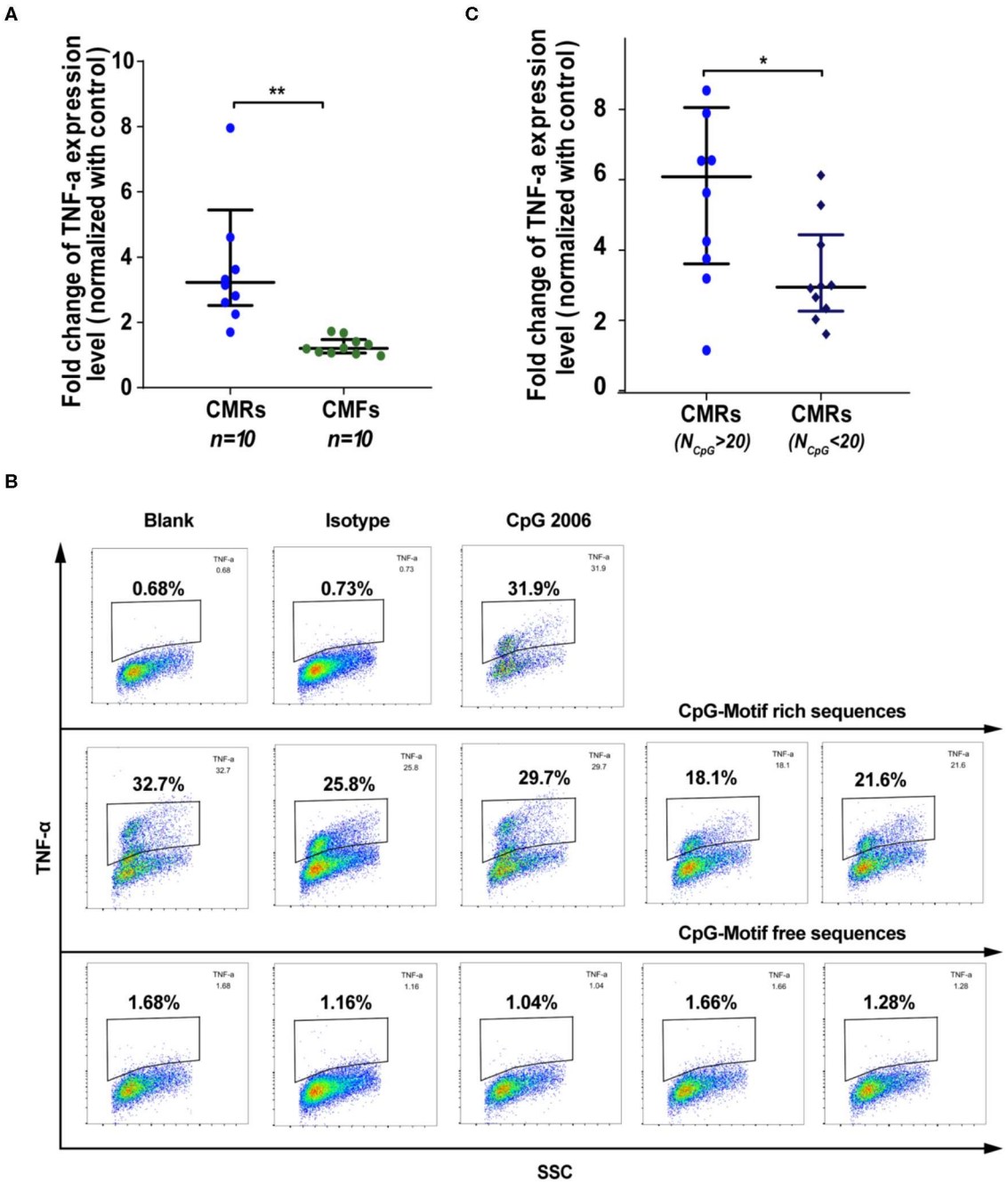

FIGURE 4 | SFcfDNA with CpG motif-rich sequences from RA patients induces TNF-α expression in THP-1 cells. **(A)** TNF-α regulation after stimulation with CMRs and CpG-motif free (CMFs) (250 ng/2 × 10^5 cells, respectively). Fold change of THP-1 expression was normalized against the control group. **(B)** Percentage of THP-1 cells expressing TNFα expression following stimulation of CMRs from SFcfDNA. **(C)** TNF-α expression induced by CMRs containing different numbers of CpG groups. **(A,C)** Statistical significance was calculated by non-parametric Mann–Whitney test, *$0.01 < P < 0.05$, **$0.001 < P < 0.01$. Data are presented as median with interquartile range.

show that there was a significant difference in plasma cfDNA levels between patients and healthy individuals (median: 41.3 vs. 32.1 ng/ml) (**Figure 1A**), and the median SFcfDNA level in RA patients was 38.8-fold higher than that in OA individuals (3,182 vs. 82 ng/ml) (**Figure 1B**). Furthermore, the median cfDNA concentration in the SF was ∼77-fold higher than that in the plasma in RA (3,182 and 41.3 ng/ml, respectively). These data confirm increased plasma and substantially high SF cfDNA levels in the relatively larger RA patient cohort (80 cases), and the fact that super high cfDNA concentrations are anatomically

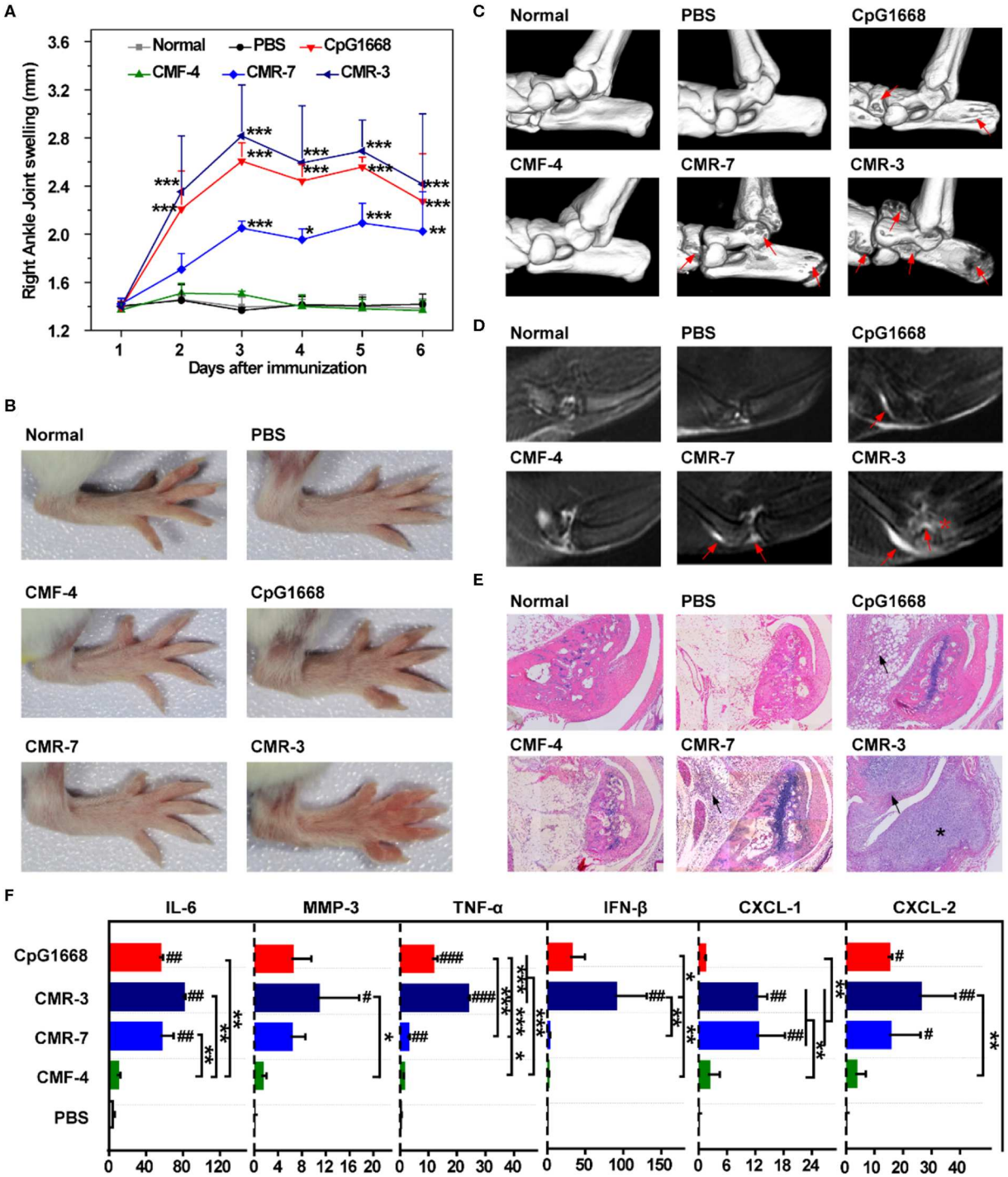

FIGURE 5 | Challenge of BALB/c mice with high-frequency CMR sequences. **(A)** Swelling of the right ankle joint as measured by the change in ankle diameter ($n = 5$). **(B)** Photos of right hindpaws on day 3 after challenge with specific sequences. **(C)** Representative 3D micro-CT images of the ankle joints of mice after administration for 6 days (resolution: 19 μm). Red arrows indicate bone destruction. **(D)** Representative T2-weighted MRI images of ankle joints of different groups at day 6. The effusion in the joint is highlighted by red arrows. Bone erosion in the CMR-3 group is highlighted with a red asterisk. **(E)** Representative HE staining of ankle joints of mice 6 days after administration (×200). Inflammatory cell infiltration in the articular cavity is indicated with black arrows. Bone destruction in mice treated with CMR-3 is highlighted with an asterisk. **(F)** mRNA level of related cytokines and MMP-3 of shinbones at day 6 after immunization. Relative mRNA expression was normalized to β-Actin. **(A,F)** Significance was calculated by one-way ANOVA. $^{\#}0.01 < P < 0.05$, $^{\#\#}0.001 < P < 0.01$, $^{\#\#\#}P < 0.001$ vs. PBS group. $^{*}0.01 < P < 0.05$, $^{**}0.001 < P < 0.01$, $^{***}P < 0.001$ between two groups. Data are presented as mean with SD.

restricted within joints strengthens the proposal that cfDNA may be implicated in onset and development of RA.

Cellular Stimulatory Function of SF cfDNA From RA Patients

To further define the pathological relevance of SF cfDNA, we determine if SFcfDNA can induce inflammatory response. SFcfDNA isolated from both RA and OA patients was used to stimulate THP-1 cells, a human monocyte cell line, which express TLR-9 and STING DNA sensors via transfection. Owing to the high variation in SFcfDNA concentrations seen in OA patients (24 ng/ml−1 μg/ml), we pooled synovial fluid from 10 separate OA cases to obtain enough cfDNA to stimulate inflammatory cells, and from 10 separate RA cases as a compared group. Results indicated that SFcfDNA from both RA and OA patients can stimulate THP-1 cells to produce inflammatory cytokine (TNF-α). SFcfDNA from RA patients was even more potent at low doses (250 ng/2 × 10^5 cells) (**Figure 2A**). Moreover, SFcfDNA from RA patients could stimulate primary SFMICs (**Supplementary Figure 1A**) and FLSs (**Supplementary Figure 1B**) to produce pro-inflammatory cytokines. Briefly, flow cytometer analysis showed that an average of 13.8% of SFMICs expressed TNF-α after SFcfDNA stimulation (**Figure 2B**), which was further confirmed by measuring TNF-α expression in SFMIC culture supernatant by ELISA (**Figure 2C**). Moreover, expression of IL-6 and IL-8 was elevated after SF cfDNA challenging FLSs (**Figure 2D**). However, no increased expression of IL-1β, TNF-α, or IFN-α was observed with FLSs, even present at a dose as high as 1 μg/ml (**Supplementary Figure 1C**). Thus, our results directly demonstrate the flammatogenic property of RA global SF cfDNA *in vitro*.

Genomic Landscape and Molecular Feature of SFcfDNA From RA

To identify and characterize individual inflammatogenic SFcfDNA molecules, we investigated the genomic distribution and sequence features of SFcfDNA from RA ($n = 50$) and OA ($n = 23$) patients using whole-genome shotgun sequencing (27). The patients were all female with an average age of 48.5 (±12.7) years old in the RA group and 51.0 (±6.2) years old in the OA group (**Supplementary Table 1**). Sequencing generated a total of 3.7 billion paired-end 125-bp reads, of which 94.9% (median) passed quality control. Of these post-QC reads, 95.4% (∼42.3 million per sample) on average aligned uniquely to human genome (**Supplementary Figure 2**). The number of sequencing reads for each sample is listed in **Supplementary Table 4**. Uneven distribution of reads across each chromosome was observed, and this intra-chromosomal variation was common among all samples, likely due to sequencing artifacts. However, the number of reads mapped to each 50-kb sliding window per chromosome in each of the samples remained consistent among all chromosomes. The sample-specific normalized factors were calculated using the number of reads per 50-kb sliding window to account for the differences in total sequencing yields among samples. Sequence densities of different regions in all the samples were analyzed. Overall comparison of sequence densities across the whole genome did not show any distinct regions with deeper coverages in the RA group (**Figure 3A**). However, the analysis, focused on epigenetically relevant CpG-island regions, revealed that the majority of these sequences had higher sequence densities on average in RA patient samples compared to the counterparts in OA patients. More specifically, 71 CpG-motif-rich (CMR) sequences were identified using the Wilcoxon rank-sum test for between-group comparison with Bonferroni-corrected alpha level (**Figure 3B**), and can be classified into two subgroups, CpG-motif-rich sequences with equal to or >20 CpG dinucleotides (CMR^{high}) and CpG-motif-rich sequences with <20 CpG dinucleotides (CMR^{low}). These CpG-islands were distributed across every chromosome, although there were more in chromosomes 1 and 19. More importantly, one-way clustering plot showed that RA and OA patients could be separated by the frequencies of these 71 CMR sequences, which could be potentially used as biomarkers to distinguish between OA and RA (**Figure 3C**).

Considering that hypomethylated DNA sequences (like mitochondrial DNA and bacterial DNA) are believed to induce a greater inflammatory response (28, 29), we next compared the total methylation levels of SFcfDNA between RA ($n = 50$) and OA ($n = 30$) patients. The global methylation level of SFcfDNA in RA patients was found to be significantly lower than that in OA patients (**Figure 3D**). Next, we randomly chose two specific CMR^{high} sequences, CMR-3 and CMR-7, to compare their methylation statuses in SFcfDNA between RA and OA patients (both $n = 24$). The results showed that both of the sequences were significantly more hypomethylated in RA patients compared to those in OA patients (**Figures 3E,F**).

Taken together, these results provide the first evidence that SFcfDNAs in RA are enriched with specific CMR sequences, which are hypomethylated.

Specific SFcfDNA Molecules Induce Potent Proinflammatory Effects *in vitro*

Hypomethylated CpG-motif-rich (CMR) sequences were previously shown to have a strong pro-inflammatory capability (30, 31), and epigenetic changes were reported to occur in RA-related cells (32, 33). Thus, we hypothesized that the 71 CpG-enriched sequences identified in SFcfDNA of RA patients might be responsible for the inflammatory responses induced *in vitro* by total RA SFcfDNA as described above. To test this, we investigated whether RA CpG-motif-rich RA-CMR^{high} could trigger strong inflammatory response in THP-1 cells with RA CpG-motif free (RA-CMF) sequences of the same length served as control. The individually purified CMR and CMF molecules were obtained by amplifying RA SFcfDNA via PCR with specific primers (**Supplementary Figure 3** and **Supplementary Tables 5**, **6**). The cell-based analysis showed that the RA-CMR^{high} could robustly stimulate THP-1 cells to express inflammatory mediator TNF-α, with its levels reaching 1.3- to 4.2-fold higher than those induced by RA-CMFs (**Figure 4A**). Also, intracellular staining revealed a similar finding. Specifically, TNF-α was produced in

25.3% on average of THP-1 cells in the presence of RA-CMR^{high}; in contrast, only did 1.36% of RA-CMFs-stimulated THP-1 cells, displaying 18.6-fold difference in the ability of inducing intracellular TNF-α production (**Figure 4B**). Moreover, among the 71 CpG-motif-rich sequences identified in this study, 10 RA-CMR^{high} sequences induced higher TNF-α expression levels than did nine RA-CMR^{low} sequences (5.9- vs. 3.9-fold) (**Figure 4C** and **Supplementary Table 6**). This is consistent with a previous study showing that CpG density correlates with the ability to induce inflammation (31). Next, we explored the signal cascade activation by the RA-CMR sequences in THP-1 cells. Two RA-CMR sequences (CMR-3 and CMR-7), CpG 2006, and one RA-CMF sequence (CMF-4) were used. The results show that CMR-3 and CMR-7 highly up-regulated TNF-α expression as that of CpG 2006 (**Supplementary Figure 4A**). On the contrary, CMF-4 hardly activated TNF-α expression. In terms of IFN-β expression, all sequences were stimulated at a low extent, and no significant difference was found between CMRs, CpG, and CMF. After knocking down TLR-9 by siRNA, TNF-α induction obviously declined in CMRs and CpG group compared to the wild-type group, while the significant alteration of IFN-β was not observed in all groups (**Supplementary Figure 4B**). Thus, RA-CMRs mainly induced inflammatory response through the TLR-9 pathway. Since we translocated cfDNA sequences into the cell with Lipofectamine, we need to make sure that the sequences could enter into the endosome and interact with TLR-9. Cy3-labeled CpG 2006 was transfected to the THP-1 cells with Lipo2000, and another known endosomal transfection reagent, DOTAP, was used as control (34, 35). The results show that both transfection reagents can translocate CpG 2006 into the endosome of the THP-1 cell (**Supplementary Figure 4C**). Overall, analysis of the stimulated human monocytic cell line THP-1 confirms the potent *in vitro* inflammatogenic property of the individual RA-CMR^{high} molecules identified by short-gun genomic sequencing.

The Specific RA-CMR^{high} Molecules Induce Joint Inflammation *in vivo*

Given that RA-CMR^{high} was shown to induce strong inflammatory responses in THP-1 cells (**Figures 4A–C**), we next investigated whether these hypomethylated RA-CMR^{high} molecules could induce RA-like joint arthritis in mice. CMR-3, CMR-7, CMF-4, and CpG 1,668 (6 μg/kg, respectively) were injected into the articular cavity of knees in mice on days 1 and 4, as described previously (36). Following the knee joint challenging, assessment of disease status was conducted, including the joint swelling scores (**Figures 5A,B**), micro-CT examination of bone erosion (**Figure 5C** and **Supplementary Figure 5A**), MRI studies of effusion in the knee joints, swelling of the suprapatellar bursa and bone erosion (**Figure 5D** and **Supplementary Figure 5B**), histopathological exam (**Figure 5E** for ankle joints, **Supplementary Figure 5C** for knee joints, and **Supplementary Figure 5D** for histology scores), as well as mRNA levels of cytokines in the shinbones (**Figure 5F**). Similar with what was observed in the positive control (CpG 1668) group, the mice treated with two individual hypomethylated RA-CMR^{high} molecules CMR3 and CMR-7 developed joint arthritis within 3–4 days. This RA-CMR^{high}-induced arthritis was characterized by severe joint or paw swelling and joint inflammation with massive leukocyte infiltration and bone erosion, as evidenced by assessing the disease parameters (**Figures 5A–F**). When evaluated with the same methods, in contrast, mice injected with PBS or CMF-4 had no joint inflammation and bone destruction observed (**Figures 5A–F**). These findings confirm the inflammatogenic ability of the RA-CMR^{high} but not RA-CMF molecules to induce joint arthritis *in vivo*.

DISCUSSION

By this work, we further support the observation of abnormal high cfDNA content in the plasma of RA. Moreover, we found that cfDNA content from synovial fluid of RA was much higher than that of OA patients, implying important roles of cfDNA to RA. Previous researches on cfDNA focused on quantitative measurement and biomarker functions, and we have shown that using cationic materials to scavenge cfDNAs may reduce inflammatory symptoms of the RA rat model (36–38). However, the pathogenetic functions of cfDNA in RA remained unclear. Now we showed that SFcfDNA from RA patients elicits robust expression and production of proinflammatory cytokines not only in THP-1 cells but also in primary SFMICs and FLSs from the same RA patients. It is noteworthy that SFcfDNA from OA patients does not have the proinflammatory stimulation ability *in vitro* when applied at the same doses as those from RA patients. Thus, for the first time, the present study provides a direct evidence that, unlike the OA SFcfDNA, the global RA SFcfDNA is inflammatogenic, facilitating the potent induction of inflammatory mediators (TNF-α and IL-6) that are critical for RA pathogenesis. More importantly, through whole genome shotgun sequencing, 71 CpG-motif-rich sequences were found with high frequencies in SFcfDNA from RA patients. One-way clustering plot analysis allows to classify RA and OA patients based on the CpG contents of their SFcfDNA. We found that the unique sequences in SFcfDNA of RA patients are able to mediate the pro-inflammatory cytokine induction. Among the characterized SFcfDNAs, RA-CMR can stimulate greater production of inflammatory cytokines than RA-CMF. Moreover, the immunostimulatory ability of SFcfDNAs correlates with the density of CpG distribution. These *in vitro* results were validated in an animal model where RA-CMR^{high}, but not RA-CMF, is able to induce even more severe joint inflammation and bone erosion. As reported previously, hypo-methylated CpG-rich sequences have a strong pro-inflammation capability (30), and bacterial DNA is highly pro-inflammatory because unmethylated CpG motifs are present at the expected frequency of 1 per 16 dinucleotides in the bacterial DNA (31). Also, in the pathological condition of rheumatoid arthritis, epigenetic change has been observed in many studies (32, 33). Therefore, for the first

time, with high-resolution analysis, we have demonstrated the characteristic features of cfDNA molecules in RA.

Like RA, SLE is another autoimmune disease, and the elevated cfDNA in plasma of patients was first reported in 1966 (39). Since then, the quantity and quality of cfDNAs in SLE have been studied. For example, high frequency G + C-rich DNA fragments showed more affinity to DNA antibody (40), and drug inhibited T-cell DNA methylation can induce autoimmune syndrome (41). Recently, hypomethylation of cfDNA in SLE was also reported by high-resolution analysis with massive parallel genomic and methylomic sequencing study (42). However, there is still no report to show high inflammatogenic-specific sequences of cfDNA. Therefore, our understanding on qualitative feature exampled by RA case will be also valuable to other cfDNA-induced autoimmune diseases. We may give a hint that there are distinct sequences in total cfDNAs that are relevant to certain autoimmune disease and even cancer. In RA patients, the functions of DNase I in circulation, DNase II in lysosomes, and cytoplasmic TrexI are deficient (6, 43, 44). The abnormal DNAases matter in the digestion of RA patient's genomic DNA, and therefore, the remained sequences of cfDNA in circulation become specific to RA development. The questions like the relationships between these cfDNA fragments and DNAase certainly need to be disclosed.

In conclusion, for the first time, we have demonstrated that the qualitative feature of cfDNA is important for the pathogenic development of RA. We show that high-frequency CMRs in SFcfDNA of RA patients stimulate a strong inflammatory response. Therefore, this work supplies not only a strategy to classify RA and OA patient but also a target of treating RA.

DATA AVAILABILITY STATEMENT

Our raw sequence files were deposited in the GSA database (https://bigd.big.ac.cn/gsa/), with the accession number of CRA002467. Other raw data supporting the conclusions of this article will be made available by the authors, without undue reservation, to any qualified researcher.

ETHICS STATEMENT

The studies involving human participants were reviewed and approved by General Hospital of Guangzhou Military Command PLA, Sun Yat-sen Memorial Hospital, the First Affiliated Hospital of Sun Yat-sen University. The patients/participants provided their written informed consent to participate in this study. The animal study was reviewed and approved by the Ethics Committee of the School of Life Science, Sun Yat-sen University. Written informed consent was obtained from the individual(s) for the publication of any potentially identifiable images or data included in this article.

AUTHOR CONTRIBUTIONS

CD carried out majority of the experiments. YL and SG carried out sequencing experiments and bioinformatic analysis. CS assisted with sequencing. HL assisted with part of the experiments. LD and SW provided patient samples and clinical discussion. JS provided medical imaging and analysis. KL provided discussion and language polishing. YC supervised experiments and wrote the manuscript. LW supervised the sequencing experiments and bioinformatic analysis. LL conceived the study, supervised all experiments, and wrote the manuscript.

FUNDING

This work was supported by the National Natural Science Foundation of China (Grant Nos. 21875290 and 81671612), the Guangdong Innovative and Entrepreneurial Research Team Program (No. 2013S086), and the Natural Science Foundation of Guangdong Province (No. 2014A030312018).

SUPPLEMENTARY MATERIAL

The Supplementary Material for this article can be found online at: https://www.frontiersin.org/articles/10.3389/fimmu.2020.00662/full#supplementary-material

REFERENCES

1. Marsman G, Zeerleder S, Luken BM, Extracellular histones, cell-free DNA, or nucleosomes: differences in immunostimulation. *Cell Death Dis*. (2016) 7:e2518. doi: 10.1038/cddis.2016.410
2. Nishimoto S, Fukuda D, Higashikuni Y, Tanaka K, Hirata Y, Murata C, et al. Obesity-induced DNA released from adipocytes stimulates chronic adipose tissue inflammation and insulin resistance. *Sci Adv*. (2016) 2:e1501332. doi: 10.1126/sciadv.1501332
3. Woo SR, Fuertes MB, Corrales L, Spranger S, Furdyna MJ, Leung MY, et al. STING-dependent cytosolic DNA sensing mediates innate immune recognition of immunogenic tumors. *Immunity*. (2014) 41:830–42. doi: 10.1016/j.immuni.2014.10.017
4. Duvvuri B, Lood C. Cell-free DNA as a biomarker in autoimmune rheumatic diseases. *Front Immunol*. (2019) 10:502. doi: 10.3389/fimmu.2019.00502
5. Moreira VG, Prieto B, Rodriguez JS, Alvarez FV. Usefulness of cell-free plasma DNA, procalcitonin and C-reactive protein as markers of infection in febrile patients. *Ann Clin Biochem*. (2010) 47:253–8. doi: 10.1258/acb.2010.009173
6. Kawane K, Ohtani M, Miwa K, Kizawa T, Kanbara Y, Yoshioka Y, et al. Chronic polyarthritis caused by mammalian DNA that escapes from degradation in macrophages. *Nature*. (2006) 443:998–1002. doi: 10.1038/nature05245
7. Porat A, Giat E, Kowal C, He M, Son M, Latz E, et al. DNA-mediated interferon signature induction by SLE serum occurs in monocytes through two pathways: a mechanism to inhibit both pathways. *Front Immunol*. (2018) 9:2824. doi: 10.3389/fimmu.2018.02824
8. Tian J, Avalos AM, Mao SY, Chen B, Senthil K, Wu H, et al. Toll-like receptor 9-dependent activation by DNA-containing immune complexes is mediated by HMGB1 RAGE. *Nat Immunol*. (2007) 8:487–96. doi: 10.1038/ni1457
9. Winfield JB, Faiferman I, Koffler D. Avidity of anti-DNA antibodies in serum and IgG glomerular eluates from patients with systemic lupus erythematosus.

Association of high avidity antinative DNA antibody with glomerulonephritis. *J Clin Invest*. (1977) 59:90–6. doi: 10.1172/JCI108626
10. Chamilos G, Gregorio J, Meller S, Lande R, Kontoyiannis DP, Modlin RL, et al. Cytosolic sensing of extracellular self-DNA transported into monocytes by the antimicrobial peptide LL37. *Blood*. (2012) 120:3699–707. doi: 10.1182/blood-2012-01-401364
11. Deng GM, Nilsson IM, Verdrengh M, Collins LV, Tarkowski A. Intra-articularly localized bacterial DNA containing CpG motifs induces arthritis. *Nat Med*. (1999) 5:702–5. doi: 10.1038/9554
12. Miyata M, Kobayashi H, Sasajima T, Sato Y, Kasukawa R. Unmethylated oligo-DNA containing CpG motifs aggravates collagen-induced arthritis in mice. *Arthritis Rheum*. (2000) 43:2578–82. doi: 10.1002/1529-0131(200011)43:11<2578::AID-ANR27>3.0.CO;2-V
13. Collins LV, Hajizadeh S, Holme E, Jonsson IM, Tarkowski A. Endogenously oxidized mitochondrial DNA induces *in vivo* and *in vitro* inflammatory responses. *J Leukoc Biol*. (2004) 75:995–1000. doi: 10.1189/jlb.0703328
14. Nagata S, Kawane K. Autoinflammation by endogenous DNA. *Adv Immunol*. (2011) 110:139–61. doi: 10.1016/B978-0-12-387663-8.00004-1
15. Leadbetter EA, Rifkin IR, Hohlbaum AM, Beaudette BC, Shlomchik MJ, Marshak-Rothstein A. Chromatin-IgG complexes activate B cells by dual engagement of IgM and Toll-like receptors. *Nature*. (2002) 416:603–7. doi: 10.1038/416603a
16. Zhong XY, von Muhlenen I, Li Y, Kang A, Gupta AK, Tyndall A, et al. Increased concentrations of antibody-bound circulatory cell-free DNA in rheumatoid arthritis. *Clin Chem*. (2007) 53:1609–14. doi: 10.1373/clinchem.2006.084509
17. Hashimoto T, Yoshida K, Hashimoto N, Nakai A, Kaneshiro K, Suzuki K, et al. Circulating cell free DNA: a marker to predict the therapeutic response for biological DMARDs in rheumatoid arthritis. *Int J Rheum Dis*. (2017) 20:722–30. doi: 10.1111/1756-185X.12959
18. Rykova E, Sizikov A, Roggenbuck D, Antonenko O, Bryzgalov L, Morozkin E, et al. Circulating DNA in rheumatoid arthritis: pathological changes and association with clinically used serological markers. *Arthritis Res Ther*. (2017) 19:85. doi: 10.1186/s13075-017-1295-z
19. Bolger AM, Lohse M, Usadel B. Trimmomatic: a flexible trimmer for Illumina sequence data. *Bioinformatics*. (2014) 30:2114–20. doi: 10.1093/bioinformatics/btu170
20. Li H, Durbin R. Fast and accurate long-read alignment with Burrows-Wheeler transform. *Bioinformatics*. (2010) 26:589–95. doi: 10.1093/bioinformatics/btp698
21. Liao Y, Smyth GK, Shi W. featureCounts: an efficient general purpose program for assigning sequence reads to genomic features. *Bioinformatics*. (2014) 30:923–30. doi: 10.1093/bioinformatics/btt656
22. Lee SM, Kim HJ, Ha YJ, Park YN, Lee SK, Park YB, et al. Targeted chemo-photothermal treatments of rheumatoid arthritis using gold half-shell multifunctional nanoparticles. *ACS Nano*. (2013) 7:50–7. doi: 10.1021/nn301215q
23. Ostergaard M, Peterfy CG, Bird P, Gandjbakhch F, Glinatsi D, Eshed I, et al. The OMERACT rheumatoid arthritis magnetic resonance imaging (MRI) scoring system: updated recommendations by the OMERACT MRI in Arthritis Working Group. *J Rheumatol*. (2017) 44:1706–12. doi: 10.3899/jrheum.161433
24. Quan L, Zhang Y, Crielaard BJ, Dusad A, Lele SM, Rijcken CJF, et al. Nanomedicines for inflammatory arthritis: head-to-head comparison of glucocorticoid-containing polymers, micelles, and liposomes. *ACS Nano*. (2014) 8:458–66. doi: 10.1021/nn4048205
25. Xu X, Shen H. AB0111 the underlying pathogenic effect of impared Dnase I activity on rheumatoid arthritis. *Ann Rheum Dis*. (2016) 75:934. doi: 10.1136/annrheumdis-2016-eular.1626
26. Dunaeva M, Buddingh BC, Toes RE, Luime JJ, Lubberts E, Pruijn GJ. Decreased serum cell-free DNA levels in rheumatoid arthritis. *Auto Immun Highlights*. (2015) 6:23–30. doi: 10.1007/s13317-015-0066-6
27. Fan HC, Blumenfeld YJ, Chitkara U, Hudgins L, Quake SR. Noninvasive diagnosis of fetal aneuploidy by shotgun sequencing DNA from maternal blood. *Proc Natl Acad Sci USA*. (2008) 105:16266–71. doi: 10.1073/pnas.0808319105
28. West AP, Shadel GS. Mitochondrial DNA in innate immune responses and inflammatory pathology. *Nat Rev Immunol*. (2017) 17:363–75. doi: 10.1038/nri.2017.21
29. El Kebir D, Jozsef L, Pan W, Wang L, Filep JG. Bacterial DNA activates endothelial cells and promotes neutrophil adherence through TLR9 signaling. *J Immunol*. (2009) 182:4386–94. doi: 10.4049/jimmunol.0803044
30. Krieg AM, Yi AK, Matson S, Waldschmidt TJ, Bishop GA, Teasdale R, et al. CpG motifs in bacterial DNA trigger direct B-cell activation. *Nature*. (1995) 374:546–9. doi: 10.1038/374546a0
31. Bird AP. CpG-rich islands and the function of DNA methylation. *Nature*. (1986) 321:209–13. doi: 10.1038/321209a0
32. Liu Y, Aryee MJ, Padyukov L, Fallin MD, Hesselberg E, Runarsson A, et al. Epigenome-wide association data implicate DNA methylation as an intermediary of genetic risk in rheumatoid arthritis. *Nat Biotechnol*. (2013) 31:142–7. doi: 10.1038/nbt.2487
33. Nakano K, Boyle DL, Firestein GS. Regulation of DNA methylation in rheumatoid arthritis synoviocytes. *J Immunol*. (2013) 190:1297–303. doi: 10.4049/jimmunol.1202572
34. Almofti MR, Harashima H, Shinohara Y, Almofti A, Baba Y, Kiwada H. Cationic liposome-mediated gene delivery: biophysical study and mechanism of internalization. *Arch Biochem Biophys*. (2003) 410:246–53. doi: 10.1016/S0003-9861(02)00725-7
35. Yasuda K, Ogawa Y, Kishimoto M, Takagi T, Hashida M, Takakura Y. Plasmid DNA activates murine macrophages to induce inflammatory cytokines in a CpG motif-independent manner by complex formation with cationic liposomes. *Biochem Biophys Res Commun*. (2002) 293:344–8. doi: 10.1016/S0006-291X(02)00210-3
36. Liang H, Peng B, Dong C, Liu L, Mao J, Wei S, et al. Cationic nanoparticle as an inhibitor of cell-free DNA-induced inflammation. *Nat Commun*. (2018) 9:4291. doi: 10.1038/s41467-018-06603-5
37. Holl EK, Shumansky KL, Borst LB, Burnette AD, Sample CJ, Ramsburg EA, et al. Scavenging nucleic acid debris to combat autoimmunity and infectious disease. *Proc Natl Acad Sci USA*. (2016) 113:9728–33. doi: 10.1073/pnas.1607011113
38. Peng B, Liang H, Li Y, Dong C, Shen J, Mao HQ, et al. Tuned cationic dendronized polymer: molecular scavenger for rheumatoid arthritis treatment. *Angew Chem Int Ed Engl*. (2019) 58:4254–8. doi: 10.1002/anie.201813362
39. Tan EM, Kunkel HG. Characteristics of a soluble nuclear antigen precipitating with sera of patients with systemic lupus erythematosus. *J Immunol*. (1966) 96:464–71.
40. Sano H, Takai O, Harata N, Yoshinaga K, Kodama-Kamada I, Sasaki T. Binding properties of human anti-DNA antibodies to cloned human DNA fragments. *Scand J Immunol*. (1989) 30:51–63. doi: 10.1111/j.1365-3083.1989.tb01188.x
41. Richardson B, Scheinbart L, Strahler J, Gross L, Hanash S, Johnson M. Evidence for impaired T cell DNA methylation in systemic lupus erythematosus and rheumatoid arthritis. *Arthritis Rheum*. (1990) 33:1665–73. doi: 10.1002/art.1780331109
42. Chan RW, Jiang P, Peng X, Tam LS, Liao GJ, Li EK, et al. Plasma DNA aberrations in systemic lupus erythematosus revealed by genomic and methylomic sequencing. *Proc Natl Acad Sci USA*. (2014) 111:E5302–11. doi: 10.1073/pnas.1421126111
43. Xu XY, Yang WF, Zhang SG, Zhao Q, Linag LJ, Wang X, et al. Correlation of DNase I in serum and synovial fluid with inflammatory activity in patients with rheumatoid arthritis. *Nan Fang Yi Ke Da Xue Xue Bao*. (2016) 36:1204–8. doi: 10.3969/j.issn.1673-4254.2016.09.07

44. Neidhart M, Karouzakis E, Schumann GG, Gay RE, Gay S, Trex-1 deficiency in rheumatoid arthritis synovial fibroblasts. *Arthritis Rheum*. (2010) 62:2673–9. doi: 10.1002/art.27567

Conflict of Interest: The authors declare that the research was conducted in the absence of any commercial or financial relationships that could be construed as a potential conflict of interest.

Copyright © 2020 Dong, Liu, Sun, Liang, Dai, Shen, Wei, Guo, Leong, Chen, Wei and Liu. This is an open-access article distributed under the terms of the Creative Commons Attribution License (CC BY). The use, distribution or reproduction in other forums is permitted, provided the original author(s) and the copyright owner(s) are credited and that the original publication in this journal is cited, in accordance with accepted academic practice. No use, distribution or reproduction is permitted which does not comply with these terms.

frontiers in Immunology

ORIGINAL RESEARCH
published: 05 May 2020
doi: 10.3389/fimmu.2020.00845

A Pauci-Immune Synovial Pathotype Predicts Inadequate Response to TNFα-Blockade in Rheumatoid Arthritis Patients

Alessandra Nerviani, Maria Di Cicco, Arti Mahto, Gloria Lliso-Ribera, Felice Rivellese, Georgina Thorborn, Rebecca Hands, Mattia Bellan, Daniele Mauro, Marie-Astrid Boutet, Giovanni Giorli, Myles Lewis, Stephen Kelly, Michele Bombardieri, Frances Humby and Costantino Pitzalis**

Experimental Medicine and Rheumatology, William Harvey Research Institute, Queen Mary University of London, London, United Kingdom

OPEN ACCESS

Edited by:
Erminia Mariani, University of Bologna, Italy

Reviewed by:
Maria I. Bokarewa, University of Gothenburg, Sweden
Lucy R. Wedderburn, University College London, United Kingdom

***Correspondence:**
Alessandra Nerviani
a.nerviani@qmul.ac.uk
Costantino Pitzalis
c.pitzalis@qmul.ac.uk

Specialty section:
This article was submitted to Autoimmune and Autoinflammatory Disorders, a section of the journal Frontiers in Immunology

Received: *16 December 2019*
Accepted: *14 April 2020*
Published: *05 May 2020*

Citation:
Nerviani A, Di Cicco M, Mahto A, Lliso-Ribera G, Rivellese F, Thorborn G, Hands R, Bellan M, Mauro D, Boutet M-A, Giorli G, Lewis M, Kelly S, Bombardieri M, Humby F and Pitzalis C (2020) A Pauci-Immune Synovial Pathotype Predicts Inadequate Response to TNFα-Blockade in Rheumatoid Arthritis Patients. Front. Immunol. 11:845. doi: 10.3389/fimmu.2020.00845

Objectives: To assess whether the histopathological features of the synovium before starting treatment with the TNFi certolizumab-pegol could predict clinical outcome and examine the modulation of histopathology by treatment.

Methods: Thirty-seven RA patients fulfilling UK NICE guidelines for biologic therapy were enrolled at Barts Health NHS trust and underwent synovial sampling of an actively inflamed joint using ultrasound-guided needle biopsy before commencing certolizumab-pegol and after 12-weeks. At 12-weeks, patients were categorized as responders if they had a DAS28 fall >1.2. A minimum of 6 samples was collected for histological analysis. Based on H&E and immunohistochemistry (IHC) staining for CD3 (T cells), CD20 (B cells), CD138 (plasma cells), and CD68 (macrophages) patients were categorized into three distinct synovial pathotypes (lympho-myeloid, diffuse-myeloid, and pauci-immune).

Results: At baseline, as per inclusion criteria, DAS28 mean was 6.4 ± 0.9. 94.6% of the synovial tissue was retrieved from the wrist or a metacarpophalangeal joint. Histological pathotypes were distributed as follows: 58% lympho-myeloid, 19.4% diffuse-myeloid, and 22.6% pauci-immune. Patients with a pauci-immune pathotype had lower levels of CRP but higher VAS fatigue compared to lympho- and diffuse-myeloid. Based on DAS28 fall >1.2, 67.6% of patients were deemed as responders and 32.4% as non-responders. However, by categorizing patients according to the baseline synovial pathotype, we demonstrated that a significantly higher number of patients with a lympho-myeloid and diffuse-myeloid pathotype in comparison with pauci-immune pathotype [83.3% (15/18), 83.3 % (5/6) vs. 28.6% (2/7), $p = 0.022$) achieved clinical response to certolizumab-pegol. Furthermore, we observed a significantly higher level of post-treatment tender joint count and VAS scores for pain, fatigue and global health in pauci-immune in comparison with lympho- and diffuse-myeloid patients but no differences in the number of swollen joints, ESR and CRP. Finally, we confirmed a significant fall in the number of CD68+ sublining macrophages post-treatment in

responders and a correlation between the reduction in the CD20+ B-cells score and the improvement in the DAS28 at 12-weeks.

Conclusions: The analysis of the synovial histopathology may be a helpful tool to identify among clinically indistinguishable patients those with lower probability of response to TNFα-blockade.

Keywords: synovial tissue, anti-TNF, pathotype, rheumatoid arthritis, certolizumab-pegol

INTRODUCTION

Rheumatoid Arthritis (RA) is a chronic inflammatory autoimmune disease characterized by persistent inflammation of synovial tissue. If not adequately treated, it can lead to progressive structural damage and subsequent disability (1). Early diagnosis and the introduction of advanced therapeutics for RA patients has resulted in substantial improvements in clinical outcomes. However, irrespective of drug choice or therapeutic target, response rates have remained stubbornly fixed with approximately 60% of patients attaining a modest 20% improvement in disease activity (ACR20), while only around 20% of patients achieving remission (2). In addition, the mechanisms responsible for such variable response to therapy are still unknown, and there are no biomarkers in regular clinical use which are predictive of treatment response to individual therapeutic agents (3). This is reflected in the most recent EULAR recommendations for the management of RA (4) that support the use of any of the available targeted therapeutics following failure on conventional synthetic (cs) DMARDs, implying a "trial and error" approach to treatment. Such an approach leaves a huge unmet need and exposes patients to a therapeutic lottery of drugs, which they may not respond to and which may cause unnecessary adverse effects. Thus, there has been considerable interest in trying to identify biomarkers of treatment response in the diseased tissue (5), as the search in peripheral blood has been largely unsuccessful (3). Heterogeneity in the quantity and quality of synovial cellular infiltrate is well recognized, and clustering of patients into three histological categories (pathotypes) has recently been described in a large early RA cohort as (i) *lympho-myeloid*, characterized by well-organized B or plasma cell aggregates and rich in macrophages; (ii) *diffuse-myeloid*, with predominant macrophages within the sublining tissue and lacking B/plasma cell aggregates, and (iii) *pauci-immune*, with scant infiltration of immune cells and prevalence of resident fibroblasts (6). Importantly, synovial molecular signatures have also been identified to associate with each pathotype (7). Moreover, synovial pathotypes and molecular signatures in the baseline biopsy are associated with clinical phenotypes, clinical response to csDMARDs, radiologic progression 12 months after the original biopsy (6, 7), and predict future requirement for biologic therapy (8). These data suggest that synovial biomarkers may be useful tools to stratify patients' response to biologic therapy. TNF inhibitors (TNFi) are the most widely prescribed biologic drugs in RA, and thus biomarkers of responses have been the most intensively sought. However, whilst levels of TNFα in the peripheral blood have repeatedly and consistently proven to be ineffective predictors (9), synovial TNFα expression and factors such as the presence of synovial B cell aggregates or specific gene signatures have been variably associated with clinical outcomes (10–12).

In this study, therefore, capitalizing on the current understanding of rheumatoid synovial histopathology, we aimed to investigate whether specific histological features in synovium prior to starting treatment with the TNFi certolizumab-pegol could predict clinical outcome, and furthermore we examined the modulation of histopathology by treatment.

METHODS

Patients

Thirty-seven RA patients [using the 1987 revised American College of Rheumatology (ACR) classification criteria] (13) fulfilling UK National Institute for Health and Care Excellence (NICE) prescribing guidelines for biologic therapy (i.e., failure of at least two csDMARDs and highly active disease demonstrated by DAS28 > 5.1) (14) were enrolled in the study at Barts Health NHS trust. Patients were excluded from the study if daily oral prednisolone dose exceeded 10 mg or if they have previously received any biologic treatment, including non-anti-TNF agents. Routine demographics including age, seropositivity for rheumatoid factor and anti-citrullinated peptide antibodies, disease duration, concomitant therapy and disease activity assessment (DAS28) were performed at baseline. Patients underwent synovial sampling of an actively inflamed joint using ultrasound (US)—guided needle biopsy as previously described (15) with collection of pre-biopsy US images. US images of the biopsied joints were scored for both synovial thickening (ST) and Power-Doppler (PD) using the EULAR/OMERACT US semi-quantitative synovitis score system (0–3) (16). Patients were subsequently commenced on standard treatment with subcutaneous certolizumab-pegol (400 mg at 0–2–4-weeks, then 200 mg every other week). Twelve-weeks after starting treatment, the number of swollen and tender joints (28 joint count), patient visual analog score (VAS) for pain, fatigue, global health and physician assessment of global health were recorded along with Health Assessment Questionnaire (HAQ). Patients were categorized as responders to therapy if a DAS28 fall >1.2 was demonstrated between baseline and 12-weeks, and non-responders if it did not. At 12-weeks, patients were consented to undergo a second synovial biopsy of the same joint sampled as at baseline. The study was approved by the local ethics committee (Rec. No. 10/H0801/47) and

written informed consent was obtained from all patients prior to inclusion.

Histological Assessment of the Synovial Tissue

A minimum of 6 samples was retrieved for histological analysis from each biopsy procedure for subsequent paraffin embedding. Following H&E staining of 3 μm-cut paraffin-embedded sections, synovial tissue underwent immunohistochemical (IHC) staining for CD3 (T cells), CD20 (B cells), CD138 (plasma cells), and CD68 (macrophages), as previously described (17). Synovial tissue was deemed as gradable if there was a visible lining layer and/or presence of macrophages in the sublining. Two independent scorers expert in synovial tissue histology quantified the degree of the immune infiltrate using a semi-quantitative score (0–4) as previously described (17). Subsequently, synovial samples were categorized into three distinct synovial pathotypes based on the following criteria: (i) Lympho-myeloid, if $CD20^+$ B-cells score $\geq$ 2 and/or $CD138^+$ plasma cells score $>$ 2; (ii) Diffuse-myeloid, if $CD68^+$ sublining (SL) macrophages score $\geq$ 2, $CD20^+$ B-cells score $\leq$ 1 and $CD138^+$ plasma cells score $\leq$ 2; Pauci-immune, if CD68SL macrophages score $<$ 2 and $CD3^+$ T cells score, $CD20^+$ B cells score, and $CD138^+$ plasma cells score $<$ 1 (6).

Statistical Analysis

Statistical analyses were performed using GraphPad Prism version 8.2.1. A $p < 0.05$ was considered statistically significant. Differences in continuous variables between two groups were analyzed by T-test or Mann-Whitney U-test depending on normality. Differences in variables between three or more groups were assessed through one-way ANOVA or Kruskal-Wallis with Dunn's correction test. Wilcoxon matched-pairs rank test was used to compare matched samples (e.g., pre- and post-treatment variables in the same patient). Chi-squared or Fisher's exact test was applied to analyze the significance of the association between categorical variables. Spearman's correlation test was used to assess the presence of significant correlations between variables. Multiple logistic regression analysis was performed with GraphPad Prism version 8.3.1. The binary clinical response (based on DAS28 improvement $\geq$1.2) was used as the outcome. The primary model was defined by the main effect of the pathotype only. Additional models were adjusted by the inclusion of several covariates such as age, gender, RF/CCP status and baseline DAS28. The Sankey diagram in **Figure 5** was plotted using SankeyMATIC (http://sankeymatic.com).

RESULTS

Patients' Characteristics

Patients' baseline demographic and clinical features are summarized in **Table 1**. Briefly, as expected in a population of established RA, ∼80% of patients were female, and the average age was 51.3 ± 11.7 years. About 70% of patients were either rheumatoid factor (RF) or anti-cyclic citrullinated peptide (CCP) antibody positive. As per the inclusion criteria of the study, all patients had high disease activity (DAS28 6.4 ± 0.9). All patients were previously exposed to csDMARDs treatment but were naïve to any biologics, and 35.1% of patients were on concomitant steroid treatment ($\leq$10 mg per day) at the time of the recruitment.

TABLE 1 | Baseline characteristics of the population included in the study ($n = 37$).

Female % (*n*)		81% (30)
Age years (mean ± *SD*)		51.3 ± 11.7
Disease duration years (mean ± *SD*)		6.3 ± 5.8
Smoking status	Previous % (*n*)	38.9% (14)
	Current % (*n*)	22.2% (8)
RF+ % (*n*)		64.9% (24)
Anti-CCP+ % (*n*)		64.9% (24)
RF+ or Anti-CCP+ % (*n*)		70.3% (26)
ESR mm/h (mean ± *SD*)		31.1 ± 25.8
CRP mg/l mean (mean ± *SD*)		10.7 ± 20.2
TJ/28 (mean ± *SD*)		18 ± 8
SJ/28 (mean ± *SD*)		10 ± 4
VAS GH patient (mean ± *SD*)		82.1 ± 13.9
VAS GH physician (mean ± *SD*)		73.7 ± 15.2
VAS pain (mean ± *SD*)		67.8 ± 24.9
VAS tiredness (mean ± *SD*)		55.1 ± 25.2
HAQ (mean ± *SD*)		1.7 ± 0.7
DAS28 (mean ± *SD*)		6.4 ± 0.9
DMARDs	MTX % (*n*)	24.3% (9)
	LFN % (*n*)	5.4% (2)
	MTX+HCQ % (*n*)	43.3% (16)
	MTX+SSZ % (*n*)	24.3% (9)
	MTX+SSZ+HCQ % (*n*)	2.7% (1)
Steroid treatment % (*n*)		35.1% (13)
Biopsied joint	MCP % (*n*)	21.6% (8)
	Elbow % (*n*)	2.7% (1)
	Knee % (*n*)	2.7% (1)
	Wrist % (*n*)	73% (27)
US BJ	Synovial Thickening (mean ± *SD*)	2.4 ± 0.6
	Power Doppler (mean ± *SD*)	1.6 ± 1

SD, Standard Deviation; n, number; RF, Rheumatoid Factor; CCP, Cyclic Citrullinated Peptide; ESR, erythrocyte sedimentation rate; CRP, C-Reactive Protein; TJ, Tender Joints; SJ, Swollen Joints; VAS, Visual Analog Scale (0-100); GH, Global Health; HAQ, Health Assessment Questionnaire; DAS, Disease Activity Score; DMARDs, Disease Modifying Anti-Rheumatic Drugs; MTX, methotrexate; LFN, leflunomide; HCQ, hydroxychloroquine; SSZ, sulfasalazine; MCP, metacarpophalangeal; US BJ, Ultrasound Biopsied Joint.

Histological Classification

A total of 37 patients were recruited to the study and underwent a synovial biopsy at study entry (baseline). 28/37 patients subsequently consented to a second synovial biopsy at 12-weeks follow up (**Figure 1A**, **Supplementary Figures 1, 2**). 31/37 baseline synovial biopsies and 22/28 12-weeks repeated biopsies yielded synovial tissue of sufficient quality for subsequent histological analysis. Demographics and clinical features of patients classified as "ungraded" (6 patients at baseline and 6 patients at 12-weeks) as well as those of patients who did not undergo a repeated synovial biopsy post-treatment are

summarized in **Supplementary Tables 1, 2**. At baseline, 58% (18/31) were classified as lympho-myeloid, 19.4% (6/31) as diffuse-myeloid, and 22.6% (7/31) as pauci-immune (**Figure 1B**). Representative immunohistological images are shown in **Figure 1C**, and the relative degree of immune cell infiltrate per pathotype shown in **Figure 1D**. 94.6% of the synovial tissue was retrieved from the wrist or a metacarpophalangeal joint (**Figure 1E**). There was no difference in the pathotype distribution among the various biopsy sites (**Figure 1F**).

Synovial Pathotypes and Baseline Clinical Features

We next evaluated whether there were significant differences in clinical parameters between patients stratified according to baseline synovial pathotype (**Table 2**). We demonstrated significantly lower levels of C-Reactive Protein (CRP) (**Figure 2A**) but higher VAS fatigue score (**Figure 2B**) in patients with a pauci-immune compared to lympho- and diffuse-myeloid pathotypes. The US Power Doppler (USPD) score of the biopsied joint was significantly higher in lympho-myeloid patients, while the US synovial thickening (USST), measured on gray-scale, was comparable among the three pathotypes (**Figures 2C,D**). This suggests that although the total proliferative cellular burden is the same across the pathotypes there are differences in the nature of the inflammatory milieu between the pathotypes, with increased vascularity observed in the lympho-myeloid pathotype.

Baseline Synovial Histological Pathotypes Associate With 12-Weeks Response to Certolizumab-Pegol

Twelve-weeks after commencing certolizumab-pegol, 25/37 patients (67.6%) were classified as responders and 12/37 (32.4%) as non-responders based on a DAS28 fall >1.2 (ΔDAS28 response). We next stratified patients according to synovial pathotype and evaluated whether there were significant differences in clinical outcomes between groups. We demonstrated that a significantly higher number of patients with a lympho-myeloid and diffuse-myeloid pathotype in comparison with pauci-immune pathotype [83.3% (15/18), 83.3 % (5/6) vs. 28.6% (2/7), Fisher test $p = 0.022$] were classified as responders to therapy. A similar distribution was observed when EULAR response criteria were applied: in this case, the rate of EULAR non-responders was 16.7% in both lympho-myeloid and diffuse-myeloid in comparison to 57.1% in pauci-immune patients (**Figure 3A**). Consistent with this, we also observed a significant fall in DAS28 score pre- and post-treatment in both the lympho-myeloid and the diffuse-myeloid groups [6.4 ± 1 to 3.9 ± 1.5 ($p < 0.001$) and 6.5 ± 0.8 to 3.2 ± 1.2 ($p = 0.002$) respectively] but not in the pauci-immune group [6.7 ± 1 to 5.2 ± 1.6 ($p = 0.06$)] (**Figure 3B**). Using a dichotomic classification of the pathotypes (lympho-myeloid and diffuse-myeloid vs. pauci-immune) we observed a significantly lower response in the pauci-immune group (Fisher test $p = 0.01$). The sensitivity of this test as a predictor of response was 83% with a specificity of 71%; the positive predictive value was 90% and the negative predictive value 56%. A logistic regression model including the pathotype alone mirrored the results of the Fisher test ("Model 1" in **Supplementary Table 3**). The histological classification remained significant when the model was adjusted for age, gender and RF/CCP status ("Model 2" in **Supplementary Figure 2**) as well as in a larger model including also DAS28 at baseline ("Model 3" in **Supplementary Figure 2**).

An Inadequate Response to Certolizumab-Pegol in Patients Categorized as Pauci-Immune Pathotype Is Driven by Higher Levels of Tender Joint Counts and Patient-Reported-Outcomes

As patients with a baseline pauci-immune histological pattern were less likely to respond to certolizumab-pegol, we next evaluated differences in individual components of clinical response between pathotype groups at 12-weeks.

We demonstrated a significantly higher level of post-treatment tender joint count and VAS scores for pain, fatigue and global health in pauci-immune in comparison with lympho- and diffuse-myeloid patients (**Figure 4A**): conversely, there were no significant differences in the number of swollen joints, ESR and CRP at 12-weeks post-treatment between pathotype groups.

Furthermore, when evaluating changes in individual components of the DAS28 score between baseline and 12-weeks follow up we saw the most significant falls in ESR, tender joint count, swollen joint count and VAS global health in the lympho-myeloid group. In the pauci-immune group only ESR level and swollen joint count significantly decreased after treatment (**Figure 4B**). Overall, this data suggests that while anti-TNF therapy is highly effective in the "inflammatory" pathotypes, it is less effective at reducing joint tenderness, pain and overall health scores in the pauci-immune patients.

Clinical Response at 12-Weeks Associates With a Reduction in the Number of Sublining Macrophages and Size of Synovial B Cells Aggregates

In order to evaluate the changes in synovial histopathology between baseline and 12-weeks, we focused on a subset of 17 patients who had gradable synovial tissue at both time-points (**Supplementary Table 1**). At 12-weeks, of these 17 patients, 47% (8/17) were classified as lympho-myeloid, 17.7% (3/17) as diffuse-myeloid and 35.3% (6/17) as pauci-immune pathotype. Overall, 70.6% patients maintained the same pathotype as baseline, 23.5% changed to a less inflammatory and 5.9% to a more inflammatory histological patter. We then evaluated the change in synovial pathotype per patient between baseline and 12-weeks. We observed that, following anti-TNF treatment, the percentage of lympho-myeloid decreased from 58 to 47% while the number of pauci-immune patients increased from 22.6 to 35.3%. Furthermore, in the absence of B cell aggregates at baseline, patients did not develop B cells and/or

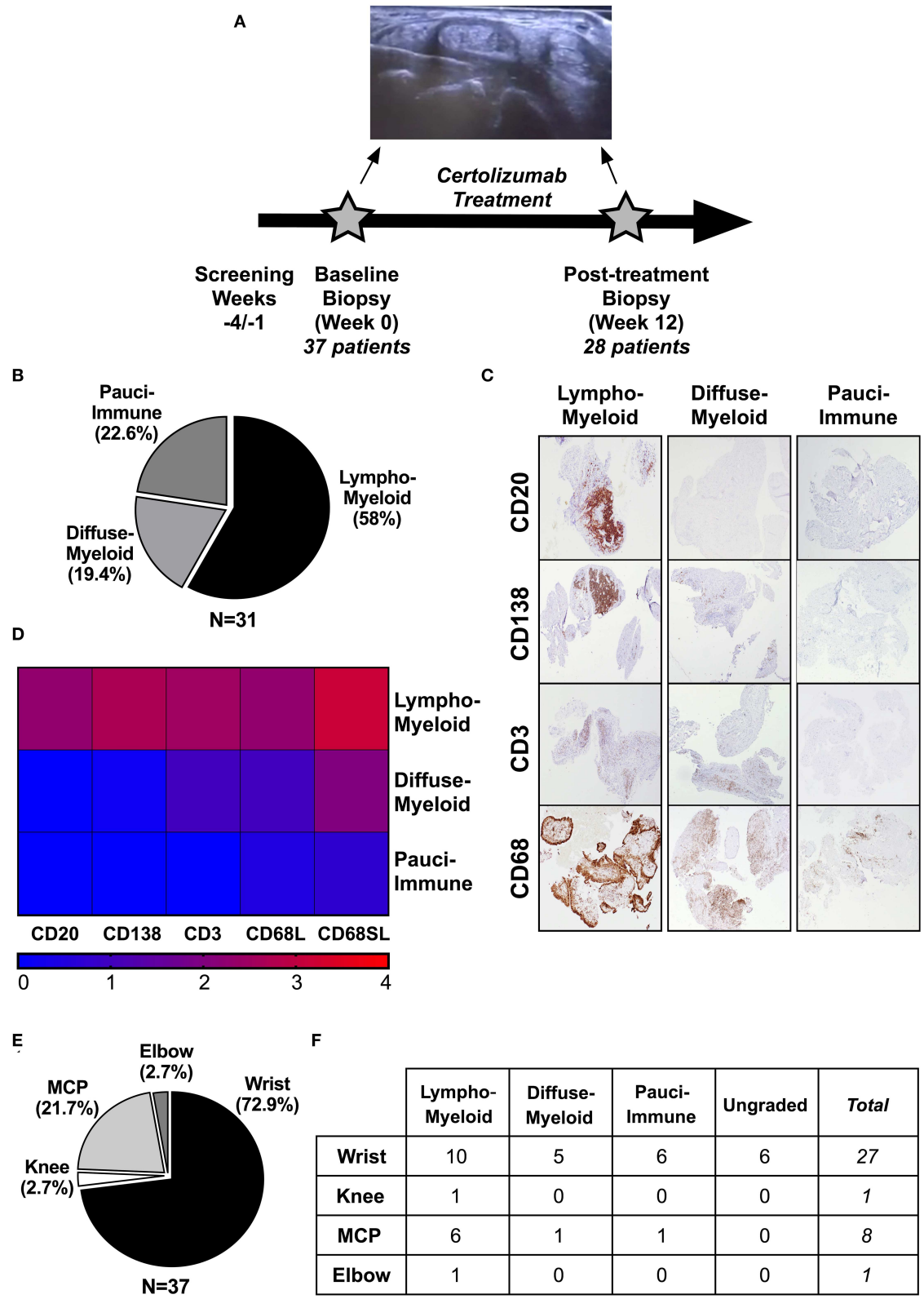

	Lympho-Myeloid	Diffuse-Myeloid	Pauci-Immune	Ungraded	*Total*
Wrist	10	5	6	6	*27*
Knee	1	0	0	0	*1*
MCP	6	1	1	0	*8*
Elbow	1	0	0	0	*1*

FIGURE 1 | (A–F) Design of the study and histological characterization of the synovial tissue. **(A)** Timeline of the study, which included a baseline US-guided needle synovial biopsy at week 0 (37 patients) and a second biopsy of the same joint after 12-weeks of treatment with certolizumab-pegol (28 patients). At the top,

(Continued)

FIGURE 1 | representative gray-scale transverse section of an US-guided wrist biopsy showing the needle entering the joint space underneath the IV extensor tendons compartment. **(B)** Distribution (%) of synovial pathotypes at baseline. **(C)** Representative images of immunohistochemistry staining of synovial tissue for immune cells markers and classification in three pathotypes: *lympho-myeloid*, *diffuse-myeloid* and *pauci-immune*. Original magnification 4x. **(D)** Heatmap showing the degree of infiltration of immune cells (CD20, B-cells; CD138, plasma cells; CD3, T-cells; CD68L, macrophages of the lining; CD68SL, macrophages of the sublining) in each pathotype. **(E)** Distribution (%) of biopsied joints. **(F)** Histological pathotype according to synovial biopsy site. MCP, metacarpophalangeal. Fisher's test: not significant.

TABLE 2 | Analysis of baseline features by pathotype.

		Lymphoid-Myeloid (58%, *n* = 18)	Diffuse-Myeloid (19.4%, *n* = 6)	Pauci-Immune (22.6%, *n* = 7)	*p-value*
Female % (*n*)		77.8% (14)	100% (6)	100% (7)	0.356[a]
Age years (mean ± *SD*)		50.4 ± 10.8	47.5 ± 17.6	54.7 ± 11.8	0.577[b]
Disease duration years (mean ± *SD*)		5.05 ± 3.7	4.8 ± 5.3	5.1 ± 6.3	0.992[b]
RF+ % (*n*)		72.2% (13)	50% (2)	71.4% (5)	0.588[a]
ACPA + % (*n*)		72.2% (13)	50% (3)	57.1% (4)	0.595[a]
RF or ACPA + % (*n*)		77.8% (14)	50% (3)	71.4% (5)	0.418[a]
ESR mm/h (mean ± *SD*)		30.53 ± 24.74	54.5 ± 33.2	25.4 ± 21.2	0.107[b]
ESR mm/h (mean ± *SD*)		30.53 ± 24.74	54.5 ± 33.2	25.4 ± 21.2	0.107[b]
CRP mg/l (mean ± *SD*)		8.9 ± 6.6	30.6 ± 46.2	2.2 ± 3.9	*0.020[b]
TJ/28 (mean ± *SD*)		17.4 ± 8.7	13 ± 6.4	22.6 ± 4.3	0.087[b]
SJ/28 (mean ± *SD*)		10.5 ± 5	8.7 ± 2.7	9.3 ± 4.9	0.675[b]
VAS GH pt (mean ± *SD*)		83.5 ± 13.6	72.7 ± 16.4	86.3 ± 16.3	0.230[b]
VAS GH phys (mean ± *SD*)		79.9 ± 12.6	65.2 ± 22	71 ± 12.5	0.112[b]
VAS pain (mean ± *SD*)		63.9 ± 27.9	54.7 ± 25.2	87.2 ± 16.6	0.101[b]
VAS tiredness (mean ± *SD*)		47.8 ± 22.6	46.7 ± 29	76.5 ± 17.5	*0.038[b]
HAQ (mean ± *SD*)		1.7 ± 0.7	1.4 ± 0.8	2 ± 0.8	0.451[b]
DAS28 (mean ± *SD*)		6.4 ± 1	6.5 ± 0.8	6.7 ± 1	0.787[b]
Steroid % (n)		27.8% (5)	50% (3)	42.9% (3)	0.595[a]
USST biopsied joint		2.6 ± 0.6	2 ± 0.6	2.4 ± 0.5	0.112[b]
USPD biopsied joint		2.1 ± 1	1 ± 0.9	1.1 ± 0.7	*0.023[b]
Steroid treatment % (*n*)		27.8% (5)	50% (3)	42.8 (3)	0.595[a]
DMARDs	MTX % (*n*)	33.3% (6)	0% (0)	14.3% (1)	[c] >0.999
	LFN % (*n*)	5.55% (1)	0% (0)	14.3% (1)	
	MTX+HCQ % (*n*)	27.8% (5)	66.7% (4)	57.1% (4)	
	MTX+SSZ % (*n*)	27.8% (5)	33.3% (2)	14.3% (1)	
	MTX+SSZ+HCQ % (*n*)	5.55% (1)	0% (0)	0% (0)	

*Baseline characteristics were compared by Fisher's exact test[a] or Kruskal-Wallis with post-hoc Dunn's test[b] as appropriate. [c]DMARDs treatment distribution was analyzed as monotherapy vs. multiple DMARDs in lympho/diffuse-myeloid vs. pauci-immune. *p < 0.05 was considered statistically significant. SD, Standard Deviation; n, number; RF, Rheumatoid Factor; CCP, Cyclic Citrullinated Peptide; ESR, erythrocyte sedimentation rate; CRP, C-Reactive Protein; TJ, Tender Joints; SJ, Swollen Joints; VAS, Visual Analog Scale (0–100); GH, Global Health; HAQ, Health Assessment Questionnaire; DAS, Disease Activity Score; DMARDs, Disease Modifying Anti-Rheumatic Drugs; MTX, methotrexate; LFN, leflunomide; HCQ, hydroxychloroquine; SSZ, sulfasalazine; MCP, metacarpophalangeal; USST, Ultrasound Synovial Thickening; USPD, Ultrasound Power-Doppler.*

plasma cells post-treatment, and so there was no transition to the most inflammatory pathotype (lympho-myeloid) at 12-weeks (**Figure 5A**).

Next, we assessed the change in CD68+ sublining macrophages between baseline and 12-weeks in responders and non-responders to certolizumab-pegol and observed a significant fall of this cell subset in responder patients (**Figure 5B**). We also confirmed a significant correlation between change in CD68+ sublining macrophages and change in DAS28 score between baseline and 12-weeks (**Figure 5C**). Similarly, we evaluated whether modulation of synovial CD20+ B cells at 12-weeks was related to clinical response. We analyzed patients with a lympho-myeloid pathotype at baseline who had a suitable synovial tissue for histological characterization post-treatment (11 patients). Only one patient was deemed as non-responder; therefore, in terms of clinical response, we did not detect any significant difference between patients with persistence (8/11, from baseline lympho-myeloid to lympho-myeloid at 12-weeks) or complete resolution of CD20+ B-cells aggregates (3/11, from baseline lympho-myeloid to diffuse-myeloid or pauci-immune at 12-weeks). We next stratified responders patients into those with a change in CD20 scores of ≥ 0 between baseline and 12-weeks, meaning same or higher B-cell score post-treatment, and those with a change of <0 (indicating a lower B-cell score

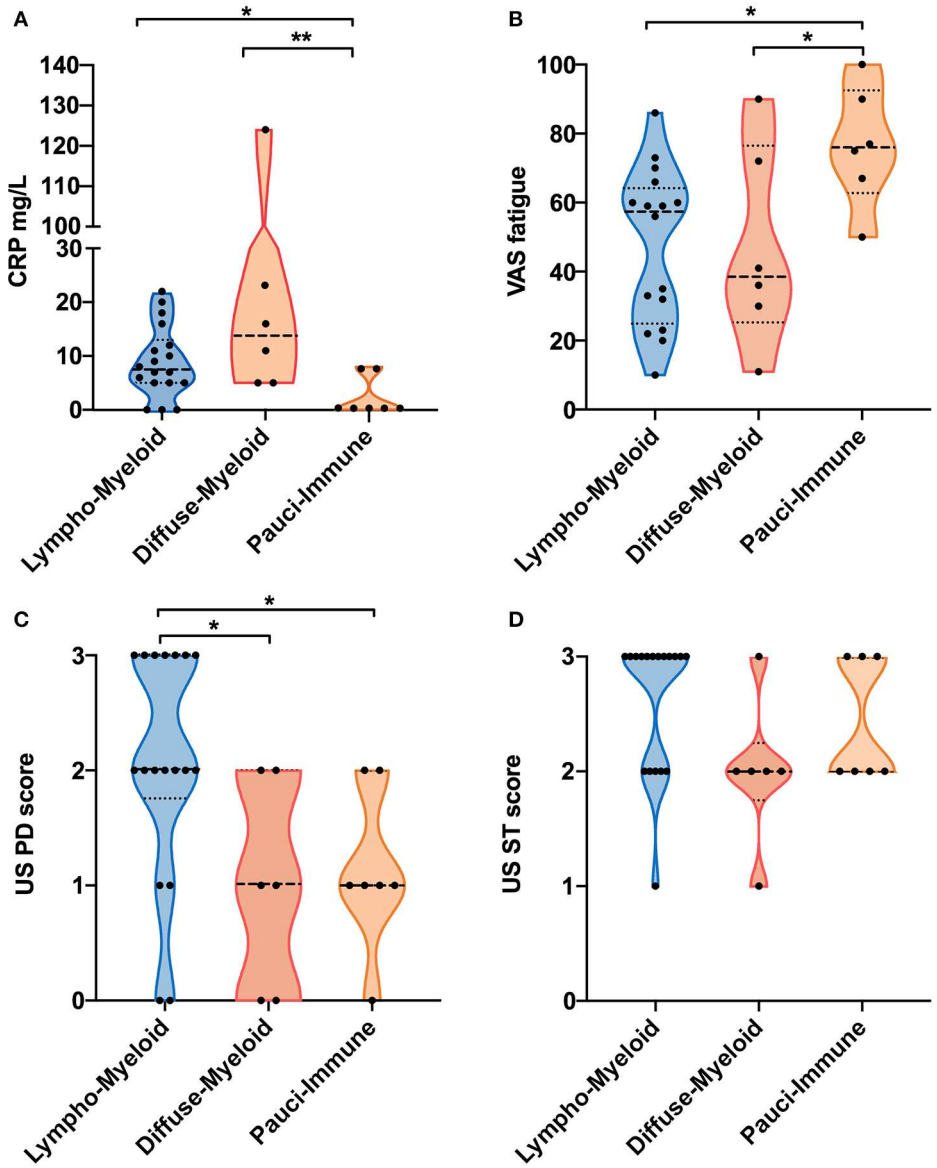

FIGURE 2 | (A–D) Violin plots showing differences in CRP **(A)**, VAS fatigue (0–100) **(B)**, ultrasound (US) Power-Doppler (PD) score (0–3) **(C)** and US synovial thickening (ST) score measured in gray-scale (0–3) **(D)** of the biopsied joints between pathotype groups. Median and interquartile ranges are represented by thick and thin dotted lines, respectively. $^{**}p < 0.01$, $^{*}p < 0.05$, Kruskal-Wallis with *post-hoc* multiple comparison on 31 patients.

at 12-weeks); then, we evaluated the mean change in DAS28 scores between the two groups. Our results suggested that patients with a reduction in the CD20+ B-cells score after treatment had a significantly greater improvement of the disease activity score at 12-weeks (**Figure 5D**). We also assessed the relationship between absolute change in DAS28 and differences in the CD20+ B-cell scores between baseline and 12-weeks and showed a significant correlation ($r = 0.66$, $p < 0.05$), suggesting that clinical improvement is associated with falls in CD20 scores and clinical worsening with increased scores (**Figure 5E**). These data demonstrate that depletion of synovial sublining macrophages and B cells are important factors in responsiveness to anti-TNF treatment.

DISCUSSION

Despite the considerable improvement in outcomes for RA patients since the introduction of TNFi therapy, clinicians are still unable to reliably identify patients most likely to respond to specific therapies, which remains a huge unmet clinical need. The identification of peripheral blood biomarkers of clinical response to TNFi therapy has been largely unsuccessful (3) and so focus has shifted to the examination of the primary site of inflammation in RA, i.e. synovial tissue (5). Early studies on this topic recognized the heterogeneity of rheumatoid synovitis and the presence of high- and low-inflammation synovial tissue, with the former being associated with higher disease activity and

A

	Lymphoid-Myeloid (58%, n=18)	Diffuse-Myeloid (19.4%, n=6)	Pauci-Immune (22.6%, n=7)	*p value*
	ΔDAS28 Response			
Responders	83.3% (15)	83.3% (5)	28.6% (2)	***0.022**
Non-Responders	16.7% (3)	16.7% (1)	71.4% (5)	
	EULAR Response			
Good Responders	38.9% (7)	50% (3)	14.3% (1)	0.355
Moderate Responders	44.4% (8)	33.3% (2)	28.6% (2)	
Non-Responders	16.7% (3)	16.7% (1)	57.1% (4)	
	ΔDAS28 [12 weeks - baseline]			
ΔDAS28 (mean ± SD)	-2.5 ± 1.1	-3.2 ± 1.8	-1.5 ± 1	0.061

B

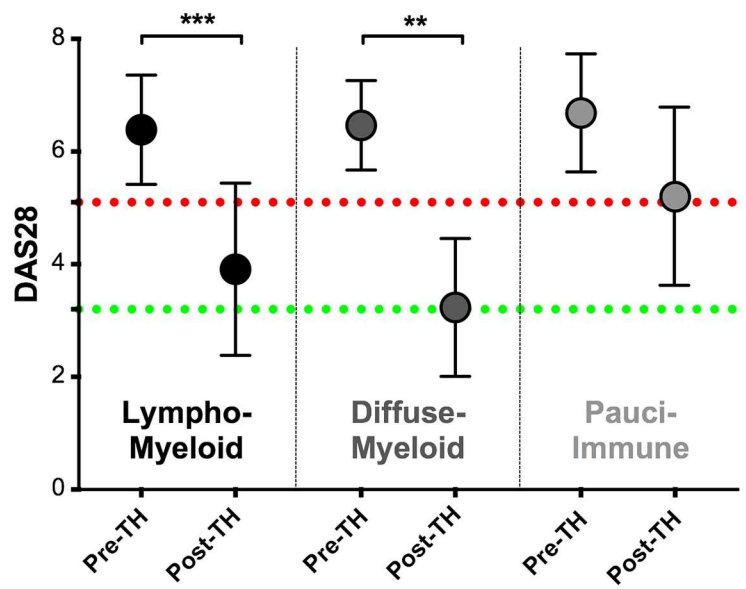

FIGURE 3 | (A) Table summarizing clinical response rates by pathotypes to certolizumab-pegol at 12-weeks. ΔDAS28 was calculated by subtracting the baseline-DAS28 value from the 12-weeks-DAS28; DAS28 fall > 1.2 defined "responders." Distribution of response rates was tested by Fisher's exact test while differences in ΔDAS28 by Kruskal-Wallis with Dunn's test. SD, standard deviation. **(B)** Comparison of pre- (pre-TH) and post-treatment (post-TH) DAS28 by pathotype. ***$p < 0.001$, **$p < 0.01$, Kruskal-Wallis with *post-hoc* Dunn's multiple comparison test on 31 patients. Red dotted line represents DAS28 5.1 ("high disease activity"); green dotted line represents DAS28 3.2 ("low disease activity").

systemic markers of inflammation (18). More recently, numerous studies defining the cellular and molecular composition of the rheumatoid synovium both at single-cell (19, 20) and whole-tissue (6, 7) level have confirmed the heterogeneity and complexity of the tissue in its diseased state as well as its association with clinical phenotypes.

Here, we characterized for the first time the baseline features of the synovial tissue of a homogeneous group of 37 inadequate

A

Post-Treatment Parameters	Lymphoid-Myeloid (58%, n=18)	Diffuse-Myeloid (19.4%, n=6)	Pauci-Immune (22.6%, n=7)	*p value*
ESR mm/h (mean ± SD)	21.7 ± 17.4	21.6 ± 17.4	12.7 ± 8.7	0.436
CRP mg/l (mean ± SD)	4.2 ± 5.7	3.2 ± 5	0.7 ± 1.9	0.318
TJ/28 (mean ± SD)	6.6 ± 8.7	2.2 ± 2.1	13.9 ± 7.2	***0.029**
SJ/28 (mean ± SD)	2.8 ± 2.7	2.2 ± 1.5	4.4 ± 2.4	0.239
VAS GH Pt (mean ± SD)	38 ± 23.2	24 ± 29	76.3 ± 23.1	***0.002**
VAS GH Phy (mean ±SD)	35.8 ± 24.4	22.5 ± 19	59.3 ± 16.9	***0.023**
VAS Pain (mean ± SD)	34.3 ± 24.9	22 ± 22.1	67.2 ± 24.6	***0.008**
VAS Fatigue (mean ± SD)	37.7 ± 27	23.8 ± 26.3	80.3 ± 16.8	***0.001**
HAQ (mean ± SD)	1.1 ± 0.8	0.8 ± 0.7	1.5 ± 1	0.411

B

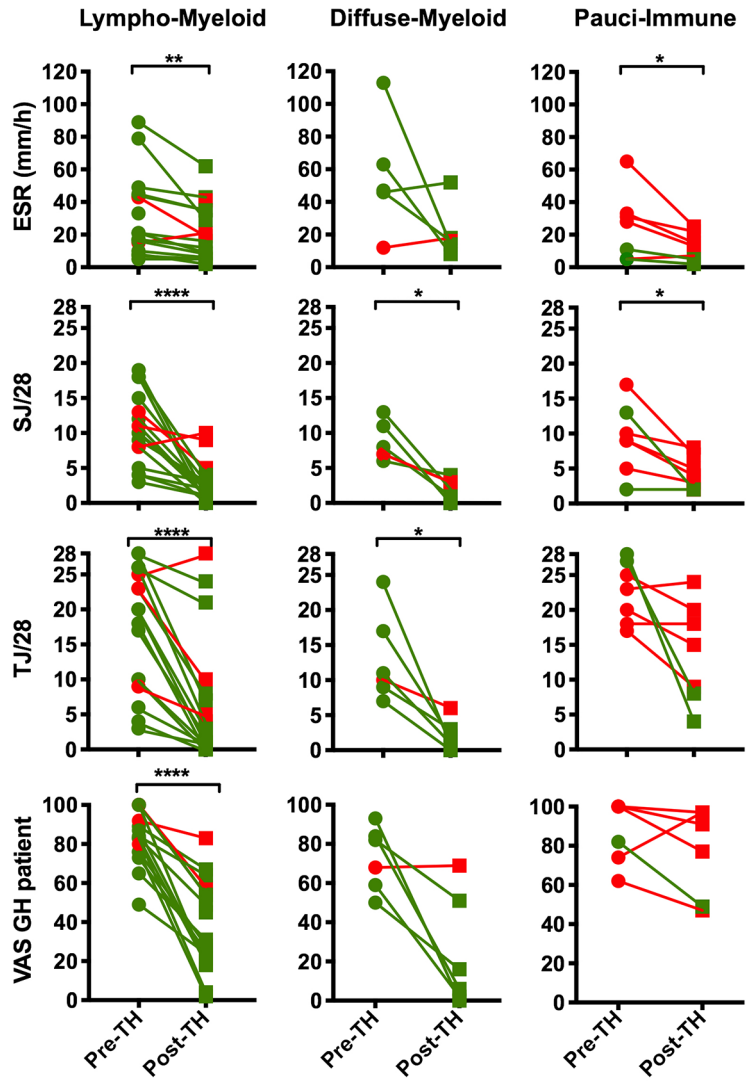

FIGURE 4 | (A) Table summarizing the comparison by pathotype of the patients' clinical features at 12-weeks post-treatment (*Kruskal-Wallis with Dunn's correction). Significantly different variables are in bold. **(B)** Comparison of pre- (pre-TH) and post-treatment (post-TH) individual parameters of the DAS28 by pathotype. p values were calculated with Wilcoxon

(Continued)

FIGURE 4 | matched-pairs rank test (31 patients); ****$p < 0.0001$, ***$p < 0.001$, **$p < 0.01$, *$p < 0.05$. Green dots and line: "responders"; red dots and lines: "non-responders". SD, Standard Deviation; ESR, erythrocyte sedimentation rate; CRP, C- Reactive Protein; TJ, Tender Joints; SJ, Swollen Joints; VAS, Visual Analog Scale (0–100); GH, Global Health; pt, patient; phy, physician; tir, tiredness; HAQ, Health Assessment Questionnaire.

responders to csDMARDs by applying a histologic algorithm previously validated in a different and independent large cohort of early RA patients and evaluated whether synovial histological characteristics prior-to-treatment correlated with clinical response to the TNFα inhibitor certolizumab-pegol.

Firstly, we confirmed the presence of all three synovial pathotypes as described early in the disease and prior to any treatment intervention (6, 7). These include a pauci-immune pathotype, which, despite the absence of infiltrating inflammatory cells, can be detected in RA patients with active disease fulfilling UK NICE criteria for starting biologic treatment (DAS28 > 5.1). The relative prevalence of the lympho-myeloid pathotypes in this RA cohort with established, more longstanding disease was higher than in early, untreated RA [58% vs. 39% (6)]. This is in line with the recent observation in early RA that patients characterized by a lympho-myeloid pathotype at disease onset are more likely to progress in terms of increasing joint damage as assessed on x-ray and are subsequently more likely to require biologic therapy at 12 months follow up (8).

The relationship between the baseline histological characteristics and the clinical response was assessed at 12-weeks by the change in the DAS28 pre- and post-treatment, since improvement in DAS28 < 1.2 at 12-weeks has been shown to be the best predictor of inadequate response at 1 year (21, 22). Overall, 67.6% of the treated patients improved their baseline DAS28 of ≥1.2 and were deemed as responders, aligned with the standard rates of response to TNFα inhibitors in clinical trials (23). However, when patients were categorized according to the baseline histological pattern, the rate of responders enriched from 67.6% up to 83.3% in both the lympho-myeloid and diffuse-myeloid pathotypes; conversely, a pauci-immune synovitis, i.e. scanty synovial inflammatory infiltrate, associated with a significantly lower rate of response (28.6%), impaired reduction of the DAS28 from pre- to post-treatment and higher absolute values of DAS28 at 12-weeks. Notably, and in line with these results, a pauci-immune-fibroblast signature in synovium of treatment-naïve patients (independent from the cohort included in this manuscript) has been found to be associated with resistance to csDMARDs in early-RA (7).

Moreover, by dissecting the post-treatment DAS28 into its individual variables, we demonstrated that the main drivers of the inadequate response in the pauci-immune patients at 12-weeks were the high number of tender joints and the patient global health VAS score whereas ESR and swollen joint count were comparable among the three pathotypes. All the patient-reported-outcomes recorded at 12-weeks, including fatigue and pain, were consistently higher in pauci-immune patients. Thus, although anti-TNF therapy reduced ESR and CRP in pauci-immune patients, it was less effective at reducing joint tenderness and pain scores in pauci-immune patients compared to the other pathotypes. Interestingly, the dissociation of pain scores from markers of inflammation has been recently described in a group of patients bearing a molecularly-defined "low inflammatory" subtype of synovitis characterized by the up-regulation of neurogenesis pathways and TGF-β (24). Thus, altogether, these data support the notion of a distinct "hyperalgesic" clinical phenotype linked to the pauci-immune pathotype. The role played by the synovial histopathology in predicting the response to TNFi has been long debated, particularly, because of the discordant findings coming from various observational studies. To date, chief attention has been given to lymphocytic structures within the synovial tissue. Their presence has been associated with the achievement of clinical response in some (25), though, not all studies (26); alternatively, it has been proposed that the disruption of the lymphoid follicles is instead critical for the success of the treatment (26), hence leaving the question substantially unanswered. Similarly, molecular analysis of the synovial tissue showed that, in some cases, an up-regulation of inflammation-related and myeloid genes characterized responder patients (11, 12) whereas, in others, high synovial content of pro-inflammatory IL7-receptor and IL-18 predicted the absence of response to TNFα blockade (27).

Here, our results suggest that both the baseline high-inflammatory pathotypes lympho-myeloid and diffuse-myeloid, differentiated by the presence/absence of B and/or plasma cell aggregates but both sharing a substantial infiltration by macrophages, had significantly better chances to respond to TNFα inhibition by certolizumab-pegol than patients with a pauci-immune pathotype. Our findings are in line with previous data demonstrating that a myeloid gene signature (12) as well as higher levels of synovial TNFα (28) pre-treatment predict enhanced response to TNFα-blockade. Conversely, the virtual absence of immune cells seems favoring the absence of clinical response, which may be potentially driven by other pathways including maladaptive pain response.

Finding that clinical response to certolizumab-pegol is significantly associated with a fall in CD68+ sublining macrophages is in line with the well-established literature recognizing the decrease in synovial macrophages as a validated biomarker of the clinical efficacy of various therapeutic interventions (29, 30). Several studies involving the use of anti-TNFα agents, including our previous observations (31), have already shown that the reduction in the number of sublining macrophages from baseline, also at early time-points after starting the treatment, associated with clinical response in RA (32, 33); we have here further confirmed this evidence. This early reduction in sublining CD68-positive cells in future responders to TNFi has also been mirrored in the peripheral blood by the change in myeloid-related-protein (MRP) 8/14 (34).

We also showed that if B cells and plasma cells are absent at baseline, as occurs in the diffuse-myeloid and pauci-immune pathotypes, there is no evolution toward a lympho-myeloid

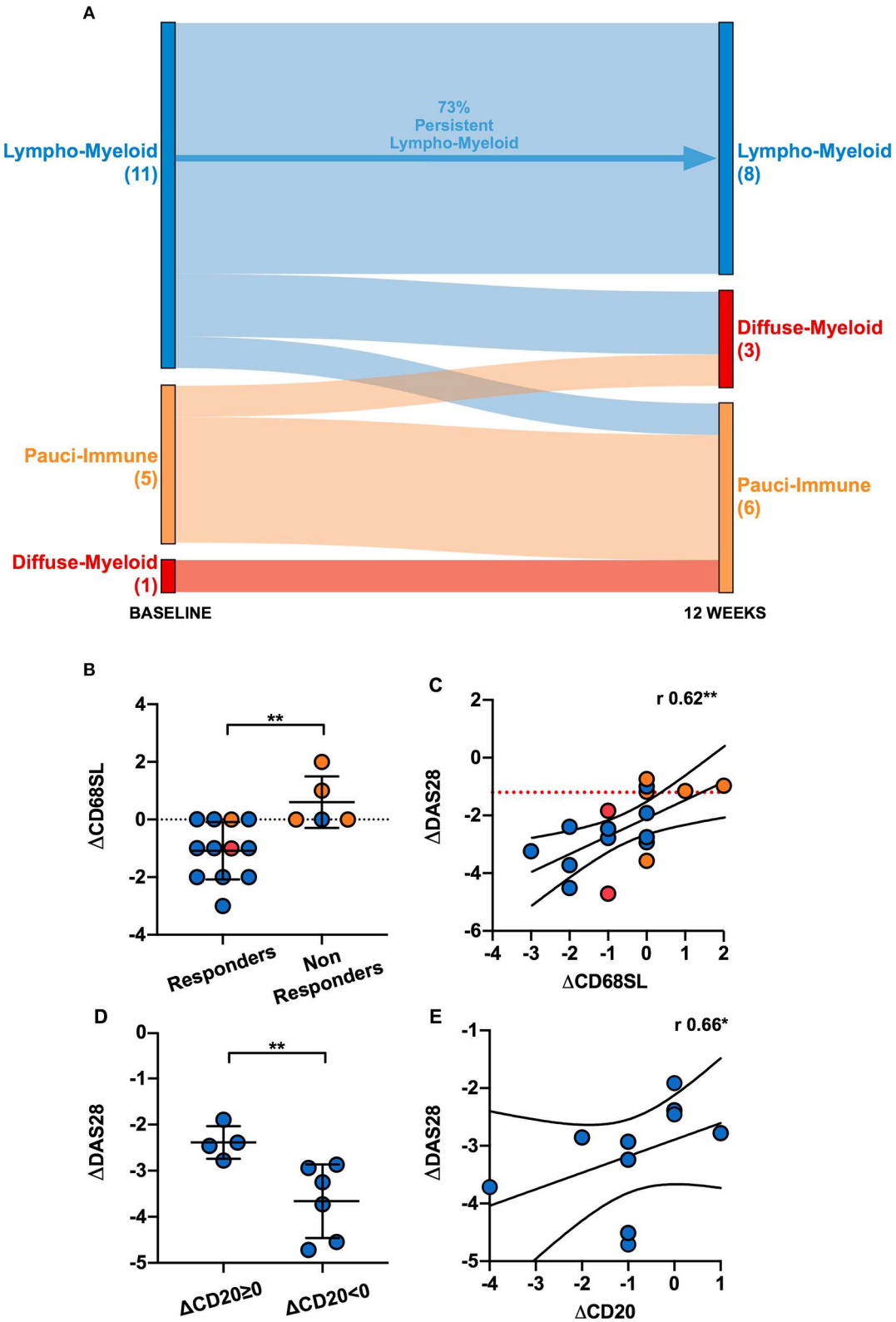

FIGURE 5 | (A) Sankey diagram representing the shift of pathotypes from pre- to post-treatment of the 17 patients who had gradable tissue both at baseline and 12-weeks. **(B)** Comparison of the delta (Δ) CD68 sublining (SL) score between responders and non-responders. ΔCD68SL is the difference in the CD68SL

(Continued)

FIGURE 5 | semi-quantitative score (0–4) between post- and pre-treatment. Mean and standard deviation shown. $^{**}p < 0.01$ (Mann-Whitney). **(C)** Correlation plot showing $\Delta DAS28^{[12-weeks-baseline]}$ and $\Delta CD68SL^{[12-weeks-baseline]}$; r Spearman coefficient of correlation, $^{**}p < 0.01$. **(D)** Comparison of ΔDAS28 between patients with same/higher ($\Delta CD20 \geq 0$) or reduced $CD20^+$ B-cells score ($\Delta CD20 < 0$) post treatment. $^{**}p < 0.01$ (Mann-Whitney, mean and standard deviation shown). **(E)** Correlation plot showing $\Delta DAS28^{[12-weeks-baseline]}$ and $\Delta CD20^{[12-weeks-baseline]}$. r Spearman coefficient of correlation, $^{**}p < 0.01$. Only responder lympho-myeloid patients were analyzed in **(D,E)** (10 patients). **(B–E)** Individual dots are color-coded by pathotype (*blue*, lympho-myeloid; *red*, diffuse-myeloid; *orange*, pauci-immune).

pathotype after treatment, in agreement with early works demonstrating a reduced synovial cellular infiltration upon treatment with infliximab (35). We observed that a decrease in the $CD20^+$ B-cell score post-treatment associated with improvement in the DAS28. Thus, depletion of synovial sublining macrophages and B cells are important factors for effective response to anti-TNF treatment. Overall, these data suggest that a shift toward a less inflammatory synovial environment after treatment associates with greater improvement in clinical disease activity, in line with similar observations in early RA patients following csDMARD therapy (7). Because certolizumab-pegol exerts its action by dampening inflammation through inhibition of TNFα, it is reasonable that it does not adequately target the pauci-immune pathotype. Hence, the development of novel therapeutics targeting the fibroblastic synovial component and aberrant nociceptive pathways may be required in the pauci-immune patient cohort and support the notion that a personalized medicine, biomarker driven approach to treating patients with arthritis is required.

In conclusion, we have demonstrated that the analysis of the synovial histopathology may be a valuable tool to discern among clinically indistinguishable patients those with less chance of responding to TNFα-blockade, and additional research efforts are required to properly target the pauci-immune pathotype.

DATA AVAILABILITY STATEMENT

The datasets generated for this study are available on request to the corresponding author.

ETHICS STATEMENT

The studies involving human participants were reviewed and approved by Rec. No. 10/H0801/47 (NRES Committee London Central). The patients/participants provided their written informed consent to participate in this study.

AUTHOR CONTRIBUTIONS

All authors have contributed to different degrees to patient recruitment, data generation, data analysis, and writing and/or revising the manuscript.

FUNDING

This was an Investigator Initiated Study (IIS) sponsored by the host Institution: Queen Mary University of London and part-funded by UCB Pharmaceutical Company, which provided the study drug (certolizumab-pegol). Neither the sponsor, nor UCB participated in the study design, data collection or interpretation. Funding for infrastructure support to the Center for Experimental Medicine and Rheumatology (EMR): Arthritis Research UK Experimental Treatment Center [grant number 20022]. AN funded by Versus Arthritis Clinical Lectureship in Experimental Medicine and Rheumatology [grant number 21890].

ACKNOWLEDGMENTS

We thank all patients who participated to this study, clinical staff who helped with recruitment and laboratory staff who helped with the processing of the histological samples.

SUPPLEMENTARY MATERIAL

The Supplementary Material for this article can be found online at: https://www.frontiersin.org/articles/10.3389/fimmu.2020.00845/full#supplementary-material

REFERENCES

1. Safiri S, Kolahi AA, Hoy D, Smith E, Bettampadi D, Mansournia MA, et al. Global, regional and national burden of rheumatoid arthritis 1990-2017: a systematic analysis of the global burden of disease study 2017. *Ann Rheum Dis*. (2019) 78:1463–71. doi: 10.1136/annrheumdis-2019-215920
2. Salliot C, Finckh A, Katchamart W, Lu Y, Sun Y, Bombardier C, et al. Indirect comparisons of the efficacy of biological antirheumatic agents in rheumatoid arthritis in patients with an inadequate response to conventional disease-modifying antirheumatic drugs or to an anti-tumour necrosis factor agent: a meta-analysis. *Ann Rheum Dis*. (2011) 70:266–71. doi: 10.1136/ard.2010.132134
3. Cuppen BVJ, Welsing PMJ, Sprengers JJ, Bijlsma JWJ, Marijnissen ACA, van Laar JM, et al. Personalized biological treatment for rheumatoid arthritis: a systematic review with a focus on clinical applicability. *Rheumatology*. (2016) 55:826–39. doi: 10.1093/rheumatology/kev421
4. Machold KP, Stamm TA, Nell VPK, Pflugbeil S, Aletaha D, Steiner G, et al. Very recent onset rheumatoid arthritis: clinical and serological patient characteristics associated with radiographic progression over the first years of disease. *Rheumatology*. (2007) 46:342–9. doi: 10.1093/rheumatology/kel237
5. Pitzalis C, Kelly S, Humby F. New learnings on the pathophysiology of RA from synovial biopsies. *Curr Opin Rheumatol*. (2013) 25:334–44. doi: 10.1097/BOR.0b013e32835fd8eb
6. Humby F, Lewis M, Ramamoorthi N, Hackney JA, Barnes MR, Bombardieri M, et al. Synovial cellular and molecular signatures stratify clinical response to csDMARD therapy and predict radiographic progression in early rheumatoid arthritis patients. *Ann Rheum Dis*. (2019) 78:761–72. doi: 10.1136/annrheumdis-2018-214539

7. Lewis MJ, Barnes MR, Blighe K, Goldmann K, Rana S, Hackney JA, et al. Molecular portraits of early rheumatoid arthritis identify clinical and treatment response phenotypes. *Cell Rep*. (2019) 28:2455–70.e5. doi: 10.1016/j.celrep.2019.07.091
8. Lliso-Ribera G, Humby F, Lewis M, Nerviani A, Mauro D, Rivellese F, et al. Synovial tissue signatures enhance clinical classification and prognostic/treatment response algorithms in early inflammatory arthritis and predict requirement for subsequent biological therapy: Results from the pathobiology of early arthritis cohort (PEAC). *Ann Rheum Dis*. (2019) 78:1642–52. doi: 10.1136/annrheumdis-2019-215751
9. Buch MH, Reece RJ, Quinn MA, English A, Cunnane G, Henshaw K, et al. The value of synovial cytokine expression in predicting the clinical response to TNF antagonist therapy (infliximab). *Rheumatology*. (2008) 47:1469–75. doi: 10.1093/rheumatology/ken261
10. Lindberg J, Wijbrandts CA, van Baarsen LG, Nader G, Klareskog L, Catrina A, et al. The gene expression profile in the synovium as a predictor of the clinical response to infliximab treatment in rheumatoid arthritis. *PLoS ONE*. (2010) 5:e11310. doi: 10.1371/journal.pone.0011310
11. van der Pouw Kraan TC, Wijbrandts CA, van Baarsen LG, Rustenburg F, Baggen JM, Verweij CL, et al. Responsiveness to anti-tumour necrosis factor alpha therapy is related to pre-treatment tissue inflammation levels in rheumatoid arthritis patients. *Ann Rheum Dis*. (2008) 67:563–6. doi: 10.1136/ard.2007.081950
12. Dennis G, Holweg CTJ, Kummerfeld SK, Choy DF, Setiadi AF, Hackney JA, et al. Synovial phenotypes in rheumatoid arthritis correlate with response to biologic therapeutics. *Arthritis Res Ther*. (2014) 16:R90. doi: 10.1186/ar4555
13. Arnett FC, Edworthy SM, Bloch DA, McShane DJ, Fries JF, Cooper NS, et al. The American Rheumatism Association 1987 revised criteria for the classification of rheumatoid arthritis. *Arthritis Rheum*. (1988) 31:315–24. doi: 10.1002/art.1780310302
14. NICE. *Adalimumab, Etanercept, Infliximab, Certolizumab Pegol, Golimumab, Tocilizumab and Abatacept for Rheumatoid Arthritis Not Previously Treated With DMARDs or After Conventional DMARDs Only Have Failed*. Technology appraisal guidance (2017). p. 1–82.
15. Kelly S, Humby F, Filer A, Ng N, Di Cicco M, Hands RE, et al. Ultrasound-guided synovial biopsy: a safe, well-tolerated and reliable technique for obtaining high-quality synovial tissue from both large and small joints in early arthritis patients. *Ann Rheum Dis*. (2015) 74:611–7. doi: 10.1136/annrheumdis-2013-204603
16. Naredo E, Möller I, Cruz A, Carmona L, Garrido J. Power doppler ultrasonographic monitoring of response to anti-tumor necrosis factor therapy in patients with rheumatoid arthritis. *Arthritis Rheum*. (2008) 58:2248–56. doi: 10.1002/art.23682
17. Humby F, Bombardieri M, Manzo A, Kelly S, Blades MC, Kirkham B, et al. Ectopic lymphoid structures support ongoing production of class-switched autoantibodies in rheumatoid synovium. *PLoS Med*. (2009) 6:e1. doi: 10.1371/journal.pmed.0060001
18. van Baarsen LGM, Wijbrandts CA, Timmer TCG, van Der Pouw-kraan TCTM, Tak PP, Verweij CL. Synovial tissue heterogeneity in rheumatoid arthritis in relation to disease activity and biomarkers in peripheral blood. *Arthritis Rheum*. (2010) 62:1602–7. doi: 10.1002/art.27415
19. Stephenson W, Donlin LT, Butler A, Rozo C, Bracken B, Rashidfarrokhi A, et al. Single-cell RNA-seq of rheumatoid arthritis synovial tissue using low-cost microfluidic instrumentation. *Nat Commun*. (2018) 9:710–91. doi: 10.1038/s41467-017-02659-x
20. Zhang F, Wei K, Slowikowski K, Fonseka CY, Rao DA, Kelly S, et al. Defining inflammatory cell states in rheumatoid arthritis joint synovial tissues by integrating single-cell transcriptomics and mass cytometry. *Nat Immunol*. (2019) 20:928–42. doi: 10.1038/s41590-019-0378-1
21. van der Heijde D, Keystone EC, Curtis JR, Landewé RB, Schiff MH, Khanna D, et al. Timing and magnitude of initial change in disease activity score 28 predicts the likelihood of achieving low disease activity at 1 year in rheumatoid arthritis patients treated with certolizumab pegol: a analysis of the RAPID 1 trial. *J Rheumatol*. (2012) 39:1326–33. doi: 10.3899/jrheum.111171
22. Berenbaum F, Pham T, Claudepierre P, de Chalus T, Joubert J-M, Saadoun C, et al. Early non-response to certolizumab pegol in rheumatoid arthritis predicts treatment failure at one year. Data from a randomised Phase III clinical trial. *Joint Bone Spine*. (2017) 85:59–64. doi: 10.1016/j.jbspin.2017.01.011
23. Smolen JS, Aletaha D. Rheumatoid arthritis therapy reappraisal: strategies, opportunities and challenges. *Nat Rev Rheumatol*. (2015) 11:276–89. doi: 10.1038/nrrheum.2015.8
24. Orange DE, Agius P, DiCarlo EF, Robine N, Geiger H, Szymonifka J, et al. Machine learning integration of rheumatoid arthritis synovial histology and RNAseq data identifies three disease subtypes. *Arthritis Rheumatol*. (2018) 70:690-701. doi: 10.1002/art.40428
25. Klaasen R, Thurlings RM, Wijbrandts CA, van Kuijk AW, Baeten D, Gerlag DM, et al. The relationship between synovial lymphocyte aggregates and the clinical response to infliximab in rheumatoid arthritis: a prospective study. *Arthritis Rheum*. (2009) 60:3217–24. doi: 10.1002/art.24913
26. Cañete JD, Celis R, Moll C, Izquierdo E, Marsal S, Sanmartí R, et al. Clinical significance of synovial lymphoid neogenesis and its reversal after anti-tumour necrosis factor alpha therapy in rheumatoid arthritis. *Ann Rheum Dis*. (2009) 68:751–6. doi: 10.1136/ard.2008.089284
27. Badot V, Galant C, Nzeusseu Toukap A, Théate I, Maudoux A-L, Van den Eynde BJ, et al. Gene expression profiling in the synovium identifies a predictive signature of absence of response to adalimumab therapy in rheumatoid arthritis. *Arthritis Res Ther*. (2009) 11:R57. doi: 10.1186/ar2678
28. Ulfgren AK, Andersson U, Engström M, Klareskog L, Maini RN, Taylor PC. Systemic anti-tumor necrosis factor alpha therapy in rheumatoid arthritis down-regulates synovial tumor necrosis factor alpha synthesis. *Arthritis Rheum*. (2000) 43:2391–6. doi: 10.1002/1529-0131(200011)43:11<2391::AID-ANR3>3.0.CO;2-F
29. Haringman JJ, Gerlag DM, Zwinderman AH, Smeets TJM, Kraan MC, Baeten D, et al. Synovial tissue macrophages: a sensitive biomarker for response to treatment in patients with rheumatoid arthritis. *Ann Rheum Dis*. (2005) 64:834–8. doi: 10.1136/ard.2004.029751
30. Wijbrandts CA, Vergunst CE, Haringman JJ, Gerlag DM, Smeets TJM, Tak PP. Absence of changes in the number of synovial sublining macrophages after ineffective treatment for rheumatoid arthritis: implications for use of synovial sublining macrophages as a biomarker. *Arthritis Rheum*. (2007) 56:3869–71. doi: 10.1002/art.22964
31. Humby F, Kelly S, Hands R, Rocher V, DiCicco M, Ng N, et al. Use of ultrasound-guided small joint biopsy to evaluate the histopathologic response to rheumatoid arthritis therapy: recommendations for application to clinical trials. *Arthritis Rheumatol*. (2015) 67:2601–10. doi: 10.1002/art.39235
32. Smeets TJM, Kraan MC, van Loon ME, Tak P-P. Tumor necrosis factor alpha blockade reduces the synovial cell infiltrate early after initiation of treatment, but apparently not by induction of apoptosis in synovial tissue. *Arthritis Rheum*. (2003) 48:2155–62. doi: 10.1002/art.11098
33. Smith MD, Barg E, Weedon H, Papengelis V, Smeets T, Tak PP, et al. Microarchitecture and protective mechanisms in synovial tissue from clinically and arthroscopically normal knee joints. *Ann Rheum Dis*. (2003) 62:303–7. doi: 10.1136/ard.62.4.303
34. Choi IY, Gerlag DM, Holzinger D, Roth J, Tak PP. From synovial tissue to peripheral blood: myeloid related protein 8/14 is a sensitive biomarker for effective treatment in early drug development in patients with rheumatoid arthritis. *PLoS ONE*. (2014) 9:e106253. doi: 10.1371/journal.pone.0106253
35. Taylor PC, Peters AM, Paleolog E, Chapman PT, Elliott MJ, McCloskey R, et al. Reduction of chemokine levels and leukocyte traffic to joints by tumor necrosis factor alpha blockade in patients with rheumatoid arthritis. *Arthritis Rheum*. (2000) 43:38–47. doi: 10.1002/1529-0131(200001)43:1<38::AID-ANR6>3.0.CO;2-L

Conflict of Interest: The authors declare that the research was conducted in the absence of any commercial or financial relationships that could be construed as a potential conflict of interest.

Copyright © 2020 Nerviani, Di Cicco, Mahto, Lliso-Ribera, Rivellese, Thorborn, Hands, Bellan, Mauro, Boutet, Giorli, Lewis, Kelly, Bombardieri, Humby and Pitzalis. This is an open-access article distributed under the terms of the Creative Commons Attribution License (CC BY). The use, distribution or reproduction in other forums is permitted, provided the original author(s) and the copyright owner(s) are credited and that the original publication in this journal is cited, in accordance with accepted academic practice. No use, distribution or reproduction is permitted which does not comply with these terms.

frontiers in Immunology

REVIEW
published: 13 May 2020
doi: 10.3389/fimmu.2020.00937

Transcriptional Regulation of Osteoclastogenesis: The Emerging Role of KLF2

*Daniela Rolph and Hiranmoy Das**

Department of Pharmaceutical Sciences, Jerry H. Hodge School of Pharmacy, Texas Tech University Health Sciences Center, Amarillo, TX, United States

Dysregulation of osteoclastic differentiation and its activity is a hallmark of various musculoskeletal disease states. In this review, the complex molecular factors underlying osteoclastic differentiation and function are evaluated. The emerging role of KLF2 in regulation of osteoclastic differentiation is examined, specifically in the context of rheumatoid arthritis in which it has been most extensively studied among the musculoskeletal diseases. The therapies that exist to manage diseases associated with osteoclastogenesis are numerous and diverse. They are varied in their mechanisms of action and in the outcomes they produce. For this review, therapies targeting osteoclasts will be emphasized, though it should be noted that many therapies exist which bolster the action of osteoblasts. A new targeted molecular approach is under investigation for the future potential therapeutic development of rheumatoid arthritis.

Keywords: rheumatoid arthritis, osteoclasts, KLF2, differentiation, transcriptional regulation

OPEN ACCESS

Edited by:
Daniela Frasca,
University of Miami, United States

Reviewed by:
Fayez Safadi,
Northeast Ohio Medical University, United States
A. K. M. Nawshad Hossian,
University of Louisiana at Monroe, United States

***Correspondence:**
Hiranmoy Das
hiranmoy.das@ttuhsc.edu

Specialty section:
This article was submitted to Autoimmune and Autoinflammatory Disorders, a section of the journal Frontiers in Immunology

Received: *10 December 2019*
Accepted: *22 April 2020*
Published: *13 May 2020*

Citation:
Rolph D and Das H (2020) Transcriptional Regulation of Osteoclastogenesis: The Emerging Role of KLF2. Front. Immunol. 11:937. doi: 10.3389/fimmu.2020.00937

INTRODUCTION

Bone is a dynamic tissue which is constantly being remodeled. Its organic and inorganic components are formed by osteoblasts and degraded by osteoclasts. Bone critically contributes to systemic metabolic processes and regulation of blood calcium by acting as a reservoir, which can be liberated or stored as needed due to the specialized actions of osteoclasts and osteoblasts. Osteoclasts are specialized bone cells of myeloid origin that participate in skeletal turnover by resorbing bone. They are tissue-specific macrophage derivatives that exert their resorptive actions by carving out pits in bone via chemical secretions. Osteoclasts are critical to bone repair from micro-damage due to daily wear and tear and also play an important role in fracture healing (1). The dysregulation of their differentiation and activity, however, is a critical component of several diverse disease states of musculoskeletal origin. Impaired bone remodeling has varied and serious consequences, both locally and systemically.

Osteoclasts act in concert with osteoblasts and osteocytes, the other cells that make up bone tissue. Osteoblasts are bone-forming cells of mesenchymal origin that deposit the proteins and minerals that form the bone matrix. Osteoblasts modulate osteoclastic differentiation and activity by producing paracrine factors and other signaling molecules. Osteoblasts produce macrophage-colony stimulating factor (M-CSF) and receptor activator of NF-κB ligand (RANKL), key promoters of osteoclastogenesis (2). Moreover, they inhibit osteoclastic function by secreting osteoprotegerin (OPG) (3). Osteoblasts regulate osteoclasts via mechanisms distinct from the classical means of osteoclastic induction; they also exert their effects via the Wnt pathway, through Semaphorin 3A signaling, and IL-34, among others (4, 5). Osteocytes are bone resident cells; they

are derived from osteoblasts that have become embedded in the matrix they produced. They are the most plentiful skeletal cells, comprising 90–95% of all bone cells. Osteocytes are important signaling cells; they produce soluble factors that regulate bone homeostasis (6). They respond to mechanical stress to induce bone remodeling by promoting osteoblast and osteoclast activity (7). They produce sclerostin, a secreted product that inhibits bone formation by osteoblasts (8). Moreover, they are capable of producing the cytokines that regulate osteoclastic differentiation and function.

OSTEOCLAST ORIGIN AND DIFFERENTIATION

Osteoclasts are myeloid cells derived from hematopoietic progenitors. They originate from the fusion of preosteoclastic cells, becoming multi-nucleated cells in the process (9). Terminally differentiated osteoclasts secrete proteases and acids that mediate their resorptive activity. Osteoclastogenesis depends on two principal hematopoietic factors that are both necessary and sufficient for differentiation: RANKL and M-CSF, also known as colony stimulating factor (CSF-1) (10). Together, these promote expression of osteoclast-specific genes. Moreover, expression of a number of other genes exerts significant influence on the osteogenic process.

The RANKL/RANK/OPG axis critically regulates osteoclastogenesis (11). Developing and mature osteoclasts express RANK, a transmembrane signaling receptor responsible for activating downstream pathways that promote osteoclastic differentiation, activation, and survival. The ligand for this receptor is RANKL, a tumor necrosis factor (TNF)-related polypeptide that is secreted by osteogenic cells to promote *de novo* bone formation as well as remodeling. OPG is a secreted TNF receptor (TNFR)-related protein that is known as a decoy receptor for RANKL. RANKL binding to OPG instead of RANK forestalls osteoclastogenesis and bone resorption. A proper OPG/RANK ratio is critical for balanced bone remodeling (12).

Abbreviations: ATP, Adenosine triphosphate; CCL3, chemokine ligand 3; ChIP, Chromatin immunoprecipitation; COX-2, Cyclooxygenase-2; CSF-1, Colony stimulating factor-1; DMARD, Disease-modifying anti-rheumatic drug; ERK, Extracellular signal-regulated kinase; HAT, histone acetylase transfer; HCl, Hydrochloric acid; HDAC, Histone deacetylase; HDACi, HDAC inhibitor; HSC, Hematopoietic stem cell; Ids, Inhibitors of differentiation; IFN-γ, Interferon gamma; IKK, IκB kinase; IRF2BP2, IFN regulatory factor 2 binding protein 2; IRF8, Interferon regulatory factor; IκB, Inhibitor of κB; JNK, c-Jun N-terminal kinase; KLF, Krüppel-like factor; Lhx2, LIM homeobox 2; MafB, V-maf avian musculoaponeurotic fibrosarcoma oncogene homolog B; MAPK, Mitogen activated protein kinase; mBSA, Methylated bovine serum albumin; MCP-1, Monocyte chemoattractant protein-1; M-CSF, Macrophage colony stimulating factor; MITF, Microphthalmia-associated transcription factor; MMP9, Matrix metalloproteinase; NFATc1, Nuclear factor of activated T cells, cytoplasmic 1; NSAID, Nonsteroidal anti-inflammatory drug; OPG, osteoprotegerin; PAI-1, Plasminogen activator inhibitor; PI3K, Phosphoinositide 3-kinase; PLCγ, Phospholipase C gamma; RA, Rheumatoid arthritis; RANK, Receptor activator of NFκB; RANKL, RANK ligand; ROS, Reactive oxygen species; sRANKL, Soluble RANKL; TNF, Tumor necrosis factor; TNFR, TNF receptor; TRAF, TNF-receptor associated factor; TRAP, Tartrate-resistant acid phosphatase; WT, Wild type.

OSTEOCLAST FUNCTION AND REGULATION

Osteoclasts participate in skeletal turnover by resorbing, or degrading, bone (13). They are polarized cells which create a microenvironment optimal for breaking down the organic and mineral structure of bone. Osteoclasts secrete hydrochloric acid (HCl), which functions to lower pH at the site of bone resorption. Furthermore, they secrete the protease cathepsin K, which works optimally at a lower pH (14). These chemical and enzymatic mechanisms form pits in bone, allowing for future deposition of new bone by osteoblasts.

Osteoclastic activity is essential for balanced bone remodeling (15). Bones constantly experience stress from the mechanical loads placed on them; osteoclasts aid in recovery from micro-damage. In the event of larger-scale damage, osteoclasts promote fracture healing to restore bones to full function. Bone is unique among tissues for its ability to recover from injury without the formation of scar tissue thanks to the orchestrated actions of osteoblasts and osteoclasts.

ROLE OF REACTIVE OXYGEN SPECIES IN OSTEOCLASTOGENESIS

At high concentrations, reactive oxygen species (ROS) can stress cells and bring about deleterious effects. At lower concentrations, however, they can serve as second messengers in various signaling pathways. ROS have been observed to activate mature osteoclasts to enhance bone resorption (16). Their role in osteoclastic cell development has likewise been demonstrated: ROS, including superoxide and hydrogen peroxide, have been identified as important mediators of the osteoclastogenic process, regulating expression of critical proteins such as p38 and JNK (17). Moreover, RANKL has been shown to generate ROS in osteoclastic precursors (18).

CELLULAR INFLUENCE

Skeletal remodeling depends on the harmoniously orchestrated interplay between bone formation by osteoblasts and bone resorption by osteoclasts. Osteoclasts, therefore, develop in an environment populated by several other cell lineages and rely on signals from these cells to develop and function. As has been discussed previously, osteoblasts provide the signals for osteoclastogenesis in the form of secreted RANKL. Moreover, it is increasingly evident that immune cells play a critical role in osteoclastic differentiation, as osteoclasts and their precursors are sensitive to signals from pro- and anti-inflammatory cytokines. This contributes to the pathogenesis of several diseases and provides clues into how bone remodeling changes as people age.

In the past few decades, the role of immune influence on skeletal homeostasis has emerged as a prominent field of study. Chronic upregulation of inflammatory cytokines in individuals of advanced age, termed "inflammaging," has been shown to influence bone health (19). During the process of bone resorption, there is intense cross-talk between

osteoclasts and T cells. T cells secrete cytokines that promote osteoclastic differentiation and activity; furthermore, osteoclasts produce molecules that in turn activate T cells (20). This is especially important in diseases such as rheumatoid arthritis (RA) that have a well-established immune component, but is an important consideration in all diseases related to osteoclastic dysfunction.

OSTEOCLASTS' ROLE IN HEALTH AND DISEASE STATES

Osteoclast dysfunction is a hallmark of a number of disease states. Osteoporosis is the most common metabolic disease, affecting over 10 million people over the age of 50 in the United States alone (21). Osteoporosis usually develops later in life and occurs when bone resorption by osteoclasts outpaces formation by osteoblasts, leading to fragile and brittle bones which are prone to fracture. Osteopetrosis is characterized by abnormally increased bone mass. It is caused by defects in osteoclast differentiation and function (22). It is a hereditary disease marked by mutations in a number of genes encoding proteins important to osteoclastic development and function. Other diseases that affect bone, such as osteoarthritis and bone metastases, are marked by inflammation that exacerbates osteoclastic activity (23, 24). While aberrant osteoclastic activity is implicated in many diseases, in-depth discussion of these diseases is beyond the scope of this review; we will here focus on RA, the impact of osteoclasts on disease progression, and the therapies that may help mitigate the destructiveness of this disease.

RHEUMATOID ARTHRITIS

RA is an autoimmune disease characterized by inflammation and deterioration of small joints. Osteoclasts are the principal mediators of bone destruction in RA. These osteoclasts are activated by signals from T cells. Cross-talk between RANKL and IFN-γ has been shown to be critical for osteoclastic activation in RA (25). Inflammatory cytokines, especially TNF-α, IL-1, and IL-6, promote accelerated bone loss in RA. TNF-α is considered to be particularly important in RA pathogenesis, as it is a known inducer of RANKL and M-CSF expression (26, 27), yet also induces osteoclastic differentiation independent of RANK/RANKL (28). T helper cells can be sub-classified into Th1 and Th2 cells, distinguished by the cytokines they produce. Th1 cells produce IFN-γ and IL-2, while Th2 cells produce IL-4, IL-5, and IL-10. In RA, the ratio of these cell populations is skewed toward the Th1 phenotype, yet the RA synovium is characterized by nearly absent IFN-γ and IL-2 expression, indicating a dysfunction in these cells (29). The anti-osteoclastic activity of IFN-γ is therefore lost; furthermore, these defective Th1 cells can induce inflammatory cytokines, including RANKL, bringing about a microenvironment in which osteoclastic differentiation and activity are greatly increased.

RHEUMATOID ARTHRITIS THERAPY

Most of the treatments for RA focus on inhibiting the proliferation of aberrantly activated immune cells. This in turn affects osteoclasts indirectly, as they rely on signals from activated T cells for their own differentiation and activation. Treatment objectives for RA are to stop inflammation, alleviate symptoms, and prevent long-term damage to joints and organs. NSAIDs are used to relieve pain and inflammation associated with RA. Corticosteroids, including prednisone and its active metabolite prednisolone, have immunosuppressive properties and are therefore used to mitigate inflammation. Administered at low doses, they help patients manage pain and stiffness, while higher doses are prescribed to manage inflammatory flare-ups (30). Methotrexate is a common disease modifying anti-rheumatic drug (DMARD) with anti-proliferative and immunosuppressive properties (31). As a chemotherapeutic agent, it acts as an inhibitor of the enzyme dihydrofolate reductase and therefore halts thymine synthesis, preventing DNA replication and subsequent mitotic division. At the lower dose used to treat RA, it reduces the growth of rapidly dividing cells, including those of the immune system. The specifics of its mechanism of action in autoimmune diseases, however, are not entirely understood (32). TNF-α inhibiting therapies are used to attenuate inflammation in RA. These therapies have been shown to attenuate osteoclastogenic differentiation and activation by reducing B cell-surface RANKL expression as well as lowering serum levels of soluble RANKL (sRANKL) (33).

Despite numerous treatment options, RA remains a difficult disease to manage due to its complex immune underpinnings and degenerative nature. Hence, it is important to develop improved therapeutics which act via novel mechanisms. As will be discussed later in this review, KLF2 plays critical roles in regulating osteoclast differentiation and function and thus is a promising target for the development of new therapies.

REGULATION OF OSTEOCLASTOGENESIS

Cytokines

Human osteoclastogenesis is regulated by two essential cytokines, M-CSF and RANKL. Moreover, it is affected by expression of pro-inflammatory cytokines, as the growing field of osteoimmunology reveals.

Macrophage Colony Stimulating Factor

M-CSF is critical for the survival, proliferation, and differentiation of early osteoclastic precursor cells. It is produced by mesenchymal cells and their derivatives in the bone marrow microenvironment (34). Secretion of M-CSF is constitutive, yet regulated by several other factors. Following the withdrawal of estrogen after menopause, for instance, M-CSF levels increase due to increased circulating levels of the inflammatory molecules IL-1 and TNF-α (35). Furthermore, increased serum levels of parathyroid hormone promote elevated secretion of M-CSF (36).

M-CSF binds to the cell surface receptor c-Fms, bringing about dimerization and tyrosine kinase activation (**Figure 1**) (38). Receptor autophosphorylation promotes downstream

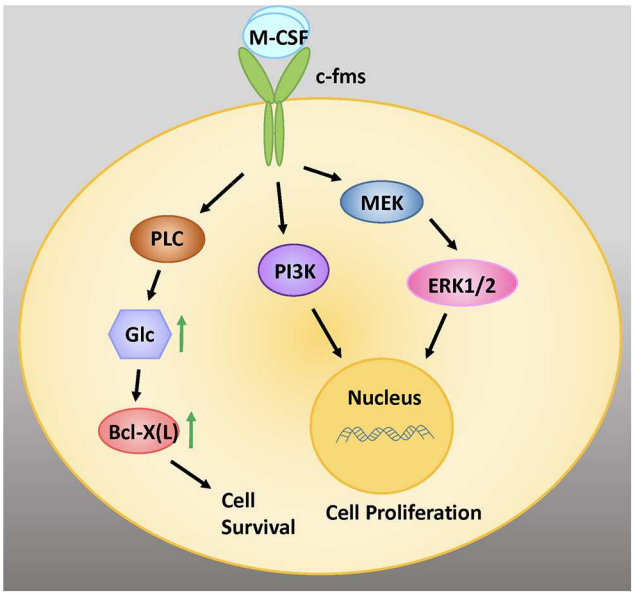

FIGURE 1 | M-CSF signaling is critical for the survival, proliferation, and differentiation of early osteoclastic precursor cells. M-CSF binds to the cell surface receptor c-fms, a tyrosine kinase receptor. Intracellular signaling via the MEK/ERK and PI3 Kinase (PI3K) signaling pathways promote cell proliferation. Signaling via PLC increases intracellular glucose (glc), which increases levels of the anti-apoptotic protein Bcl-X(L), leading to cell survival. Adapted from Stanley and Chitu, *Cold Spring Harb Perspect Biol*, 2014 (37).

signaling that triggers a number of intracellular pathways, including extracellular signal-regulated kinases 1 and 2 (ERK1/2), phosphoinositide 3-kinase (PI3K), and phospholipase C gamma (PLCγ) signaling. Downstream signaling by mitogen activated protein kinases (MAPKs) including ERK has been shown to be instrumental for osteoclast development and function (39).

Receptor Activator of NF-κB Ligand

Receptor Activator of NF-κB Ligand (RANKL) is instrumental for the terminal differentiation of myeloid cells into osteoclasts. RANKL binds to its transmembrane receptor RANK and induces intracellular signaling pathways, which include TRAF6 and c-Fos. These signaling cascades selectively activate nuclear factor of activated T cells, cytoplasmic 1 (NFATc1), a transcription factor critically important for expression of osteoclast-specific genes (40).

Osteoclastogenesis is regulated in part by the balance between RANK and OPG, the decoy receptor for RANKL. OPG is produced by osteoblasts and osteocytes and is either expressed on these cells' surfaces or secreted into the bone marrow space. OPG acts as a decoy receptor for RANKL, binding it and thereby preventing its interaction with RANK on pre-osteoclast cells (41).

Transcription Factors

Following initiation of osteoclastogenesis by M-CSF and RANKL, a number of downstream pathways and gene regulation mechanisms are activated. Osteoclastic differentiation requires activation of transcription factors including microphthalmia-associated transcription factor (MITF), c-Fos, NF-κB, and NFATc1. These transcription factors promote the expression of genes critical for osteoclast phenotype and function. Recently, Kruppel-like factor (KLF) 2 has also emerged as an important regulator of osteoclastic differentiation and activity.

Microphthalmia-Associated Transcription Factor

MITF regulates the development and activity of several cell lineages, including osteoclasts. The isoform MITF-E, which is significantly upregulated in developing osteoclasts but is virtually absent in macrophages, is induced by RANKL and has been shown to be critically important for osteoclastogenesis (42). Moreover, MITF-E has more recently been shown to regulate osteoclastogenesis by modulating the activity of NFATc1 (43). MITF is activated downstream of p38 MAP kinase, which in turn is activated as a result of RANKL signaling. MITF is crucial to the expression of genes encoding osteoclast-specific proteins tartrate-resistant acid phosphatase (TRAP) and cathepsin K (2).

NFATc1, NF-κB, and c-Fos

NFATc1 is a transcription factor that is amplified downstream of RANKL activation (11). RANKL signaling via TNF-receptor associated factor 6 (TRAF6) leads to auto-amplification of NFATc1, the master transcription factor regulating osteoclastogenesis (44). Intermediate signals downstream of TRAF6 are mediated via NF-κB and c-Fos (**Figure 2**) (45).

NF-κB is a family of transcription factors that mediate a number of cellular processes. Notably, NF- κB signaling is involved in inflammatory gene transcription; moreover, it is known to mediate RANKL induced osteoclastogenesis (46). In the absence of an activator ligand, the p50 and p65 subunits of NF-κB are inhibited by their interaction with the inhibitor of κB (IκB) protein, which prevents their nuclear translocation. In the "on" state, IκB is phosphorylated by IκB kinase (IKK), which marks it for polyubiquitination and subsequent proteasomal degradation (47). The free subunits of NF-κB then translocate to the nucleus where they modulate gene transcription. NF-κB signaling is initiated in cells by a variety of stimuli, including cytokines, immune modulators, and other factors. Intracellular signaling cascades are activated not only by RANKL but also by TNF-α, IL-1, and radical oxygen species (ROS), among others. The receptors for these molecules often associate with intracellular adaptor proteins such as TRAFs that facilitate recruitment of the downstream signaling molecules that bring about NF-κB activation. c-Fos is a proto-oncogene that critically regulates osteoclastogenesis (48). Like NF-κB, it is a transcription factor that is activated downstream of RANKL, TNF-α, and IL-1 signaling (49). Moreover, evidence suggests that c-Fos regulates RANK expression (50).

Given the importance of NF-κB in RA pathogenesis, it seems to be a sensible target for RA therapeutic development, however, none have been approved for use in patients (51). While it is important to keep exploring this trajectory, it is critical to investigate the therapeutic potential of emerging targets. Emerging findings show that KLF2 regulates most of

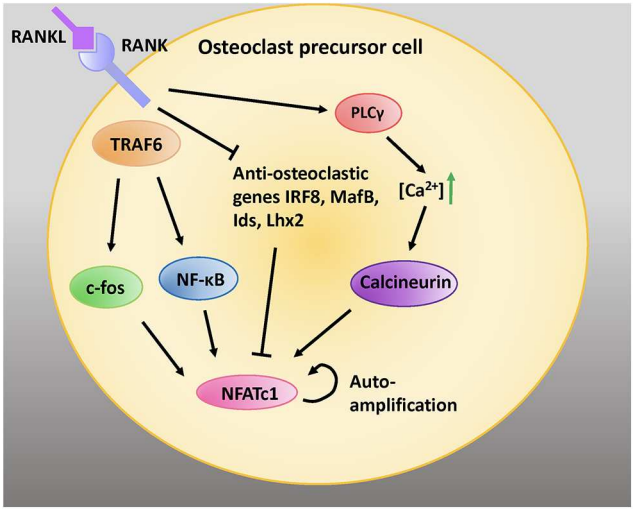

FIGURE 2 | RANK/RANKL signaling is critical for osteoclastic differentiation and function. RANKL binding to RANK expressed on the cell surface of preosteoblastic cells activates intracellular adaptor protein TRAF6. Activation of c-fos and NF-κB pathways induces the NFATc1 gene. Moreover, activation of PLCγ increases intracellular calcium concentrations; this activates the protein calceineurin, which leads to recruitment of NFATc1 to its own promoter which further induces NFATc1. RANK signaling inhibits the anti-osteoclastic genes interferon regulatory factor 8 (IRF8), V-maf avian musculoaponeurotic fibrosarcoma oncogene homolog B (MafB), inhibitors of differentiation (Ids), and LIM homeobox 2 (Lhx2), which inhibit NFATc1 expression. Adapted from Kim and Kim, *J Bone Metab*, 2014 (45).

the inflammatory genes that are regulated by NF-κB, therefore, next we focus on emphasizing the role of KLF2 in regulation of osteoclast differentiation and function in the context of RA and beyond.

KLF2

KLF Structure and Function

Krüppel-like factors (KLF) are a family of DNA-binding zinc-finger proteins that can act as either transcriptional activators or repressors. Eighteen members of the KLF family have been identified so far. Their expression varies widely among tissues, pointing to the specific functions of each isoform (52). KLF family proteins are associated with development, metabolic regulation, and maintenance of homeostasis in diverse organs and tissues, from the heart to muscles to blood cells. Many are essential to life: global knockout of most KLF isoforms *in vivo* causes severe complications or death. KLF4 is especially well-known to researchers due to the role it plays in embryogenesis and for its groundbreaking utility in induced pluripotent stem cell reprograming (53–55).

KLF proteins play a significant role in physiological processes including cell differentiation, growth, and proliferation, as well as in responses to stressors such as apoptosis. Changes in their activity are associated with diverse pathologies, from cardiovascular disease to metabolic aberrations to cancer (56). They share homology with the transcription factor Sp1, which binds CG-rich regions of DNA with its zinc-finger structure; Sp1 and KLF are often classified as members of a common family. The Sp1/KLF family regulates the expression of genes with diverse functions in cell maintenance, development, and homeostasis (57).

KLFs in Bone Biology

Several KLF proteins are involved in bone health and disease. KLF5, expressed in osteoblasts and chondrocytes but not in osteoclasts, is associated with cartilage degradation. This process is mediated by increasing transcription of MMP9 (58). KLF15 has been shown to be upregulated by glucocorticoids, and in turn to impair osteoblast differentiation and bone formation (59). A recent publication demonstrates that KLF10 mediates chondrocyte hypertrophy during development (60). KLF4 expression increases in response to inflammatory stimuli in macrophages and mediates pro-inflammatory signaling pathways in these cells, which may have effects on bone biology given that osteoclasts are derived from myeloid precursors (61). KLF2, discussed in detail below, has been shown to play a critical role in osteoclast and osteoblast development and activity. Further investigation in the field may reveal skeletal involvement of other KLF isoforms.

Physiologic Roles of KLF2

KLF2, also known as lung KLF, is expressed during embryonic development in vascular endothelial cells and is upregulated in endothelial cells subjected to shear stress from prolonged laminar blood flow (62). Homozygous KLF2 knockout is embryonic lethal due to the critical role that KLF2 plays in promoting vessel integrity (63). KLF2 is best known for its importance in lung function, cardiovascular development, and for its atheroprotective qualities (64–66). Moreover, it is a critical regulator of blood cell development, as it promotes erythropoiesis and T cell trafficking (67, 68). Emerging evidence suggests that it also plays a key role in cell differentiation and cellular response to inflammatory stimuli. For instance, KLF2 expression in endothelial cells is suppressed by pro-inflammatory cytokines IL-1β and TNF-α, both of which contribute to the pathogenesis of atherosclerosis. Moreover, myeloid-specific KLF2 deletion results in spontaneous activation of pro-inflammatory myeloid cell activation (69). TNF-α inhibits KLF2 by activating NF-κB and histone deacetylases (HDAC) 3 and 4 (70). In turn, KLF2 has been shown to regulate NF-κB mediated activities, including hypoxia inducible factor (HIF-1α) transcription in monocytes (69, 71). While it does not affect p65 accumulation in the nucleus, KLF2 strongly inhibits its transcriptional activity (72, 73). KLF2 inhibits NF-κB activity via direct interaction with epigenetic regulator p300 and PCAF, which are essential co-activators of NF-κB-directed transcriptional activity (72, 74). Moreover, KLF2 overexpression inhibits intracellular pathways that depend on IL-1β signaling (75). More specifically in the context of RA, global deletion of KLF2 attenuates expression of MMP9 and inflammatory cytokines, contributing to elevated osteoclastogenesis and more aggressive disease progression (76).

Animal Models in KLF2 Studies

The development of animal models for the study of KLF2 is complicated by the fact that global knockout of the gene is embryonic lethal; absent KLF2 precludes proper formation of the vasculature in the developing pup (67). Endothelial KLF2 is essential for life at all stages, and endothelial deletion of KLF2 in adult mice is likewise lethal (77). For that reason, conditional KLF2 knockout in mice is a valuable tool to study the effects of this molecule. To overcome this challenge, two different knockout models are used in the studies detailed below: one is a hemizygous KLF2 knockout, in which the mice have a single copy of the gene instead of the two copies present in wild type animals (76, 78). The other is a monocyte-specific knockout characterized by normal expression of KLF2 in all tissues excluding the monocytes, which don't express any KLF2 (76).

K/BxN serum-induced RA is a useful model to study the immunologic forces at play in RA pathogenesis (79). To induce arthritis in this model, serum from arthritic transgenic K/BxN mice is injected into the foot pad of naïve mice. Signs of arthritis are evident within a few days of injection. The inflammation resulting from serum injection is caused by the formation of autoantibodies against endogenous glucose-6-phosphate isomerase, which leads to immune complexes that activate cells associated with the innate immune response. This reaction mimics the autoimmune nature of RA and this makes for a powerful model for the study of inflammation related to the progression of disease. Similar KLF2 dynamics are observed in K/BxN-induced RA models as well as in samples obtained from RA patients, indicating that this model accurately recapitulates the disease state in humans.

Emerging Roles of KLF2 in Bone Metabolism

It is well-established that KLF2 inhibits pro-inflammatory activation of monocytes (**Figure 3**) (72). Moreover, studies investigating the effects of KLF2 in the context of RA show that, in mouse models of the disease, KLF2 modulates monocyte differentiation and function (78). In this study, KLF2 hemizygous mice were found to express higher levels of pro-inflammatory genes encoding monocyte chemoattractant protein 1 (MCP-1), cyclooxygenase-2 (COX-2), and plasminogen activator inhibitor-1 (PAI-1) than wild type (WT) controls. These molecules exert a pro-inflammatory influence in the context of RA by recruiting monocytes to the synovium, promoting angiogenesis in synovial tissue, and promoting fibrin accumulation in joint tissues, respectively (81–83). Moreover, methylated bovine serum albumin (mBSA) and IL-1β induced arthritis caused greater damage to cartilage and bones in KLF2 hemizygous mice compared to WT controls. In the RA models, higher recruitment of inflammatory monocytes to the joints was observed in KLF2 hemizygous mice compared to WT controls. Bone marrow-derived monocytes cultured *ex vivo* from KLF2 hemizygous mice underwent osteoclastic differentiation much more readily than cells taken from WT mice; moreover, the former osteoclasts possessed more aggressive pit-forming capacity, a measure of their function. Together, the data indicate that KLF2 plays an important role in attenuating inflammation and inhibiting osteoclastogenic differentiation and function in RA.

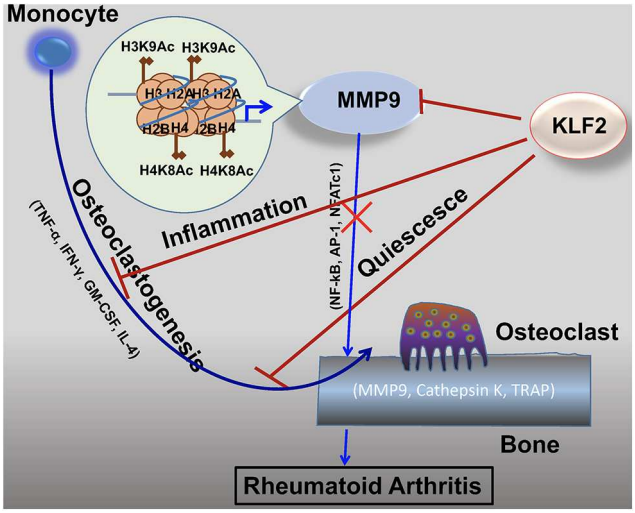

FIGURE 3 | KLF2 attenuates osteoclastogenesis via several complementary mechanisms. KLF2 plays a role in epigenetic modulation of the pro-osteoclastogenic molecule MMP9; data from our lab show that KLF2 knockdown significantly increased enrichment of the active histone marks H3K9Ac and H4K8Ac and respective histone acetylase transfer (HAT) enzymes P300 and PCAF at the enrichment sites for the MMP9 gene (80). KLF2 inhibits pro-inflammatory markers, thereby further inhibiting monocytic activation (72). Furthermore, KLF2 promotes cell quiescence, decreasing osteoclastic activation and function. Altogether, its effects prevent excessive osteoclastic activity, slowing RA disease progression.

While KLF2 has a demonstrable role in osteoclastogenesis, the mechanisms governing this interaction are not well-understood (**Figure 4**). Recent reports detail work done in a K/BxN serum-induced model of rheumatoid arthritis which further illumines the role of KLF2 in regulating disease progression (80). In this study, RA induction was more pronounced in KLF2 hemizygous ($KLF2^{+/-}$) mice compared to wild type (WT) animals; more ankle swelling and more severe immunohistochemical signs of inflammation and tissue damage were detected in the $KLF2^{+/-}$ mice, whereas WT animals showed only mild signs of arthritic pathogenesis. After 7 days of arthritic induction, osteoclast precursor cells were isolated from the bone marrow of $KLF2^{+/-}$ and WT animals and cultured *in vitro*. After 3 and 6 days of culture, osteoclastic differentiation was evaluated by TRAP staining; significantly higher numbers of TRAP stained cells were observed in the $KLF2^{+/-}$ population compared to the WT population. Moreover, differentiated osteoclasts from the $KLF2^{+/-}$ population expressed higher levels of the osteoclastic markers matrix metalloproteinase 9 (MMP9), NFATc1, and v-ATPase than WT cells. Expression of inflammatory molecules was also evaluated in cells isolated from the bone marrow of $KLF2^{+/-}$ and WT mice: q-PCR revealed that cells obtained from $KLF2^{+/-}$ animals express higher levels of the pro-inflammatory molecules IL-1β, IL-6, and TNF-α, higher levels of the chemokines CCL3 and MCP-1, and lower levels of the anti-inflammatory cytokine IL-10 than cells collected from the control group. These findings are consistent with the inflammatory

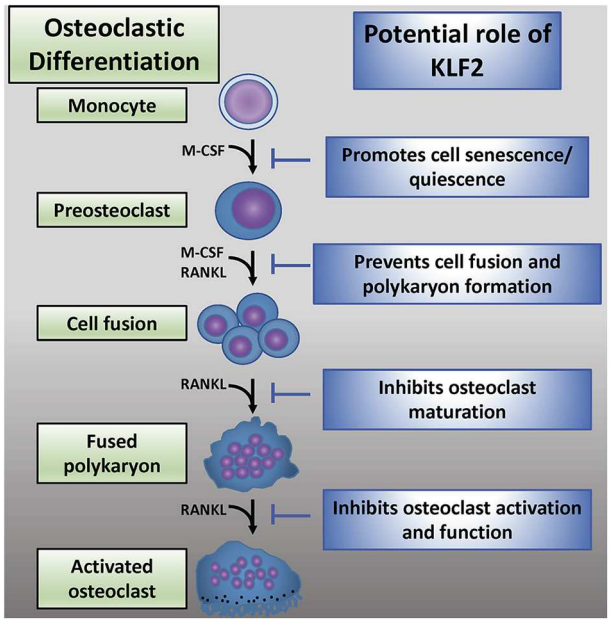

FIGURE 4 | The emerging role of KLF2 in osteoclastic regulation. Osteoclastic differentiation from myeloid precursor cells is critically regulated by M-CSF and RANKL (2). KLF2 may play an inhibitory role at several stages of osteoclastic differentiation, maturation, and activation (72).

nature of RA pathogenesis and demonstrate that KLF2 may play a protective role in bones and surrounding tissue by attenuating inflammation in arthritic joints.

In a subsequent study, K/BxN serum-induced arthritic induction was performed in a monocyte-specific conditional KLF2 knockout mouse model in order to determine whether KLF2 expression in monocytes is important for RA pathogenesis (76). Conditional KLF2$^{-/-}$ mice showed pronounced ankle swelling which caused joint stiffness and impaired movement, whereas WT (KLF2$^{+/+}$) mice showed minimal ankle swelling or distortion. At the tissue level, conditional KLF2$^{-/-}$ mice showed more severe cartilage and subchondral bone degradation, as well as synovial thickening and hyperplasia; moreover, pannus formation and excessive production of fibrous tissue was observed, which is indicative of severe RA progression. To determine the role of monocytes in RA pathogenesis, bone marrow cells were isolated to study osteoclastogenesis and expression of inflammation-related markers. Increased expression levels of MCP-1, IL-1, IL-6, TNF-α, and MMP9 were observed in conditional KLF2$^{-/-}$ mice compared to KLF2$^{+/+}$ mice. In order to evaluate effects of monocyte-specific KLF2 knockout on osteoclastic differentiation and resorptive activity, bone marrow cells were harvested from conditional KLF2$^{-/-}$ and KLF2$^{+/+}$ mice after induction of arthritis. These cells were cultured *in vitro* in osteoclastic differentiation medium and stained for TRAP on days 3 and 6 of culture; much higher counts of TRAP+ cells were identified in the conditional KLF2$^{-/-}$ mice compared to WT animals. Furthermore, osteoclasts were differentiated and cultured on ivory slices to evaluate their pit forming capacity; again, cells from conditional KLF2$^{-/-}$ mice formed much more aggressive osteoclasts. Finally, MMP9 and MMP13 expression was evaluated in differentiated cells; expression of these molecules was significantly elevated in conditional KLF2$^{-/-}$ mice relative to WT controls. These findings support the hypothesis that monocytic expression of KLF2 is critical for attenuating these cells' potential for osteogenic induction and inflammatory reactions.

In order to determine whether K/BxN serum-induced arthritis has any effects on KLF2 expression in monocytes, monocytes were isolated from C57BL/6 mice 7 days after induction of arthritis and q-PCR was performed to determine expression of various markers. Results indicated decreased KLF2 expression in both the bone marrow and in blood monocytes of arthritic mice relative to healthy controls. Furthermore, arthritic mice expressed increased levels of pro-osteoclastic markers TNF-α, MCP-1, MMP1, and MMP9. This indicates that KLF2 expression wanes over the course of arthritic induction, which allows for an increase in expression of pro-inflammatory proteins.

In human arthritic joints, immunohistochemical analysis was carried out to evaluate recruitment of activated (CD68^{+}) monocytes to the inflammatory sites of RA tissues. More severe pathologic clinical manifestations were observed in human RA patients. Significant numbers of CD68^{+} monocytes were identified in all RA tissues evaluated in both the lining and sublining layers. Infiltration of numerous cell types was detected in inflamed RA tissues but not in healthy control tissues. q-PCR was carried out in order to evaluate expression of various molecules in peripheral monocytes in healthy vs. diseased patients. Importantly, this analysis revealed significantly decreased expression of KLF2 in monocytes obtained from diseased patients, as well as increased levels of the inflammatory factors TNF-α, MCP-1, MMP1, and MMP9. While a causal role is not established, these data suggest that a decreased level of KLF2 expression and concomitant increased levels of pro-inflammatory molecules are associated with RA pathogenesis not only in animal models of the disease but also in humans with symptoms of active RA.

It was observed that KLF2 knockdown increased MMP9 and NF-κB (p65) expression, and that KLF2 overexpression attenuated MMP9 and p65 levels. In order to better understand how KLF2 regulates MMP9, epigenetic studies were performed. Enrichment sites for epigenetic marks on the MMP9 promoter were identified and chromatin immunoprecipitation (ChIP) analysis and q-PCR were carried out. These experiments revealed that knockdown of KLF2 significantly increased enrichment of the active histone marks H3K9Ac and H4K8Ac and respective histone acetylase transfer (HAT) enzymes P300 and PCAF at the enrichment sites for the MMP9 gene. These findings indicate that KLF2 plays an important role in epigenetic modulation of the gene encoding MMP9. By inhibiting transcription of this gene, the destructive nature of osteoclasts is largely curtailed.

To test the therapeutic potential of KLF2, we have induced KLF2 using a pharmacological compound, histone deacetylase inhibitor (HDACi) and found that KLF2 expression was increased in myeloid cells both *in vitro* and *in vivo*. Induction of KLF2 significantly reduced osteoclastic

differentiation of monocytes and decreased expression of matrix metalloproteinases in myeloid cells. Specifically in mice, induction of KLF2 in immune cells reduced arthritic inflammation and attenuated joint destruction. Furthermore, co-immunoprecipitation confirmed the direct interaction between KLF2 and HDAC4, thereby providing the groundwork to understand the molecular mechanisms whereby KLF2 regulates RA pathogenesis (80). Altogether, these data demonstrate a novel protective role of KLF2 in regulation of RA severity and progression.

Because KLF2 has demonstrable roles in regulation of RA pathogenesis, it is a promising therapeutic target. Moreover, further research into the pathways downstream of KLF2 activity may elucidate more signaling molecules that can be targeted to modulate disease progression and severity. Moreover, because KLF2 affects osteoclastogenesis, it may be a suitable target for a number of disease states associated with impaired osteoclast differentiation and function.

Similar findings have been reported by other labs showing that KLF2 overexpression in bone marrow-derived macrophages cultured in M-CSF and RANKL leads to lower rates of osteoclastic differentiation compared to control cells (84). Moreover, KLF2 overexpressing cells have lower mRNA expression of cFos, NFATc1, and TRAP and reduced levels of cFos and NFATc1 protein expression. Conversely, KLF2 downregulation with siRNA increases osteoclastic differentiation and leads to decreased expression of cFos, NFATc1, and RANKL mRNA as well as decreased levels of cFos and NFATc1 protein expression. They also found that KLF2 overexpression in primary osteoblasts cultured in osteoblastic differentiation medium containing BMP2, β-glycerophosphate, and ascorbic acid enhances their function by increasing expression of Runx2, alkaline phosphatase (ALP), and bone sialoprotein (BSP). Furthermore, KLF2 silencing decreases osteoblastic differentiation, as evidenced by significantly reduced ALP activity, bone nodule formation, and calcification, as well as decreased expression of osteoblastic marker genes compared to control cells.

This study also identified IFN regulatory factor 2 binding protein 2 (IRF2BP2), a regulator of KLF2, as a potential regulator of osteoclastogenesis and osteoblastogenesis. IRF2BP2 has been shown in several diverse research settings to attenuate inflammation; however, it has been studied less extensively than KLF2 (85, 86). In these studies, IRF2BP2 overexpression in osteoclast precursor cells significantly increases KLF2 expression, decreases osteoclastogenesis, and reduces expression of cFos and NFATc1 at the mRNA and protein levels and RANKL at the mRNA level. Moreover, IRF2BP2 overexpression in osteoblast precursors increases their expression of KLF2 and promotes osteoblastic differentiation and function by increasing expression of Runx2, ALP, and BSP. These findings indicate that IRF2BP2 mediates its effects on osteoblasts and osteoclasts by modulating KLF2. While IRF2BP2 overexpression inhibits osteoclastogenesis, its inhibitory effect is significantly reduced by silencing KLF2 with siRNA. In osteoblasts, IRF2BP2 overexpression increases differentiation, as evidenced by increased Runx2 and ALP expression and increased bone nodule formation; KLF2 silencing in these cells abrogates these effects. While the available data indicate that IRF2PB2 has a strong association with KLF2, the latter molecule appears to be more immediately important for the regulation of osteoclasts and osteoblasts. IRF2PB2 may be a promising anti-inflammatory target in the context of RA therapeutic development, however, much more is known about the role of KLF2 in this disease state. Moreover, it is not well-understood whether IRF2BP2 mediates osteoclast and osteoblast differentiation and function exclusively via KLF2 regulation or if it has effects independent of this downstream mediator.

A growing body of evidence supports the hypothesis that KLF2 regulates not only osteoclasts but also osteoblasts. A report indicates that KLF2 is expressed in osteoblast precursors as well as in mature terminally differentiated cells (87). This study found that osteoblasts cultured for 9 days in an osteogenic medium containing BMP2, β-glycerophosphate, and ascorbic acid expressed higher level of KLF2 throughout the differentiation process at both the mRNA and protein level. Moreover, cells cultured in osteogenic medium express higher levels of the osteoblastic marker genes ALP, osteocalcin, and osterix. Runx2 is a transcription factor that serves as the master controller for osteoblastic differentiation as well as the bone forming functions of mature osteoblasts (88). ALP, osteocalcin, and osterix genes are regulated by Runx2, which was also increased in expression throughout the differentiation process in a time-dependent manner at both the mRNA and protein levels. siRNA-mediated KLF2 knockdown led to reduced expression of Runx2, ALP, osteocalcin, and osterix in cells cultured in osteogenic medium, implying that KLF2 is a critical regulator of osteogenic differentiation. Moreover, KLF2 overexpression significantly enhanced Runx2, ALP, osteocalcin, and osterix expression at the mRNA and protein levels in osteoblastic progenitors cultured in osteogenic medium, further supporting the role of KLF2 in osteoblastic differentiation. KLF2 promotes osteoblastic activity by increasing expression of Runx2; importantly, immunoprecipitation experiments performed in HEK293T cells (human embryonic kidney cells) revealed that KLF2 physically interacts directly with Runx2 and thus promotes expression of ALP, osterix, and osteocalcin in osteoblast precursor cells. These findings illustrate the important role that KLF2 plays in promoting healthy skeletal remodeling and bone function.

Taken together, the data from our lab and those presented by other research groups provide a well-rounded view of the mechanisms by which KLF2 attenuates bone resorption and promotes bone formation. In the context of RA, curtailing the aggressiveness of osteoclasts is especially important, but the additional positive effects of KLF2 on osteoblasts indicate that this molecule may be a useful target in a number of diseases affecting the bones. Currently, most available medications aim to either reduce bone resorption or promote bone formation, but targeting KLF2 may lead to the development of therapies with dual functions. This emerging focus of study deserves the attention of researchers and holds great promise for future therapeutic developments.

CONCLUSIONS AND FUTURE DIRECTIONS

Osteoclasts play a critical role in human health and disease. They resorb bone in response to a number of factors secreted by resident bone cells as well as cells of immune system. They are necessary for the maintenance of skeletal health and maintaining homeostasis: insufficient activity leads to dense bones, while excessive activity results in brittle and fragile bones. While the role of osteoclasts in diseases such as osteoporosis is well-understood, how their dysfunction contributes to other diseases remains unknown. Moreover, certain targets represent untapped therapeutic potential; as new molecular pathways regulating osteoclasts are elucidated, new medications may be developed to treat osteoclast-related diseases. One such molecular target is KLF2: while its role in vascular development has been well-established, the mechanisms by which it regulates monocytes' differentiation into osteoclasts, as well as their activation and function are gradually being discovered. Moreover, their role in the promotion of osteoblastic differentiation and function further supports their utility as a target in bone metabolic diseases. Modulating KLF2 may prove useful to treat diseases involving osteoclasts.

AUTHOR CONTRIBUTIONS

Both authors contributed in writing manuscript and constructing figures.

FUNDING

This work was supported in part by National Institutes of Health grants, R01AR068279 (NIAMS), STTR 1R41EY024217 (NEI), and STTR 1R41AG057242 (NIA).

REFERENCES

1. Schell H, Lienau J, Epari DR, Seebeck P, Exner C, Muchow S, et al. Osteoclastic activity begins early and increases over the course of bone healing. *Bone*. (2006) 38:547–54. doi: 10.1016/j.bone.2005.09.018
2. Boyle W, Simonet WS, Lacey D. Osteoclast differentiation and activation. *Nature*. (2003) 337–42. doi: 10.1038/nature01658
3. Simonet WS, Lacey DL, Dunstan CR, Kelley M, Chang MS, Luthy R, et al. Osteoprotegerin: a novel secreted protein involved in the regulation of bone density. *Cell*. (1997) 89:309–19. doi: 10.1016/S0092-8674(00)80209-3
4. Yamashita T, Takahashi N, Udagawa N. New roles of osteoblasts involved in osteoclast differentiation. *World J Orthop*. (2012) 3:175–81. doi: 10.5312/wjo.v3.i11.175
5. Rolph DN, Deb M, Kanji S, Greene CJ, Das M, Joseph M, et al. Ferutinin directs dental pulp-derived stem cells towards the osteogenic lineage by epigenetically regulating canonical Wnt signaling. *Biochim Biophys Acta Mol Basis Dis*. (2018) 1866:165314. doi: 10.1016/j.bbadis.2018.10.032
6. Schaffler MB, Kennedy OD. Osteocyte signaling in bone. *Curr Osteoporos Rep*. (2012) 10:118–25. doi: 10.1007/s11914-012-0105-4
7. Burr DB, Martin RB, Schaffler MB, Radin EL. Bone remodeling in response to in vivo fatigue microdamage. *J Biomech*. (1985) 18:189–200. doi: 10.1016/0021-9290(85)90204-0
8. Poole KE, van Bezooijen RL, Loveridge N, Hamersma H, Papapoulos SE, Lowik CW, et al. Sclerostin is a delayed secreted product of osteocytes that inhibits bone formation. *FASEB J*. (2005) 19:1842–4. doi: 10.1096/fj.05-4221fje
9. Miyamoto T. Regulators of osteoclast differentiation and cell-cell fusion. *Keio J Med*. (2011) 60:101–5. doi: 10.2302/kjm.60.101
10. Boyce BF. Advances in the regulation of osteoclasts and osteoclast functions. *J Dent Res*. (2013) 92:860–7. doi: 10.1177/0022034513500306
11. Boyce BF. Advances in osteoclast biology reveal potential new drug targets and new roles for osteoclasts. *J Bone Miner Res*. (2013) 28:711–22. doi: 10.1002/jbmr.1885
12. Wada T, Nakashima T, Hiroshi N, Penninger JM. RANKL-RANK signaling in osteoclastogenesis and bone disease. *Trends Mol Med*. (2006) 12:17–25. doi: 10.1016/j.molmed.2005.11.007
13. Boyce BF, Rosenberg E, de Papp AE, Duong LT. The osteoclast, bone remodelling and treatment of metabolic bone disease. *Eur J Clin Invest*. (2012) 42:1332–41. doi: 10.1111/j.1365-2362.2012.02717.x
14. Blair HC. How the osteoclast degrades bone. *Bioessays*. (1998) 20:837–46. doi: 10.1002/(SICI)1521-1878(199810)20:10<837::AID-BIES9>3.0.CO;2-D
15. Hadjidakis DJ, Androulakis II. Bone remodeling. *Ann N Y Acad Sci*. (2006) 1092:385–96. doi: 10.1196/annals.1365.035
16. Garrett IR, Boyce BF, Oreffo RO, Bonewald L, Poser J, Mundy GR. Oxygen-derived free radicals stimulate osteoclastic bone resorption in rodent bone *in vitro* and *in vivo*. *J Clin Invest*. (1990) 85:632–9. doi: 10.1172/JCI114485
17. Rhee SG. Redox signaling: hydrogen peroxide as intracellular messenger. *Exp Mol Med*. (1999) 31:53–9. doi: 10.1038/emm.1999.9
18. Lee NK, Choi YG, Baik JY, Han SY, Jeong DW, Bae YS, et al. A crucial role for reactive oxygen species in RANKL-induced osteoclast differentiation. *Blood*. (2005) 106:852–9. doi: 10.1182/blood-2004-09-3662
19. Pietschmann P, Mechtcheriakova D, Meshcheryakova A, Foger-Samwald U, Ellinger I. Immunology of osteoporosis: a mini-review. *Gerontology*. (2016) 62:128–37. doi: 10.1159/000431091
20. D'Amico L, Roato I. Cross-talk between T cells and osteoclasts in bone resorption. *Bonekey Rep*. (2012) 1:82. doi: 10.1038/bonekey.2012.82
21. Wright NC, Looker AC, Saag KG, Curtis JR, Delzell ES, Randall S, et al. The recent prevalence of osteoporosis and low bone mass in the United States based on bone mineral density at the femoral neck or lumbar spine. *J Bone Miner Res*. (2014) 29:2520–6. doi: 10.1002/jbmr.2269
22. Stark Z, Savarirayan R. *Osteopetrosis*. *Orphanet J Rare Dis*. (2009) 4:5. doi: 10.1186/1750-1172-4-5
23. Findlay DM, Atkins GJ. Osteoblast-Chondrocyte interactions in osteoarthritis. *Curr Osteoporos Rep*. (2014) 12:127–34. doi: 10.1007/s11914-014-0192-5
24. Maurizi A, Rucci N. The osteoclast in bone metastasis: player and target. *Cancers*. (2018) 10:218. doi: 10.3390/cancers10070218
25. Sato K, Takayanagi H. Osteoclasts, rheumatoid arthritis, and osteoimmunology. *Curr Opin Rheumatol*. (2006) 18:419–26. doi: 10.1097/01.bor.0000231912.24740.a5
26. Zhang YH, Heulsmann A, Tondravi MM, Mukherjee A, Abu-Amer Y. Tumor necrosis factor-alpha (TNF) stimulates RANKL-induced osteoclastogenesis via coupling of TNF type 1 receptor and RANK signaling pathways. *J Biol Chem*. (2001) 276:563–8. doi: 10.1074/jbc.M008198200
27. Kitaura H, Zhou P, Kim HJ, Novack DV, Ross FP, Teitelbaum SL. M-CSF mediates TNF-induced inflammatory osteolysis. *J Clin Invest*. (2005) 115:3418–27. doi: 10.1172/JCI26132
28. Kobayashi K, Takahashi N, Jimi E, Udagawa N, Takami M, Kotake S, et al. Tumor necrosis factor α stimulates osteoclast differentiation by a mechanism independent of the ODF/RANKL-RANK interaction. *J Exp Med*. (2000) 191:275–86. doi: 10.1084/jem.191.2.275
29. Schulze-Koops H, Kalden JR. The balance of Th1/Th2 cytokines in rheumatoid arthritis. *Best Pract Res Clin Rheumatol*. (2001) 15:677–91. doi: 10.1053/berh.2001.0187
30. O'Dell JR. Therapeutic strategies for rheumatoid arthritis. *N Engl J Med*. (2004) 350:2591–602. doi: 10.1056/NEJMra040226

31. Shinde CG, Venkatesh MP, Kumar TM, Shivakumar HG. Methotrexate: a gold standard for treatment of rheumatoid arthritis. *J Pain Palliat Care Pharmacother*. (2014) 28:351–8. doi: 10.3109/15360288.2014.959238
32. Brown PM, Pratt AG, Isaacs JD. Mechanism of action of methotrexate in rheumatoid arthritis, and the search for biomarkers. *Nat Rev Rheumatol*. (2016) 12:731–42. doi: 10.1038/nrrheum.2016.175
33. Perpetuo IP, Caetano-Lopes J, Rodrigues AM, Campanilho-Marques R, Ponte C, Canhao H, et al. Effect of tumor necrosis factor inhibitor therapy on osteoclasts precursors in rheumatoid arthritis. *Biomed Res Int*. (2017) 2017:2690402. doi: 10.1155/2017/2690402
34. Udagawa N, Takahashi N, Akatsu T, Tanaka H, Sasaki T, Nishihara T, et al. Origin of osteoclasts: mature monocytes and macrophages are capable of differentiating into osteoclasts under a suitable microenvironment prepared by bone marrow-derived stromal cells. *Proc Natl Acad Sci USA*. (1990) 87:7260–4. doi: 10.1073/pnas.87.18.7260
35. Kimble RB, Srivastava S, Ross FP, Matayoshi A, Pacifici R. Estrogen deficiency increases the ability of stromal cells to support murine osteoclastogenesis via an interleukin-1and tumor necrosis factor-mediated stimulation of macrophage colony-stimulating factor production. *J Biol Chem*. (1996) 271:28890–7. doi: 10.1074/jbc.271.46.28890
36. Weir EC, Lowik CW, Paliwal I, Insogna KL. Colony stimulating factor-1 plays a role in osteoclast formation and function in bone resorption induced by parathyroid hormone and parathyroid hormone-related protein. *J Bone Miner Res*. (1996) 11:1474–81. doi: 10.1002/jbmr.5650111014
37. Stanley ER, Chitu V. CSF-1 receptor signaling in myeloid cells. *Cold Spring Harb Perspect Biol*. (2014) 6:1–21. doi: 10.1101/cshperspect.a021857
38. Ross FP. M-CSF, c-Fms, and signaling in osteoclasts and their precursors. *Ann N Y Acad Sci*. (2006) 1068:110–6. doi: 10.1196/annals.1346.014
39. Lee K, Seo I, Choi MH, Jeong D. Roles of mitogen-activated protein kinases in osteoclast biology. *Int J Mol Sci*. (2018) 19:3004. doi: 10.3390/ijms19103004
40. Takayanagi H, Kim S, Koga T, Nishina H, Isshiki M, Yoshida H, et al. Induction and activation of the transcription factor NFATc1 (NFAT2) integrate RANKL signaling in terminal differentiation of osteoclasts. *Dev Cell*. (2002) 3:889–901. doi: 10.1016/S1534-5807(02)00369-6
41. Boyce BF, Xing L. Functions of RANKL/RANK/OPG in bone modeling and remodeling. *Arch Biochem Biophys*. (2008) 473:139–46. doi: 10.1016/j.abb.2008.03.018
42. Lu SY, Li M, Lin YL. Mitf induction by RANKL is critical for osteoclastogenesis. *Mol Biol Cell*. (2010) 21:1763–71. doi: 10.1091/mbc.e09-07-0584
43. Lu SY, Li M, Lin YL. Mitf regulates osteoclastogenesis by modulating NFATc1 activity. *Exp Cell Res*. (2014) 328:32–43. doi: 10.1016/j.yexcr.2014.08.018
44. Takayanagi H. The role of NFAT in osteoclast formation. *Ann N Y Acad Sci*. (2007) 1116:227–37. doi: 10.1196/annals.1402.071
45. Kim JH, Kim N. Regulation of NFATc1 in osteoclast differentiation. *J Bone Metab*. (2014) 21:233–41. doi: 10.11005/jbm.2014.21.4.233
46. Abu-Amer Y. NF-κB signaling and bone resorption. *Osteoporos Int*. (2013) 24:2377–86. doi: 10.1007/s00198-013-2313-x
47. Brown KD, Claudio E, Siebenlist U. The roles of the classical and alternative nuclear factor-kappaB pathways: potential implications for autoimmunity and rheumatoid arthritis. *Arthritis Res Ther*. (2008) 10:212. doi: 10.1186/ar2457
48. Grigoriadis AE, Wang ZQ, Cecchini MG, Hofstetter W, Felix R, Fleisch HA, et al. c-Fos: a key regulator of osteoclast-macrophage lineage determination and bone remodeling. *Science*. (1994) 266:443–8. doi: 10.1126/science.7939685
49. Boyce BF, Yamashita T, Yao Z, Zhang Q, Li F, Xing L. Roles for NF-κB and c-Fos in osteoclasts. *J Bone Miner Metab*. (2005) (Supp1. 23):1–5. doi: 10.1007/BF03026317
50. Arai A, Mizoguchi T, Harada S, Kobayashi Y, Nakamichi Y, Yasuda H, et al. Fos plays an essential role in the upregulation of RANK expression in osteoclast precursors within the bone microenvironment. *J Cell Sci*. (2012) 125:2910–7. doi: 10.1242/jcs.099986
51. Makarov SS. NF-kappa B in rheumatoid arthritis: a pivotal regulator of inflammation, hyperplasia, and tissue destruction. *Arthritis Res*. (2001) 3:200–6. doi: 10.1186/ar300
52. Pollak NM, Hoffman M, Goldberg IJ, Drosatos K. Kruppel-like factors: crippling and un-crippling metabolic pathways. *JACC Basic Transl Sci*. (2018) 3:132–56. doi: 10.1016/j.jacbts.2017.09.001
53. Takahashi K, Tanabe K, Ohnuki M, Narita M, Ichisaka T, Tomoda K, et al. Induction of pluripotent stem cells from adult human fibroblasts by defined factors. *Cell*. (2007) 131:861–72. doi: 10.1016/j.cell.2007.11.019
54. Chen K, Long Q, Xing G, Wang T, Wu Y, Li L, et al. Heterochromatin loosening by the Oct4 linker region facilitates Klf4 binding and iPSC reprogramming. *EMBO J*. (2020) 39:e99165. doi: 10.15252/embj.201899165
55. Takahashi K, Yamanaka S. Induction of pluripotent stem cells from mouse embryonic and adult fibroblast cultures by defined factors. *Cell*. (2006) 126:663–76. doi: 10.1016/j.cell.2006.07.024
56. McConnell BB, Yang VW. Mammalian Kruppel-like factors in health and diseases. *Physiol Rev*. (2010) 90:1337–81. doi: 10.1152/physrev.00058.2009
57. Kadonaga JT, Carner KR, Masiarz FR, Tjian R. Isolation of cDNA encoding transcription factor Sp1 and functional analysis of the DNA binding domain. *Cell*. (1987) 51:1079–90. doi: 10.1016/0092-8674(87)90594-0
58. Shinoda Y, Ogata N, Higashikawa A, Manabe I, Shindo T, Yamada T, et al. Kruppel-like factor 5 causes cartilage degradation through transactivation of matrix metalloproteinase 9. *J Biol Chem*. (2008) 283:24682–9. doi: 10.1074/jbc.M709857200
59. Yang Y, Su Y, Wang D, Chen Y, Liu Y, Luo S, et al. Tanshinol rescues the impaired bone formation elicited by glucocorticoid involved in KLF15 pathway. *Oxid Med Cell Longev*. (2016) 2016:1092746. doi: 10.1155/2016/1092746
60. Lee JM, Ko JY, Park JW, Lee WK, Song SU, Im GI. KLF10 is a modulatory factor of chondrocyte hypertrophy in developing skeleton. *J Orthop Res*. (2020). doi: 10.1002/jor.24653. [Epub ahead of print].
61. Feinberg MW, Cao Z, Wara AK, Lebedeva MA, Senbanerjee S, Jain MK. Kruppel-like factor 4 is a mediator of proinflammatory signaling in macrophages. *J Biol Chem*. (2005) 280:38247–58. doi: 10.1074/jbc.M509378200
62. Dekker RJ, Von Soest S, Fontijn RD, Salamanca S, de Groot PG, VanBavel E, et al. Prolonged fluid shear stress induces a distinct set of endothelial cell genes, most specifically lung Kruppel-like factor (KLF2). *Blood*. (2002) 100:1689–98. doi: 10.1182/blood-2002-01-0046
63. Kuo CT, Veselits ML, Barton KP, Lu MM, Clendenin C, Leiden JM. The LKLF transcription factor is required for normal tunica media formation and blood vessel stabilization during murine embryogenesis. *Genes Dev*. (1997) 11:2996–3006. doi: 10.1101/gad.11.22.2996
64. Parmar KM, Nambudiri V, Dai G, Larman HB, Gimbrone MA Jr, Garcia-Cardena G. Statins exert endothelial atheroprotective effects via the KLF2 transcription factor. *J Biol Chem*. (2005) 280:26714–9. doi: 10.1074/jbc.C500144200
65. Wani MA, Wert SE, Lingrel JB. Lung Kruppel-like factor, a zinc finger transcription factor, is essential for normal lung development. *J Biol Chem*. (1999) 274:21180–5. doi: 10.1074/jbc.274.30.21180
66. Chiplunkar AR, Lung TK, Alhashem Y, Koppenhaver BA, Salloum FN, Kukreja RC, et al. Kruppel-like factor 2 is required for normal mouse cardiac development. *PLoS ONE*. (2013) 8:e54891. doi: 10.1371/journal.pone.0054891
67. Basu P, Morris PE, Haar JL, Wani MA, Lingrel JB, Gaensler KM, et al. KLF2 is essential for primitive erythropoiesis and regulates the human and murine embryonic beta-like globin genes *in vivo*. *Blood*. (2005) 106:2566–71. doi: 10.1182/blood-2005-02-0674
68. Carlson CM, Endrizzi BT, Wu J, Ding X, Weinreich MA, Walsh ER, et al. Kruppel-like factor 2 regulates thymocyte and T-cell migration. *Nature*. (2006) 442:299–302. doi: 10.1038/nature04882
69. Mahabeleshwar GH, Kawanami D, Sharma N, Takami Y, Zhou G, Shi H, et al. The myeloid transcription factor KLF2 regulates the host response to polymicrobial infection and endotoxic shock. *Immunity*. (2011) 34:715–28. doi: 10.1016/j.immuni.2011.04.014
70. Huddleson JP, Srinivasan S, Ahmad N, Lingrel JB. Fluid shear stress induces endothelial KLF2 gene expression through a defined promoter region. *Biol Chem*. (2004) 385:723–9. doi: 10.1515/BC.2004.088
71. Jha P, Das H. KLF2 in Regulation of NF-κB-mediated immune cell function and inflammation. *Int J Mol Sci*. (2017) 18:2383. doi: 10.3390/ijms18112383
72. Das H, Kumar A, Lin Z, Patino WD, Hwang PM, Feinberg MW, et al. Kruppel-like factor 2 (KLF2) regulates proinflammatory activation of monocytes. *Proc Natl Acad Sci USA*. (2006) 103:6653–8. doi: 10.1073/pnas.0508235103

73. Nayak L, Goduni L, Takami Y, Sharma N, Kapil P, Jain MK, et al. Kruppel-like factor 2 is a transcriptional regulator of chronic and acute inflammation. *Am J Pathol*. (2013) 182:1696–704. doi: 10.1016/j.ajpath.2013.01.029
74. Deng WG, Zhu Y, Wu KK. Role of p300 and PCAF in regulating cyclooxygenase-2 promoter activation by inflammatory mediators. *Blood*. (2004) 103:2135–42. doi: 10.1182/blood-2003-09-3131
75. SenBanerjee S, Lin Z, Atkins GB, Greif DM, Rao RM, Kumar A, et al. KLF2 Is a novel transcriptional regulator of endothelial proinflammatory activation. *J Exp Med*. (2004) 199:1305–15. doi: 10.1084/jem.20031132
76. Das M, Deb M, Laha D, Joseph M, Kanji S, Aggarwal R, et al. Myeloid Kruppel-like factor 2 critically regulates K/BxN serum-induced arthritis. *Cells*. (2019) 8:908. doi: 10.3390/cells8080908
77. Sangwung P, Zhou G, Nayak L, Chan ER, Kumar S, Kang DW, et al. KLF2 and KLF4 control endothelial identity and vascular integrity. *JCI Insight*. (2017) 2:e91700. doi: 10.1172/jci.insight.91700
78. Das M, Lu J, Joseph M, Aggarwal R, Kanji S, McMichael BK, et al. Kruppel-Like factor 2 (KLF2) regulates monocyte differentiation and functions in mBSA and IL-1 beta-Induced arthritis. *Curr Mol Med*. (2012) 12:113–25. doi: 10.2174/156652412798889090
79. Christensen AD, Haase C, Cook AD, Hamilton JA. K/BxN serum-transfer arthritis as a model for human inflammatory arthritis. *Front Immunol*. (2016) 7:213. doi: 10.3389/fimmu.2016.00213
80. Das M, Laha D, Kanji S, Joseph M, Aggarwal R, Iwenofu OH, et al. Induction of Kruppel-like factor 2 reduces K/BxN serum-induced arthritis. *J Cell Mol Med*. (2019) 23:1386–95. doi: 10.1111/jcmm.14041
81. Koch AE, Kunkel SL, Harlow LA, Johnson B, Evanoff HL, Haines GK, et al. Enhanced production of monocyte chemoattractant protein-1 in rheumatoid arthritis. *J Clin Invest*. (1992) 90:772–9. doi: 10.1172/JCI115950
82. Woods JM, Mogollon A, Amin MA, Martinez RJ, Koch AE. The role of COX-2 in angiogenesis and rheumatoid arthritis. *Exp Mol Pathol*. (2003) 74:282–90. doi: 10.1016/S0014-4800(03)00019-4
83. Van Ness K, Chobaz-Peclat V, Castellucci M, So A, Busso N. Plasminogen activator inhibitor type-1 deficiency attenuates murine antigen-induced arthritis. *Rheumatology*. (2002) 41:136–41. doi: 10.1093/rheumatology/41.2.136
84. Kim I, Kim JH, Kim K, Seong S, Kim N. The IRF2BP2-KLF2 axis regulates osteoclast and osteoblast differentiation. *BMB Rep*. (2019) 52:469–74. doi: 10.5483/BMBRep.2019.52.7.104
85. Chen HH, Keyhanian K, Zhou X, Vilmundarson RO, Almontashiri NA, Cruz SA, et al. IRF2BP2 reduces macrophage inflammation and susceptibility to atherosclerosis. *Circ Res*. (2015) 117:671–83. doi: 10.1161/CIRCRESAHA.114.305777
86. Cruz SA, Hari A, Qin Z, Couture P, Huang H, Lagace DC, et al. Loss of IRF2BP2 in Microglia increases inflammation and functional deficits after focal ischemic brain injury. *Front Cell Neurosci*. (2017) 11:201. doi: 10.3389/fncel.2017.00201
87. Hou Z, Wang Z, Tao Y, Bai J, Yu B, Shen J, et al. KLF2 regulates osteoblast differentiation by targeting of Runx2. *Lab Invest*. (2019) 99:271–80. doi: 10.1038/s41374-018-0149-x
88. Liu TM, Lee EH. Transcriptional regulatory cascades in Runx2-dependent bone development. *Tissue Eng Part B Rev*. (2013) 19:254–63. doi: 10.1089/ten.teb.2012.0527

Conflict of Interest: The authors declare that the research was conducted in the absence of any commercial or financial relationships that could be construed as a potential conflict of interest.

Copyright © 2020 Rolph and Das. This is an open-access article distributed under the terms of the Creative Commons Attribution License (CC BY). The use, distribution or reproduction in other forums is permitted, provided the original author(s) and the copyright owner(s) are credited and that the original publication in this journal is cited, in accordance with accepted academic practice. No use, distribution or reproduction is permitted which does not comply with these terms.

frontiers in Immunology

ORIGINAL RESEARCH
published: 15 May 2020
doi: 10.3389/fimmu.2020.00936

Spine and Sacroiliac Joints Lesions on Magnetic Resonance Imaging in Early Axial-Spondyloarthritis During 24-Months Follow-Up (Italian Arm of SPACE Study)

*Mariagrazia Lorenzin[1], Augusta Ortolan[1], Mara Felicetti[1], Stefania Vio[2], Marta Favero[1], Pamela Polito[1], Carmelo Lacognata[2], Vanna Scapin[2], Andrea Doria[1] and Roberta Ramonda[1]**

[1] Rheumatology Unit, Department of Medicine–DIMED, University of Padova, Padova, Italy, [2] Radiology Unit, University of Padova, Padova, Italy

OPEN ACCESS

Edited by:
Erminia Mariani,
University of Bologna, Italy

Reviewed by:
Maria Sole Chimenti,
Policlinico Tor Vergata, Italy
Ennio Lubrano,
University of Molise, Italy

***Correspondence:**
Roberta Ramonda
roberta.ramonda@unipd.it

Specialty section:
This article was submitted to Autoimmune and Autoinflammatory Disorders, a section of the journal Frontiers in Immunology

Received: 17 December 2019
Accepted: 22 April 2020
Published: 15 May 2020

Citation:
Lorenzin M, Ortolan A, Felicetti M, Vio S, Favero M, Polito P, Lacognata C, Scapin V, Doria A and Ramonda R (2020) Spine and Sacroiliac Joints Lesions on Magnetic Resonance Imaging in Early Axial-Spondyloarthritis During 24-Months Follow-Up (Italian Arm of SPACE Study). Front. Immunol. 11:936. doi: 10.3389/fimmu.2020.00936

Objectives: Our study aimed to identify: (1) the prevalence of spine and pelvis magnetic resonance imaging (MRI-spine and MRI-SIJ) inflammatory and structural lesions in patients (pts) with a diagnosis of axial spondyloarthritis (axSpA); (2) the predictive factors for a severe disease pattern with a higher probability of radiographic progression.

Materials and Methods: Seventy-five pts with low back pain (LBP) (≥3 months, ≤2 years, onset ≤45 years) underwent physical examination, questionnaires, laboratory tests, X-rays, MRI-spine, and MRI-SIJ at baseline (T0) and during a 24-months follow-up. Two expert rheumatologists made axSpA diagnosis and classification (according ASAS criteria). MRI-spine, MRI-SIJ and X-rays were scored independently by 2 readers following the SPARCC, mSASSS, and mNY-criteria. According to ASAS criteria, 21 pts fulfilled imaging arm only and 29 clinical arm with/without imaging arm; 25 pts did not fulfill ASAS criteria.

Results: At T0 the mean ± SD LBP onset was 28.51 ± 8.05 years, 45.3% pts were male, 38.7% were HLA-B27+; 56% showed bone marrow oedema (BMO) at MRI-spine and 64% at MRI-SIJ. Signs of enthesitis were found in 58% pts in the thoracic spine. Eighteen (24%) pts presented BMO at MRI-spine with a negative MRI-SIJ. The prevalence of BMO lesions and the SPARCC SIJ and spine score decreased during the follow-up in the 2 cohorts meeting ASAS criteria. An early onset of LBP, a lower use of NSAIDs, a BASDAI>4 were identified as predictors of spine structural damage; the high SPARCC SIJ score appeared to be a predictor of SIJ structural damage. A higher mSASSS was predicted by a lower age of onset of LBP. Predictor of higher SPARCC spine was a higher NSAIDs and of higher SPARCC SIJ score the HLA-B27 positivity with increased inflammatory biomarkers.

Conclusions: At T0 a significant prevalence of BMO lesions was observed both in SIJ and spine, with predominant involvement of thoracic district. Since positive MRI-spine

images were observed in the absence of sacroiliitis, these findings seem to be relevant in the axSpA diagnosis. Early age of disease onset, long duration of LBP, increased inflammatory biomarkers, higher use of NSAIDs, male gender, HLA-B27 positivity, SPARCC SIJ score>2 appeared predictors of radiological damage and activity.

Keywords: diagnostic imaging, inflammatory biomarkers, low back pain, spine, disease process

INTRODUCTION

Spondyloarthritis (SpA) is a group of chronic inflammatory rheumatic diseases that share overlapping features and can be subdivided into axial SpA (axSpA) and peripheral SpA (pSpA) (1–3). AxSpA mainly affects the spine and the sacroiliac joints (SIJ), has an early onset at young age and can be further subdivided between non-radiographic (nr-axSpA) and radiographic axSpA (r-axSpA), the latter also known as ankylosing spondylitis (AS) (2). With the development of new effective treatment strategies, the need to identify patients in an earlier stage of disease has increased (3, 4). Early onset nr-axSpA may present as a very active disease with axial pain symptoms responding quickly and effectively to therapy. Therefore, the identification of these early forms becomes a priority in order to establish the most appropriate treatment (1, 3). *The Assessment of SpondyloArthritis International Society* (ASAS) has established classification criteria to identify patients with early stage axSpA (3); the imaging arm of the criteria requires the presence of sacroiliitis on magnetic resonance imaging (MRI) or on X-rays in addition to one SpA feature for patients with chronic low back pain (LBP) with onset $\leq$ 45 years of age. Conventional X-rays of SIJ, still frequently used to detect sacroiliitis, do not appear to provide adequate information to classify patients with suspected early axSpA, as they detect only structural bone damage, indicative of a more advanced disease stage (3, 5). Thus, MRI represents an important additional screening option since it can detect inflammatory lesions of SIJ in patients with early-onset axSpA without evidence of radiographic sacroiliitis (6). Positive MRI-SIJ scans were defined by the *ASAS/Outcome Measures in Rheumatology MRI working group* (ASAS/OMERACT) as the presence of inflammatory lesions such as *bone marrow edema* (BMO) which is highly suggestive of SpA (6) (**Figures 1A,B**). Whether structural SIJ lesions should be added to this definition and whether structural and inflammatory spinal lesions could contribute to detecting axSpA remains a matter of debate (7). Inflammatory spinal lesions on MRIs may nevertheless occur in the absence of SIJ involvement (8, 9). These lesions include BMO adjacent to vertebral endplates at the attachment of the annulus fibrosus to the vertebral rim and at the insertion of anterior and posterior longitudinal ligaments, both within the facet joints (**Figures 2A,B**). Since there is evidence that spondylitis may also occur prior to -or even without- sacroiliitis, it was deemed important to define the characteristics of a MRI-spine considered positive for inflammation. The ASAS/OMERACT working group thus defined MRI-spine criteria of inflammatory lesions (spondylitis) and structural changes (fat deposition) (7). Imaging of the thoracic spine, often involved in axSpA, has instead not yet been taken into consideration in evaluation of structural damage (10–12). The goal of this study was to determine the prevalence of spine and SIJ lesions on MRI and their correlation with clinical and disease activity indices in patients with early axSpA included in the *SpondyloArthritis-Caught-Early* (SPACE) Italian cohort at baseline (T0) and during a 24-months follow-up. Secondary objectives included evaluation of: (a) the role of imaging in the diagnostic process of axSpA with or without SIJ involvement; (b) evolution of MRI features over time and their relationship to radiographic damage; (c) predictors of radiological progression and severe disease.

MATERIALS AND METHODS

Patients

The SPACE study is an on-going observational prospective cohort multi-center study II level evidence (Netherlands, Norway, Sweden, Italy). Patients who were at least 16 years old, suffering by chronic inflammatory LBP ($\geq$3 months, $\leq$2 years, onset $<$ 45 years) of unknown origin and referred to a rheumatologist were included. In the present study only patients from our center were considered. Approval by local Medical Ethics Committee (Azienda Ospedaliera di Padova [approval no. 2438P]) was obtained. Informed consent was required from the patients prior to inclusion. Eligible patients underwent physical examinations and laboratory tests following a standardized protocol at baseline (T0) and at 6, 12, 24 months (T6, T12, T24). The patients also completed questionnaires on disease activity, physical functioning, pain and disease-related impairment. SIJ and spinal plain radiographs and MRIs were performed at T0, T12 and T24. Axial pain and MRI lesions were localized in 4 sites: cervical/thoracic/lumbar spine and SIJ. X-rays and MRI images were read by two expert radiologists (SV and VS), while 2 experienced rheumatologists (RR and ML) made axSpA diagnosis and classified subjects according to ASAS criteria (3). The patients were subdivided into three cohorts: those fulfilling only the imaging arm of ASAS axSpA criteria (*axSpA imaging arm*), those fulfilling the clinical arm of ASAS axSpA criteria in presence/absence of imaging arm (*axSpA clinical±imaging arm)* and those not fulfilling ASAS axSpA criteria (*not full ASAS axSpA*). A detailed description of the recruitment and clinical assessment of the SPACE cohort has previously been published (13, 14). At T0 all the patients were being treated with non-steroidal anti-inflammatory drugs (NSAIDs). Afterwards, patients were being treated according to best clinical practice, with no limitation on pharmacological treatments, physical therapies or other treatments.

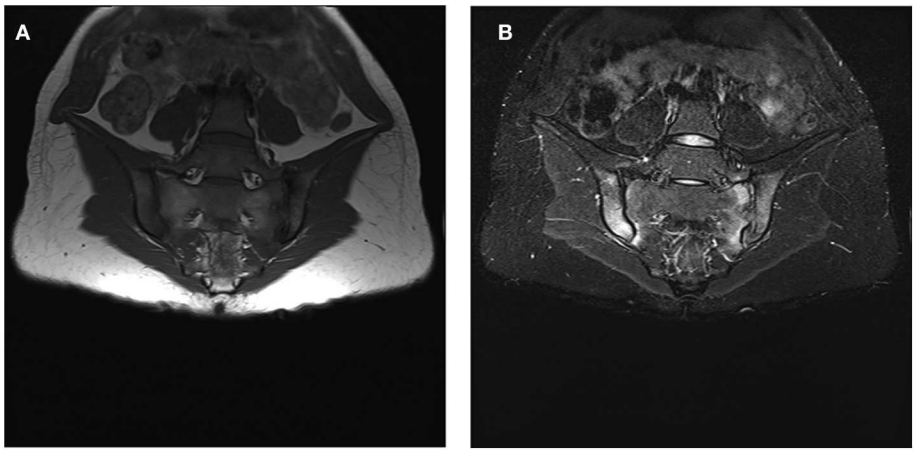

FIGURE 1 | (A,B): Bone marrow oedema (BMO) signs at both SIJ. **(A)** hypointense signal at the sacral and iliac superior and inferior third region of both right and left SIJ in sequence T1. **(B)** corresponding iperintense signal at the sacral and iliac superior and inferior third region of both right and left SIJ in sequence STIR. The written informed consent was obtained from the individual for the publication of these images.

FIGURE 2 | (A,B) Anterior spondylitis. **(A)** hypointense signal at the anterior-superior corner of L1 (white ring) in sequence T1 **(B)** corresponding hyperintense signal at the anterior-superior corner of L1 in sequence STIR (white ring). The written informed consent was obtained from the individual for the publication of these images.

Methods

Physician Clinical, Questionnaires', and Biochemical Assessments

The clinical evaluation focused on an examination of the spine, SIJ and entheses, using the *Bath Ankylosing Spondylitis Metrology Index* (*BASMI)* and the *Maastricht Ankylosing enthesitis Spondilities Score (MASES*). The patients' disease activity and physical functioning were assessed using self-reported questionnaires and composite indices: the *Bath Ankylosing Spondylitis Disease Activity Index (BASDAI)*, the *Bath Ankylosing Spondylitis Functional Index (BASFI)*, the *Ankylosing Spondylitis disease activity score (ASDAS)*, the *Visual Analogue Scale (VAS) pain*, the *VAS night pain*, the *VAS disease activity*, the *Bath Ankylosing Spondylitis Patient Global Score (BASG1)*, the *BASG2*, the *Health Assessment Questionnaire (HAQ)*. Biochemical parameters included the erythrocyte sedimentation rate (ESR) (Westergren method in mm after 1 h; normal range 0–15 mm/h) and C-reactive protein (CRP) (ELISA in mg/l; Research & Diagnostic Systems, Inc., expressed in mg/L, normal range 0–6 mg/L). DNA was also collected to perform HLA-B (complement-dependent microlymphocytic assay). Bank serum was be stored at −70C. Serum for the assays was separated by centrifugation at 3,000 rpm for 10 min. All blood samples were analyzed twice using the same method.

MRI and Radiographs Assessments

MRI-SIJ and MRI-spine were performed using a 1.5 T scanner Magnetom Harmony, Siemens AG Medical Solutions, Munich, with phased-array surphace coil, acquiring T1-weighted turbo spin echo (T1TSE; TR 583/TE 9.4) and short-tau inversion recovery (STIR; TR 2980/TE47) sequences. The coronal oblique and sagittal views of the SIJ and spine were taken, with a slice

thickness of 4 mm. Lateral view radiographs of the cervical and lumbar spine and anterior-posterior view radiographs of the pelvis were taken. The images were obtained with a Philips vertical bucky, with a focus-film distance of 140 cm, film size of 18 × 43 cm. MRI images were analyzed according to ASAS/OMERACT criteria (6, 7). The inflammatory positive MRI images were scored using the *Spondyloarthritis Research Consortium of Canada* (SPARCC) score (15, 16). For spine and SIJ X-rays the *Stoke Ankylosing Spondylitis Spinal Score (SASSS) system* modified by Creemers (mSASSS) (10) and mNY criteria (5) were used. All readers were blinded for clinical and laboratory data, and for the results of the other imaging methods. The temporal sequence of the images was unblinded to radiologists for the scoring. When two readers (SV and VS) both scored an SIJ image positive according to ASAS/OMERACT and mNY, the image was considered positive. In case of disagreement, an adjudicator was introduced (CL). If the primary readers agreed on a positive (or negative) MRI-SIJ, the mean SPARCC scores were calculated based on the scores of these primary readers. In cases of disagreement, the mean scores were based on the consensus scores of the adjudicator and 1 primary reader. A similar process was followed for calculating the mean SPARCC scores in the MRI-spine. The adjudicator (CL) was also introduced in case of disagreement between the readers regarding the presence/absence of spine radiological lesions on X-rays. In cases of agreement, the mean score between the 2 readers was calculated for mSASSS. Intra and inter-observer reliability was assessed.

Statistical Analysis

The Cohen's Kappa test was used to assess the intra and inter-observational reliability between the two rheumatologists and radiologists. The non-parametric Kruskal-Wallis test (one-way ANOVA for ranks) for repeated measurements followed by the Dunn's multiple Comparison test were used to compare the clinical (BASMI, MASES), bioumoral (ESR,CRP), functional (BASFI, HAQ, BASG1, BASG2, VAS pain, VAS night pain, VAS disease activity) and disease activity indices (BASDAI, ASDAS) at T0, T6, T12 and T24. The same method was used to compare the imaging scores (mSASSS, score SIJ mNY, SPARCC SIJ, and SPARCC spine) at T0, T12 and T24 in all patients and among the three cohorts (*axSpA imaging arm, axSpA clinical±imaging arm and not full ASAS axSpA*). A linear regression analysis was performed to identify baseline predictors of inflammation and radiological progression of the disease evaluated using as outcomes mSASSS, score SIJ mNY, SPARCC SIJ and SPARCC spine indices at T24. The following independent variables were considered in the univariable analysis: female sex, age of LBP onset, duration of LBP, presence of HLA-B27, elevated inflammation indices, BASDAI>4, use of NSAIDs, SPARCC SIJ score>2. The significant independent variables ($p < 0.1$) at univariable analysis were introduced in the multivariable models. The radiographic progression of SIJ from T0 to T24 was defined as (17): (1) transition from nr-axSpA to r-axSpA according to the mNY criteria; (2) change of >1 degree of sacroiliitis but ignoring the transition from degree 0 to 1 of sacroiliitis. The radiographic progression of the spine from T0 to T24 was defined as (18) an increase in mSASSS score >2 over the course of 2 years of observation. All statistical analyses were performed using the SPSS 13.0 program (SSPS Inc, IL, USA). The values of $p < 0.05$ were considered statistically significant.

RESULTS

Seventy-five patients with chronic inflammatory LBP were enrolled. According to the ASAS criteria for axSpA, **21** (28%) patients were classified as *axSpA imaging arm*, **29** (38.7%) patients as *axSpA clinical±imaging arm* and **25** (33.3%) patients as *not full ASAS criteria for axSpA*. The agreement between the two clinicians was good (k 0.75). The average age at LBP onset was 28.51 ± 8.05 years, 45.3% were male, 38.7% were HLA-B27+. Thirty-nine (52%) of patients presented an exclusive axial involvement, while 36 (48%) of patients also had peripheral involvement. A high prevalence of psoriasis and heel enthesitis was observed (33.3 and 72%, respectively). Other characteristics of the patients, including typical SpA features, have been reported in **Table 1** and have previously been published (19). Out of all 75 patients, 37.3, 56, 100, and 64%, respectively, complained of cervical/thoracic/lumbar/buttock pain. We found a higher prevalence of HLA-B27, male gender, uveitis, increased serological markers and alternating buttock pain among subjects with MRI-SIJ+ for BMO lesions; instead a higher prevalence of inflammatory bowel diseases (IBD) in those with MRI-spine+ for BMO lesions. The other SpA features were comparable between subjects with MRI-SIJ+ and/or MRI-spine+ (**Table 1**). The clinical (MASES, BASMI), disease activity (BASDAI, ASDAS), functional (HAQ, BASFI, VAS pain, VAS pain night, VAS disease activity, BASG1, BASG2) indices as well as inflammatory biomarkers (ESR, CRP) were analyzed and measured at T0, T6, T12, and T24. Out of all 75 patients, 90.7% were evaluated at **T6**, of these 78.7% patients at **T12**, of these 72% at **T24**.

(A) The Prevalence of the Inflammatory and Structural Lesions on MRI at T0

The inter-observer reliability of MRI-SIJ and MRI-spine between two expert readers was good to moderate (kappa 0.75 for inflammatory lesions and 0.62 for structural lesions on MRI-spine; kappa 0.76 for inflammatory lesions and 0.64 for structural lesions on MRI-SIJ, respectively). The inter-observer reliability of X-rays was good (kappa 0.81 for spine radiological lesions and kappa 0.79 for SIJ radiological lesions). Moreover, intra-observer reliability was good for all spine and SIJ images on X-rays and MRI (respectively, kappa 0.78 for spine and 0.84 for SIJ on X-Rays and kappa 0.80 for spine and 0.82 for SIJ on MRI). Fifty-two (69.3%) patients presented structural and/or inflammatory lesions on MRI-SIJ at T0 (on the right SIJ in 63% of the patients and on left one in 59% of the patients). BMO lesions were observed in 48 (64%) patients (58% on the right SIJ and 50% on the left one) and structural lesions on MRI-SIJ in 33 (44%) patients (37% on the right SIJ and 30% on the left one). Fifty (66.7%) patients had inflammatory and/or structural lesions on the MRI-spine at T0. BMO lesions on the anterior corner of the spine were observed

TABLE 1 | Baseline features of all LBP patients in relation to the presence of BME lesions on MRI-spine and on MRI-SIJ.

Baseline features of all patients with inflammatory LBP	Total patients *n* = 75	MRI-SIJ + / MRI-SPINE ±, *n* = 48	vs.	MRI-SIJ – / MRI-SPINE ±, *n* = 27	p§	MRI-SPINE + / MRI-SIJ ±, *n* = 44	vs.	MRI-SPINE – / MRI-SIJ ±, *n* = 31	p§
Age of onset LBP, mean (± SD)	28.51 (± 8.05)	28.44 (± 7.24)		28.63 (± 9.48)	ns	28.11 (± 7.92)		29.06 (± 8.33)	ns
Male, n (%)	34 (45.3%)	27 (56.25%)		7 (25.93%)	<0.05	20 (45.45%)		14 (45.16%)	ns
Duration (months) di LBP, mean (± SD)	13.37 (± 6.14)	14.25 (± 6.38)		11.81 (± 5.47)	ns	13.77 (±.67)		12.81 (± 5.39)	ns
Only axial involvement, n (%)	39 (52%)	25 (52.08%)		14 (51.85%)	ns	25 (56.82%)		14 (45.16%)	ns
Axial and peripheral involvment, n (%)	36 (48%)	23 (47.92%)		13 (48.15%)	ns	19 (43.18%)		17 (54.84%)	ns
HLA-B27 positive, n (%)	29 (38.7%)	26 (54.17%)		3 (11.11%)	<0.05	19 (43.18%)		10 (32.26%)	<0.05
Positive family history of SpA, n (%)	35 (46.7%)	24 (50%)		11 (40.74%)	ns	20 (45.45%)		15 (48.39%)	ns
Peripheral arthritis, n (%)	34 (45.3%)	23 (47.92%)		11 (40.74%)	ns	19 (43.18%)		15 (48.39%)	ns
Psoriasis, n (%)	25 (33.3%)	17 (35.42%)		8 (29.63%)	ns	13 (29.55%)		12 (38.71%)	ns
Dactylitis, n (%)	15 (20%)	8 (16.67%)		7 (25.93%)	ns	5 (11.36%)		10 (32.26%)	ns
Heel enthesitis, n (%)	54 (72%)	33 (68.75%)		21 (77.78%)	ns	29 (65.91%)		25 (80.65%)	ns
Uveitis, n (%)	7 (9.3%)	7 (14.58%)		0 (%)	<0.05	4 (9.09%)		3 (9.68%)	<0.05
IBD, n (%)	9 (12%)	4 (8.33%)		5 (18.52%)	<0.05	7 (15.91%)		2 (6.45%)	<0.05
Preceding infections, n (%)[†]	4 (5.3%)	3 (6.25%)		1 (3.70%)	ns	2 (4.55%)		2 (6.45%)	ns
Good response to NSAIDs, n (%)	73 (97.3%)	47 (97.92%)		26 (96.30%)	ns	43 (97.73%)		30 (96.77%)	ns
Elevated CRP/ESR, n (%)	42 (56%)	29 (60.42%)		13 (48.15%)	<0.05	24 (54.55%)		18 (58.06%)	ns
Cervical pain, n (%)	28 (37.3%)	16 (33.33%)		12 (44.44%)	ns	18 (40.91%)		10 (32.26%)	ns
Thoracic pain, n(%)	42 (56%)	31 (64.58%)		11 (40.74%)	ns	25 (56.82%)		17 (54.84%)	ns
Buttock pain, n (%)	48 (64%)	35 (72.92%)		13 (48.15%)	<0.05	31 (70.45%)		17 (54.84%)	ns
Alternating buttock pain, n (%)	37 (49.3%)	29 (60.42%)		8 (29.63%)	<0.05	26 (59.10%)		11 (35.48%)	<0.05
Morning stiffness, n (%)	57 (76%)	37 (77.08%)		20 (74.07%)	ns	36 (81.82%)		21 (67.74%)	ns
Night pain, n(%)	71 (94.7%)	46 (95.83%)		25 (92.60%)	ns	43 (97.73%)		28 (90.32%)	ns
Sacroiliitis MRI *, n (%)	48 (64%)	48 (100%)		0 (0%)	<0.05	29 (65.91%)		19 (61.29%)	<0.05
Sacroiliitis x-ray **, n (%)	25 (33.3%)	19 (39.58%)		6 (22.22%)	<0.05	17 (38.64%)		8 (25.81%)	<0.05
Weight (kg), mean (± SD)	70.22 (± 16.15)	71.25 (± 15.87)		68.05 (± 16.98)	ns	66.60 (± 11.12)		75.5 (± 20.65)	ns
Height (cm), mean (± SD)	170.6 (± 8.67)	172.23 (± 8.73)		167.71 (± 7.91)	ns	170.41 (± 8.42)		170.88 (± 9.15)	ns

HLA-B27, human leukocyte antigen; LBP, low back pain; IBD, inflammatory bowel disease; CRP, C-reactive protein; ESR, erythrocyte sedimentation rate; MRI, magnetic resonance imaging; SpA, spondyloarthritis; SIJ, sacroiliac joints; NSAID, non-steroidal antiinflammatory drugs; MRI+, presence of inflammatory lesions; MRI–r, absence of inflammatory lesions; ±, presence or absence of inflammatory lesions.

**sacroiliitis on MRI according ASAS/EULAR criteria. **sacroiliitis on X-Rays according modified New York criteria (0–4). [†] balanitis, urethritis, or cervicitis. p§, anova (Kruskal Wallis) a t0: $p < 0.05$; SD = deviation standard.*

TABLE 2 | The prevalence of inflammatory and structural lesions at T0 and T24 in three cohorts (*axSpA imaging arm, axSpA clinical ± imaging arm, not full ASAS axSpA*).

	T0 MRI evaluation		
	axSpA imaging arm	**axSpA clinical ± imaging arm**	**Not full ASAS axSpA**
Total number of patients	21 (28%)	29 (38.7%)	25 (33.3%)
SIJ total lesions	21 (100%)	27 (93.1%)	4 (16%)
BMO lesions	21 (100%)	27 (93.1%)	0 (0%)
Sclerosis lesions	10 (47.6%)	14 (48.28%)	0 (0%)
Fatty lesions	7 (33.3%)	2 (6.9%)	4 (16%)
Erosions lesions	8 (38.1%)	3 (10.3%)	0 (0%)
Spine total lesions	20 (95.2%)	19 (65.5%)	11 (44%)
BMO lesions	18 (85.7%)	15 (51.7%)	9 (36%)
Enthesitis lesions	17 (80.9%)	19 (65.5%)	11 (44%)
Fatty lesions	6 (28.6%)	7 (24.1%)	4 (16%)
Sclerosis/syndesmophytes lesions	6 (28.6%)	6 (20.7%)	3 (12%)
Erosions lesions	2 (9.5%)	2 (6.9%)	1 (4%)
	T24 MRI evaluation		
	axSpA imaging arm	**axSpA clinical ± imaging arm**	**Not full ASAS axSpA**
Total number of patients	16 (29.6%)	22 (40.7%)	16 (29.6%)
SIJ total lesions	16 (100%)	15 (68.2%)	1 (6.3%)
BMO lesions	9 (56.3%)	13 (59.1%)	0 (0%)
Sclerosis lesions	7 (43.8%)	10 (45.5%)	0 (0%)
Fatty lesions	6 (37.5%)	4 (18.2%)	1 (6.3%)
Erosions lesions	3 (18.8%)	2 (9.1%)	0 (0%)
Spine total lesions	11 (68.8%)	4 (18.2%)	7 (43.8%)
BMO lesions	7 (43.8%)	5 (22.7%)	5 (31.3%)
Enthesitis lesions	7 (43.8%)	6 (27.3%)	7 (43.8%)
Fatty lesions	6 (37.5%)	4 (18.2%)	4 (25%)
Sclerosis/syndesmophytes lesions	7 (43.8%)	3 (13.6%)	2 (12.5%)
Erosions lesions	1 (6.3%)	2 (9.1%)	0 (0%)

MRI, magnetic resonance imaging; SIJ, sacroiliac joints; BMO, bone marrow oedema; axSpA, Axial Spondyloarthritis; T0, 0 months; T24, 24 months.

in 42 (56%) patients (cervical/thoracic/lumbar regions: 19, 39, and 33%, respectively). Structural spine lesions were detected in 28 (37.3%) patients (cervical/thoracic/lumbar regions: 18, 14, and 19%, respectively). Signs of enthesitis were found in 47 (62.7%) patients: (cervical/thoracic/lumbar spine: 8, 58, and 11%, respectively). At T0 18 patients (8 fulfilling *axSpA clinical±imaging arm* and 10 not fulfilling ASAS axSpA criteria) with inflammatory lesions on MRI-spine showed no abnormalities in SIJ, while 11 (14.7%) patients without active sacroiliitis on MRI-SIJ did not present MRI-spine lesions.

(B) The Prevalence and Type of MRI Lesions in the 3 Cohorts at T0 and T24

The prevalence of inflammatory and structural MRI lesions in the three cohorts is outlined in **Table 2**. As it could be expected, an increased prevalence of structural lesions on MRI-SIJ was found at T0 in the *axSpA imaging arm* and *axSpA clinical±imaging arm* compared to those who did *not fulfill ASAS axSpA criteria*. In the cohorts who met axial ASAS criteria, a higher prevalence of inflammatory and structural spinal lesions was observed, as well as a decrease of MRI lesions during the follow-up period.

(C) Analysis of Clinical, Serological, Disease Activity, Imaging Indices in Overall Patients, and in the 3 Cohorts Over 24 Months Follow-Up

All indices (values expressed as mean and standard deviation-SD), analyzed by Kruskal-Wallis test are reported in **Table 3** [data previously published elsewhere (19)]. Considering the whole population, a significant decrease in the following variables was noted from T0 to T24: MASES ($p = 0.008$), BASG1 ($p = 0.02$), BASG2 ($p < 0.0001$), HAQ ($p = 0.0002$), VAS pain ($p = 0.01$), VAS pain night ($p = 0.04$), VAS disease activity ($p = 0.05$), BASFI ($p = 0.02$), BASDAI ($p < 0.0001$), ASDAS ($p < 0.0001$). Conversely, BASMI, ESR, and CRP did not significantly decrease. Considering the patients subdivided in the 3 cohorts, a downward trend in all functional and disease activity indices was observed, which in some cases was significant

TABLE 3 | Clinical, functional, disease activity, and serological indices values from T0 to T24 in the whole group of patients ($n = 75$) and in three cohorts (axSpA imaging arm, axSpA clinical ± imaging arm, not full ASAS axSpA).

		BASMI	MASES	BASFI	HAQ	BASG1	BASG2	VAS pain	VAS dis act	VAS pain N	BASDAI	ASDAS	ESR	CRP
axSpA imaging arm	T0	1 (1.18)	3.33 (2.65)	17.43 (20.21)	0.34 (0.53)	3.43 (2.79)	5.71 (3.02)	3.48 (2.82)	3.81 (3.03)	3.24 (3.33)	39.50 (25.99)	2.29 (0.86)	17.52 (12.98)	4.81 (3.61)
	T6	0.80 (1.15)	3.30 (2.85)	17.95 (22.52)	0.21 (036)	3.15 (2.87)	4.80 (2.48)	3.40 (2.72)	3.35(2.91)	2.90 (2.92)	29.17 (26.19)	2.14 (0.98)	13.55(11.59)	3.04 (2.01)
	T12	0.39 (0.78)	3.06 (2.98)	12.67 (12.82)	0.15 (0.31)	2.01(2.03)	3.71 (2.44)	3.47 (2.61)	3.18 (2.74)	2.06 (2.34)	29.06 (26.71)*	1.78 (0.87)*	15.06 (10.23)	4.06 (2.98)
	T24	0.44 (0.63)	2.06 (2.11)*	9.25 (8.12)**	0.14 (0.38)**	2.29 (2.23)*	2.71 (2.64)**	1.75 (1.77)*	1.81 (1.71)*	1.56 (1.93)*	18.72 (18.25)**	1.36 (0.56)**	11.13(5.73)**	3.13 (1.31)
axSpA clinical ± imaging arm	T0	0.76 (1.02)	3.41 (2.35)	13.680 (15.14)	0.30 (0.38)	3.52 (2.77)	5.10 (2.77)	4.10 (2.97)	4.07 (3.15)	4.17 (3,57)	44.27 (25.03)	2.61 (0.56)	15.14 (11.76)	3.17 (3.32)
	T6	0.54 (0.86)	2.58 (2.39)	15.85 (20.65)	0.21 (0.37)	2.73(2.54)	3.84 (2.31)	3.08 (2.64)	3.19 (2.80)	2.62 (2.70)	35.11 (24.70)	1.95 (0.79)	14.88 (9.27)	3.12 (2.19)
	T12	0.43 (0.79)	2.39 (2.90)	11.04 (15.63)	0.10 (0.25)	2.67 (2.33)	3.33 (2.12)	2.41 (2.04)*	2.92 (2.22)	2.25 (2.26)*	25.48 (17.78)**	1.59 (0.54)*	12.73 (9.39)	4.05 (6.31)
	T24	0.50 (0.86)	2.09 (2.37)*	10.27 (14.29)*	0.10 (0.23)*	1.50 (1.87)**	1.91 (1.98)**	2.23 (2.20)*	2.18 (2.32)*	2.36 (2.32)*	20.73 (18.76)***	1.33 (0.69)***	10.86 (5.54)*	3.59 (3.84)
Not full ASAS axSpA	T0	0.92 (1.08)	3.56 (2.47)	22.44 (25.75)	0.52 (0.55)	4.64 (3.35)	5.28 (2.94)	5.08 (3.23)	5.04 (3.35)	4.20 (3.33)	53.48 (24.97)	2.66 (0.88)	21.68 (21.19)	4.24 (3.28)
	T6	0.96 (1.22)	3.43 (2.59)	17.52 (21.71)	0.34 (0.41)	4.26 (3.01)	4.82 (3.52)	4.52 (3.36)	4.30 (3.21)	3.48 (3.17)	45.66 (27.37)	2.51 (1.19)	19.73 (17.01)	6.35 (10.33)
	T12	0.65 (0.81)	2.40 (2.14)	12.38 (14.63)*	0.20 (0.29)	3.35 (2.69)	3.18 (2.46)	3.58 (3.17)	4.70 (3.16)	3.10 (3.01)	31.26 (19.67)*	2.02 (0.99)	16.06 (13.06)	4.22 (3.67)
	T24	0.50 (0.73)	2.40 (2.14)*	12.84 (12.63)**	0.15 (0.22)**	3.33 (2.19)*	3.67 (2,32)*	2.81 (2.32)**	2.81 (2.26)*	3.00 (2.59)*	24.80 (19.67)**	1.34 (0.61)*	14.25 (10.21)**	3.63 (2.03)
Total patients with IBP, $n = 75$	T0	0.88 (1.08)	3.44 (2.45)	17.65 (20.64)	0.39 (0.49)	3.87 (2.99)	5.33 (2.87)	4.25 (3.05)	4.32 (2.18)	3.92 (3.40)	46.01 (25.07)	2.54 (0.77)	17.99 (15.85)	3.98 (3.42)
	T6	0.75 (1.08)	3.07 (2.59)	17.01 (21.26)	0,25 (0,38)	3.36 (2.83)	4.45 (2.82)	3.65 (2.95)	3.61 (2.97)	2.98 (2.91)	36.90 (26.51)	2.19 (1.01)	16.09 (13.05)	4.29 (6.33)
	T12	0.49 (0.79)	2.59 (2.67)	11.95 (14.30)*	0,16 (0,30)**	2.67 (2.38) *	3.40 (2.29)**	3.08 (2.61)	3.57 (2.77)	2.47 (2.54)	28.37 (21.05)**	1.79 (0.82)**	14.48 (10.80)*	4.10 (4.62)
	T24	0.48 (0.75)	2.12 (2.13)**	10.73 (12.12)**	0,14 (0,29)***	2.25 (2.17) **	2.63 (2.24)***	2.26 (2.12)**	2.26 (2.14)**	2.28 (2.30)**	21.34 (18.07)***	1.34 (0.61)***	11.94 (7.30)**	3.46 (2.75)

Data are expressed as mean ± SD. The test Kruskal Wallis repeated measures test and Dunn's multiple comparison test were used.

****$p < 0.0001$ vs. T0, **$p < 0.001$ vs. T0, *$p < 0.01$ vs. T0.*

BASMI, bath ankylosing score metrology index; MASES, maastricht ankylosing spondilities enthesitis score; BASFI, bath ankylosing spondylitis functional index; HAQ, health assessment questionnaire; BASG1, bath ankylosing spondylitis patient global score 1; BASG2, bath ankylosing spondylitis patient global score 2; ESR, erytrocyte sedimentation rate; CRP, C-reactive protein; BASDAI, bath ankylosing spondylitis disease activity index; ASDAS, ankylosing spondylitis disease activity score; VAS pain, visual analog scale pain; VAS dis act, visual analog scale disease activity; VAS pain N, visual analog scale pain night.

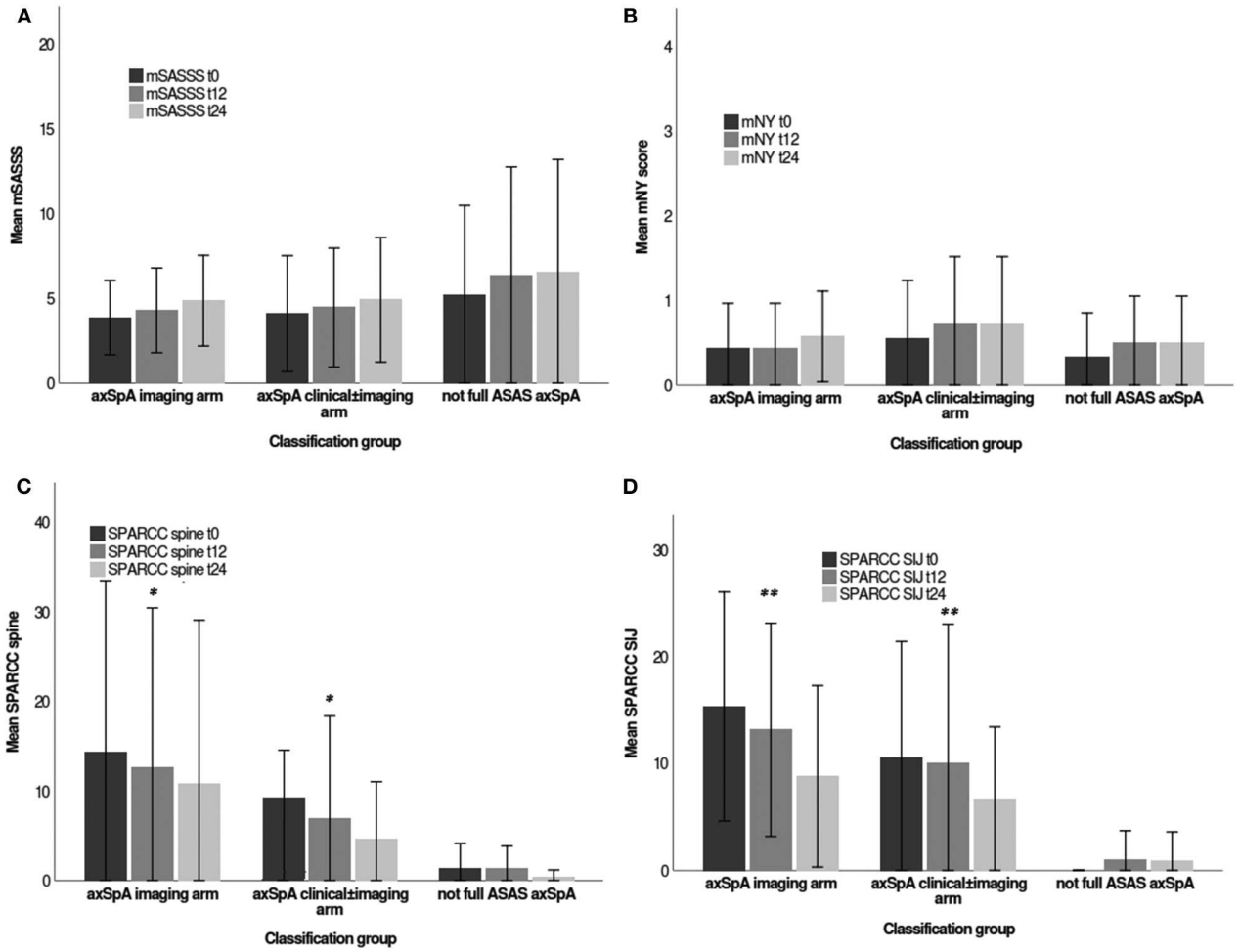

FIGURE 3 | (A–D) Imaging indices values (mSASSS, mNY score, SPARCC spine, SPARCC SIJ), expressed as mean (deviation standard) from T0 to T24 in the three cohorts (*axSpA imaging arm, axSpA clinical±imaging arm, not full ASAS axSpA*). *$p < 0.01$ vs. T0, **$p < 0.001$ vs. T0. Stoke Ankylosing Spondylitis Spinal Score (SASSS) system modified by Creemers (mSASSS); modified criteria of New York (mNY) score; Spondyloarthritis Research Consortium of Canada (SPARCC); Sacroiliac joint (SIJ). The written informed consent was obtained from the individual for the publication of these images.

(see **Table 3**); however, no significant differences were found among the cohorts. A significant downtrend of SPARCC SIJ and SPARCC spine score was also observed in *axSpA imaging arm* and *axSpA clinical±imaging arm* cohorts (**Figures 3A–D**).

(D) Regression Analysis to Identify the Predictors of Disease Activity and Radiological Progression

A regression analysis was performed to identify any baseline predictors of radiological activity on MRI at T24 (measured by continuous variables such as SPARCC SIJ and SPARCC spine) and of structural damage at T24 (measured by continuous variables such as mSASSS and SIJ mNY score and dichotomous variables such as presence/absence of structural lesions on X rays of SIJ and spine). As shown in **Tables 4–6**, at the multivariate analysis radiological spine structural damage was independently predicted by an early onset of LBP, a lower use of NSAIDs, a BASDAI>4. Radiological SIJ structural damage was independently predicted by high SPARCC SIJ score. A higher mSASSS was independently predicted by a lower age of onset of LBP. Predictive factors of increased radiological activity were: a higher NSAIDs intake for a higher SPARCC spine score and the HLA-B27 positivity and increased serological inflammatory markers for a higher SPARCC SIJ score, respectively.

(E) Evaluation of the Pelvic and Spinal Radiographic Progression From T0 to T24

In our study SIJ radiographic progression (17) and spine radiographic progression (18) were not significant from T0 to T24.

DISCUSSION

Our study highlighted the presence of BMO both in the SIJ and in the spine, especially the thoracic spine. BMO seemed to be positively associated to HLA-B27 and inflammatory serological

TABLE 4 | Baseline predictors factors of mSASSS score at T24.

Independent variables	Univariable analysis		Multivariable analysis	
	coeff (IC)	*p*	coeff (IC)	*p*
Female sex	−0.80 (−2.55, 0.93)	0.359	–	–
LBP onset age	0.21 (0.11, 0.30)	0.000	0.19 (0.09, 0.29)	0.000
Duration of LBP	0.02 (−0.12, 0.16)	0.770	–	–
HLA-B27+	−0.72 (−2.5, 1.08)	0.428	–	–
Increased ESR/CRP	0.97 (−0.80, 2.75)	0.278	–	–
BASDAI >=4	−0.48 (−2.22, 1.26)	0.583	–	–
Use of NSAIDs	2.63 (−0.22, 5.48)	0.070	1.22 (−1.46, 3.90)	0.367
SPARCC SIJ >2	0.91 (−0.84, 2.55)	0.233	–	–

LBP, low back pain; HLA-B27, human leukocyte antigen B27; CRP, C-reactive protein; ESR, erythrocyte sedimentation rate; BASDAI, bath ankylosing spondylitis disease activity index; NSAIDs, non-steroidal antiinflammatory drugs; SPARCC, spondyloarthritis research consortium of Canada; SIJ,sacroiliac joints; mSASSS, modified Stoke ankylosing spondylitis spinal score (SASSS) system; T24, 24 months.

TABLE 5 | Baseline predictors factors of SPARCC spine score and SPARCC SSJ score at T24.

SPARCC spine score

Independent variables	Univariable analysis		Multivariable analysis	
	coeff (IC)	*p*	coeff (IC)	*p*
Female sex	−0.14 (−0.56, 0.28)	0.511	–	–
LBP onset age	−0.01 (−0.04, 0.00)	0.152	−0.02 (−0.05, 0.00)	0.124
Duration of LBP	0.02 (−0.01, 0.05)	0.154	0.02 (−0.01, 0.05)	0.192
HLA-B27+	0.35 (−0.06, 0.78)	0.099	0.12 (−0.33, 0.58)	0.582
Increased ESR/CRP	0.11 (−0.31, 0.54)	0.583	–	–
BASDAI>=4	−0.39(−0.81, 0.01)	0.058	−0.33 (−.73, 0.07)	0.104
Use of NSAIDs	0.60 (−0.26, 1.48)	0.168	0.88 (0.01, 1.75)	0.046
SPARCC SIJ>2	0.44 (−0.42, 0.65)	0.311	–	–

SPARCC SSJ score

Independent variables	Univariable analysis		Multivariable analysis	
	coeff (IC)	*p*	coeff (IC)	*p*
Female sex	−3.59 (−9.54, 2.36)	0.233	–	–
LBP onset age	−0.36 (−0.72, −0.004)	0.047	−0.25 (−0.60, 0.08)	0.140
Duration of LBP	0.00 (−0.48, 0.49)	0.980	–	–
HLA-B27+	9.41 (3.64, 15.18)	0.002	8.87 (3.08, 14.65)	0.003
Increased ESR/CRP	4.46 (−1.59, 10.51)	0.146	5.74 (0.15, 11.34)	0.044
BASDAI >=4	−3.94 (−9.85, 1.96)	0.187	−3.14 (−8.55, 2.26)	0.250
Use of NSAIDs	3.87 (−6.09, 13.84)	0.441	–	–

LBP, low back pain; HLA-B27, human leukocyte antigen B27; CRP, C-reactive protein; ESR, erythrocyte sedimentation rate; BASDAI, bath ankylosing spondylitis disease activity index; NSAIDs, non-steroidal antiinflammatory drugs; SPARCC, spondyloarthritis research consortium of Canada; SIJ, sacroiliac joints; T24, 24 months.

indices at the SIJ level, moreover it was negatively associated with NSAIDs use at the spine level. When present, BMO tended to decrease during follow-up, after beginning an adequate therapy for axSpA.

The advent and development of new imaging methods in the last two decades has increased the interest to diagnose axSpA forms in the earlier stages—before structural damage has occurred—aiming at an earlier and more effective treatment (3, 4, 20, 21). MRI has a high sensitivity in detection of inflammatory lesions of the spine and SIJ, hence its widespread use in clinical practice, especially in assessing patients with suspected axSpA and/or a history of chronic inflammatory LBP (6, 7, 22–25). MRI-SIJ is useful since it reveals the pathological lesions which led to an axSpA diagnosis (6). Based on the definition of the ASAS/OMERACT criteria, an MRI-SIJ is considered positive if at least one BMO, highly suggestive for SpA, is present on ≥2 consecutive slices or if ≥2 bone inflammatory lesions are visible on a single slice (26, 27). Nevertheless, a SPARCC score >2—widely used because it measures inflammation on a continuous scale with good sensitivity to change (15, 16)—can be used to define a positive MRI-SIJ (ASAS definition) in clinical trials (28). Some studies have recently considered inflammatory and structural lesions observed on MRI-spine in SpA patients (7, 22): the most frequent and specific lesions are the BMO of the anterior vertebral corners, which is an expression of anterior osteitis (29); other possible lesions are fatty lesions—replacement of vertebral corners with fatty tissue—though they appear to be less specific for SpA and of later appearance (30–32). Likewise to previous studies, including those from ASAS/OMERACT MRI study group, the prevalence and type of both inflammatory and structural lesions in our study were analyzed in subjects with LBP and suspected early axSpA. In our study population, a higher prevalence of BMO lesions compared to structural lesions, has been noted at MRI, confirming the ability of this method in the visualization of inflammatory lesions. A significant prevalence of BMO lesions was observed in both SIJs and the spinal district, with predominant localization in the vertebral anterior corner. This observation, in keeping with previous studies, highlights the importance of spine involvement in the initial stage of the inflammatory process in axSpA (3, 29, 33, 34). This data are especially interesting in the nr-axSpA forms without sacroiliitis on MRI, suggesting that the inclusion of spine BMO lesions at MRI among the classification criteria for axSpA would decrease the number of false negative patients. In some studies, it has been shown that the determination of ≥3 inflammatory lesions (BMO) in the anterior vertebral site (anterior spondylitis) in subjects younger than 45 years increases the likelihood of axSpA diagnosis (32, 35, 36). On the other hand, although the appearance of multiple structural (at least three) and *fatty* lesions increases the probability of axSpA (37), it has been reported that these lesions tend to increase with aging and can be found even in healthy individuals or in those affected with other spinal degenerative diseases (38, 39). In a recent study the presence on MRI of ≥ 5 spinal inflammatory lesions or ≥ 5 spinal fatty lesions—unlike the presence of ≥3 spinal lesions—appears to discern between axSpA patients and non-SpA patients, while maintaining >95% specificity (40). Furthermore, while an association between inflammatory MRI lesions and LBP has been confirmed, it remains unclear whether axSpA spinal lesions could be associated with pain (41). Therefore, the inclusion of MRI-spine lesions

TABLE 6 | Baseline predictors factors of spine or pelvis structural lesions at T24.

Spine structural lesions (presence = 1; absence = 0)

Independent variables	Univariable analysis		Multivariable analysis	
	OR (IC)	*p*	coeff (IC)	*p*
Female sex	0.93 (0.69, 1.26)	0.661	–	–
LBP onset age	0.90 (0.84, 0.97)	0.006	0.89 (0.82, 0.97)	0.010
Duration of LBP	0.97 (0.90, 1.05)	0.495	–	–
HLA-B27+	1.22 (0.48, 3.08)	0.672	–	–
Increased ESR/CRP	0.46 (0.16, 1.31)	0.147	0.57 (0.16, 1.93)	0.369
BASDAI >=4	2.15 (0.79, 5.85)	0.131	4.05 (1.15, 14.24)	0.029
Use of NSAIDs	0.07 (0.008, 0.65)	0.019	0.09 (0.008, 0.99)	0.049
SPARCC SIJ >2	1.28 (0.59, 2.44)	0.531	–	–

Pelvis structural lesions (presence = 1; absence = 0)

Independent variables	Univariable analysis		Multivariable analysis	
	OR (IC)	*p*	coeff (IC)	*p*
Female sex	0.45 (0.17, 1.18)	0.107	0.65 (0.21, 2.01)	0.462
LBP onset age	0.98 (0.92, 1.03)	0.527	–	–
Duration of LBP	1.00 (0.92, 1.08)	0.951	–	–
HLA-B27+	1.45 (0.58, 3.60)	0.423	–	–
Increased ESR/CRP	1.27 (0.48, 3.35)	0.629	–	–
BASDAI >=4	0.43 (0.16, 1.14)	0.091	0.60 (0.19, 1.84)	0.375
Use of NSAIDs	1.77 (0.32, 9.84)	0.511	–	–
SPARCC SIJ >2	1.07 (1.026, 1.13)	0.003	1.07 (1.01, 1.12)	0.007

LBP, low back pain; HLA-B27, human leukocyte antigen B27; CRP, C-reactive protein; ESR, erythrocyte sedimentation rate; BASDAI, bath ankylosing spondylitis disease activity index; NSAIDs, non-steroidal antiinflammatory drugs; SPARCC, spondyloarthritis research consortium of Canada; SIJ, sacroiliac joints; T24, 24 months; OR, Odds Ratio.

in classification criteria is currently under discussion owing to its increased sensitivity—albeit with a reduced specificity. In the present study, MRI-spine also showed a high prevalence of inflammatory lesions attributable to enthesitis (47 patients) mostly in the thoracic district (58%) (42), suggesting an early involvement of this site in the initial stage of axSpA. We found no significant variations in the radiological progression of SIJ and spine evaluated by SIJ mNY and mSASSS scores from T0 to T24, according to definitions used in previous studies (17, 18). These results may be explained by the very early disease stage of our patients and the relatively short follow-up (24 months is a minimal timeframe to observe any significant radiological changes). A downward trend of radiological activity measured by ΔSPARCC SIJ and ΔSPARCC spine and of prevalence of inflammatory lesions on spinal and pelvic MRIs was observed in the 2 cohorts that met the ASAS criteria, probably due to the pharmacological treatment initiated after baseline evaluation and the diagnosis of axSpA (**Figures 4A–F**). However, due to the non-homogeneity in therapy and reduced sample size ($n = 54$ patients) at T24 with available imaging, a comparative analysis on the ΔSPARCC SIJ and the ΔSPARCC spine by treatment type was not possible. Several studies systematically evaluated the concomitant use of MRI-spine and MRI-SIJ in patients with suspected axSpA and healthy controls, highlighting an improved diagnostic capacity for the two techniques together compared to MRI-SIJ only (8, 43). However, other authors claim that this procedure only increases the level of diagnostic probability in patients with suspected axSpA due to the inclusion of false positives (37–39, 44). In another recent study the prevalence of lesions on MRI-spine in patients with ≤3-year duration of chronic LBP included in SPACE and DESIR cohorts, was found in very few patients without sacroiliitis on X-rays or MRI-SIJ: 3/447 (1%) patients in SPACE cohort and 8/382 (2%) in DESIR cohort, respectively. The conclusion of this study was that the addition of MRI-spine in ASAS axSpA criteria yielded few newly classified patients (45). On the opposite, our study suggests that the use of MRI-spine along with MRI-SIJ could add a relevant information which can be useful in the diagnosis and in the the follow-up. In fact, at T0 we found 24% patients with positive MRI-spine and negative MRI-SIJ, as well as 14.7% patients with negative MRI-spine and positive MRI-sacroiliitis. Predictors of radiological damage and activity in our population were: early age of disease onset and long duration of LBP, increased inflammatory biomarkers, higher use of NSAIDs, male gender, HLA-B27 positivity and a SPARCC SIJ score>2, in keeping with previous studies (46, 47). Moreover, in our study we observed as curiuos aspect that patients with positive MRI-spine had higher prevalence of IBD, instead patients with positive MRI-SIJ presented more frequently uveitis. Our study also investigated whether there were differences in clinical indices of disease activity according to the presence or absence of signs of sacroiliitis on X-rays and MRIs. Despite the differences at T0 in the three cohorts in the prevalence of sacroiliitis on MRIs, X-rays, and SPARCC SIJ score, no differences were found in clinical and disease activity indices. Patients with active MRI sacroiliitis did not show higher disease activity indices compared to those without inflammatory changes in the SIJs or those with initial signs of radiographic sacroiliitis. In contrast, several studies reported higher values of clinical, functional and disease activity indices in AS and r-axSpA in patients with long disease duration vs. subjects with nr-axSpA (46, 48–52). In our study a significant reduction of functional and disease activity indices was observed in all patients throughout the follow-up period. Nevertheless, no markedly significant decrease of these indices was observed in one cohort vs. the others. The improvement of these indices may depend on the successful pharmacological treatment after the diagnosis of axSpA.

Some of the limitations of this study pertain to the small sample size, the early disease stage which could limit the potential to detect radiographic changes, and the variability of treatments in the three cohorts. Conversely, the strengths are the prospective study design and the central reading by two expert radiologists.

CONCLUSIONS

A high prevalence of inflammatory lesions on MRI-SIJ and MRI-spine was found in our patients. Since inflammatory lesions on MRI-spine can occur in the absence of SIJ involvement, the use of MRI-spine alongside MRI-SIJ may add a relevant information

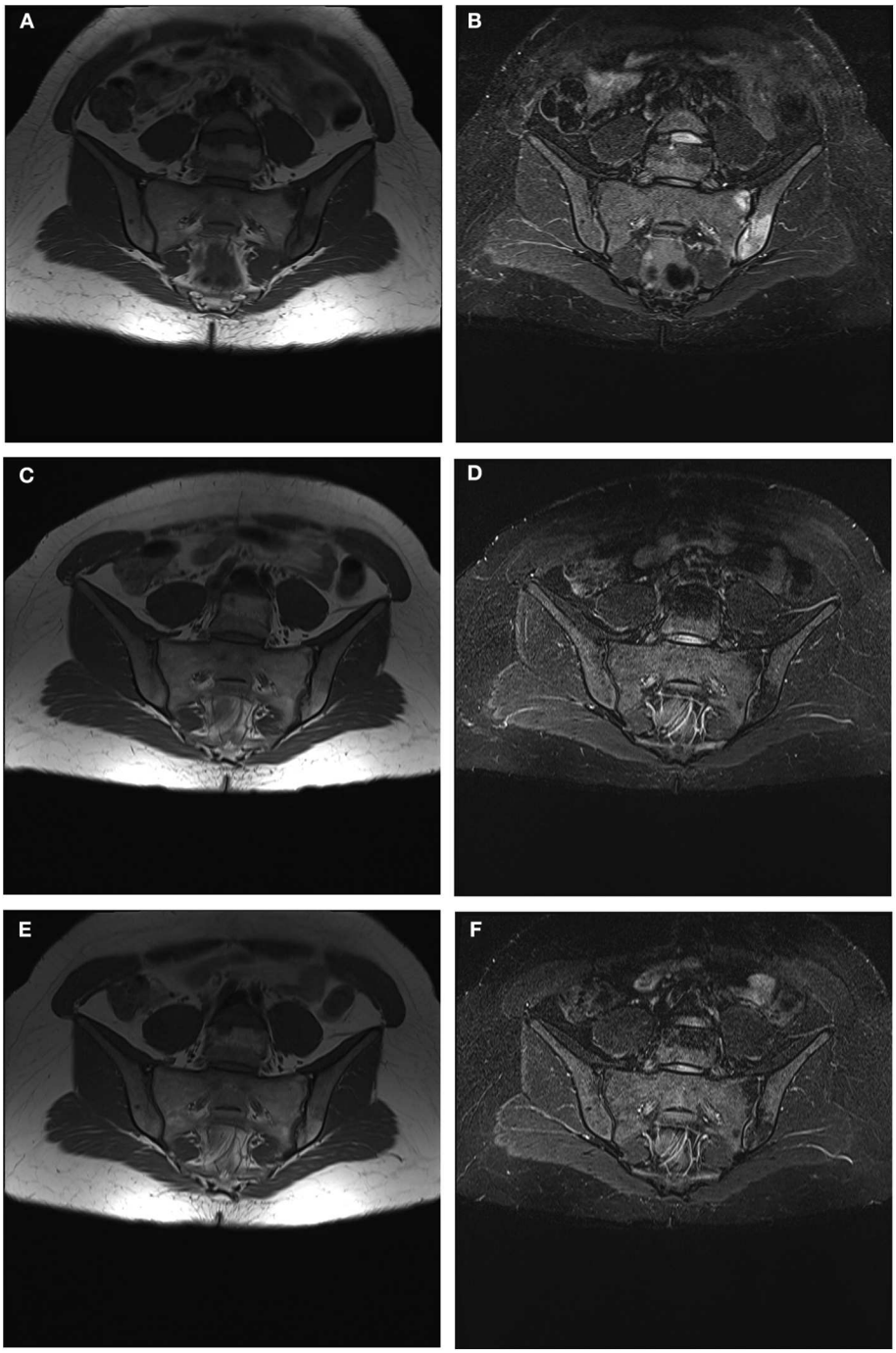

FIGURE 4 | (A–F) Progressive reduction until disappearance of BMO signs and subsequent corresponding appearance of signs of adipose metaplasia on left SIJ during a follow up period of 24 months. **(A)** MRI-SIJ at T0 in T1 sequence **(B)** MRI-SIJ at T0 in STIR sequence **(C)** MRI-SIJ at T12 in T1 sequence **(D)** MRI-SIJ at T12 in STIR sequence **(E)** MRI-SIJ at T24 in T1 sequence **(F)** MRI-SIJ at T24 in STIR sequence. The written informed consent was obtained from the individual for the publication of these images.

which can be useful in the diagnosis, especially of nr-axSpA. As of today, no studies assessed the involvement of the thoracic spine by means of a spinal structural damage scoring method. Notably, we observed a significant involvement of the thoracic region in our patients which warrants further investigation. In the current study, different types of axial involvement—presence/absence of sacroiliitis—were not associated to significant differences in clinical severity and disease activity indices in all three cohorts.

DATA AVAILABILITY STATEMENT

The datasets generated for this study are available on request to the corresponding author.

ETHICS STATEMENT

The studies involving human participants were reviewed and approved by the Medical Ethics Committee, Leiden University Medical Center (approval no. P08.105); and Azienda Ospedaliera di Padova (approval no. 2438P). The patients/participants provided their written informed consent to participate in this study.

AUTHOR CONTRIBUTIONS

ML participated in drafting the manuscript as well as gathering, analyzing, and interpreting the data. RR and AD conceived and designed the study, participated in data processing and drafting the manuscript. CL, SV, and VS participated in performing spine and pelvis X-rays and MRIs and participated in reading the images. AO, MFe, PP, and MFa participated in gathering, analyzing, and interpreting the data. All the authors have made substantive intellectual contributions to the study, have reviewed the article, and have given final approval for the version being submitted.

ACKNOWLEDGMENTS

The authors wish to thank Eric Frank Nde for his assistance in editing the English version. The authors also wish to thank Mariagrazia Lorenzin for her contribution in performing and reporting results of this research in the Ph.D. thesis *Spine and sacroiliac joints on nuclear magnetic resonance imaging and research of serological biomarkers predictive of severity and disease activity in early axial spondyloarthritis*.

REFERENCES

1. Sieper J, Poddubnyy D. Axial spondyloarthritis. *Lancet*. (2017) 390:73–84. doi: 10.1016/S0140-6736(16)31591-4
2. Rudwaleit M, Landewé R, van der Heijde D, Listing J, Brandt J, Braun J, et al. The development of Assessment of Spondyloarthritis international Society classification criteria for axial spondyloarthritis (part I): classification of paper patients by expert opinion including uncertainty appraisal. *Ann Rheum Dis*. (2009) 68:770–6. doi: 10.1136/ard.2009.108217
3. Rudwaleit M, van der Heijde D, Landewé R, Listing J, Akkoc N, Brandt J, et al. The development of Assessment of Spondyloarthritis international Society classification criteria for axial spondyloarthritis (part II): validation and final selection. *Ann Rheum Dis*. (2009) 68:777–83. doi: 10.1136/ard.2009.108233
4. van der Heijde D, Ramiro S, Landewé R, Baraliakos X, Van den Bosch F, Sepriano A, et al. 2016 update of the ASAS-EULAR management recommendations for axial spondyloarthritis. *Ann Rheum Dis*. (2017) 76:978–91. doi: 10.1136/annrheumdis-2016-210770
5. Van der Linden S, Valkenburg HA, Cats A. Evaluation of diagnostic criteria for ankylosing spondylitis. A proposal for modification of the New York criteria. *Arthritis Rheum*. (1984) 27:361–8. doi: 10.1002/art.1780270401
6. Rudwaleit M, Jurik AG, Hermann KG, Landewé R, van der Heijde D, Baraliakos X, et al. Defining active sacroiliitis on magnetic resonance imaging (MRI) for classification of axial spondyloarthritis: a consensual approach by the ASAS/OMERACT MRI group. *Ann Rheum Dis*. (2009) 68:1520–7. doi: 10.1136/ard.2009.110767
7. Hermann KG, Baraliakos X, van der Heijde DM, Jurik AG, Landewé R, Marzo-Ortega H, et al.; Assessment in SpondyloArthritis international Society (ASAS). Assessment in SpondyloArthritis international Society (ASAS). Descriptions of MRI-spine lesions and definition of a positive MRI of the spine in axial spondyloarthritis: a consensual approach by the ASAS/OMERACT MRI study group. *Ann Rheum Dis*. (2012) 71:1278–88. doi: 10.1136/ard.2011.150680
8. van der Heijde D, Sieper J, Maksymowych WP, Brown MA, Lambert RG, Rathmann SS, et al. Spinal inflammation in the absence of sacroiliac joint inflammation on magnetic resonance imaging in patients with active non radiographic axial spondyloarthritis. *Arthritis Rheumatol*. (2014) 66:667–73. doi: 10.1002/art.38283
9. Braun J, Baraliakos X, Golder W, Brandt J, Rudwaleit M, Listing J, et al. Magnetic resonance imaging examinations of the spine in patients with ankylosing spondylitis, before and after successful therapy with infliximab: evaluation of a new scoring system. *Arthritis Rheum*. (2003) 48:1126–36. doi: 10.1002/art.10883
10. Creemers MC, Franssen MJ, van't Hof MA, Gribnau FW, van de Putte LB, van Riel PL. Assessment of outcome in ankylosing spondylitis: an extended radiographic scoring system. *Ann Rheum Dis*. (2005) 64:127–9. doi: 10.1136/ard.2004.020503
11. Salaffi F, Carotti M, Garofalo G, Giuseppetti GM, Grassi W. Radiological scoring methods for ankylosing spondylitis: a comparison between the bath ankylosing spondylitis radiology index and the modified stoke ankylosing spondylitis spine score. *Clin Exp Rheumatol*. (2007) 25:67–74.
12. Spoorenberg A, de Vlam K, van der Linden S, Dougados M, Mielants H, van de Tempel H, et al. Radiological scoring methods in ankylosing spondylitis: reliability and change over 1 and 2 years. *J Rheumatol*. (2004) 31:125–32.
13. Van den Berg R, de Hooge M, van Gaalen F, Reijnierse M, Huizinga T, van der Heijde D. Percentage of patients with spondyloarthritis in patients referred because of chronic back pain and performance of classification criteria: experience from the spondyloarthritis caught early (SPACE) cohort. *Rheumatol*. (2013) 52:1492–9. doi: 10.1093/rheumatology/ket164
14. Lorenzin M. *Spine and sacroiliac joints on nuclear magnetic resonance imaging and research of serological biomarkers predictive of severity and disease activity in early axial spondyloarthritis* (dissertation/PhD thesis). University of Padova, Padova, Italy (2018).
15. Maksymowych WP, Inman RD, Salonen D, Dhillon SS, Williams M, Stone M, et al. Spondyloarthritis Research Consortium of Canada magnetic resonance imaging index for assessment of sacroiliac joint inflammation in ankylosing spondylitis. *Arthritis Rheum*. (2005) 53:703–9. doi: 10.1002/art.21445
16. Maksymowych WP, Inman RD, Salonen D, Dhillon SS, Krishnananthan R, Stone M, et al. Spondyloarthritis Research Consortium of Canada magnetic resonance imaging index for assessment of spinal inflammation in ankylosing spondylitis. *Arthritis Rheum*. (2005) 53:502–9. doi: 10.1002/art.21337
17. Dougados M, Sepriano A, Molto A, van Lunteren M, Ramiro S, de Hooge M, et al. Sacroiliac radiographic progression in recent onset axial spondyloarthritis: the 5-year data of the DESIR cohort. *Ann Rheum Dis*. (2017) 76:1823–8. doi: 10.1136/annrheumdis-2017-211596
18. Poddubnyy D, Rudwaleit M, Haibel H, Listing J, Märker-Hermann E, Zeidler H, et al. Effect of non-steroidal anti-inflammatory drugs on radiographic spinal progression in patients with axial spondyloarthritis: results from the German Spondyloarthritis Inception Cohort. *Ann Rheum Dis*. (2012) 71:1616–22. doi: 10.1136/annrheumdis-2011-201252
19. Lorenzin M, Ortolan A, Felicetti M, Favero M, Vio S, Zaninotto M, et al. Serological biomarkers in early axial spondyloarthritis during 24-months follow up (Italian Arm of Space Study). *Front Med*. (2019) 6:177. doi: 10.3389/fmed.2019.00177

20. Sieper J, van der Heijde D, Landewé R, Brandt J, Burgos-Vagas R, Collantes-Estevez E, et al. New criteria for inflammatory back pain in patients with chronic back pain: a real patient exercise by experts from the Assessment of SpondyloArthritis international Society (ASAS). *Ann Rheum Dis*. (2009) 68:784–8. doi: 10.1136/ard.2008.101501
21. Rudwaleit M. New approaches to diagnosis and classification of axial and peripheral spondyloarthritis. *Curr Opin Rheumatol*. (2010) 22:375–80. doi: 10.1097/BOR.0b013e32833ac5cc
22. Lukas C, Braun J, van der Heijde D, Hermann KG, Rudwaleit M, Østergaard M, et al. ASAS/OMERACT MRI in AS Working Group. 2007 Scoring inflammatory activity of the spine by magnetic resonance imaging in ankylosing spondylitis: a multireader experiment. *J Rheumatol*. (2007) 34:862–70.
23. Weber U, Pfirrmann C WA, Kissling RO, Hodler J, Zanetti M. Whole body MR imaging in ankylosing spondyltis: a descriptive pilot study in patient with suspected early and active confirmed ankylosing spondylitis. *BMC Musuloskelet Disord*. (2007) 8:20. doi: 10.1186/1471-2474-8-20
24. Kiltz U, Baraliakos X, Karakostas P, Igelmann M, Kalthoff L, Klink C, et al. Do patients with non-radiographic axial spondylarthritis differ from patients with ankylosing spondylitis? *Arthritis Care Res*. (2012) 64:1415–22. doi: 10.1002/acr.21688
25. Paternotte S, van der Heijde D, Claudepierre P, Rudwaleit M, Dougados M. Evaluation of the validity of the different arms of the ASAS set of criteria for axial spondyloarthritis and description of the different imaging abnormalities suggestive of spondyloarthritis: data from the DESIR cohort. *Ann Rheum Dis*. (2015) 74:746–51. doi: 10.1136/annrheumdis-2013-204262
26. Baraliakos X, van der Heijde D, Braun J, Landewé RB. OMERACT magnetic resonance imaging initiative on structural and inflammatory lesions in ankylosing spondylitis–report of a special interest group at OMERACT 10 on sacroiliac joint and spine lesions. *J Rheumatol*. (2011) 38:2051–4. doi: 10.3899/jrheum.110423
27. de Hooge M, van den Berg R, Navarro-Compán V, van Gaalen F, van der Heijde D, Huizinga T, et al. Magnetic resonance imaging of the sacroiliac joints in the early detection of spondyloarthritis: no added value of gadolinium compared with short tau inversion recovery sequence. *Rheumatology*. (2013) 52:1220–4. doi: 10.1093/rheumatology/ket012
28. van den Berg R, de Hooge M, Bakker PA, van Gaalen F, Navarro-Compán V, Fagerli KM, et al. Metric Properties of the SPARCC Score of the Sacroiliac joints - data from baseline, 3-month, and 12-month followup in the SPACE cohort. *J Rheumatol*. (2015) 42:1186–93. doi: 10.3899/jrheum.140806
29. Kim NR, Choi JY, Hong SH, Jun WS, Lee JW, Choi JA, et al. "MR corner sign": value for predicting presence of ankylosing spondylitis. *AJR Am J Roentgenol*. (2008) 191:124–8. doi: 10.2214/AJR.07.3378
30. Bennett AN, Rehman A, Hensor EM, Marzo-Ortega H, Emery P, McGonagle D. The fatty Romanus lesion: a non-inflammatory spinal MRI lesion specific for axial spondyloarthropathy. *Ann Rheum Dis*. (2010) 69:891–4. doi: 10.1136/ard.2009.112094
31. Bennett AN, Rehman A, Hensor EM, Marzo-Ortega H, Emery P, McGonagle D. Evaluation of the diagnostic utility of spinal magnetic resonance imaging in axial spondylarthritis. *Arthritis Rheum*. (2009) 60:1331–41. doi: 10.1002/art.24493
32. Weber U, Hodler J, Kubik RA, Rufibach K, Lambert RG, Kissling RO, et al. Sensitivity and specificity of spinal inflammatory lesions assessed by whole-body magnetic resonance imaging in patients with ankylosing spondylitis or recent-onset inflammatory back pain. *Arthritis Rheum*. (2009) 61:900–8. doi: 10.1002/art.24507
33. Baraliakos X, Landewé R, Hermann KG, Listing J, Golder W, Brandt J, et al. Inflammation in ankylosing spondylitis: a systematic description of the extent and frequency of acute spinal changes using magnetic resonance imaging. *Ann Rheum Dis*. (2005) 64:730–4. doi: 10.1136/ard.2004.029298
34. Ez-Zaitouni Z, Bakker PA, van Lunteren M, Berg IJ, Landewé R, van Oosterhout M, et al. Presence of multiple spondyloarthritis (SpA) features is important but not sufficient for a diagnosis of axial spondyloarthritis: data from the SPondyloArthritis Caught Early (SPACE) cohort. *Ann Rheum Dis*. (2017) 76:1086–92. doi: 10.1136/annrheumdis-2016-210119
35. Hermann KG, Althoff CE, Schneider U, Zühlsdorf S, Lembcke A, Hamm B, et al. Magnetic resonance imaging of spinal changes in patients with spondyloarthritis and correlation with conventional radiography. *Radiographics*. (2005) 25:559–70. doi: 10.1148/rg.253045117
36. Lambert RG, Pederson SJ, Maksymowych WP. Active inflammatory lesions detected by magnetic resonance imaging in the spine of patients with spondyloarthritis- definitions, assessment system, and reference image set. *J Rheumatol*. (2009) 84:3–17. doi: 10.3899/jrheum.090616
37. Song IH, Hermann KG, Haibel H, Althoff CE, Poddubnyy D, Listing J, et al. Relationship between active inflammatory lesions in the spine and sacroiliac joints and new development of chronic lesions on whole-body MRI in early axial spondyloarthritis: results of the ESTHER trial at week 48. *Ann Rheum Dis*. (2011) 70:1257–63. doi: 10.1136/ard.2010.147033
38. Stäbler A, Baur A, Krüger A, Weiss M, Helmberger T, Reiser M. St. 1998 Differential diagnosis of erosive osteochondrosis and bacterial spondylitis: magnetic resonance tomography (MRT). *Rofo*. (1998)166:193–9.
39. Resnick D, Shaul SR, Robins JM. Diffuse idiopathic skeletal hyperostosis (DISH): Forestier's disease with extraspinal manifestations. *Radiology*. (1975) 115:513–24. doi: 10.1148/15.3.513
40. de Hooge M, van den Berg R, Navarro-Compán V, Reijnierse M, van Gaalen F, Fagerli K, et al. Patients with chronic back pain of short duration from the SPACE cohort: which MRI structural lesions in the sacroiliac joints and inflammatory and structural lesions in the spine are most specific for axial spondyloarthritis? *Ann Rheum Dis*. (2016) 75:1308–14. doi: 10.1136/annrheumdis-2015-207823
41. de Hooge M, de Bruin F, de Beer L, Bakker P, van den Berg R, Ramiro S, et al. Is the site of back pain related to the location of magnetic resonance imaging lesions in patients with chronic back pain? Results from the spondyloarthritis caught early cohort. *Arthritis Care Res*. (2017) 69:717–23. doi: 10.1002/acr.22999
42. Lorenzin M, Ortolan A, Frallonardo P, Vio S, Lacognata C, Oliviero F, et al. Spine and sacroiliac joints on magnetic resonance imaging in patients with early axial spondyloarthritis: prevalence of lesions and association with clinical and disease activity indices from the Italian group of SPACE study. *Reumatismo*. (2016) 68:72–82. doi: 10.4081/reumatismo.2016.885
43. Reveille JD. Biomarkers for diagnosis, monitoring of progression, and treatment responses in ankylosing spondylitis and axial spondyloarthritis. *Clin Rheumatol*. (2015) 34:1009–18. doi: 10.1007/s10067-015-2949-3
44. Weber U, Zubler V, Zhao Z, Lambert RG, Chan SM, Pedersen SJ, et al. Does spinal MRI add incremental diagnostic value to MRI of the sacroiliac joints alone in patients with non-radiographic axial spondyloarthritis? *Ann Rheum Dis*. (2015) 74:985–92. doi: 10.1136/annrheumdis-2013-203887
45. Ez-Zaitouni Z, Bakker PA, van Lunteren M, de Hooge M, van den Berg R, Reijnierse M, et al. The yield of a positive MRI of the spine as imaging criterion in the ASAS classification criteria for axial spondyloarthritis: results from the SPACE and DESIR cohorts. *Ann Rheum Dis*. (2017) 76:1731–6. doi: 10.1136/annrheumdis-2017-211486
46. Poddubnyy D, Rudwaleit M, Haibel H, Listing J, Märker-Hermann E, Zeidler H, et al. Rates and predictors of radiographic sacroiliitis progression over 2 years in patients with axial spondyloarthritis. *Ann Rheum Dis*. (2011) 70:1369–74. doi: 10.1136/ard.2010.145995
47. Bennett AN, McGonagle D, O'Connor P, Hensor EM, Sivera F, Coates LC, et al. Severity of baseline magnetic resonance imaging-evident sacroiliitis and HLA-B27 status in early inflammatory back pain predict radiographically evident ankylosing spondylitis at eight years. *Arthritis Rheum*. (2008) 58:3413–18. doi: 10.1002/art.24024
48. Pedersen SJ, Sørensen IJ, Garnero P, Johansen JS, Madsen OR, Tvede N, et al. ASDAS, BASDAI and different treatment responses and their relation to biomarkers of inflammation, cartilage and bone turnover in patients with axial spondyloarthritis treated with TNFα inhibitors. *Ann Rheum Dis*. (2011) 70:1375–81. doi: 10.1136/ard.2010.138883
49. Pedersen SJ, Sørensen IJ, Lambert RG, Hermann KG, Garnero P, Johansen JS, et al. Radiographic progression is associated with resolution of systemic inflammation in patients with axial spondylarthritis treated with tumor necrosis factor α inhibitors: a study of radiographic progression, inflammation on magnetic resonance imaging, and circulating biomarkers of inflammation,

angiogenesis, and cartilage and bone turnover. *Arthritis Rheum*. (2011) 63:3789–800. doi: 10.1002/art.30627

50. De Vries MK, van Eijk IC, van der Horst-Bruinsma IE, Peters MJ, Nurmohamed MT, Dijkmans BA, et al. Erythrocyte sedimentation rate, C-reactive protein level, and serum amyloid a protein for patient selection and monitoring of anti-tumor necrosis factor treatment in ankylosing spondylitis. *Arthritis Rheum*. (2009) 61:1484–90. doi: 10.1002/art.24838
51. Poddubnyy DA, Rudwaleit M, Listing J, Braun J, Sieper J. Comparison of a high sensitivity and standard C reactive protein measurement in patients with ankylosing spondylitis and non-radiographic axial spondyloarthritis. *Ann Rheum Dis*. (2010) 69:1338–41. doi: 10.1136/ard.2009.120139
52. Visvanathan S, Wagner C, Marini JC, Baker D, Gathany T, Han J, et al. Inflammatory biomarkers, disease activity and spinal disease measures in patients with ankylosing spondylitis after treatment with infliximab. *Ann Rheum Dis*. (2008) 67:511–7. doi: 10.1136/ard.2007.071605

Conflict of Interest: The authors declare that the research was conducted in the absence of any commercial or financial relationships that could be construed as a potential conflict of interest.

Copyright © 2020 Lorenzin, Ortolan, Felicetti, Vio, Favero, Polito, Lacognata, Scapin, Doria and Ramonda. This is an open-access article distributed under the terms of the Creative Commons Attribution License (CC BY). The use, distribution or reproduction in other forums is permitted, provided the original author(s) and the copyright owner(s) are credited and that the original publication in this journal is cited, in accordance with accepted academic practice. No use, distribution or reproduction is permitted which does not comply with these terms.

frontiers in Immunology

REVIEW
published: 03 June 2020
doi: 10.3389/fimmu.2020.01108

Infectious Triggers in Periodontitis and the Gut in Rheumatoid Arthritis (RA): A Complex Story About Association and Causality

Burkhard Möller[1]*, *Florian Kollert*[1], *Anton Sculean*[2] and *Peter M. Villiger*[1]

[1] Department for Rheumatology, Immunology and Allergology, Inselspital—University Hospital of Bern, Bern, Switzerland,
[2] Department of Periodontology, School of Dental Medicine, University of Bern, Bern, Switzerland

Rheumatoid arthritis (RA) is a systemic immune mediated inflammatory disease of unknown origin, which is predominantly affecting the joints. Antibodies against citrullinated peptides are a rather specific immunological hallmark of this heterogeneous entity. Furthermore, certain sequences of the third hypervariable region of human leukocyte antigen (HLA)-DR class II major histocompatibility (MHC) molecules, the so called "shared epitope" sequences, appear to promote autoantibody positive types of RA. However, MHC-II molecule and other genetic associations with RA could not be linked to immune responses against specific citrullinated peptides, nor do genetic factors fully explain the origin of RA. Consequently, non-genetic factors must play an important role in the complex interaction of endogenous and exogenous disease factors. Tobacco smoking was the first environmental factor that was associated with onset and severity of RA. Notably, smoking is also an established risk factor for oral diseases. Furthermore, smoking is associated with extra-articular RA manifestations such as interstitial lung disease in anatomical proximity to the airway mucosa, but also with subcutaneous rheumatoid nodules. In the mouth, *Porphyromonas gingivalis* is a periodontal pathogen with unique citrullinating capacity of foreign microbial antigens as well as candidate RA autoantigens. Although the original hypothesis that this single pathogen is causative for RA remained unproven, epidemiological as well as experimental evidence linking periodontitis (PD) with RA is rapidly accumulating. Other periopathogens such as *Aggregatibacter actinomycetemcomitans* and *Prevotella intermedia* were also proposed to play a specific immunodominant role in context of RA. However, demonstration of T cell reactivity against citrullinated, MHC-II presented autoantigens from RA synovium coinciding with immunity against *Prevotella copri* (*Pc.*), a gut microbe attracted attention to another mucosal site, the intestine. *Pc.* was accumulated in the feces of clinically healthy subjects with citrulline directed immune responses and was correlated with RA onset. In conclusion, we retrieved more than one line of evidence for mucosal sites and different microbial taxa to be potentially involved in the development of RA. This review gives an overview of infectious agents and mucosal pathologies, and discusses the current evidence for causality between different exogenous or mucosal factors and systemic inflammation in RA.

Keywords: rheumatoid arthritis, periodontitis, intestinal, mucosa, trigger

OPEN ACCESS

Edited by:
Erminia Mariani,
University of Bologna, Italy

Reviewed by:
Marta E. Alarcon-Riquelme,
Junta de Andalucía de Genómica e Investigación Oncológica (GENYO), Spain
Guenter Steiner,
Medical University of Vienna, Austria

***Correspondence:**
Burkhard Möller
Burkhard.moeller@insel.ch

Specialty section:
This article was submitted to Autoimmune and Autoinflammatory Disorders, a section of the journal Frontiers in Immunology

Received: *21 February 2020*
Accepted: *07 May 2020*
Published: *03 June 2020*

Citation:
Möller B, Kollert F, Sculean A and Villiger PM (2020) Infectious Triggers in Periodontitis and the Gut in Rheumatoid Arthritis (RA): A Complex Story About Association and Causality. Front. Immunol. 11:1108. doi: 10.3389/fimmu.2020.01108

INTRODUCTION

Rheumatoid arthritis (RA) is a common immune mediated inflammatory condition primarily affecting the joints. Despite the well-described contribution of a genetic background predominantly at the immunological synapse and the many other candidate autoantigens, the origin of this potentially devastating human disease is still enigmatic. Increasing efforts have been made in the recent past to unravel the interaction of affected subjects with their environment, but many aspects of a multitude of potential triggering factors and their respective contribution in RA pathogenesis are still unknown. The mucosal surface of the oral cavity and the gut is physiologically colonized by commensal microbes, which possess the capacity to profoundly shape the repertoire of adaptive immune responses. It is one of the most fascinating current perspectives to employ this way of immune system regulation for therapeutic or preventive purposes.

An immune response against citrullinated peptides is the most specific immunological marker of RA. Citrullinated peptides are abundant in many types of inflammation, RA synovitis with all antigens for the most relevant fine-specificities of anti-citrullinated protein antibodies (ACPAs) (1–5), in extra-articular RA manifestations (6), but also in non-RA related inflammation (7) as well as in *Porphyromonas gingivalis* (*Pg.*) induced periodontitis (PD) (8). Already in the pre-clinical phase, RA patients develop ACPAs against an increasing numbers of epitopes (9). Affinity maturation of ACPA paratopes appears to cause the antigen spreading (10), but little is really understood or even proven how this phenomenon occurs. A persistent response of ACPA expressing plasmablasts predominantly of an IgA isotype suggests one or several persistent mucosal triggers in this process (11). Moreover, the highest diagnostic specificity of IgA-isotypic ACPA further supports the assumption that the most specific immune system activation in RA is happening at mucosal sites (12).

In the following chapters, we try to review parts of the overwhelming amount of data which we think is of most probable relevance. We will follow different currently proposed tracks of RA pathogenesis from genetic and environmental risk factors to microbial species and microbial communities, from innate inflammatory to adaptive immune responses and ultimately to associations with some of the characteristic features of RA. In order to sensitize the readers, we strongly recommend to scrutinize the proposed relationships in view of the Bradford–Hill criteria for causality (13). Among them, we believe that the highest attention should be given to the reported strengths of association, reproducibility, specificity, temporality, and the overall coherence of epidemiological and experimental findings.

INBORN FACTORS IN RA

RA is apparently not very strong clustered in families, but the genetic background of RA was in the focus of pathogenesis oriented research until the decryption of the human genome at the turn of the millennium and in the following years (14, 15). In a nationwide sibling study in the UK from 1993, monozygotic twins had about four times higher RA concordance rates than dizygotic twins (16). More recently, in the largest registry study on the inheritance of RA in Sweden, the odds for RA heritability was about three in first degree relatives and about two in second degree relatives, irrespective of the affected being parent, sibling or offspring (17). Both studies independently point to a significant genetic background of RA, which may confer to about 50% of disease risk. Today genetics in RA are still an important aspect of research with a new focus on personalized medicine, as an individually tailored approach for the minimization of the large inter-individual variability response to therapy (18).

The strongest genetic risk factor for RA is a specific peptide sequence in the type II human leukocyte antigen (HLA) or major histocompatibility complex (MHCII) of only six amino acids, called the shared epitope motif. Shared epitope motifs are especially frequent in native Americans (19). MHCII molecules play a crucial role in the presentation of antigens, and their association with RA is a consistent finding in many populations of different ancestry (20–24). MHCII molecules are central in directing adaptive immune responses. Only a few alleles in the DRB1 molecule, which are coding for QKRAA [Q (glutamine) K (lysine) R (arginine) and AA (alanine-alanine], QRRAA, or RRRAA amino acid sequences in the positions 70–74 of the third hypervariable region, have a strong association with RA. However, other alleles in the HLA complex (25) as well as dozens other non-HLA genes appear to also confer to the genetic risk of RA, but to a much lesser extent (26). Other sufficiently robust RA associated genes are single nucleotide polymorphism (SNP) in the PTPN22 gene, which codes for a non-receptor lymphoid protein phosphatase and negative regulator of presentation of immune complex derived antigens (27) and a specific allele in human PADI4 (28). Other genetic associations were too inconsistently associated with RA to mention in this brief overview.

Recently, X-ray crystallography studies could demonstrate citrullinated as well as non-citrullinated vimentin peptides in the binding groove of HLA-DRB1 molecules (29). This finding suggests that the genetic background of MHC molecules is directly linked to the antigenicity of specific peptides. Interestingly, recent data demonstrate an effect of the shared epitope on the gut microbiome in clinically healthy study populations (30). Thus, it is tempting to speculate that RA-related MHC alleles affect the presentation of disease relevant antigens and the symbiotic coexistence of the host and its microbiota by the same key MHCII molecules. However, other researchers suggested an alternative and probably antigen independent explanation for the association of MHC molecules with RA (31, 32).

Another inborn X-chromosomal risk factor for RA is the female sex. Notably, although female subjects are about two to three times more often affected by RA in the general population, familial RA aggregation appears not to be affected by sex (17). Female RA preponderance seems to be limited to the reproductive phase of life, but late onset RA appears to be similar prevalent in male and in female (33). We currently have no consistent data on an inappropriate inactivation of X-chromosomal genes in RA (34). Furthermore, as indicated by the preferential disease onset in the menopause, RA onset or

flares in the first year after delivery but treatment-independent amelioration of disease activity during pregnancy, the role of the female sex hormones in RA appears to be complex (35, 36). As for all large epidemiological studies, it has to be kept in mind that the results are strongly depending on the robustness of disease definition, e.g., autoantibody status, which can be a major challenge in the field (17). Furthermore, the strength of observed association with sex appears to be affected by ancestry, by disease severity, by disease onset during life time or parity (37). Although the research field on the vaginal microbiome and female health is rapidly growing, we did not retrieve any specific literature on this topic in relation to RA.

AGE AND BEHAVIORAL RISK FACTORS FOR RA

RA as well as RF and ACPA associated types of juvenile idiopathic arthritis may start at any phase of lifetime. However, RA incidence is highest in the fifth and sixth life decade. This fact may hint to the important non-genetic factors, which become only active under certain circumstances. Life style factors also appear to be relevant, as age- and sex-standardized incidences were lower in densely populated areas and in individuals with high educational level (34). Depending on sex, RA occurred in a study from Sweden more often in male farmers, brick layers, and electric or electronic workers, and in female preferentially in nurse assistants and social science related workers (38).

Smoking is one of the best established environmental risk factors especially for RF-positive RA and especially in men (39). Tobacco smoking was the first environmental factor that was associated with the onset RA (40, 41), but smoking can explain the severity of RA only to some extent (42). Furthermore, smoking is associated with extra-articular RA disease manifestations such as interstitial lung disease (43) and subcutaneous rheumatoid nodules (44). The mechanisms of how smoking might affect RA must be further elucidated. Moreover, with the given focus of this review, smoking is also an established risk factor for periodontitis (45).

The influence of diet on the onset and course of RA is since a long time a matter of an intensive debate. Mediterranean diet as well as antioxidant and fruit-rich diet have been proposed to be protective (46–48), while obesity seems to have negative effects on the risk for the development of RA. However, any observed effects of diet on the RA disease risk were rather small, and even bariatric surgery appeared to be without effect on RA status, despite its obvious consequences for the nutritional status as well as for the intestinal microbiome (49, 50). Coffee or tea consumption appears to be irrelevant for the onset of RA (46). Alcohol consumption in contrast to smoking does not seem play a relevant role in the incidence of RA (51), but appears to have modest effects on PD (52).

INVASIVE INFECTIOUS TRIGGERS

One of the most frequent causes of an inflammation is an invasive infection. However, RA in contrast to reactive arthritis starts very rarely with a clinically apparent infection. Following the classic postulates of Robert Koch for the proof of a microbial origin of disease, RA would not be proven infectious origin (53). However, an imperfect but repeatedly significant association of specific MHCII alleles necessary to develop RA may indicate a relevant role of host response mechanisms for an infection with low disease penetrance, which could have prevented the discovery of an infectious origin of RA.

Following the first of Koch's postulates of an infectious disease origin, a microbial agent or at least some of its components should have been detected in RA joints. A landmark study on this topic was published in 2003 (54), when authors searched for bacteria-derived muramic acid by gas chromatography-mass spectrometry (GC-MS) as well as bacterial 16s or 23s rRNA by polymerase chain reaction in RA synovium. This study was positive in a few patients with longstanding RA, but in similar frequency as in control subjects (54). In another study, bacterial DNA from *Pg.* was identified in 15% of RA samples, which was significantly more frequent than in the 3% of synovial fluid from control subjects (55).

Zhao et al. (56) reported the presence of bacterial 16s rRNA from many different species in synovial materials from RA and control samples, which draws any species-specific invasive infection to cause RA into question. However, this notable finding should be confirmed in an independent study. An invasive infection in RA must not necessarily be proven in the joint. In RA associated vasculopathy, *Methylobacterium oryzae* was detected in the aortic adventitia in 3 out of 11 biopsies, but different bacterial species were detected by 16s rRNA sequencing in 4 out of 11 control samples (57). As far as we know, *Methylobacterium oryzae* has never been isolated from RA joints.

Viral infections are since a long time handled as a potential infectious trigger of RA. In a recent systematic review, an overall poor quality of studies on RA incidence upon viral exposure was reported. The risk of RA onset appeared to be somewhat increased after Parvo B19 [$n = 12$ studies, OR = 1.77 (95% CI: 1.11–2.80), $p = 0.02$], hepatitis C virus [$n = 7$ studies, OR = 2.82 (95% CI: 1.35–5.90), $p = 0.006$] and possibly also after EBV infection (58). In summary, we have some evidence for infectious triggers, but only limited evidence for an invasive infection causing RA. Furthermore, all the few positive studies for an invasive infection in RA are still awaiting independent confirmation.

DISEASE MODELS FOR MUCOSAL INFECTIONS AND DYSBIOSIS

In animal models, major effects of oral as well as of intestinal infectious triggers could be observed on incidence and severity of arthritis (**Table 1**). Furthermore, inoculation of some specific periopathogens in the oral cavity appeared to affect the composition of the gut microbiome. However, there also exists experimental evidence from the K/BXN serum transfer model in C57BL/6 mice that an existing arthritis might not only be consequence of intestinal dysbiosis, but may act back

TABLE 1 | Mucosal inflammation in arthritis models.

Model	Animals	Challenge	Microbial stimulation	ACPA status	References
K/BxN	C57BL/6	K/BxN serum	Intestinal *Pg.* on three occasions	Not reported	(59)
CIA	BALB/c	CII + FA	*Pg.* after 3d antibiotics	Unknown	(60)
AIA	DR4-IE-tg	FA	CEP-1 and REP-1 from human and *Pg.*	Positive	(61)
	MHC II (–/) wt				
	C57BL/6				
CIA	DBA/1	CII + FA	*Pg.* W83 wt. and PPAD-	Positive	(62)
CIA	DBA/1	CII + FA	Oral *Pg.* infection	Unknown	(63)
CIA	BALB/C	CII + FA	*Pg.* vs. PPAD def. *Pg.*	Positive	(64)
CIA	B10.RIII mice	CII + FA	*Pg.*, *T. denticola*, *T. forsythia*	Unknown	(65)
CIA	(HLA)-DR1 humanized C57BL/6	CII + FA	Oral *Pg.* infection after 7d SMZ-TMP	Positive	(66)
SKG	ZAP-70 mut	Laminarin	*Pg.* i.p.	Positive	(67)
CIA	DQB1-tg B6	CII + FA	*Prevotella histicola*	unknown	(68)
CIA	DBA/1	CII + FA	*P. gingivalis*, *P. intermedia*	Pos., unchanged	(69)
CIA	DBA/1	CII + FA	Antibiotics	Unknown	(70)
AIA, CIA	TH17–/– C57BL/6	CII+ FA	Antibiotics, Jackson microbiota	Unknown	(71)
CIA	F1 (DBA/1 × B10.Q)	CII + FA	*P. gingivalis*	Unknown	(72)
CIA	DBA/1	CII + FA	Antibiotics before and after challenge	Negative	(70)
	Lewis rats		*P. gingivalis*, *P. intermedia*	Positive	(73)

CII + FA, Type II collagen and FA Freund's adjuvant; CEP, citrullinated alpha enolase from human or Pg.; K/BXN serum transfer model, Serum from F1 generation of T-cell receptor transgenic KRN mice with autoimmune-prone non-obese diabetic (NOD) mice (74). Pg., Porphyromonas gingivalis; REP arginine bearing alpha enolase from human or Pg.

on mucosal inflammation by down-regulation of several pro-resolving mediators (59). As compared to control mice, the gut protective mediator resolvin became metabolized to its inactive 17-oxo metabolite, when arthritis was induced by K/BxN serum transfer. Furthermore, the mucosal expression of anti-inflammatory IL-10, the number of goblet cells and the expression of tight junction molecules was reduced in arthritic mice, thereby increasing the gut permeability for microbes (59). Increased gut mucosal permeability upon serum transfer was further aggravated upon *Pg.* inoculation directly in the stomach, but administration of resolvin in arthritic *Pg.*–inoculated mice normalized mucosal IL-10 expression and gut permeability and ameliorated arthritis. This study elegantly demonstrates how a weakened gut barrier can be critical for the pathogenic action of intestinal microbes (59).

In the study of Flak et al. (59), an oral pathobiont was directly inoculated into the stomach, thereby preventing Pg-induced PD. In the meantime, a correlation of oral and intestinal mucosal colonization was confirmed for several times and in different arthritis models (**Table 1**). However, most of the data come from collagen induced arthritis (CIA), which typically develops a rapidly erosive but self-limiting disease without citrulline specific immune responses. Nevertheless, as a conclusion of a rapidly increasing number of animal experiments, we have strong evidence that arthritis-relevant triggers of the immune system could be initiated by commensal or facultative human pathogens in the oral as well as in the intestinal mucosa.

PERIODONTITIS

Healthy squamous epithelium of the mouth or cylinder epithelium of the gut and respiratory mucosa should represent a sufficient defense line against invading microbes of low virulence. However, these mucosal tissues show important anatomical differences, which may warrant more attention than what is currently reported.

The gingival mucosa especially in the close proximity of teeth represents a weak point in the barrier against invasive microorganisms. The periodontal tissue is perfect site for longstanding commensal colonization and a nidus of dysbiotic biofilm for a permanent immune stimulation. With a 3.47 billion people estimate (95% CI: 3.27–3.68), oral disorders are globally the number one among all level three burden of disease conditions (75). Nutritional components such as carbohydrate intake and other behavioral factors such as standard and habits of dental hygiene as well a smoking are likely to have a major influence on the microbial colonization and thus on both the evolution of caries and periodontitis during lifetime. According to recent global estimates, 743 million people worldwide are affected by severe PD (76).

PD is characterized clinically by bleeding or suppuration upon probing due to pocket formation and loss of supporting alveolar bone (77). In contrast, the gingivitis is characterized by a bleeding of the gingiva without pocket formation and bone loss. PD is triggered by so-called lead bacteria, which are mostly facultative anaerobic pathogens. It is assumed that these ubiquitous taxa are present in every human's oral cavity, but in such small numbers that they can be kept in check by the natural microbiota and the host immune system. Socransky categorized PD triggering bacteria into four different complexes (78), the early colonizer which are mainly streptococci, followed by so called bridge species such as Fusobacteria and *Prevotellaceae*, which create an ideal livelihood for the most aggressive microbes.

More recently, a new periodontal disease model, i.e., the polymicrobial synergy and dysbiosis (PSD) model, has been proposed (79) (**Figure 1B**). Peridontitis in the PSD model is initiated by a synergistic and dysbiotic microbial community rather than by select "periopathogens," such as the "red complex." In this polymicrobial synergy, different members or specific gene combinations within the community fulfill distinct roles which may act synergistically in order to form and stabilize a disease-provoking microbiota. In this model certain microbial species, termed "keystone pathogens" play a crucial role to modulate the host response in ways that impair immune surveillance and shift the balance from homeostasis to dysbiosis. The so called "keystone pathogens" also increase the virulence of the entire microbial community through interactive communication with accessory pathogens.

To the "key stone" pathogens belong the facultative anaerobic bacteria *Pg.*, *Treponema denticola*, *Tannerella forsythia*, and *Aggregatibacter actinomycetemcomitans* (*Aa.*). These pathogens are strongly related to the flora found in deep periodontal pockets associated with advanced periodontal disease (80). *Pg.* possesses some virulence factors of special interest in the context of RA: it has its own citrullinating enzyme, Porphyromonas peptidylarginine deiminase (PPAD), which is expressed on the outer membrane of *Pg.* and differs from human PAD's in its Ca^{2+} independent enzymatic activity (62). Furthermore, PPAD in contrast to human PAD is capable of citrullinating C-terminal arginine residues, which are generated by another *Pg.*-derived enzyme, arginine specific gingipain (Rgp) protease (81). The coordinated activity of these two microbial enzymes is unique in having the capacity of generating known RA autoantigens such as C-terminal citrullinated fibrinogen and enolase without aid of human enzymes (82).

One of the first cross-sectional RA association studies with PD goes back to 1997 (83), when the nowadays available modern biological and targeted immunosuppressive therapies were not available. Many patients were at that time in advanced stages of RA and handicaps in accurately performing oral hygiene measures were likely present in this population with longstanding RA. By using nationwide health care data for PD, the number of reimbursed dental treatment courses for PD as well as the costs for PD therapy before the onset of RA were significantly increased in a large Taiwanese case-control study (84). As compared to health care insurance patients in a database without PD, patients with PD but without dental scaling (HR = 1.89, 95% CI: 1.56–2.29) had the highest RA risk, followed by PD patients who had received PD therapy (HR: 1.35, 1.09–1.67 (85). In some studies, the oral microbiome appears to be altered in RA anyway and irrespective of the co-existence of PD (86, 87), and even in orally healthy subjects (88), but the composition of the oral microbiome was not in all association studies associated with RA (89).

In RA association studies for specific periodontal microbes, *Pg.* was on basis of its citrullinating properties of self- and foreign-antigens the first candidate periodontopathogen to be studied in context of RA (90–92). Infection of the gums by *Pg.* and PD is probably not the same, as *Pg.* alone at very low colonization levels was not sufficient to cause periodontitis in germfree mice, but disrupted the host-microbial homeostasis and caused severe PD when added to a community of commensal microbiota (93, 94). Furthermore, *Pg.* in contrast to typically health associated oral commensals was eliminated from the feces, elicited systemic immune responses and induced pathological changes in the liver, which supports the importance of an oral-gut connection (93).

Better understandable in respect of these experimental findings was that the frequency of PD as well as of immune responses against *Pg.* was increased in a British study in ACPA positive subjects without arthritis (95). In a Western Chinese study, *Pg.* was expanded in patients with established RA, but reduced in ACPA positive high-risk individuals (96). ACPA positivity in contrast was not linked to immunity against *Pg.* in the French early RA study cohort (97). Furthermore, in treatment naïve patients with arthralgia, inflammation was rather linked to the presence of PD than the presence of *Pg.* (98). Moreover, PAD expression and citrullination in the periodontium was neither associated with the presence of *Pg.* nor with *Aa.*, another interesting common pathogen PD in context of RA (99). In a study in patients with established RA, antibodies against *Pg.* derived arginine gingipain type B (RgpB) were associated with RA, but smoking interacted with PD as well as with RA (100). Finally, as a summary from three studies in patients with established RA, the presence of *Pg.* in the gingival crevicular fluid as well as *Pg.* directed antibody response appeared to be more closely associated with PD than with RA (86, 91, 101). Other cell- and surface receptor-specific data will be discussed in the respective chapters.

The second already mentioned periodontal pathogen with specific features of interest in context of RA, *Aa.*, induces the pore-forming toxin leukotoxin-A (LtxA), thereby releasing citrullinating enzymes from neutrophils (102). A third periodontal taxa to be briefly discussed in context of RA is *Prevotella intermedia* (*Pi.*) and Prevotella_6 (P_6). *Pi.* causes citrullination of different peptides in the crevicular fluid, among them peptides from Tenascin-5. Anti-tenascin-5 antibodies were detected in 18% of pre-RA and in about 50% of sera from patients with manifest RA with a specificity of 98% (103). P_6 was identified in the Western Chinese study population in high-risk individuals for RA and in patients with established RA (96).

Pathology of PD

Gingivitis and PD are a continuum of diseases of the teeth supporting tissues (**Figures 1A–D**). In 1976, Roy Page and Hubert Schroeder described PD as the host response to a lasting accumulation of dental plaque. They described the entire process in four phases, an "initial," an "early," an "established," and an "advanced" stage of lesions (104, 105). Initial lesions were characterized by an inflammatory infiltrate of mainly neutrophils, early lesions predominated by macrophages and lymphocytes and later phases of PD with more complex cellular infiltrates.

In gingivitis and the initial stage of PD, the junctional epithelium starts to produce prostaglandin E2 (PGE2) and other chemotactic mediators (106). This leads to enhanced

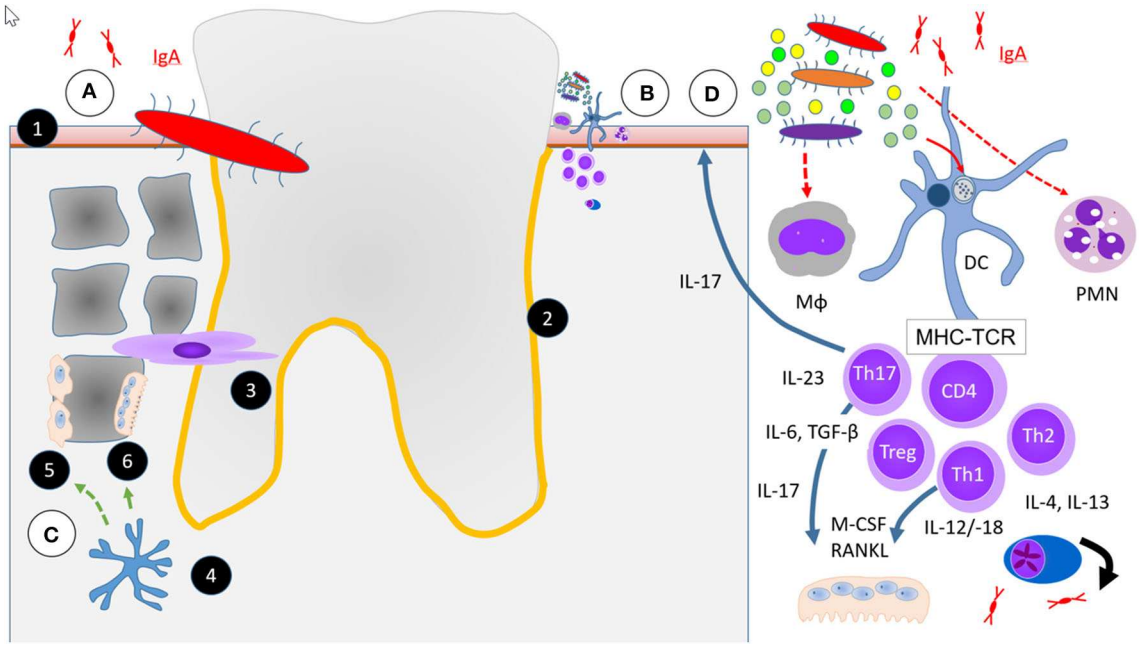

FIGURE 1 | Simplified scheme of four hypotheses or aspects in the etiopathogenesis of periodontitis (PD) relevant to RA. **(A)** Falsified scenario of a single specific infectious microbial pathogen, i.e., *P. gingivalis*. **(B)** Current hypothesis of an increasing multitude of microbes necessary to initiate and maintain PD the polymicrobial synergy and dysbiosis model (PSD) and immune response in RA. **(C)** Osteoimmunology. **(D)** Excessive or unresolved inflammatory response. (1) Squamous epithelium, (2) Periodontal space (orange line), (3) Fibroblast periodontal ligament cells, (4) Osteocyte control Wnt-signaling by Sclerostin and DKK-1 (green dashed arrow) in (5) Osteoblasts and activate (6) Osteoclasts by RANKL (green solid arrow). Abbreviations for different immune cells: Mϕ are macrophages, DC dendritic cells, PMN neutrophils, $CD4^+$, Th1, Th2, Th17, and Treg are some of a much larger multitude of T cell subsets in PD. MHC, major histocompatibility complex and TCR, T cell receptor represent the immunological synapse of antigen-specific immune response. All other abbreviations of soluble factors are explained in the text.

permeability of the endothelium, accumulation of numerous neutrophils, and evasion from the junctional epithelium into the gingival sulcus. The mucosal epithelium starts to proliferate and an apical migration of the junctional epithelium may be observed. Detachment of the junctional mucosa from the enamel defines disease progression from initial to an early disease stage, while deeper pockets are characteristic for an established stage. From this stage onwards the epithelial defense line is growing and the retention of the dysbiotic biofilm at the same time facilitated.

In parallel to the epithelial alterations and cellular infiltrates, the subepithelial matrix stroma becomes increasingly affected. Periodontal ligament cells and other fibroblasts start to proliferate. Furthermore, osteoblasts and other progenitor cells differentiate into osteoclasts and start to degrade the bone matrix, which is the main criterion of advanced PD. Page and Schroeder already reported from longitudinal observations that established lesions did not necessarily progress to bone resorption and edentulism, but could remain stable indefinitely. This led them to conclude that an appropriate level of host response and maintenance of a stable balance despite the persistence of a dysbiotic biofilm could be achieved in chronic PD (104, 107). Variants in the MHC II complex definitely have an important impact on the strength of adaptive immune responses, and an overwhelming amount of data from around the globe shows their importance for the development of RA (20–24). In comparison, the strongest known genetic associations for PD are observed with genes outside the MHC II complex (23, 24, 108), and they are much weaker. Thus, RA and PD are not linked to each other by their genetic background. In the following, we will discuss the potential role of different cell types for the onset of PD with a perspective of its relevance for RA.

Since the early descriptive studies of PD (107), major advances in knowledge about the biology of PD could be achieved by interventional studies in various PD models. Experiments were performed in knock-in and knock-out animals and even germfree mice. Some came to fascinating novel results that changed the view on PD, but most of these data are yet unrelated to systemic (auto-)immunity or arthritis. At this place, we like to refer to the excellent review of Hajishengallis and Korostoff (104) for a comprehensive overview, but we want to briefly discuss here some of the central results and the findings with highest probability to be relevant for RA.

Resident Periodontal Cells

The alveolar bone is the indispensable mechanically stable ground for the fixation of the teeth and covered by the periodontal and gingival epithelium and subepithelial stroma. In between of teeth and the bone, the architecture of the periodontal tissue is defined by collagen fibers, glycoproteins, and many other macromolecules. To allow a stable fixation of the teeth in the cavities of alveolar bone, oblique, and horizontal type-1 collagen fibers are circumferentially strained

around the teeth. This extracellular matrix is synthesized and continuously reshaped for the changing demands over time by resident periodontal ligament (PDL) cells and fibroblasts. However, in their capacity of producing high amounts of tissue degrading matrix metalloproteinases (MMPs) in an activated state, they resemble to some extent fibroblast-like cells in the RA synovium. PDL are also capable of phagocytosing and processing pathogenic periodontal microbes such as *Aa.* (109). Upon stimulation, e.g., with viable *Pg.*, PDL express increased amounts of the inflammatory cytokines IL-1β, IL-6, TNF, as well as chemokines such as IL-8, CCL3, CXCL12, and monocyte chemotactic protein MCP-1 (110). Notably, PDL and fibroblasts of other subgingival localization appear to respond differently to inflammatory stimuli (111). However, despite their capacity of transiently elevating the expression of MHC II molecules upon stimulation with pro-inflammatory cytokines, even potently cytokine-stimulated PDL do not express CD40 or CD80 co-stimulatory molecules, which are fundamentally important characteristics of professional APC (109).

Alveolar bone loss is hardly reversible and a hallmark of the most advanced stage of PD (**Figure 1C**). Until recently, when we compare PD with a cacophonic symphony of the oral and dental health, microbial invasion was believed to be the conductor and the host's inflammatory response the orchestra of PD. The bone tissue was until recently exclusively believed to be the passively suffering audience, with the osteoclasts among them at best as applauding listeners. Recently, it became clear that osteocytes play an active and central role in PD by expressing receptor activator of nuclear factor kappaB ligand (RANKL) (112). Together with macrophage colony stimulating factor (M-CSF) which stimulates the proliferation of osteoclast progenitors (113), RANKL is the key stimulus of osteoclast formation (114, 115). When a mixture of *Pg.* and *Fusobacterium nucleatum*, two frequent dysbiotic bacterial strains were several times inoculated into the periodontal tissue of osteocyte-specific RANKL-deleted mice, osteoclast numbers were not increased nor were the bony surfaces eroded. In contrast, the same PD-associated bacteria mixture increased osteoclast numbers and caused severe alveolar bone loss in wild type mice (112).

Osteocytes do not only express RANKL, but they also express other mediators with major relevance for anabolic processes in the bone. Wnt/β-catenin (named by homologies to the wingless gene in Drosophila and int-1 oncogene in mice) is a major signaling pathway for osteoblast formation and differentiation (116). This pathway is of central importance in the embryonic osteogenesis and later in life for bone homeostasis. Wnt/β-catenin signaling in osteoblasts is under control of sclerostin and dickkopf-1 related protein (DKK1). Sclerostin antagonizes canonical Wnt-signaling directly by binding to the LRP5/6 receptor, while DKK1 exerts its action by binding to the Wnt co-receptor (116, 117). Osteocytes express and secrete sclerostin and DKK1 (118).

Sclerostin appears to be involved in the etiopathogenesis of PD, as knock out mice had a slightly ameliorated PD phenotype (119) and antibodies against sclerostin inhibited the progression of PD (116). Even more interesting, sclerostin antibodies were able to ameliorate inflammation and to partially revert PD related bone damage (118). In conclusion, osteocytes are a source of important mediators of bone in periodontitis. In human PD, sclerostin concentrations were locally elevated in the gingival crevicular fluid only from diseased sites (120), hereby indicating a locally restricted response of osteocytes. This finding seems to be specific for sclerostin, as concentrations of TNF and a soluble activator of the Wnt-pathway, Wnt-5a, appeared to be altered in a similar way (120). In opposite to this local finding, sclerostin in contrast to DKK1 concentrations were elevated on a systemic level in the sera of PD patients (121). In difference to PD, elevated DKK1 but not sclerostin serum concentrations were related to joint damage progression in RA (106). Furthermore, although the biological importance of sclerostin for the negative effects on bone formation were recently shown in arthritic rats (122), the periodontal bone loss in PD is restricted to the gums, and a direct link to the joint erosions in RA remains currently unexplained by soluble factors. However, it could be interesting to study the relevance of sclerostin and DKK1 on a systemic level for other bone-specific aspects of human RA such as osteoporosis, abnormal bone geometry and accelerated thinning of metacarpal bones (123–125).

Innate Immunity

With their main function of phagocytosis and elimination of pathogens, polymorphic nuclear cells (PMN) are the dominant cell population in gingivitis (**Figure 1D**). Given the relevance of infectious noxes in PD, it appears rational to assume that an impaired elimination of dysbiotic bacteria by defective PMN might be critical. However, a normal frequency of PD in patients with a severe X-linked defect in the nicotinamide adenine dinucleotide phosphate (NADPH)-oxidase necessary for the respiratory burst of phagocytes (104, 126) suggests only a secondary role of bacterial elimination by neutrophils for the prevention of PD.

We have increasing evidence that a periodontopathogen such as *Pg.* may circumvent elimination despite an originally intact neutrophil biology. PMN migrate along chemokine gradients such as C′5a or C′3a complement factor concentrations through the capillary endothelium, the submucosal stroma and gingival epithelium. Intriguingly, therapeutic blockade of the C′5 receptor in a prophylactic protocol prevented PD, respectively application in a therapeutic manner alleviated PD in a *Pg.* induced periodontitis model (127). Notably, *Pg.* can use the C′5a receptor in crosstalk with toll-like receptor 2 (TLR-2) to induce proteasomal degradation of the Toll-like receptor-2 adaptor myeloid differentiation primary response protein-88 (MyD88) in neutrophils and other phagocytes (128). The resulting lack in MyD88 impairs the rapid activation of the inflammasome complex and affects the host defense against dysbiotic microbes, but the same initial process activates a phospho-inositol-3 kinase (Pi3K) dependent pro-inflammatory pathway.

TLR-2 is a pivotal receptor for innate immune processes in neutrophils, in monocytes and in macrophages (129). Activation of TLR-2 appears to be crucial for the development of PD, as TLR-2 deficient mice are normally resistant to *Pg.* induced PD (130). Adoptive cell transfer of TLR-2 positive monocytes and macrophages enables *Pg.* to induce PD in TLR-2 deficient

mice (130). Furthermore, TLR-2 may mediate longer bacterial persistence in macrophages and stimulate TNF-dependent osteoclast activation (130, 131).

Macrophages are directed *in vitro* to M1 in the presence of lipopolysaccharides (LPS), granulocyte-monocyte colony stimulating factor (GM-CSF), and interferon-gamma (IFN-γ), and are characterized by CD86 surface expression, inducible nitric oxide synthase (iNOS), TNF, interleukin 1 beta (IL-1β), IL-6, IL12, and IL-23 expression. M2 macrophages in contrast origin from alternative activation in a Th2 dominated cytokine milieu with excess of IL-4 and IL-13 from Th2 differentiated T cells. M2 cells are characterized by CD206, IL-10, and transforming-growth factor beta (TGF-β) expression (132). Both, M1 as well as M2 macrophages are present in human PD, but periodontal macrophages appear to be predominantly polarized to the classically activated M1 phenotype (133, 134).

Switching From Innate to Adaptive Immunity

A low number of lymphocytes, predominantly $CD4^+$ and $CD8^+$ and a few γδ T cells can be found in the healthy periodontium (**Figure 1D**) (135). Upon activation by antigen-presenting cells, naive $CD4^+$ T cells can be polarized into distinct effector T helper (Th) cell subsets; Th1, Th2, Th17, and regulatory T (Treg) cells, depending on the local cytokine milieu.

Dendritic cells (DCs) are the best studied APCs in mucosal tissues. DCs can be subdivided into predominantly resident DCs and those with migratory potential. For the spreading of RA relevant antigens, the latter appear to be of greater interest (136). With regard to their migratory capacity, *Pg.* is capable of inducing CCR6 expression in $CD1c^+$ DCs, as the CCL20 ligand of CCR6 was elevated in *Pg.* induced PD (137). Non-canonical DC maturation by *Pg.* is reported to occur with or without GM-CSF/IL-4, and *Pg.*-infected DCs become resistant to apoptosis and inflammatory pyroptosis (138).

The 67 kDa minor fimbriae Mfa-1 bacterial adhesion molecule is known for inducing the expression of dendritic cell-specific intercellular adhesion molecule-3-grabbing non-integrin (DC-SIGN) or CD209 (138). Mfa-1 is a DC-SIGN ligand, and the 41 kDa major fimbriae protein FimA a TLR2 agonist (139). DC-SIGN and TLR-2 are two different pattern recognition receptors (PRRs) on DCs, and their activation has divergent consequences for the survival of *Pg.* (138). TLR2/4 deficiency ameliorates the course of PD to the costs of more extensive bacterial spreading throughout the body due to insufficient bacterial containment or killing (140). Uptake of *Pg.* into DC by interaction of Mfa-1 with DC-SIGN resulted in lower intracellular killing and higher intracellular content of *Pg.* in single membrane phagosomes, where the bacteria survived intracellularly after prevention of phagolysosome formation. Furthermore, interaction of Mfa-1 with DC-SIGN in stably transfected monocytic cell lines induced lower expression levels of CD80, CD83, and CD86 co-stimulatory molecules, and secreted significantly lower levels of inflammatory cytokines IL-1β, IL-6, IL-8, IL-12 p70, and TNF (139). In contrast, uptake of *Pg.* in the absence of DC-SIGN upon single activation of TLR-2 and autophagy was associated with endosomal lysis and reduced survival of *Pg.* (138).

Another receptor on DCs for fimbriae proteins is C-X-C chemokine receptor type 4 (CXCR4), which is also present on DCs in RA synovium (141). Activation of the CXCR4 receptor appears to be beneficial for the severity of PD by disrupting immunosurveillance, but with the consequence of prolonged bacterial persistence (142, 143). As another interesting finding, CXCR4 inhibition appears to be beneficial in terms of a lower expression of oncogenes (144). Upon activation of the MAP kinase pathway, *Pg.* may induce protective genes against oxidative stress and apoptosis in mDCs via forkhead box class-O protein FOXO1 (143). Control of FOXO1 in DCs reduced the cleavage of caspase-3 and decreased the expression of pro-apoptotic proteins Bax and Bim (144). Myeloid DCs had a better longevity and propagated the generation of local Treg by Indole amine 2,3 dioxygenase (Ido1) activity in the presence of *Pg.* (144).

FOXO1 transcription factors appear to be essential for the mucosal immunity, as they do not only regulate DCs, but pro-inflammatory signaling molecules (TLR-2, TLR-4, IL-1β, and TNF), wound healing factors such as TGF-β and vascular endothelial growth factor (VEGF), integrins, a proliferation inducing ligand (APRIL) and B-lymphocyte stimulator (Blys), T-regulatory modulators (Foxp3 and CTLA-4), antioxidants and DNA repair enzymes in different immune relevant cell populations (145). In conclusion, *Pg.* infected and apoptosis resistant mDC can lead to local immunological tolerance, but are at the same time a good candidate for spreading the key pathobiont of PD into other organs and tissues.

$CD207^+$ (langerin) positive Langerhans cells (LC) are potent immune regulators, but are in contrast to conventional myeloid DCs resident cells predominantly in the periodontal epithelium (146). They are important mediators of *Pg.* induced local Th17 differentiation, but have only little effect on the migratory capacity of conventional mDCs (146). Myeloid CD207-DCs could migrate from the lamina propria into the regional lymph nodes. We speculate that non-Langerhans DC are more likely to have an impact on systemic immune response or microbial spreading. Furthermore, the generation of Th1 cells as well as regulatory T cells was not affected in mice lacking LC (146). Notably, despite a deficiency of Th17 cells, alveolar bone resorption by osteoclasts was not affected by a lack of LC (146).

Adaptive Immune Response

T and B cell infiltrates are abundantly present in established and in advanced PD (104) (**Figure 1D**). T cells become locally primed, according to the dominating cytokine milieu, into Th1, Th2, or Th17 cells, to provide locally active inflammatory, regulatory, or immune activating signals. Th17 cells are divided into two subsets; homeostatic Th17 cells which accumulate in the periodontal space in an IL-6 dependent manner, and locally expanding Th17 cells which require both, IL6 and mostly monocyte derived

IL-23 for local expansion. Genetic as well as therapeutic blockade of IL-17 diminished the amount of inflammatory response in PD as well as bone loss, but propagated fungal infections (147).

Plasma cells are also present in chronic PD. The occurrence of IL-35 and IL-37 expression appears to be beneficial to the local inflammatory process, as both cytokines inhibited osteoclast formation at least *in vitro* (148). However, these findings appear to be controversial to other studies, and we retrieved surprisingly little original data on the role of plasma cells as local antibody secreting cells (149).

Probably more interesting for the systemic aspects of mucosa driven autoimmunity in RA is the total lack of reports regarding the formation of lymph follicles or other organized lymphoid structures, which appears notable in view of more than 500 histological studies that were performed in relation to PD. Thus, any canonical immune response in relation to mucosal infections requires the migration from the affected tissue to the regional lymph nodes.

Effects of PD Treatment on RA

More intensive than only standard hygienic means are necessary in the advanced stages of PD, when deeper pockets prevent an efficient reduction of pathogenic bacteria from heavily colonized dental plaques (76). Standard of care in advanced PD is non-surgical scaling and root planning (SRP) plus intensive oral hygiene, e.g., with antimicrobial chlorhexidine containing mouth rinse. This procedure reduces the periodontal microbiota at least transiently is called a one-stage full mouth disinfection (FMD), which may be completed by short term systemic antibiotic therapy (150–152). In a recently published randomized controlled trial in patients with PD plus RA, no significant effect on RA disease activity was demonstrated upon standard PD therapy (153). However, although the autoantibody profile against citrullinated peptides remained unaffected, it was shown in another uncontrolled study that FMD plus antibiotics could be beneficial for RA in some highly selected patients (154). More mechanistically, no significant changes in the peripheral blood DC or T cell population were observed upon standard non-surgical local therapy for PD (136), but myeloid DCs (mDCs) with a pro-inflammatory phenotype were reduced upon one week of antibiotic co-therapy (136). These changes in numbers of mDCs with an inflammatory phenotype to the levels of healthy control subjects was paralleled by lower Th17 to Treg ratios (136).

So far, we have only discussed the local dysbiotic periodontal colonization and the resulting inflammation that could be associated with RA, but a sufficiently large cross-sectional RA association study on the subgingival microbiome came to a negative result (89). Furthermore, it has to be kept in mind that the periodontal microbiome in RA could share relevant similarities with the microbiome on the palatinal tonsils, as it was at least demonstrated in healthy subjects (155). According to this finding, it might be worth to study whether a colonization of dysbiotic bacteria in the periodontal niches might be linked to a pathogenic antigen presentation on the tonsils in patients with RA.

INTESTINAL MUCOSA IMMUNITY

Intestinal Dysbiosis

One of the first large metagenome-wide association study (MGWAS) on the microbiome in fecal samples revealed significant differences between RA and control subjects with regard to the phylogenetic taxa, redox environment, transport, and metabolism of iron, sulfur, zinc, and arginine (156). Furthermore, significant associations were observed when the stool samples were compared to dental biofilm and saliva from the same individuals (156). Interestingly, MTX and an alternative herbal treatment partially restored the microbiome to a more normal respectively healthier state (156), an unexpected finding at that time, which resembles experimental evidence that an inflammatory status such as arthritis could act back to disrupt the mucosal integrity (59).

As to be expected are nutritional factors important modulators of the intestinal microbiome, which appears to also have important impact on systemic immunity. It was recently shown in this context that the treatment of mice with an alpha-glucosidase inhibitor affected the intestinal microbiome and alleviated CIA (141). Furthermore, vitamin D and its active 1,25 hydroxylated metabolite is not only a differentiation factor of monocytes and Th17 cells (157, 158), but vitamin D deficiency impairs the intestinal barrier function and affects the microbiome composition (74).

In 2017, N-acetylglucosamine-6-sulfatase (GNS) and filamin A (FLNA) were identified in RA as HLA-DR–presented peptide autoantigens for T and B cell responses (159). Both autoantigens had marked sequence homology with gut derived peptides from *Prevotella copri* (*Pc.*) and other gut commensals (159). Since then *Pc.* is in the focus by research on microbial species that could be implicated in the etiopathogenesis of RA (159–163). Subsequently, a *Pc.*-derived 27 kDa peptide was identified in association with new onset RA (160). In 2019, Alpizar-Rodriguez et al., reported that *Pc.* was enriched in the gut microbiome of asymptomatic European first-degree relatives of RA patients with immunity against citrullinated peptides, when their stool microbiome was compared to asymptomatic first degree relatives without ACPA (161). In the same year, *Pc.* as well as other Prevotella species were reported as being enriched in a gut MGWAS in Japanese RA patients (164). *Prevotellaceae* are also common in the periodontal pathology, but is to our knowledge not specifically associated with RA when present in the oral microbiota (165). While these studies appear to hint to potential microbial triggers of RA related immunity, it is remarkable to find in healthy subjects bearing RA-associated DRB1 alleles in association with the intestinal microbiome (30), suggesting that a RA-related genetic background could shape the microbiome.

Immune System Activation in the Intestinal Mucosa

The importance of ACPA in RA led us to search in the literature for evidence of the presence of citrullinated peptides in the mucosa. Indeed, a recent proteome analysis revealed striking differences in abundance of citrullinated proteins in the colon mucosa in RA and in healthy controls (166). However, this

study was performed in a small number of patients only and awaits replication. Furthermore, we do not know whether the citrullinated peptides represent known RA antigens.

Goblet cells and M cells are specialized epithelial intestinal cells, which are permissive for intestinal antigens from the gut lumen. Furthermore, CX3CR1$^+$ expressing dendritic cells (DC) have the capacity of sampling commensal antigens in the small intestine via transepithelial intercellular dendrites into the gut lumen (167).

Mucosa associated lymphoid tissue (MALT) is the next line of defense against invading microbes. MALT has many anatomical similarities with secondary lymphoid organs of other locations, but a specificity of MALT is its immediate vicinity to in quantity more commensal than virulent microbial factors. Invading gut commensals are rapidly killed by macrophages, but intestinal DCs can contain small numbers of live commensals for several days (168). This process is highly relevant to selectively induce a protective IgA response. At the same time, immune responses to commensal bacteria need to be restricted to the regional lymph nodes, without potentially damaging the entire immune system (168).

DC subtypes are since a couple of years in the focus of research on intestinal MALT. Circulating DC are found throughout the entire intestine. They are located in the lamina propria of the small gut, where they accumulate in lymphoid aggregates or follicles such as Peyer patches. DC engulf microbial peptides, degrade them in their phagolysosomes into presentable components via MHC molecules to antigen specific T cell receptors (TCR) of their thymus selected T lymphocyte counterparts. DCs can be subdivided into resident plasmacytoid DCs (pDCs) and mDCs in secondary lymphoid organs, and into a migratory tissue derived DC phenotype. Notably, migratory DCs can be further subdivided by their surface molecule expression profile. In context of the local induction of regulatory T cells (iTreg), CD103$^+$ α_E integrin expressing migratory DC have the selective ability to direct toward (iTreg) via production of retinoic acid, which is an important myeloid cell differentiation factor (169, 170). CD103$^+$ cells are present throughout the intestinal mucosa, but can be differentiated according to their Integrin αM CD11b expression into CD103$^+$CD11b$^+$ DCs preferentially of the small intestine and CD103$^+$CD11b$^-$ DCs, which are enriched in the colonic mucosa, in Peyer's patches and lymphoid follicles (171). As a third intestinal mucosal DC population, CD103$^-$CD11b$^-$ DCs also express CX3CR1. This DC subset is resident under control of normal commensal conditions, but can switch into a migratory phenotype with the capacity of entering regional lymph nodes upon broad-spectrum antibiotic therapy (170). At least to be briefly mentioned in this review are type 3 immune-like cells (ILC3s) a fourth non-classical type of antigen presenting cells, which are important for the inflammatory response in the gut mucosa and at least present in the synovium of arthritic joints (172, 173).

Each DC subtype appears, depending on the DC to T cell ratio and other factors, to be associated with rather specific T cell responses: CD103$^+$CD11b$^-$ DCs appear to essentially foster the generation of a Th1 expression profile, but CD103$^+$CD11b$^+$ DCs preferentially lead to either Th17 or iTreg differentiation, while CD103-CD11b$^+$ DCs appear to direct T cells to both, Th1 and Th17 responses (171, 174, 175). In the presence of IL-6 and TGF-β, T cells can either differentiate into pro-inflammatory or into immune stimulatory Th17 cells or into iTreg. Macrophage derived IL-23 is essential in directing CD4$^+$ T cells into the inflammatory Th17 phenotype. Th17 cells express different IL-17 isoforms and IL-22, which exert important functions in APCs and in epithelial cells (176, 177). After having passed the regional lymph nodes, gut derived T cells, but also B cells and plasma cells could circulate throughout the entire body, and their evasion from the circulation will be directed by specific exit signs for their integrin homing receptors. The probably most prominent representative of these molecules is α4 β7 integrin, which directs the evasion of lymphocytes at intestinal blood vessels. IgA producing plasma cells should essentially be located at the gut mucosa, but specialized regulatory microenvironments are of major relevance for the local distribution of antibody secreting plasma cells in the gut or in the bone marrow (178, 179).

PRELIMINARY CONCLUSIONS

We have aimed to collect as much as possible of the currently available clinical, epidemiological, and experimental evidence for the discussion of a causative link between mucosal inflammation and the emergence of RA (**Figure 2**). However, the amount of literature is overwhelming, and not all the potentially relevant information could be incorporated into this review simply for space and time restriction. We will now briefly discuss assembled data according to the Bradford Hill criteria of causality (13).

1. Strength of association: We identified many reports with an association, but pathogenic links between (a) periodontitis and RA, (b) oral microbiome and RA, (c) intestinal microbiome and RA as well as, (d) specific periodontal microbiota and RA were always weak.
2. Consistency: Shared epitope and the presence of ACPA were reproduced in many populations and on different continents. Reports on association of PD with RA came from different continents. Furthermore, this association was observed in populations of different ancestry. Intestinal *Prevotellaceae* were identified in association with RA in Northern America, Europe and Japan, but a Chinese study did not find this association. The microbial metagenome is probably more diverse than the human genome, but all the currently available MGWAS studies are by far smaller than the rather large and robust genetic association studies. In conclusion, although we have no formal power estimates for this statement, we believe that larger MGWAS studies are warranted.
3. Specificity: Microbes with a low level of virulence usually colonize in mixed communities. It can be assumed that this statement is likewise true for the periodontal and other localizations such as the intestinal tract. The polymicrobial synergy and dysbiosis model (PSD) is an example of how a combination of bacteria rather than a single specific species is causal in a chronic disease process like PD. Furthermore, not only *Pg.*, but different periodontal pathobionts aroused suspicion to specifically trigger different important aspects

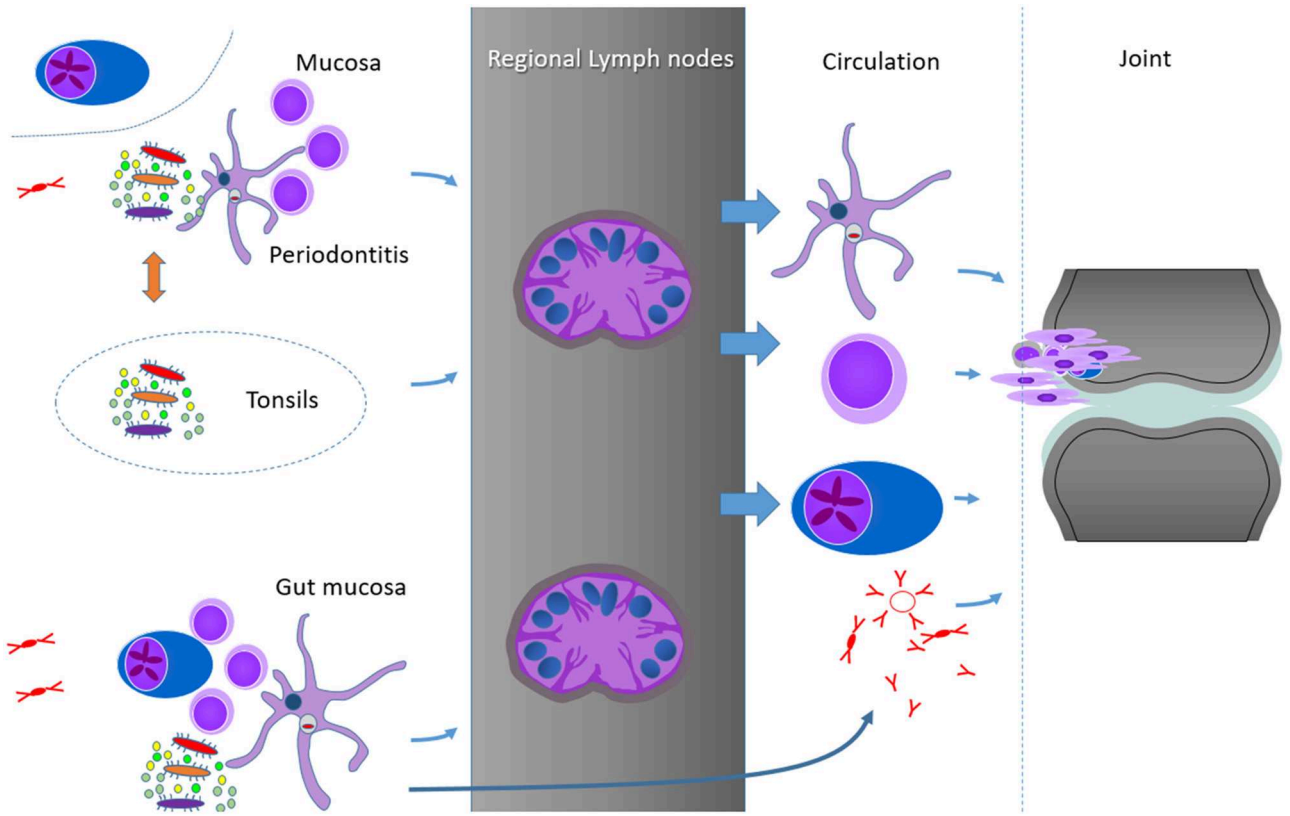

FIGURE 2 | Hypothetical summary schedule of some of the possibilities to connect the mucosal sites and RA joints, from top to bottom: persistent bacterial components in DC and other phagocytosing cells, shaping of the T cell memory at mucosal sites, plasmablasts or plasma cells and soluble factors, as exemplified by antibodies (IgG monomers, IgM pentamers, and IgA dimers). Important for the control of the mucosal responses are probably the clearing regional and secondary lymph nodes. As we identified no reports on germinal center responses in the periodontal tissues, but some similarities between the subgingival periodontal and the palatinal microbiome, we include the tonsils as another possibility of mucosal activation of immune processes in RA.

of immunity in RA. Moreover, at least in experimental settings, bacteria of the oral cavity significantly affected the intestinal microbiome. In conclusion, it is from the current perspective not a single agent, but the combination of oral and intestinal microbiota as well as other potential sites of mucosal inflammation to be followed in parallel in future studies.

4. Temporality: PD diagnosis before the onset of RA perfectly fulfills this prerequisite of causality. Furthermore, a high prevalence of intestinal *Pc.* in an ACPA-positive at risk population in a cross-sectional setting appears to fulfill this criterion, but the definitive results of longitudinal studies have to be awaited, before definiteconclusions can be made.
5. Biological gradient: A dose dependency of a single causal agent, was demonstrated in several experimental settings. However, in PD, not the most severe aggressive type but the less progressive chronic form is preferentially associated with RA. Furthermore, it is currently not clear how to quantify models of polymicrobial synergy. We currently have no information of biological gradients at hands to explain the entire process of mucosal inflammation, citrullination, ACPA-specific immunity, and arthritis. Furthermore, we yet do not know how the type, the combination of synergistic factors, or the effects of time exposure for different interacting stimuli to be designed in a composite model.
6. Biological plausibility: We identified many reports about mucosal inflammation or a specific mucosal stimulus that were associated with onset or severity of experimental arthritis. Now, albeit the detailed current knowledge about the cellular mechanisms in the intestinal immune system and in periodontal inflammation is not known, it appears essential to pursue the identification of the cellular and molecular processes between mucosal inflammation and immunization in arthritis models as well as in human disease.
7. Coherence: This review is only a small extract of all the available, but to some extent contradictory knowledge, i.e., regarding specific microbial taxa being implicated in the connection of mucosal immunity and RA. Furthermore, in terms of generalizability and the transfer of data from model to disease, questions about the ACPA status, which is different in CIA and RA, as well as the different arthritis susceptibility in male and female humans and mice should be answered.
8. Experiment: Chronic PD is a hardly reversible disease, but the effects of PD therapy on RA severity are controversial. Lower

incidence rates of RA in treated than in untreated PD patients go into this definition.

9. Analogy: Different periodontal pathogens cause a similar type of PD, and different oral or intestinal microbiota were associated with RA. However, it is too early to decide whether different exposures in terms of microbial taxa leading to RA can be interpreted as analog evidence for causality, or alternatively, as a violation of the criterion of specificity.

Taken together, we summarized the current viewpoints on putative mucosal triggers of RA in a narrative review. This paper is an incomplete compilation of the currently available supporting data for the postulated link between mucosal immunity and RA. In this summary of work in progress, several pieces of evidence appear to be of high validity. We conclude that ongoing major efforts, both on PD as well as the oral and intestinal microbiome, are warranted in order to answer the many remaining questions about the etiopathogenesis of RA.

AUTHOR CONTRIBUTIONS

AS wrote the section about periodontitis. BM wrote the other sections. All authors critically reviewed the entire manuscript for the content. In doing so, all authors agree to be accountable for the content of the work.

ACKNOWLEDGMENTS

The authors are grateful to all the collaborators on this topic in the past. Kira Herren wrote her master thesis on this topic. We are especially grateful for her preparatory work.

REFERENCES

1. van Beers JJBC, Willemze A, Stammen-Vogelzangs J, Drijfhout JW, Toes REM, M Pruijn GJ. Anti-citrullinated fibronectin antibodies in rheumatoid arthritis are associated with human leukocyte antigen-DRB1 shared epitope alleles. *Arthritis Res Ther.* (2012) 14:R35. doi: 10.1186/ar3744
2. Tilleman K, Union A, Cantaert T, De Keyser S, Daniels A, Elewaut D, et al. In pursuit of B-cell synovial autoantigens in rheumatoid arthritis: confirmation of citrullinated fibrinogen, detection of vimentin, and introducing carbonic anhydrase as a possible new synovial autoantigen. *Proteomics Clin Appl.* (2007) 1:32–46. doi: 10.1002/prca.200600221
3. Takizawa Y, Suzuki A, Sawada T, Ohsaka M, Inoue T, Yamada R, et al. Citrullinated fibrinogen detected as a soluble citrullinated autoantigen in rheumatoid arthritis synovial fluids. *Ann Rheum Dis.* (2006) 65:1013–20. doi: 10.1136/ard.2005.044743
4. Kinloch A, Tatzer V, Wait R, Peston D, Lundberg K, Donatien P, et al. Identification of citrullinated alpha-enolase as a candidate autoantigen in rheumatoid arthritis. *Arthritis Res Ther.* (2005) 7:R1421–9. doi: 10.1186/ar1845
5. Lundberg K, Nijenhuis S, Vossenaar ER, Palmblad K, van Venrooij WJ, Klareskog L, et al. Citrullinated proteins have increased immunogenicity and arthritogenicity and their presence in arthritic joints correlates with disease severity. *Arthritis Res Ther.* (2005) 7:R458–67. doi: 10.1186/ar1697
6. Bongartz T, Cantaert T, Atkins SR, Harle P, Myers JL, Turesson C, et al. Citrullination in extra-articular manifestations of rheumatoid arthritis. *Rheumatology.* (2007) 46:70–5. doi: 10.1093/rheumatology/kel202
7. Makrygiannakis D, Af Klint E, Lundberg IE, Löfberg R, Ulfgren AK, Klareskog L, et al. Citrullination is an inflammation-dependent process. *Ann Rheum Dis.* (2006) 65:1219–22. doi: 10.1136/ard.2005.049403
8. Janssen KMJ, Vissink A, De Smit MJ, Westra J, Brouwer E. Lessons to be learned from periodontitis. *Curr Opin Rheumatol.* (2013) 25:241–7. doi: 10.1097/BOR.0b013e32835d833d
9. Suwannalai P, van de Stadt LA, Radner H, Steiner G, El-Gabalawy HS, Zijde CM, et al. Avidity maturation of anti-citrullinated protein antibodies in rheumatoid arthritis. *Arthritis Rheum.* (2012) 64:1323–8. doi: 10.1002/art.33489
10. Kongpachith S, Lingampalli N, Ju C, Blum LK, Lu DR, Elliott SE, et al. Affinity maturation of the anti-citrullinated protein antibody paratope drives epitope spreading and polyreactivity in rheumatoid arthritis. *Arthritis Rheumatol.* (2019) 71:507–17. doi: 10.1002/art.40760
11. Elliott SE, Kongpachith S, Lingampalli N, Adamska JZ, Cannon BJ, Mao R, et al. Affinity maturation drives epitope spreading and generation of proinflammatory anti-citrullinated protein antibodies in rheumatoid arthritis. *Arthritis Rheumatol.* (2018) 70:1946–58. doi: 10.1002/art.40587
12. Sieghart D, Platzer A, Studenic P, Alasti F, Grundhuber M, Swiniarski S, et al. Determination of autoantibody isotypes increases the sensitivity of serodiagnostics in rheumatoid arthritis. *Front Immunol.* (2018) 9:876. doi: 10.3389/fimmu.2018.00876
13. Hill AB. The environment and disease: association or causation? *Proc R Soc Med.* (1965) 58:295–300. doi: 10.1177/003591576505800503
14. Okada Y, Wu D, Trynka G, Raj T, Terao C, Ikari K, et al. Genetics of rheumatoid arthritis contributes to biology and drug discovery. *Nature.* (2014) 506:376–81. doi: 10.1038/nature12873
15. Lander ES, Linton LM, Birren B, Nusbaum C, Zody MC, Baldwin J, et al. Initial sequencing and analysis of the human genome. *Nature.* (2001) 409:860–921. doi: 10.1038/35057062
16. Silman AJ, MacGregor AJ, Thomson W, Holligan S, Carthy D, Farhan A, et al. Twin concordance rates for rheumatoid arthritis: results from a nationwide study. *Br J Rheumatol.* (1993) 32:903–7. doi: 10.1093/rheumatology/32.10.903
17. Frisell T, Holmqvist M, Källberg H, Klareskog L, Alfredsson L, Askling J. Familial risks and heritability of rheumatoid arthritis: role of rheumatoid factor/anti-citrullinated protein antibody status, number and type of affected relatives, sex, and age. *Arthritis Rheum.* (2013) 65:2773–82. doi: 10.1002/art.38097
18. Bluett J, Barton A. Precision medicine in rheumatoid arthritis. *Rheum Dis Clin North Am.* (2017) 43:377–87. doi: 10.1016/j.rdc.2017.04.008
19. Peschken CA, Hitchon CA, Robinson DB, Smolik I, Barnabe CR, Prematilake S, et al. Rheumatoid arthritis in a north American native population: longitudinal followup and comparison with a white population. *J Rheumatol.* (2010) 37:1589–95. doi: 10.3899/jrheum.091452
20. Traylor M, Curtis C, Patel H, Breen G, Lee SH, Xu X, et al. Genetic and environmental risk factors for rheumatoid arthritis in a UK African ancestry population: The GENRA case-control study. *Rheumatol (United Kingdom).* (2017) 56:1282–92. doi: 10.1093/rheumatology/kex048
21. Liu WX, Jiang Y, Hu QX, You XB. HLA-DRB1 shared epitope allele polymorphisms and rheumatoid arthritis: a systemic review and meta-analysis. *Clin Investig Med.* (2016) 39:E182–E203. doi: 10.25011/cim.v39i6.27487
22. Gregersen PK, Silver J, Winchester RJ. The shared epitope hypothesis. An approach to understanding the molecular genetics of susceptibility to rheumatoid arthritis. *Arthritis Rheum.* (1987) 30:1205–13. doi: 10.1002/art.1780301102
23. Liukkonen J, Gürsoy UK, Könönen E, Gürsoy M, Metso J, Salminen A, et al. Salivary biomarkers in association with periodontal parameters and the periodontitis risk haplotype. *Innate Immun.* (2018) 24:439–47. doi: 10.1177/1753425918796207

24. Zupin L, Moura Rodrigues R, Navarra CO, Bevilacqua L, Catamo E, Di Lenarda R, et al. Association of *LTA* gene haploblock with periodontal disease in Italian adults. *J Periodontal Res.* (2019) 54:128–33. doi: 10.1111/jre.12609
25. Raychaudhuri S, Sandor C, Stahl EA, Freudenberg J, Lee H-S, Jia X, et al. Five amino acids in three HLA proteins explain most of the association between MHC and seropositive rheumatoid arthritis. *Nat Genet.* (2012) 44:291–6. doi: 10.1038/ng.1076
26. Viatte S, Barton A. Genetics of rheumatoid arthritis susceptibility, severity, and treatment response. *Semin Immunopathol.* (2017) 39:395–408. doi: 10.1007/s00281-017-0630-4
27. Clarke F, Purvis HA, Sanchez-Blanco C, Gutiérrez-Martinez E, Cornish GH, Zamoyska R, et al. The protein tyrosine phosphatase PTPN22 negatively regulates presentation of immune complex derived antigens. *Sci Rep.* (2018) 8:12692. doi: 10.1038/s41598-018-31179-x
28. Plenge RM, Padyukov L, Remmers EF, Purcell S, Lee AT, Karlson EW, et al. Replication of putative candidate-gene associations with rheumatoid arthritis in >4,000 samples from North America and Sweden: association of susceptibility with PTPN22, CTLA4, and PADI4. *Am J Hum Genet.* (2005) 77:1044–60. doi: 10.1086/498651
29. Scally SW, Law S-C, Ting YT, Heemst J van, Sokolove J, Deutsch AJ, et al. Molecular basis for increased susceptibility of Indigenous North Americans to seropositive rheumatoid arthritis. *Ann Rheum Dis.* (2017) 76:1915–23. doi: 10.1136/annrheumdis-2017-211300
30. Asquith M, Sternes PR, Costello M, Karstens L, Diamond S, Martin TM, et al. HLA alleles associated with risk of ankylosing spondylitis and rheumatoid arthritis influence the gut microbiome. *Arthritis Rheumatol.* (2019) 71:1642–50. doi: 10.1002/art.40917
31. de Almeida DE, Ling S, Holoshitz J. New insights into the functional role of the rheumatoid arthritis shared epitope. *FEBS Lett.* (2011) 585:3619–26. doi: 10.1016/j.febslet.2011.03.035
32. Ling S, Pi X, Holoshitz J, Rogers NE, Ignarro LJ, Voskuhl RR. The rheumatoid arthritis shared epitope triggers innate immune signaling via cell surface calreticulin. *J Immunol.* (2007) 179:6359–67. doi: 10.4049/jimmunol.179.9.6359
33. Crowson CS, Matteson EL, Myasoedova E, Michet CJ, Ernste FC, Warrington KJ, et al. The lifetime risk of adult-onset rheumatoid arthritis and other inflammatory autoimmune rheumatic diseases. *Arthritis Rheum.* (2010) 63:633–9. doi: 10.1002/art.30155
34. Chitnis S, Monteiro J, Glass D, Apatoff B, Salmon J, Concannon P, et al. The role of X-chromosome inactivation in female predisposition to autoimmunity. *Arthritis Res.* (2000) 2:399–406. doi: 10.1186/ar118
35. Alpizar-Rodriguez D, Förger F, Courvoisier DS, Gabay C, Finckh A. Role of reproductive and menopausal factors in functional and structural progression of rheumatoid arthritis: results from the SCQM cohort. *Rheumatology.* (2019) 58:432–40. doi: 10.1093/rheumatology/key311
36. Alpizar-Rodriguez D, Mueller RB, Möller B, Dudler J, Ciurea A, Zufferey P, et al. Female hormonal factors and the development of anti-citrullinated protein antibodies in women at risk of rheumatoid arthritis. *Rheumatology.* (2017) 56:1579–85. doi: 10.1093/rheumatology/kex239
37. Viatte S, Plant D, Han B, Fu B, Yarwood A, Thomson W, et al. Association of HLA-DRB1 haplotypes with rheumatoid arthritis severity, mortality, and treatment response. *JAMA.* (2015) 313:1645. doi: 10.1001/jama.2015.3435
38. Li X, Sundquist J, Sundquist K. Socioeconomic and occupational risk factors for rheumatoid arthritis: a nationwide study based on hospitalizations in Sweden. *J Rheumatol.* (2008) 35:986–91.
39. Sugiyama D, Nishimura K, Tamaki K, Tsuji G, Nakazawa T, Morinobu A, et al. Impact of smoking as a risk factor for developing rheumatoid arthritis: a meta-analysis of observational studies. *Ann Rheum Dis.* (2010) 69:70–81. doi: 10.1136/ard.2008.096487
40. Voigt LF, Koepsell TD, Nelson JL, Dugowson CE, Daling JR. Smoking, obesity, alcohol consumption, and the risk of rheumatoid arthritis. *Epidemiology.* (1994) 5:525–32.
41. Avila MH, Liang MH, Willett WC, Stampfer MJ, Colditz GA, Rosner B, et al. Reproductive factors, smoking, and the risk for rheumatoid arthritis. *Epidemiology.* (1990) 1:285–91. doi: 10.1097/00001648-199007000-00005
42. de Rooy DPC, van Nies JAB, Kapetanovic MC, Kristjansdottir H, Andersson MLE, Forslind K, et al. Smoking as a risk factor for the radiological severity of rheumatoid arthritis: a study on six cohorts. *Ann Rheum Dis.* (2014) 73:1384–7. doi: 10.1136/annrheumdis-2013-203940
43. Johnson C. Recent advances in the pathogenesis, prediction, and management of rheumatoid arthritis-associated interstitial lung disease. *Curr Opin Rheumatol.* (2017) 29:254–9. doi: 10.1097/BOR.0000000000000380
44. Wolfe F. The effect of smoking on clinical, laboratory, and radiographic status in rheumatoid arthritis. *J Rheumatol.* (2000) 27:630–7.
45. Haber J. Cigarette smoking: a major risk factor for periodontitis. *Compendium.* (1994) 15:1002, 1004–8 passim; quiz 1014.
46. Lee YH, Bae S-C, Song GG. Coffee or tea consumption and the risk of rheumatoid arthritis: a meta-analysis. *Clin Rheumatol.* (2014) 33:1575–83. doi: 10.1007/s10067-014-2631-1
47. Hu Y, Costenbader KH, Gao X, Hu FB, Karlson EW, Lu B. Mediterranean diet and incidence of rheumatoid arthritis in women. *Arthritis Care Res (Hoboken).* (2015) 67:597–606. doi: 10.1002/acr.22481
48. Hu Y, Sparks JA, Malspeis S, Costenbader KH, Hu FB, Karlson EW, et al. Long-term dietary quality and risk of developing rheumatoid arthritis in women. *Ann Rheum Dis.* (2017) 76:1357–64. doi: 10.1136/annrheumdis-2016-210431
49. Maglio C, Zhang Y, Peltonen M, Andersson-Assarsson J, Svensson P-A, Herder C, et al. Bariatric surgery and the incidence of rheumatoid arthritis - a Swedish obese subjects study. *Rheumatology.* (2020) 59:303–9. doi: 10.1093/rheumatology/kez275
50. Liu R, Hong J, Xu X, Feng Q, Zhang D, Gu Y, et al. Gut microbiome and serum metabolome alterations in obesity and after weight-loss intervention. *Nat Med.* (2017) 23:859–68. doi: 10.1038/nm.4358
51. Bae SC, Lee YH. Alcohol intake and risk of rheumatoid arthritis: a Mendelian randomization study. *Z Rheumatol.* (2019) 78:791–6. doi: 10.1007/s00393-018-0537-z
52. Wang J, Lv J, Wang W, Jiang X. Alcohol consumption and risk of periodontitis: a meta-analysis. *J Clin Periodontol.* (2016) 43:572–83. doi: 10.1111/jcpe.12556
53. Fredricks DN, Relman DA. Sequence-based identification of microbial pathogens: a reconsideration of Koch's postulates. *Clin Microbiol Rev.* (1996) 9:18–33. doi: 10.1128/CMR.9.1.18
54. Chen T, Rimpiläinen M, Luukkainen R, Möttönen T, Yli-Jama T, Jalava J, et al. Bacterial components in the synovial tissue of patients with advanced rheumatoid arthritis or osteoarthritis: analysis with gas chromatography-mass spectrometry and pan-bacterial polymerase chain reaction. *Arthritis Care Res (Hoboken).* (2003) 49:328–34. doi: 10.1002/art.11119
55. Reichert S, Haffner M, Keyßer G, Schäfer C, Stein JM, Schaller H-G, et al. Detection of oral bacterial DNA in synovial fluid. *J Clin Periodontol.* (2013) 40:591–8. doi: 10.1111/jcpe.12102
56. Zhao Y, Chen B, Li S, Yang L, Zhu D, Wang Y, et al. Detection and characterization of bacterial nucleic acids in culture-negative synovial tissue and fluid samples from rheumatoid arthritis or osteoarthritis patients. *Sci Rep.* (2018) 8:14305. doi: 10.1038/s41598-018-32675-w
57. Curran SA, Hollan I, Erridge C, Lappin DF, Murray CA, Sturfelt G, et al. Bacteria in the adventitia of cardiovascular disease patients with and without rheumatoid arthritis. *PLoS One.* (2014) 9:e98627. doi: 10.1371/journal.pone.0098627
58. Kudaeva FM, Speechley MR, Pope JE. A systematic review of viral exposures as a risk for rheumatoid arthritis. *Semin Arthritis Rheum.* (2019) 48:587–96. doi: 10.1016/j.semarthrit.2018.03.011
59. Flak MB, Colas RA, Muñoz-Atienza E, Curtis MA, Dalli J, Pitzalis C. Inflammatory arthritis disrupts gut resolution mechanisms, promoting barrier breakdown by *Porphyromonas gingivalis*. *JCI Insight.* (2019) 4:e125191. doi: 10.1172/jci.insight.125191
60. Cantley MD, Haynes DR, Marino V, Bartold PM. Pre-existing periodontitis exacerbates experimental arthritis in a mouse model. *J Clin Periodontol.* (2011) 38:532–41. doi: 10.1111/j.1600-051X.2011.01714.x
61. Kinloch AJ, Alzabin S, Brintnell W, Wilson E, Barra L, Wegner N, et al. Immunization with *Porphyromonas gingivalis* enolase induces autoimmunity to mammalian α-enolase and arthritis in DR4-IE-transgenic mice. *Arthritis Rheum.* (2011) 63:3818–23. doi: 10.1002/art.30639
62. Maresz KJ, Hellvard A, Sroka A, Adamowicz K, Bielecka E, Koziel J, et al. *Porphyromonas gingivalis* facilitates the development and progression of

destructive arthritis through its unique bacterial peptidylarginine deiminase (PAD). *PLoS Pathog.* (2013) 9:e1003627. doi: 10.1371/journal.ppat.1003627
63. Marchesan JT, Gerow EA, Schaff R, Taut AD, Shin S-Y, Sugai J, et al. *Porphyromonas gingivalis* oral infection exacerbates the development and severity of collagen-induced arthritis. *Arthritis Res Ther.* (2013) 15:R186. doi: 10.1186/ar4376
64. Gully N, Bright R, Marino V, Marchant C, Cantley M, Haynes D, et al. *Porphyromonas gingivalis* peptidylarginine deiminase, a key contributor in the pathogenesis of experimental periodontal disease and experimental arthritis. *PLoS One.* (2014) 9:e100838. doi: 10.1371/journal.pone.0100838
65. Chukkapalli S, Rivera-Kweh M, Gehlot P, Velsko I, Bhattacharyya I, Calise SJ, et al. Periodontal bacterial colonization in synovial tissues exacerbates collagen-induced arthritis in B10.RIII mice. *Arthritis Res Ther.* (2016) 18:161. doi: 10.1186/s13075-016-1056-4
66. Sandal I, Karydis A, Luo J, Prislovsky A, Whittington KB, Rosloniec EF, et al. Bone loss and aggravated autoimmune arthritis in HLA-DRβ1-bearing humanized mice following oral challenge with *Porphyromonas gingivalis*. *Arthritis Res Ther.* (2016) 18:249. doi: 10.1186/s13075-016-1143-6
67. Yamakawa M, Ouhara K, Kajiya M, Munenaga S, Kittaka M, Yamasaki S, et al. *Porphyromonas gingivalis* infection exacerbates the onset of rheumatoid arthritis in SKG mice. *Clin Exp Immunol.* (2016) 186:177–9. doi: 10.1111/cei.12847
68. Marietta EV, Murray JA, Luckey DH, Jeraldo PR, Lamba A, Patel R, et al. Suppression of inflammatory arthritis by human gut-derived prevotella histicola in humanized mice. *Arthritis Rheumatol.* (2016) 68:2878–88. doi: 10.1002/art.39785
69. Sato K, Takahashi N, Kato T, Matsuda Y, Yokoji M, Yamada M, et al. Aggravation of collagen-induced arthritis by orally administered *Porphyromonas gingivalis* through modulation of the gut microbiota and gut immune system. *Sci Rep.* (2017) 7:6955. doi: 10.1038/s41598-017-07196-7
70. Jubair WK, Hendrickson JD, Severs EL, Schulz HM, Adhikari S, Ir D, et al. Modulation of inflammatory arthritis in mice by gut microbiota through mucosal inflammation and autoantibody generation. *Arthritis Rheumatol.* (2018) 70:1220–33. doi: 10.1002/art.40490
71. Evans-Marin H, Rogier R, Koralov SB, Manasson J, Roeleveld D, Kraan PM, et al. Microbiota-dependent involvement of Th17 cells in murine models of inflammatory arthritis. *Arthritis Rheumatol.* (2018) 70:1971–83. doi: 10.1002/art.40657
72. Lübcke PM, Ebbers MNB, Volzke J, Bull J, Kneitz S, Engelmann R, et al. Periodontal treatment prevents arthritis in mice and methotrexate ameliorates periodontal bone loss. *Sci Rep.* (2019) 9:8128. doi: 10.1038/s41598-019-44512-9
73. Courbon G, Rinaudo-Gaujous M, Blasco-Baque V, Auger I, Caire R, Mijola L, et al. *Porphyromonas gingivalis* experimentally induces periodontis and an anti-CCP2-associated arthritis in the rat. *Ann Rheum Dis.* (2019) 78:594–9. doi: 10.1136/annrheumdis-2018-213697
74. Yamamoto EA, Jørgensen TN. Relationships between Vitamin D, gut microbiome, and systemic autoimmunity. *Front Immunol.* (2020) 10:3141. doi: 10.3389/fimmu.2019.03141
75. James SL, Abate D, Abate KH, Abay SM, Abbafati C, Abbasi N, et al. Global, regional, and national incidence, prevalence, and years lived with disability for 354 diseases and injuries for 195 countries and territories, 1990-2017: a systematic analysis for the Global Burden of Disease Study 2017. *Lancet.* (2018) 392:1789–858. doi: 10.1016/S0140-6736(18)32279-7
76. Jepsen S, Blanco J, Buchalla W, Carvalho JC, Dietrich T, Dörfer C, et al. Prevention and control of dental caries and periodontal diseases at individual and population level: consensus report of group 3 of joint EFP/ORCA workshop on the boundaries between caries and periodontal diseases. *J Clin Periodontol.* (2017) 44:S85–S93. doi: 10.1111/jcpe.12687
77. Bartold PM, Marshall RI, Haynes DR. Periodontitis and rheumatoid arthritis: a review. *J Periodontol.* (2005) 76:2066–74. doi: 10.1902/jop.2005.76.11-S.2066
78. Socransky SS, Haffajee AD, Cugini MA, Smith C, Kent RL. Microbial complexes in subgingival plaque. *J Clin Periodontol.* (1998) 25:134–44. doi: 10.1111/j.1600-051X.1998.tb02419.x
79. Hajishengallis G, Lamont RJ. Beyond the red complex and into more complexity: the polymicrobial synergy and dysbiosis (PSD) model of periodontal disease etiology. *Mol Oral Microbiol.* (2012) 27:409–19. doi: 10.1111/j.2041-1014.2012.00663.x
80. Gmür R, Strub JR, Guggenheim B. Prevalence of *Bacteroides forsythus* and *Bacteroides gingivalis* in subgingival plaque of prosthodontically treated patients on short recall. *J Periodontal Res.* (1989) 24:113–20. doi: 10.1111/j.1600-0765.1989.tb00865.x
81. Potempa J, Pike R, Travis J. The multiple forms of trypsin-like activity present in various strains of *Porphyromonas gingivalis* are due to the presence of either Arg-gingipain or Lys-gingipain. *Infect Immun.* (1995) 63:1176–82. doi: 10.1128/IAI.63.4.1176-1182.1995
82. Montgomery AB, Kopec J, Shrestha L, Thezenas M-L, Burgess-Brown NA, Fischer R, et al. Crystal structure of *Porphyromonas gingivalis* peptidylarginine deiminase: implications for autoimmunity in rheumatoid arthritis. *Ann Rheum Dis.* (2016) 75:1255–61. doi: 10.1136/annrheumdis-2015-207656
83. Kasser UR, Gleissner C, Dehne F, Michel A, Willershausen-Zonnchen B, Bolten WW. Risk for periodontal disease in patients with longstanding rheumatoid arthritis. *Arthritis Rheum.* (1997) 40:2248–51. doi: 10.1002/art.1780401221
84. Chen HH, Huang N, Chen YM, Chen TJ, Chou P, Lee YL, et al. Association between a history of periodontitis and the risk of rheumatoid arthritis: a nationwide, population-based, case-control study. *Ann Rheum Dis.* (2013) 72:1206–11. doi: 10.1136/annrheumdis-2012-201593
85. Chou Y-Y, Lai K-L, Chen D-Y, Lin C-H, Chen H-H. Rheumatoid arthritis risk associated with periodontitis exposure: a nationwide, population-based cohort study. *PLoS One.* (2015) 10:e0139693. doi: 10.1371/journal.pone.0139693
86. Scher JU, Ubeda C, Equinda M, Khanin R, Buischi Y, Viale A, et al. Periodontal disease and the oral microbiota in new-onset rheumatoid arthritis. *Arthritis Rheum.* (2012) 64:3083–94. doi: 10.1002/art.34539
87. Goh CE, Kopp J, Papapanou PN, Molitor JA, Demmer RT. Association between serum antibodies to periodontal bacteria and rheumatoid factor in the third national health and nutrition examination survey. *Arthritis Rheumatol.* (2016) 68:2384–93. doi: 10.1002/art.39724
88. Lopez-Oliva I, Paropkari AD, Saraswat S, Serban S, Yonel Z, Sharma P, et al. Dysbiotic subgingival microbial communities in periodontally healthy patients with rheumatoid arthritis. *Arthritis Rheumatol (Hoboken, NJ).* (2018) 70:1008–13. doi: 10.1002/art.40485
89. Mikuls TR, Walker C, Qiu F, Yu F, Thiele GM, Alfant B, et al. The subgingival microbiome in patients with established rheumatoid arthritis. *Rheumatology (Oxford).* (2018) 57:1162–72. doi: 10.1093/rheumatology/key052
90. Wegner N, Lundberg K, Kinloch A, Fisher B, Malmstrom V, Feldmann M, et al. Autoimmunity to specific citrullinated proteins gives the first clues to the etiology of rheumatoid arthritis. *Immunol Rev.* (2010) 233:34–54. doi: 10.1111/j.0105-2896.2009.00850.x
91. Lappin DF, Apatzidou D, Quirke AM, Oliver-Bell J, Butcher JP, Kinane DF, et al. Influence of periodontal disease, *Porphyromonas gingivalis* and cigarette smoking on systemic anti-citrullinated peptide antibody titres. *J Clin Periodontol.* (2013) 40:907–15. doi: 10.1111/jcpe.12138
92. Mikuls TR, Payne JB, Yu F, Thiele GM, Reynolds RJ, Cannon GW, et al. Periodontitis and *Porphyromonas gingivalis* in patients with rheumatoid arthritis. *Arthritis Rheumatol.* (2014) 66:1090–100. doi: 10.1002/art.38348
93. Sato K, Yokoji M, Yamada M, Nakajima T, Yamazaki K. An orally administered oral pathobiont and commensal have comparable and innocuous systemic effects in germ-free mice. *J Periodontal Res.* (2018) 53:950–60. doi: 10.1111/jre.12593
94. Hajishengallis G, Liang S, Payne MA, Hashim A, Jotwani R, Eskan MA, et al. Low-abundance biofilm species orchestrates inflammatory periodontal disease through the commensal microbiota and complement. *Cell Host Microbe.* (2011) 10:497–506. doi: 10.1016/j.chom.2011.10.006
95. Mankia K, Cheng Z, Do T, Hunt L, Meade J, Kang J, et al. Prevalence of periodontal disease and periodontopathic bacteria in anti-cyclic citrullinated protein antibody-positive at-risk adults without arthritis. *JAMA Netw Open.* (2019) 2:e195394. doi: 10.1001/jamanetworkopen.2019.5394
96. Tong Y, Zheng L, Qing P, Zhao H, Li Y, Su L, et al. Oral microbiota perturbations are linked to high risk for rheumatoid arthritis. *Front Cell Infect Microbiol.* (2020) 9:475. doi: 10.3389/fcimb.2019.00475

97. Seror R, Le Gall-David S, Bonnaure-Mallet M, Schaeverbeke T, Cantagrel A, Minet J, et al. Association of anti-*Porphyromonas gingivalis* antibody titers with nonsmoking status in early rheumatoid arthritis: results from the prospective French cohort of patients with early rheumatoid arthritis. *Arthritis Rheumatol (Hoboken, NJ).* (2015) 67:1729–37. doi: 10.1002/art.39118
98. Hashimoto M, Yamazaki T, Hamaguchi M, Morimoto T, Yamori M, Asai K, et al. Periodontitis and *Porphyromonas gingivalis* in preclinical stage of arthritis patients. *PLoS One.* (2015) 10:e0122121. doi: 10.1371/journal.pone.0122121
99. Engström M, Eriksson K, Lee L, Hermansson M, Johansson A, Nicholas AP, et al. Increased citrullination and expression of peptidylarginine deiminases independently of *P. gingivalis* and *A. actinomycetemcomitans* in gingival tissue of patients with periodontitis. *J Transl Med.* (2018) 16:214. doi: 10.1186/s12967-018-1588-2
100. Kharlamova N, Jiang X, Sherina N, Potempa B, Israelsson L, Quirke A-M, et al. Antibodies to *Porphyromonas gingivalis* indicate interaction between oral infection, smoking, and risk genes in rheumatoid arthritis etiology. *Arthritis Rheumatol.* (2016) 68:604–13. doi: 10.1002/art.39491
101. Smit MD, Westra J, Vissink A, Doornbos-van der Meer B, Brouwer E, van Winkelhoff AJ. Periodontitis in established rheumatoid arthritis patients: a cross-sectional clinical, microbiological and serological study. *Arthritis Res Ther.* (2012) 14:R222. doi: 10.1186/ar4061
102. Konig MF, Abusleme L, Reinholdt J, Palmer RJ, Teles RP, Sampson K, et al. *Aggregatibacter actinomycetemcomitans*-induced hypercitrullination links periodontal infection to autoimmunity in rheumatoid arthritis. *Sci Transl Med.* (2016) 8:369ra176. doi: 10.1126/scitranslmed.aaj1921
103. Schwenzer A, Quirke AM, Marzeda AM, Wong A, Montgomery AB, Sayles HR, et al. Association of distinct fine specificities of anti-citrullinated peptide antibodies with elevated immune responses to *Prevotella intermedia* in a subgroup of patients with rheumatoid arthritis and periodontitis. *Arthritis Rheumatol.* (2017) 69:2303–313. doi: 10.1002/art.40227
104. Hajishengallis G, Korostoff JM. Revisiting the Page & Schroeder model: the good, the bad and the unknowns in the periodontal host response 40 years later. *Periodontol 2000.* (2017) 75:116–51. doi: 10.1111/prd.12181
105. Page RC, Schroeder HE. Pathogenesis of inflammatory periodontal disease. A summary of current work. *Lab Invest.* (1976) 34:235–49.
106. Seror R, Boudaoud S, Pavy S, Nocturne G, Schaeverbeke T, Saraux A, et al. Increased dickkopf-1 in recent-onset rheumatoid arthritis is a new biomarker of structural severity. Data from the ESPOIR cohort. *Sci Rep.* (2016) 6:1–11. doi: 10.1038/srep18421
107. Page RC, Schroeder HE. Pathogenesis of inflammatory periodontal disease. A summary of current work. *Lab Investig.* (1976) 34:235–49.
108. Stein JM, Machulla HKG, Smeets R, Lampert F, Reichert S. Human leukocyte antigen polymorphism in chronic and aggressive periodontitis among Caucasians: a meta-analysis. *J Clin Periodontol.* (2008) 35:183–92. doi: 10.1111/j.1600-051X.2007.01189.x
109. Konermann A, Deschner J, Allam JP, Novak N, Winter J, Baader SL, et al. Antigen-presenting cell marker expression and phagocytotic activity in periodontal ligament cells. *J Oral Pathol Med.* (2012) 41:340–7. doi: 10.1111/j.1600-0714.2011.01086.x
110. Sipert CR, Morandini AC, Dionísio TJ, Machado MAAM, Oliveira SHP, Campanelli AP, et al. *In vitro* regulation of CCL3 and CXCL12 by bacterial by-products is dependent on site of origin of human oral fibroblasts. *J Endod.* (2014) 40:95–100. doi: 10.1016/j.joen.2013.09.031
111. Scheres N, Laine ML, de Vries TJ, Everts V, van Winkelhoff AJ. Gingival and periodontal ligament fibroblasts differ in their inflammatory response to viable *Porphyromonas gingivalis*. *J Periodontal Res.* (2010) 45:262–70. doi: 10.1111/j.1600-0765.2009.01229.x
112. Graves DT, Alshabab A, Albiero ML, Mattos M, Corrêa JD, Chen S, et al. Osteocytes play an important role in experimental periodontitis in healthy and diabetic mice through expression of RANKL. *J Clin Periodontol.* (2018) 45:285–92. doi: 10.1111/jcpe.12851
113. Xu F, Teitelbaum SL. Osteoclasts: new insights. *Bone Res.* (2013) 1:11–26. doi: 10.4248/BR201301003
114. Xiong J, Onal M, Jilka RL, Weinstein RS, Manolagas SC, O'Brien CA. Matrix-embedded cells control osteoclast formation. *Nat Med.* (2011) 17:1235–41. doi: 10.1038/nm.2448
115. Nakashima T, Hayashi M, Fukunaga T, Kurata K, Oh-Hora M, Feng JQ, et al. Evidence for osteocyte regulation of bone homeostasis through RANKL expression. *Nat Med.* (2011) 17:1231–4. doi: 10.1038/nm.2452
116. Nusse R, Varmus HE. Wnt genes. *Cell.* (1992) 69:1073–87. doi: 10.1016/0092-8674(92)90630-U
117. Pinzone JJ, Hall BM, Thudi NK, Vonau M, Qiang YW, Rosol TJ, et al. The role of Dickkopf-1 in bone development, homeostasis, and disease. *Blood.* (2009) 113:517–25. doi: 10.1182/blood-2008-03-145169
118. de Vries TJ, Huesa C. The osteocyte as a novel key player in understanding periodontitis through its expression of RANKL and sclerostin: a review. *Curr Osteoporos Rep.* (2019) 17:116–21. doi: 10.1007/s11914-019-00509-x
119. Kuchler U, Schwarze UY, Dobsak T, Heimel P, Bosshardt DD, Kneissel M, et al. Dental and periodontal phenotype in sclerostin knockout mice. *Int J Oral Sci.* (2014) 6:70–6. doi: 10.1038/ijos.2014.12
120. Chatzopoulos GS, Mansky KC, Lunos S, Costalonga M, Wolff LF. Sclerostin and WNT-5a gingival protein levels in chronic periodontitis and health. *J Periodontal Res.* (2019) 54:555–65. doi: 10.1111/jre.12659
121. Napimoga MH, Nametala C, Da Silva FL, Miranda TS, Bossonaro JP, Demasi APD, et al. Involvement of the Wnt-β-catenin signalling antagonists, sclerostin and dickkopf-related protein 1, in chronic periodontitis. *J Clin Periodontol.* (2014) 41:550–7. doi: 10.1111/jcpe.12245
122. Courbon G, Lamarque R, Gerbaix M, Caire R, Linossier MT, Laroche N, et al. Early sclerostin expression explains bone formation inhibition before arthritis onset in the rat adjuvant-induced arthritis model. *Sci Rep.* (2018) 8:3492. doi: 10.1038/s41598-018-21886-w
123. Sapir-Koren R, Livshits G. Postmenopausal osteoporosis in rheumatoid arthritis: The estrogen deficiency-immune mechanisms link. *Bone.* (2017) 103:102–15. doi: 10.1016/j.bone.2017.06.020
124. Aeberli D, Fankhauser N, Zebaze R, Bonel H, Möller B, Villiger PM. Effect of rheumatoid arthritis and age on metacarpal bone shaft geometry and density: a longitudinal pQCT study in postmenopausal women. *Semin Arthritis Rheum.* (2019) 50:220–7. doi: 10.1016/j.semarthrit.2019.08.003
125. Eser P, Aeberli D, Widmer J, Möller B, Villiger PM. Abnormal bone geometry at the metacarpal bone shaft of rheumatoid arthritis patients with maintained muscle bone relationship. *Arthritis Care Res.* (2011) 63:383–9. doi: 10.1002/acr.20394
126. Kohn DB, Booth C, Kang EM, Pai SY, Shaw KL, Santilli G, et al. Lentiviral gene therapy for X-linked chronic granulomatous disease. *Nat Med.* (2020) 26:200–6. doi: 10.1038/s41591-019-0735-5
127. Abe T, Hosur KB, Hajishengallis E, Reis ES, Ricklin D, Lambris JD, et al. Local complement-targeted intervention in periodontitis: proof-of-concept using a C5a receptor (CD88) antagonist. *J Immunol.* (2012) 189:5442–8. doi: 10.4049/jimmunol.1202339
128. Maekawa T, Krauss JL, Abe T, Jotwani R, Triantafilou M, Triantafilou K, et al. *Porphyromonas gingivalis* manipulates complement and TLR signaling to uncouple bacterial clearance from inflammation and promote dysbiosis. *Cell Host Microbe.* (2014) 15:768–78. doi: 10.1016/j.chom.2014.05.012
129. Su X, Yu Y, Zhong Y, Giannopoulou EG, Hu X, Liu H, et al. Interferon-γ regulates cellular metabolism and mRNA translation to potentiate macrophage activation. *Nat Immunol.* (2015) 16:838–49. doi: 10.1038/ni.3205
130. Burns E, Bachrach G, Shapira L, Nussbaum G. Cutting edge: TLR2 is required for the innate response to *Porphyromonas gingivalis*: activation leads to bacterial persistence and TLR2 deficiency attenuates induced alveolar bone resorption. *J Immunol.* (2006) 177:8296–300. doi: 10.4049/jimmunol.177.12.8296
131. Papadopoulos G, Weinberg EO, Massari P, Gibson FC, Wetzler LM, Morgan EF, et al. Macrophage-specific TLR2 signaling mediates pathogen-induced TNF-dependent inflammatory oral bone loss. *J Immunol.* (2013) 190:1148–57. doi: 10.4049/jimmunol.1202511
132. Shapouri-Moghaddam A, Mohammadian S, Vazini H, Taghadosi M, Esmaeili S-A, Mardani F, et al. Macrophage plasticity, polarization, and function in health and disease. *J Cell Physiol.* (2018) 233:6425–40. doi: 10.1002/jcp.26429
133. Yang J, Zhu Y, Duan D, Wang P, Xin Y, Bai L, et al. Enhanced activity of macrophage M1/M2 phenotypes in periodontitis. *Arch Oral Biol.* (2018) 96:234–42. doi: 10.1016/j.archoralbio.2017.03.006

134. Garaicoa-Pazmino C, Fretwurst T, Squarize CH, Berglundh T, Giannobile WV, Larsson L, et al. Characterization of macrophage polarization in periodontal disease. *J Clin Periodontol.* (2019) 46:830–9. doi: 10.1111/jcpe.13156
135. Dutzan N, Abusleme L, Konkel JE, Moutsopoulos NM. Isolation, characterization and functional examination of the gingival immune cell network. *J Vis Exp.* (2016) 2016:53736. doi: 10.3791/53736
136. Rajendran M, Looney S, Singh N, Elashiry M, Meghil MM, El-Awady AR, et al. Systemic antibiotic therapy reduces circulating inflammatory dendritic cells and Treg-Th17 plasticity in periodontitis. *J Immunol.* (2019) 202:2690–9. doi: 10.4049/jimmunol.1900046
137. Mahanonda R, Champaiboon C, Subbalekha K, Sa-Ard-Iam N, Yongyuth A, Isaraphithakkul B, et al. Memory T cell subsets in healthy gingiva and periodontitis tissues. *J Periodontol.* (2018) 89:1121–30. doi: 10.1002/JPER.17-0674
138. El-Awady AR, Miles B, Scisci E, Kurago ZB, Palani CD, Arce RM, et al. *Porphyromonas gingivalis* evasion of autophagy and intracellular killing by human myeloid dendritic cells involves DC-SIGN-TLR2 crosstalk. *PLoS Pathog.* (2015) 11:e1004647. doi: 10.1371/journal.ppat.1004647
139. Zeituni AE, Jotwani R, Carrion J, Cutler CW. Targeting of DC-SIGN on human dendritic cells by minor fimbriated *Porphyromonas gingivalis* strains elicits a distinct effector T cell response. *J Immunol.* (2009) 183:5694–704. doi: 10.4049/jimmunol.0901030
140. Chukkapalli SS, Velsko IM, Rivera-Kweh MF, Larjava H, Lucas AR, Kesavalu L. Global TLR2 and 4 deficiency in mice impacts bone resorption, inflammatory markers and atherosclerosis to polymicrobial infection. *Mol Oral Microbiol.* (2017) 32:211–25. doi: 10.1111/omi.12165
141. Timmer TCG, Baltus B, Vondenhoff M, Huizinga TWJ, Tak PP, Verweij CL, et al. Inflammation and ectopic lymphoid structures in rheumatoid arthritis synovial tissues dissected by genomics technology: identification of the interleukin-7 signaling pathway in tissues with lymphoid neogenesis. *Arthritis Rheum.* (2007) 56:2492–502. doi: 10.1002/art.22748
142. Mcintosh ML, Hajishengallis G. Inhibition of *Porphyromonas gingivalis*-induced periodontal bone loss by CXCR4 antagonist treatment. *Mol Oral Microbiol.* (2012) 27:449–57. doi: 10.1111/j.2041-1014.2012.00657.x
143. Hajishengallis G, Mcintosh ML, Nishiyama SI, Yoshimura F. Mechanism and implications of CXCR4-mediated integrin activation by *Porphyromonas gingivalis*. *Mol Oral Microbiol.* (2013) 28:239–49. doi: 10.1111/omi.12021
144. Arjunan P, Meghil MM, Pi W, Xu J, Lang L, El-Awady A, et al. Oral pathobiont activates anti-apoptotic pathway, promoting both immune suppression and oncogenic cell proliferation. *Sci Rep.* (2018) 8:1–15. doi: 10.1038/s41598-018-35126-8
145. Graves DT, Milovanova TN. Mucosal immunity and the FOXO1 transcription factors. *Front Immunol.* (2019) 10:2530. doi: 10.3389/fimmu.2019.02530
146. Bittner-Eddy PD, Fischer LA, Kaplan DH, Thieu K, Costalonga M. Mucosal langerhans cells promote differentiation of Th17 cells in a murine model of periodontitis but are not required for *Porphyromonas gingivalis* - driven alveolar bone destruction. *J Immunol.* (2016) 197:1435–46. doi: 10.4049/jimmunol.1502693
147. Dutzan N, Kajikawa T, Abusleme L, Greenwell-Wild T, Zuazo CE, Ikeuchi T, et al. A dysbiotic microbiome triggers TH17 cells to mediate oral mucosal immunopathology in mice and humans. *Sci Transl Med.* (2018) 10:eaat0797. doi: 10.1126/scitranslmed.aat0797
148. Jing L, Kim S, Sun L, Wang L, Mildner E, Divaris K, et al. IL-37- and IL-35/IL-37-producing plasma cells in chronic periodontitis. *J Dent Res.* (2019) 98:813–21. doi: 10.1177/0022034519847443
149. Zouali M. The emerging roles of B cells as partners and targets in periodontitis. *Autoimmunity.* (2017) 50:61–70. doi: 10.1080/08916934.2016.1261841
150. Aimetti M, Romano F, Guzzi N, Carnevale G. Full-mouth disinfection and systemic antimicrobial therapy in generalized aggressive periodontitis: a randomized, placebo-controlled trial. *J Clin Periodontol.* (2012) 39:284–94. doi: 10.1111/j.1600-051X.2011.01795.x
151. Keestra JAJ, Grosjean I, Coucke W, Quirynen M, Teughels W. Non-surgical periodontal therapy with systemic antibiotics in patients with untreated chronic periodontitis: a systematic review and meta-analysis. *J Periodontal Res.* (2015) 50:294–314. doi: 10.1111/jre.12221
152. van Winkelhoff AJ, Tijhof CJ, de Graaff J. Microbiological and clinical results of metronidazole plus amoxicillin therapy in *Actinobacillus actinomycetemcomitans* - associated periodontitis. *J Periodontol.* (2012) 63:52–7. doi: 10.1902/jop.1992.63.1.52
153. Monsarrat P, de Grado GF, Constantin A, Willmann C, Nabet C, Sixou M, et al. The effect of periodontal treatment on patients with rheumatoid arthritis: the ESPERA randomised controlled trial. *Joint Bone Spine.* (2019) 86:600–9. doi: 10.1016/j.jbspin.2019.02.006
154. Möller B, Bender P, Eick S, Kuchen S, Maldonado A, Potempa J, et al. Treatment of severe periodontitis may improve clinical disease activity in otherwise treatment-refractory rheumatoid arthritis patients. *Rheumatology (Oxford).* (2019) 59:243–5. doi: 10.1093/rheumatology/kez287
155. Eren AM, Borisy GG, Huse SM, Mark Welch JL. Oligotyping analysis of the human oral microbiome. *Proc Natl Acad Sci U S A.* (2014) 111:E2875–84. doi: 10.1073/pnas.1409644111
156. Zhang X, Zhang D, Jia H, Feng Q, Wang D, Liang D, et al. The oral and gut microbiomes are perturbed in rheumatoid arthritis and partly normalized after treatment. *Nat Med.* (2015) 21:895–905. doi: 10.1038/nm.3914
157. Ikeda U, Wakita D, Ohkuri T, Chamoto K, Kitamura H, Iwakura Y, Nishimura T. 1α,25-Dihydroxyvitamin D3 and all-trans retinoic acid synergistically inhibit the differentiation and expansion of Th17 cells. *Immunol Lett.* (2010) 134:7–16. doi: 10.1016/j.imlet.2010.07.002
158. Dodd RC, Cohen MS, Newman SL, Gray TK. Vitamin D metabolites change the phenotype of monoblastic U937 cells. *Proc Natl Acad Sci U S A.* (1983) 80:7538–41. doi: 10.1073/pnas.80.24.7538
159. Pianta A, Arvikar SL, Strle K, Drouin EE, Wang Q, Costello CE, et al. Two rheumatoid arthritis-specific autoantigens correlate microbial immunity with autoimmune responses in joints. *J Clin Invest.* (2017) 127:2946–56. doi: 10.1172/JCI93450
160. Pianta A, Arvikar S, Strle K, Drouin EE, Wang Q, Costello CE, et al. Evidence of the immune relevance of *Prevotella copri*, a gut microbe, in patients with rheumatoid arthritis. *Arthritis Rheumatol (Hoboken, NJ).* (2017) 69:964–75. doi: 10.1002/art.40003
161. Alpizar-Rodriguez D, Lesker TR, Gronow A, Gilbert B, Raemy E, Lamacchia C, et al. *Prevotella copri* in individuals at risk for rheumatoid arthritis. *Ann Rheum Dis.* (2019) 78:590–3. doi: 10.1136/annrheumdis-2018-214514
162. Lee YH. Causal association of gut microbiome on the risk of rheumatoid arthritis: a Mendelian randomisation study. *Ann Rheum Dis.* (2020). doi: 10.1136/annrheumdis-2019-216747. [Epub ahead of print].
163. Inamo J. Response to: 'causal association of gut microbiome on the risk of rheumatoid arthritis: a Mendelian randomisation study' by Lee. *Ann Rheum Dis.* (2020). doi: 10.1136/annrheumdis-2019-216767. [Epub ahead of print].
164. Kishikawa T, Maeda Y, Nii T, Motooka D, Matsumoto Y, Matsushita M, et al. Metagenome-wide association study of gut microbiome revealed novel aetiology of rheumatoid arthritis in the Japanese population. *Ann Rheum Dis.* (2020) 79:103–11. doi: 10.1136/annrheumdis-2019-215743
165. Laugisch O, Wong A, Sroka A, Kantyka T, Koziel J, Neuhaus K, et al. Citrullination in the periodontium–a possible link between periodontitis and rheumatoid arthritis. *Clin Oral Investig.* (2016) 20:675–83. doi: 10.1007/s00784-015-1556-7
166. Bennike TB, Ellingsen T, Glerup H, Bonderup OK, Carlsen TG, Meyer MK, et al. Proteome analysis of rheumatoid arthritis gut mucosa. *J Proteome Res.* (2017) 16:346–54. doi: 10.1021/acs.jproteome.6b00598
167. Niess JH, Brand S, Gu X, Landsman L, Jung S, McCormick BA, et al. CX_3CR1-mediated dendritic cell access to the intestinal lumen and bacterial clearance. *Science.* (2005) 307:254–8. doi: 10.1126/science.1102901
168. Macpherson AJ, Uhr T. Induction of protective IgA by intestinal dendritic cells carrying commensal bacteria. *Science.* (2004) 303:1662–5. doi: 10.1126/science.1091334
169. Coombes JL, Siddiqui KRR, Arancibia-Cárcamo CV, Hall J, Sun CM, Belkaid Y, et al. A functionally specialized population of mucosal $CD103^+$ DCs induces $Foxp3^+$ regulatory T cells via a TGF-β- and retinoic acid-dependent mechanism. *J Exp Med.* (2007) 204:1757–64. doi: 10.1084/jem.20070590
170. Mucida D, Park Y, Kim G, Turovskaya O, Scott I, Kronenberg M, et al. Reciprocal TH17 and regulatory T cell differentiation mediated by retinoic acid. *Science.* (2007) 317:256–60. doi: 10.1126/science.1145697
171. Denning TL, Norris BA, Medina-Contreras O, Manicassamy S, Geem D, Madan R, et al. Functional specializations of intestinal dendritic cell and

macrophage subsets that control Th17 and regulatory T cell responses are dependent on the T Cell/APC ratio, source of mouse strain, and regional localization. *J Immunol.* (2011) 187:733–47. doi: 10.4049/jimmunol.1002701

172. Takaki-Kuwahara A, Arinobu Y, Miyawaki K, Yamada H, Tsuzuki H, Irino K, et al. $CCR6^+$ group 3 innate lymphoid cells accumulate in inflamed joints in rheumatoid arthritis and produce Th17 cytokines. *Arthritis Res Ther.* (2019) 21:198. doi: 10.1186/s13075-019-1984-x
173. Zeng B, Shi S, Ashworth G, Dong C, Liu J, Xing F. ILC3 function as a double-edged sword in inflammatory bowel diseases. *Cell Death Dis.* (2019) 10:1–12. doi: 10.1038/s41419-019-1540-2
174. Persson EK, Uronen-Hansson H, Semmrich M, Rivollier A, Hägerbrand K, Marsal J, et al. IRF4 transcription-factor-dependent $CD103^+CD11b^+$ dendritic cells drive mucosal T helper 17 cell differentiation. *Immunity.* (2013) 38:958–69. doi: 10.1016/j.immuni.2013.03.009
175. Luda KM, Joeris T, Persson EK, Rivollier A, Demiri M, Sitnik KM, et al. IRF8 transcription-factor-dependent classical dendritic cells are essential for intestinal T cell homeostasis. *Immunity.* (2016) 44:860–74. doi: 10.1016/j.immuni.2016.02.008
176. Omenetti S, Pizarro TT. The Treg/Th17 axis: a dynamic balance regulated by the gut microbiome. *Front Immunol.* (2015) 6:639. doi: 10.3389/fimmu.2015.00639
177. Lee GR. The balance of th17 versus treg cells in autoimmunity. *Int J Mol Sci.* (2018) 19:730. doi: 10.3390/ijms19030730
178. Wilmore JR, Allman D. Here, There, and anywhere? Arguments for and against the physical plasma cell survival niche. *J Immunol.* (2017) 199:839–45. doi: 10.4049/jimmunol.1700461
179. Gommerman JL, Rojas OL, Fritz JH. Re-thinking the functions of IgA^+plasma cells. *Gut Microbes.* (2015) 5:652–62. doi: 10.4161/19490976.2014.969977

Conflict of Interest: The authors declare that the research was conducted in the absence of any commercial or financial relationships that could be construed as a potential conflict of interest.

Copyright © 2020 Möller, Kollert, Sculean and Villiger. This is an open-access article distributed under the terms of the Creative Commons Attribution License (CC BY). The use, distribution or reproduction in other forums is permitted, provided the original author(s) and the copyright owner(s) are credited and that the original publication in this journal is cited, in accordance with accepted academic practice. No use, distribution or reproduction is permitted which does not comply with these terms.

frontiers in Immunology

HYPOTHESIS AND THEORY
published: 23 July 2020
doi: 10.3389/fimmu.2020.01576

The Multifaceted Nature of Aminopeptidases ERAP1, ERAP2, and LNPEP: From Evolution to Disease

*Fabiana Paladini, Maria Teresa Fiorillo, Valentina Tedeschi, Benedetta Mattorre and Rosa Sorrentino**

Department of Biology and Biotechnology "Charles Darwin", Sapienza University of Rome, Rome, Italy

In the human genome, the aminopeptidases ERAP1, ERAP2 and LNPEP lie contiguously on chromosome 5. They share sequence homology, functions and associations with immune-mediated diseases. By analyzing their multifaceted activities as well as their expression in the zoological scale, we suggest here that the progenitor of the three aminopeptidases might be LNPEP from which the other two aminopeptidases could have derived by gene duplications. We also propose that their functions are partially redundant. More precisely, the evolutionary story of the three aminopeptidases might have been dictated by their role in regulating the renin–angiotensin system, which requires their controlled and coordinated expression. This hypothesis is supported by the many species that lack one or the other gene as well as by the lack of ERAP2 in rodents and a null expression in 25% of humans. Finally, we speculate that their role in antigen presentation has been acquired later on during evolution. They have therefore been diversified between those residing in the ER, ERAP1 and ERAP2, whose role is to refine the MHC-I peptidomes, and LNPEP, mostly present in the endosomal vesicles where it can contribute to antigen cross-presentation or move to the cell membrane as receptor for angiotensin IV. Their association with autoinflammatory/autoimmune diseases can therefore be two-fold: as "contributors" to the shaping of the immune-peptidomes as well as to the regulation of the vascular response.

Keywords: ERAP1, ERAP2, LNPEP, aminopeptidases, immune-mediated diseases

OPEN ACCESS

Edited by:
Mariagrazia Uguccioni, Institute for Research in Biomedicine (IRB), Switzerland

Reviewed by:
Uma Sriram, Lewis Katz School of Medicine at Temple University, United States
Peter M. Van Endert, Institut National de la Santé et de la Recherche Médicale (INSERM), France

****Correspondence:***
Rosa Sorrentino
rosa.sorrentino@uniroma1.it

Specialty section:
This article was submitted to Autoimmune and Autoinflammatory Disorders, a section of the journal Frontiers in Immunology

Received: *30 January 2020*
Accepted: *15 June 2020*
Published: *23 July 2020*

Citation:
Paladini F, Fiorillo MT, Tedeschi V, Mattorre B and Sorrentino R (2020) The Multifaceted Nature of Aminopeptidases ERAP1, ERAP2, and LNPEP: From Evolution to Disease. Front. Immunol. 11:1576. doi: 10.3389/fimmu.2020.01576

In the human genome ERAP1 (Endoplasmic Reticulum Aminopeptidase 1), ERAP2 (Endoplasmic Reticulum Aminopeptidase 2) and LNPEP (Leucyl and Cystinyl Aminopeptidase) lie contiguously in 200 kilobase segment on the chromosome 5q21 and share sequence and functions as aminopeptidases. They are members of the oxytocinase subfamily of M1 Zn-metallopeptidases (1, 2). Noteworthy, their protein sequences are closely related, with LNPEP showing 43 and 49% identity to ERAP1 and ERAP2, respectively, while the two ERAP enzymes are 49% identical. These observations suggest recent gene duplication events and subsequent divergence.

ERAP1 and ERAP2 are expressed in various human tissues and are regulated by interferon-gamma (IFN-γ) (3); they reside in the endoplasmic reticulum (ER) where they trim the N-terminal peptide residues to the correct length to bind the HLA-class I molecules. In fact, cytosolic peptides are delivered through channels formed by TAP (Transporter associated with antigen processing) into the ER where they will be trimmed at their N-terminal end by the ERAPs. ERAPs have

different specificities and they complement each other in shaping the antigenic repertoire: ERAP1 preferentially cleaves N-terminal hydrophobic residues whereas ERAP2 prefers positively charged amino acids. Both however cannot trim peptide bonds involving Pro. Indeed, this amino acid is frequently found at P2 in epitopes presented by HLA-I molecules sharing a Pro-permissive B pocket (4). Trimming of longer peptides probably requires the concerted action of both ERAPs and indeed ERAP1 and ERAP2 have been found to co-localize *in vivo* and to form heterodimeric complexes (5). The homologous gene LNPEP encodes a cytosolic and endosomal aminopeptidase (IRAP, Insulin-Regulated membrane Aminopeptidase) cleaving before cysteine and leucine as well as other amino acids. Endogenous peptides including arginine-vasopressin and oxytocin have been show to be processed by LNPEP. Alternative splicing results in multiple transcript variants encoding different isoforms. Interestingly, LNPEP can be found secreted in soluble form in maternal serum during normal pregnancy (6). Thanks to an additional N-terminal cytoplasmic domain, LNPEP is retained in the endosomal vesicles from where it can traffick to the cell membrane forming a type II integral membrane glycoprotein. LNPEP co-segregates with GLUT4 transporter in storage vesicles that traffic to and from the plasma membrane in insulin-responsive cells (7). Besides, LNPEP in the membrane catalyzes the final step of the angiotensinogen to angiotensin IV (AngIV) conversion and it is acknowledged as AT4 receptor (8) being in humans predominally expressed in brain and, to different extents, in heart, kidney, adrenals and blood vessels. LNPEP has a positive influence on a number of physiological and behavioral functions including blood flow, neuroprotection, synaptogenesis, long-term potentiation and memory consolidation and retrieval (9–11). LNPEP is also an essential component in the renin–angiotensin system (RAS): it degrades peptide hormones, such as oxytocin, vasopressin and angiotensin III (AngIII), and plays a role in maintaining homeostasis during pregnancy. In the evolution of human race the RAS played an important role due to its ability to control salt intake and stimulate thirst. Recent studies have unraveled roles for RAS and its main effector molecule angiotensin II (AngII) in inflammation, autoimmunity and aging (12). AngII levels can be regulated by angiotensin converting enzyme 2 (ACE2), that leads to the production of the vasodilatory heptapeptide Ang 1–7, and by other aminopeptidases including ERAPs generating AngIII (Ang 2–8) and AngIV (Ang 3–8). AngIII has similar effects to AngII, although with lower potency, in enhancing blood pressure and vasopressin release and stimulating the expression of pro-inflammatory mediators (13). AngIV exerts a protective role by increasing blood flow in the kidney and brain (12). In fact, one the most recent advance in the field, it has been the discovery of local RAS in heart, brain, pancreas, lymphatic and adipose tissue. The local RAS can operate independently or in close interaction with circulating RAS. In addition, a functional intracellular RAS has been identified highlighting several prominent effects of AngII, including pro-inflammatory, proliferative and pro-fibrotic activities (8, 14). In this context, LNPEP is involved in the inflammatory response by activating the NF-kB pathway via Ang IV (15, 16). Most interestingly, it has been demonstrated that its aminopeptidase activity is responsible for the trimming of cross-presented peptides in the endosomes of dendritic cell (DC). This observation makes LNPEP as fully belonging to the antigen presenting machinery with a prevalent role in refining extracellular epitopes. However, at the current state a contribution to the processing of intracellular epitopes traveling across the vesicles network cannot be excluded (17, 18).

DISEASE ASSOCIATIONS

The three aminopeptidases have been found associated with distinct as well as overlapping pathologies (19). This has been discussed in several reviews (2, 4, 19–21). In short, ERAP1 is associated with birdshot chorioretinopathy (22), ankylosing spondylitis (23–26) psoriasis and Behçet's disease (27) in individuals carrying the corresponding HLA-I susceptibility alleles. Interestingly, while ERAP1 haplotypes determining a higher expression associate with the first three diseases, Behçet's risk alleles induce a lower ERAP1 expression (28). Since the peptides bound to the susceptible HLA-B51 molecules carry a Pro2 or Ala2 as N-terminal anchor, it is possible that ERAP1 influences the balance of the resultant peptidomes (4, 29). In general, genetic and functional data show that the haplotypes carrying polymorphisms associated with a higher ERAP1 and/or ERAP2 expression are, in most cases, detrimental. In the case of ERAP1 this can be due to its activity as "ruler" either by destroying "protective" epitopes or by refining the susceptible peptidome (30, 31). To this regard, a recent observation has shown that in a melanoma cell, ERAP1 inhibition enhanced the predicted MHC-I binding affinity, reduced the presentation of sub-optimal long peptides and increased the presentation of many high-affinity 9–12 mers, suggesting that the baseline ERAP1 activity is destructive for many potential epitopes (32). A higher expression of ERAP2 is associated with birdshot chorioretinopathy, ankylosing spondylitis and psoriasis (4, 19, 33, 34). However, and most interestingly, this association is not in epistasis with the HLA-I susceptibility allele (35). This suggests that the two molecules do not necessarily converge in the same pathway in conferring disease susceptibility. More precisely, it allows to speculate that, while ERAP1 is fundamental in shaping the peptide repertoire for the relevant HLA-I molecules, ERAP2 can contribute different facets to disease pathogenesis. This is also suggested by the association of ERAP2 with a wider array of diseases, such as preeclampsia or IBD (36–38). At present, the relationship between ERAP1 and ERAP2 is not completely clear: there are suggestions that they can cooperate, but also that ERAP2 can regulate ERAP1 expression and activity (39, 40), modifying the peptidome and, consequently, the expression of the HLA molecules in a subtype-dependent manner (23). LNPEP has been involved in diabetes (41) and associated with psoriasis (42, 43), sharing the last feature with the other two aminopeptidases. Although not demonstrated in the literature, it is however still possible that LNPEP can contribute to disease pathogenesis by modulating the peptidome cross-presented by the HLA-I molecules (44). More interesting, although speculative, is the hypothesis that the LNPEP specific role in the

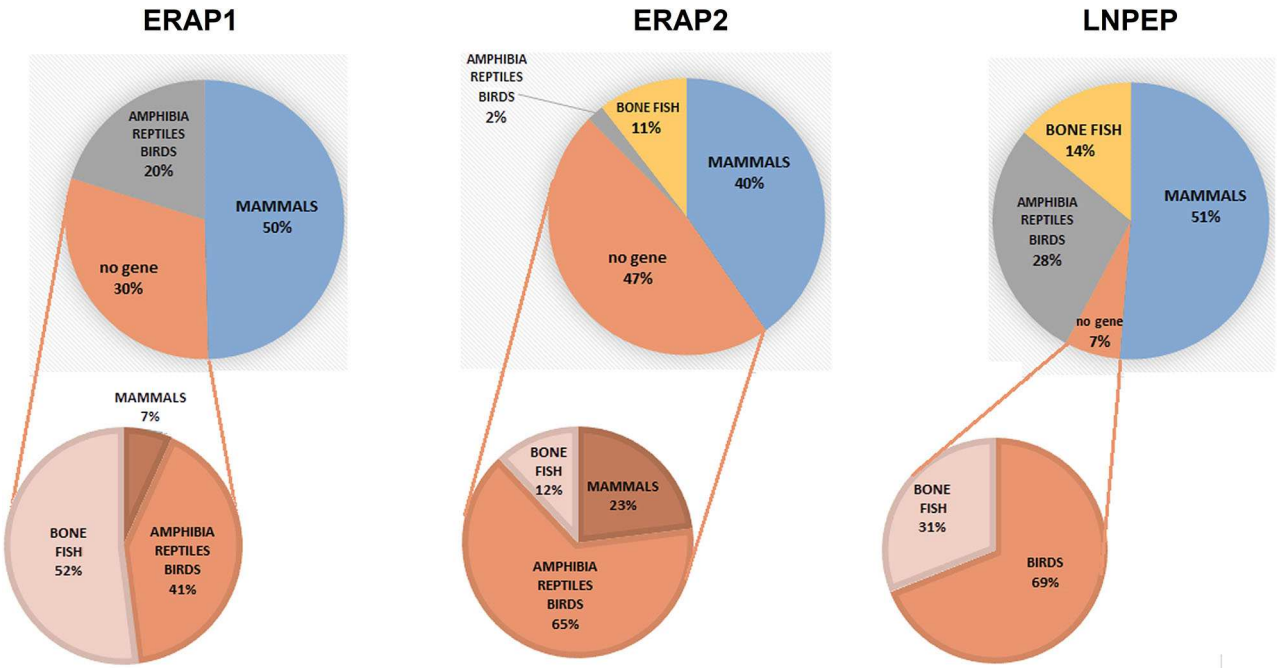

FIGURE 1 | Pie charts summarizing the expression of the orthologous genes ERAP1, ERAP2 and LNPEP along the animal classes as reported by the NCBI's Gene resource (https://www.ncbi.nlm.nih.gov/search/all/?term=orthologs). Amphibians, reptiles, and birds have been merged due to the small number of available species analyzed. The composition of the negative fraction for each gene is shown in the pie charts at the bottom.

RAS can have a strong impact in psoriasis. Several considerations support this hypothesis: angiotensin-converting enzyme gene, which is also a key component in the renin–angiotensin system, has been reported to be associated with psoriasis (45–47). Moreover, it has been shown that LNPEP genetic variants are associated with biological effects on vasopressin clearance and serum sodium regulation (48). Furthermore, the activation of the NF-kB cascade via Ang IV can play an additional role (15, 16). In the lack of conclusive data, we can assume that LNPEP can contribute to different aspects of the disease.

ARE LNPEP AND ERAP2 PARTIALLY INTERCHANGEABLE?

Here we want to consider the hypothesis that ERAP2 can exert functions affecting or at least partially overlapping with those of LNPEP, in particular in local RAS resulting from inflammation. Indeed ERAP2, besides its function as peptide trimmer, has also been found to play a role in the AngII conversion in AngIII and AngIV and consequently, in the predisposition to preeclampsia via the RAS (49, 50). It must be reminded that the association of ERAP2 with the immune-mediated diseases is in quantitative terms. Indeed, ERAP2 displays a balanced polymorphism at the SNP rs2248374 (A/G) that controls protein expression. In particular, the presence of a guanosine causes the elongation of exon 10 inducing a nonsense-mediated RNA decay, a quality-control process that destroys incorrect mRNAs. Consequently, G/G homozygotes accounting for about 25% of the population, do not express ERAP2. This has suggested that a selective pressure by infectious agents has helped to maintain a balanced selection (51). However, another possibility is that there is a redundancy in the function of the three aminopeptidases inside and outside the cells being all of them secreted. Given the function of ERAP2 in RAS, it can be hypothesized for this protein an ancillary role which makes it dispensable and even dangerous if over-expressed. This is suggested not only by the lack of ERAP2 in 25% of humans but also by its absence in rodents.

EVOLVING AMINOPEPTIDASES

To have a hint on this intriguing question, we interrogated data banks asking what the expression of ERAP1, ERAP2 and LNPEP across the species is (248 species: 127 mammals, 61 birds, 9 lizards, 4 turtles, 4 alligators, 4 amphibia, 40 bone fish) (**Supplementary Table 1**). Ortholog ERAP1, ERAP2 and LNPEP genes appear in 173 (69.8%), 131 (52.8%), and 232 (93.5%) species, respectively. ERAP1 is substantially missing in bone fish (39 species) and a large part of birds (29 species). Instead, most mammals that do not express ERAP2 are rodents, which make-up to 85% of the ERAP2 negative fraction in mammals (23 rodents together with domestic cat, rabbit, koala and common wombat). As for LNPEP, however, the species that do not express this gene are predominantly birds (69%, 11 species) and bone fish (**Figure 1**). Overall, most of the mammals express the three genes (**Figure 2A**) and they usually are in the same region of the chromosome. An exception is the lack of ERAP2 in

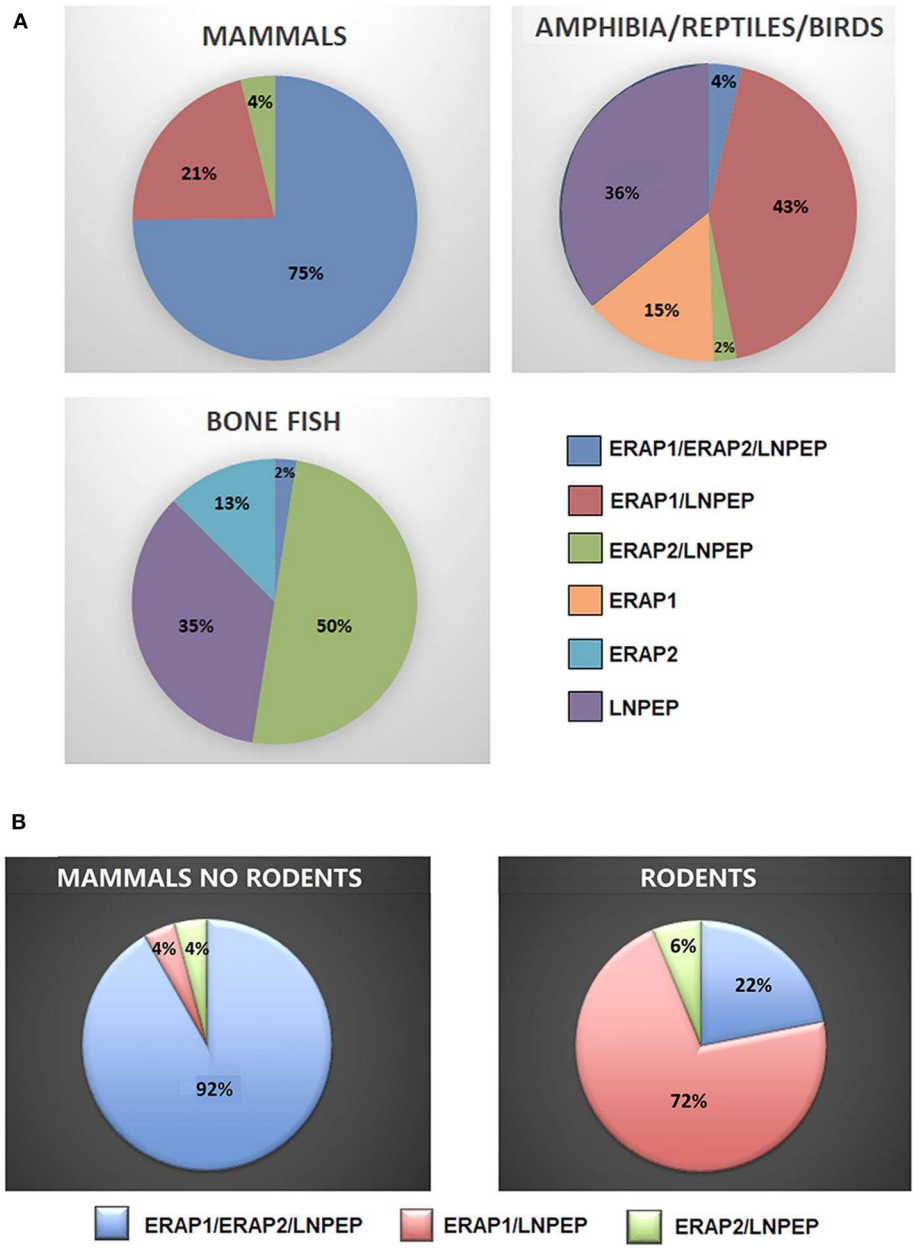

FIGURE 2 | (A) Percentages of mammals, amphibians, reptiles, birds, and bone fish expressing ERAP1, ERAP2, and/or LNPEP genes. **(B)** Percentage of ERAP1, ERAP2, and/or LNPEP genes in the mammalian class (left) extrapolating rodents (right).

rodents (**Figure 2B**). It has been suggested that ERAP2 derives from a gene duplication event of ERAP1 in mammals. This appears most unlikely since ERAP2 is present in amphibia, in fishes and even in reptiles (**Figure 1**). Interestingly, within the rodents, *Mus pahari* (shrew mouse) carries ERAP1 in a different chromosome (chr 11) than LNPEP (chr 21). Most intriguingly, a truncated form of ERAP2 is present in this species, contiguously to LNPEP. This observation could suggest that indeed ERAP2 stems from a duplication of LNPEP and that it has been lost in rodents. Besides, mouse ERAP1 is encoded by a sequence near a putative breakpoint on chromosome 13 and LNPEP is encoded on chromosome 17. Mouse ERAP2 may therefore have been destroyed by a recombinant event. In any case, ERAP2 is apparently not required for an efficient trimming in this species. Why that happened, it remains unknown. However, it confirms that ERAP2 in the antigen processing and presentation (APP) pathway is dispensable and, most probably, redundant. ERAP1 instead is present in almost the totality of mammals whereas absent in the majority of bone fish, which express ERAP2 together with LNPEP. The birds are the most interesting case. They

almost completely lack ERAP2 and the great majority (50 species) expresses LNPEP. However, there is a subset that expresses ERAP1 only, and a tiny group expressing ERAP2 only, suggesting again that there is a high degree of redundancy among these genes. ERAP2 is instead lacking in two of the three amphibia species analyzed, the only positive being *Rhinatrema bivittatum*. In reptiles LNPEP is expressed across all species whereas the expression of ERAP1 and ERAP2 appears again as alternate. In bone fish the majority of species lacks ERAP1, or both ERAP1 and ERAP2. There is however a significant percentage that expresses ERAP2 only and a very tiny subset expressing the three genes. This analysis points out a high degree of redundancy among the three aminopeptidases and shows that, in many cases, one aminopeptidase is enough to supply the needed functions. Moreover, the expression of all three of them appears to correlate with the genetic complexity with the exception of rodents where ERAP2 has been lost.

DO THE THREE AMINOPEPTIDASES HAVE AN EXTRACELLULAR ROLE?

ERAP1 has been found to be secreted by activated macrophages and, in turn, to potentiate their activation (52). More recently, it has been shown that ERAP2 also can be secreted from human monocyte-derived macrophages (MDMs) in response to IFNγ/LPS stimulation and this corresponds to an increased $CD8^+$ T cells activity (53). The mechanisms underlying these effects are not clear. However, the secretion of these molecules apparently occurs in activated macrophages and might have different outcomes: i.e., the triggering of a vascular response relevant in the inflammatory process accompanying these diseases. In humans for example, ERAP1 rs30187, a loss-of function gene variant that reduces AngII degradation *in vitro*, is associated with hypertension (54). The role of LNPEP in the RAS is well-documented as well as the association of ERAP2 with preeclampsia. We can therefore speculate that all three aminopeptidases play a role in the control of the vascular response in inflammation. In support of this theory there is their expression along the zoological scale where, in most cases, the "classical" antigen presenting functions are absent. It might be that the specific role in the complex network of antigen presentation has been acquired later on and maintained because the "trimming" function has become an essential part of a productive defense against viruses (18). A second implication is that the redundancy of their function can lead to a "quantitative" control of the three aminopeptidases so that the full expression of all of them is disfavored. In this regard, we have recently shown that the transcription of ERAP1 and ERAP2 is interlinked: the variant G at rs75862629 in the intergenic region between the two genes strongly influences the expression of the two aminopeptidases with a down-modulation of ERAP2 coupled with a significant higher expression of ERAP1 (40). Even more intriguing is the observation that the ERAP2 variants co-segregating with a lower or null expression of ERAP2 (G at rs75862629 and G at rs2248374, respectively) appear more frequent in the equatorial regions, where the malaria has been endemic. It is interesting that an evolutionary analysis of antigen presentation pathways (55) showed that positive selection has driven the recurrent appearance of ERAP2 protein-destabilizing variants during mammalian evolution in a region apparently not involved in antigen presentation. LNPEP was also found to evolve adaptively in mammals. In this case, four positively selected sites were found to be located at the C-terminal domain 4, which has been shown to possess regulatory activity. The same study points out an inter-species selection of LNPEP gene, an inter-and intra-species selection of ERAP2 gene and an intra-species selection only in the human lineage of ERAP1 gene. This suggests that the ERAP1 gene appeared consequently to that of ERAP2.

In conclusion, we propose here that the expression of the three aminopeptidases mapping on chromosome 5 in the human genome have evolved from the duplication of the precursor LNPEP gene. We also propose that their original function is in the control of the renin–angiotensin system and blood pressure. The "trimming" function has been acquired later on along the zoological scale. The most ancient function is therefore quantitatively controlled through an alternative expression in most cases. Indeed in mammals, ERAP2 has been sacrificed being absent in rodents and controlled in humans where 25% of population is null and 50% is monoallelic. These observations offer a new functional frame in which the association of the aminopeptidases with immune mediated diseases can be reconsidered.

AUTHOR CONTRIBUTIONS

FP has produced the data and the figures about the amino peptidases expression. FP, MF, and RS have written the review. This hypothesis originates from scientific discussions to which all authors have contributed. All authors contributed to the article and approved the submitted version.

FUNDING

This work was supported by Fondazione Ceschina, Lugano, Switzerland and Sapienza University, Rome, Italy.

ACKNOWLEDGMENTS

The authors wish to thank Ceschina Foundation and Sapienza (Progetti di Ateneo) for financial support.

SUPPLEMENTARY MATERIAL

The Supplementary Material for this article can be found online at: https://www.frontiersin.org/articles/10.3389/fimmu.2020.01576/full#supplementary-material

Supplementary Table 1 | Species of mammals, birds, reptiles, amphibians, and bone fish included in the analysis for the presence or absence of the genes ERAP1, ERAP2, and LNPEP.

REFERENCES

1. Rawlings ND, Barrett AJ, Bateman A. MEROPS: the database of proteolytic enzymes, their substrates and inhibitors. *Nucleic Acids Res.* (2012) 40:D343–50. doi: 10.1093/nar/gkr987
2. Papakyriakou A, Stratikos E. The role of conformational dynamics in antigen trimming by intracellular aminopeptidases. *Front Immunol.* (2017) 8:946. doi: 10.3389/fimmu.2017.00946
3. Saric T, Chang SC, Hattori A, York IA, Markant S, Rock KL, et al. An IFN-gamma-induced aminopeptidase in the ER, ERAP1, trims precursors to MHC class I-presented peptides. *Nat Immunol.* (2002) 3:1169–76. doi: 10.1038/ni859
4. López de Castro JA. How ERAP1 and ERAP2 shape the peptidomes of disease associated MHC-I proteins. *Front. Immunol.* (2018) 9:2463. doi: 10.3389/fimmu.2018.02463
5. Saveanu L, Carroll O, Lindo V, Del Val M, Lopez D, Lepelletier Y, et al. Concerted peptide trimming by human ERAP1 and ERAP2 aminopeptidase complexes in the endoplasmic reticulum. *Nat Immunol.* (2005) 6:689–97. doi: 10.1038/ni1208
6. Yamahara N, Nomura S, Suzuki T, Itakura A, Ito M, Okamoto T, et al. Placental leucine aminopeptidase/oxytocinase in maternal serum and placenta during normal pregnancy. *Life Sci.* (2000) 66:1401–10. doi: 10.1016/S0024-3205(00)00451-3
7. Li DT, Habtemichael EN, Julca O, Sales CI, Westergaard XO, DeVries SG, et al. GLUT4 Storage vesicles: specialized organelles for regulated trafficking. *Yale J Biol Med.* (2019) 92:453–70.
8. Singh KD, Karnik SS. Angiotensin receptors: structure, function, signaling and clinical applications. *J Cell Signal.* (2016) 1:111. doi: 10.4172/jcs.1000111
9. Wright JW, Kawas LH, Harding JW. A role for the brain RAS in Alzheimer's and Parkinson's diseases. *Front Endocrinol (Lausanne).* (2013) 4:158. doi: 10.3389/fendo.2013.00158
10. Andersson H, Hallberg M. Discovery of inhibitors of insulin-regulated aminopeptidase as cognitive enhancers. *Int J Hypertens.* (2012) 2012:789671. doi: 10.1155/2012/789671
11. Romero CA, Orias M, Weir MR. Novel RAAS agonists and antagonists: clinical applications and controversies. *Nat Rev Endocrinol.* (2015) 11:242–52. doi: 10.1038/nrendo.2015.6
12. Benigni A, Cassis P, Remuzzi G. Angiotensin II revisited: new roles in inflammation, immunology and aging. *EMBO Mol Med.* (2010) 2:247–57. doi: 10.1002/emmm.201000080
13. Ruiz-Ortega M, Lorenzo O, Egido J. Angiotensin III increases MCP-1 and activates NF-kappaB and AP-1 in cultured mesangial and mononuclear cells. *Kidney Int.* (2000) 57:2285–98. doi: 10.1046/j.1523-1755.2000.00089.x
14. Ruster C, Wolf G. Renin-angiotensin-aldosterone system and progression of renal disease. *J Am Soc Nephrol.* (2006) 17:2985–91. doi: 10.1681/ASN.2006040356
15. Esteban V, Ruperez M, Sánchez-López E, Rodríguez-Vita J, Lorenzo O, Demaegdt H, et al. Angiotensin IV activates the nuclear transcription factor-kappaB and related proinflammatory genes in vascular smooth muscle cells. *Circ Res.* (2005) 96:965–73. doi: 10.1161/01.RES.0000166326.91395.74
16. Ruiz-Ortega M, Esteban V, Egido J. The regulation of the inflammatory response through nuclear factor-kappab pathway by angiotensin IV extends the role of the renin angiotensin system in cardiovascular diseases. *Trends Cardiovasc Med.* (2007) 17:19–25. doi: 10.1016/j.tcm.2006.10.003
17. Saveanu L, van Endert P. The role of insulin-regulated aminopeptidase in MHC class I antigen presentation. *Front Immunol.* (2012) 3:57. doi: 10.3389/fimmu.2012.00057
18. Saveanu L, Babdor J, Lawand M, van Endert P. Insulin-regulated aminopeptidase and its compartment in dendritic cells. *Mol Immunol.* (2013) 55:153–5. doi: 10.1016/j.molimm.2012.10.013
19. Yao Y, Liu N, Zhou Z, Shi L. Influence of ERAP1 and ERAP2 gene polymorphisms on disease susceptibility in different populations. *Hum Immunol.* (2019) 80:325–34. doi: 10.1016/j.humimm.2019.02.011
20. Vitulano C, Tedeschi V, Paladini F, Sorrentino R, Fiorillo MT. The interplay between HLA-B27 and ERAP1/ERAP2 aminopeptidases: from anti-viral protection to spondyloarthritis. *Clin Exp Immunol.* (2017) 190:281–90. doi: 10.1111/cei.13020
21. Hanson AL, Morton CJ, Parker MW, Bessette D, Kenna TJ. The genetics, structure and function of the M1 aminopeptidase oxytocinase subfamily and their therapeutic potential in immune-mediated disease. *Hum Immunol.* (2019) 80:281–9. doi: 10.1016/j.humimm.2018.11.002
22. Alvarez-Navarro C, Martín-Esteban A, Barnea E, Admon A, López de Castro JA. Endoplasmic reticulum aminopeptidase 1 (ERAP1) polymorphism relevant to inflammatory disease shapes the peptidome of the birdshot chorioretinopathy-associated HLA-A*29:02 antigen. *Mol Cell Proteomics.* (2015) 14:1770–80. doi: 10.1074/mcp.M115.048959
23. Paladini F, Fiorillo MT, Tedeschi V, Cauli A, Mathieu A, Sorrentino R. Ankylosing spondylitis: a trade off of HLA-B27, ERAP, and pathogen interconnections? Focus on Sardinia. *Front Immunol.* (2019) 10:35. doi: 10.3389/fimmu.2019.00035
24. Lee YH, Song GG. Associations between ERAP1 polymorphisms and susceptibility to ankylosing spondylitis: a meta-analysis. *Clin Rheumatol.* (2016) 35:2009–15. doi: 10.1007/s10067-016-3287-9
25. Paladini F, Fiorillo MT, Tedeschi V, D'Otolo V, Piga M, Cauli A, et al. The rs75862629 minor allele in the endoplasmic reticulum aminopeptidases intergenic region affects human leucocyte antigen B27 expression and protects from ankylosing spondylitis in sardinia. *Rheumatology.* (2019) 58:2315–24. doi: 10.1093/rheumatology/kez212
26. Evans DM, Spencer CC, Pointon JJ, Su Z, Harvey D, Kochan G, et al. Interaction between ERAP1 and HLA-B27 in ankylosing spondylitis implicates peptide handling in the mechanism for HLA-B27 in disease susceptibility. *Nat Genet.* (2011) 43:761–7. doi: 10.1038/ng.873
27. Deng Y, Zhu W, Zhou X. Immune regulatory genes are major genetic factors to Behcet disease: systematic review. *Open Rheumatol J.* (2018) 12:70–85. doi: 10.2174/1874312901812010123
28. Dimopoulou C, Lundgren JD, Sundal J, Ullum H, Aukrust P, Nielsen FC, et al. Variant in ERAP1 promoter region is associated with low expression in a patient with a Behçet-like MHC-I-opathy. *J Hum Genet.* (2019) 65:325–35. doi: 10.1038/s10038-019-0709-y
29. Guasp P, Lorente E, Martín-Esteban A, Barnea E, Romania P, Fruci D, et al. Redundancy and complementarity between ERAP1 and ERAP2 revealed by their effects on the Behcet's disease-associated HLA-B*51 peptidome. *Mol Cell Proteomics.* (2019) 18:14911510. doi: 10.1074/mcp.RA119.001515
30. Martín-Esteban A, Sanz-Bravo A, Guasp P, Barnea E, Admon A, López de Castro JA. Separate effects of the ankylosing spondylitis associated ERAP1 and ERAP2 aminopeptidases determine the influence of their combined phenotype on the HLA-B*27 peptidome. *J Autoimmun.* (2017) 79:28–38. doi: 10.1016/j.jaut.2016.12.008
31. Joyce S. Immunoproteasomes edit tumors, which then escapes immune recognition. *Eur J Immunol.* (2015) 45:3241–5. doi: 10.1002/eji.201546100
32. Koumantou D, Barnea E, Martin-Esteban A, Maben Z, Papakyriakou A, Mpakali A, et al. Editing the immunopeptidome of melanoma cells using a potent inhibitor of endoplasmic reticulum aminopeptidase 1 (ERAP1). *Cancer Immunol Immunother.* (2019) 68:1245–61. doi: 10.1007/s00262-019-02358-0
33. López de Castro JA, Alvarez-Navarro C, Brito A, Guasp P, Martín-Esteban A, Sanz-Bravo A. Molecular and pathogenic effects of endoplasmic reticulum aminopeptidases ERAP1 and ERAP2 in MHC-I-associated inflammatory disorders: towards a unifying view. *Mol Immunol.* (2016) 77:193–204. doi: 10.1016/j.molimm.2016.08.005
34. Kuiper JJ, Van Setten J, Ripke S, Van 'T Slot R, Mulder F, Missotten T, et al. A genomewide association study identifies a functional ERAP2 haplotype associated with birdshot chorioretinopathy. *Hum Mol Genet.* (2014) 23:6081–7. doi: 10.1093/hmg/ddu307
35. Robinson PC, Costello ME, Leo P, Bradbury LA, Hollis K, Cortes A, et al. ERAP2 is associated with ankylosing spondylitis in HLA-B27-positive and HLA-B27-negative patients. *Ann Rheum Dis.* (2015) 74:1627–9. doi: 10.1136/annrheumdis-2015-207416
36. Kikas T, Rull K, Beaumont RN, Freathy RM, Laan M. The effect of genetic variation on the placental transcriptome in humans. *Front Genet.* (2019) 10:550. doi: 10.3389/fgene.2019.00550
37. Soltani S, Nasiri M. Association of ERAP2 gene variants with risk of pre-eclampsia among Iranian women. *Int J Gynaecol Obstet.* (2019) 145:337–42. doi: 10.1002/ijgo.12816
38. Hulur I, Gamazon ER, Skol AD, Xicola RM, Llor X, Onel K, et al. Enrichment of inflammatory bowel disease and colorectal cancer risk

variants in colon expression quantitative trait loci. *BMC Genomics.* (2015) 16:138. doi: 10.1186/s12864-015-1292-z
39. Chen H, Li L, Weimershaus M, Evnouchidou I, van Endert P, Bouvier M. ERAP1-ERAP2 dimers trim MHC I-bound precursor peptides; implications for understanding peptide editing. *Sci Rep*. (2016) 6:28902. doi: 10.1038/srep28902
40. Paladini F, Fiorillo MT, Vitulano C, Tedeschi V, Piga M, Cauli A, et al. An allelic variant in the intergenic region between ERAP1 and ERAP2 correlates with an inverse expression of the two genes. *Sci Rep.* (2018) 8:10398. doi: 10.1038/s41598-018-28799-8
41. Shibata K, Kajiyama H, Ino K, Nawa A, Nomura S, Mizutani S, et al. P-LAP/IRAPinduced cell proliferation and glucose uptake in endometrial carcinoma cells via insulin receptor signaling. *BMC Cancer.* (2007) 7:15. doi: 10.1186/1471-2407-7-15
42. Cheng H, Li Y, Zuo XB, Tang HY, Tang XF, Gao JP, et al. Identification of a missense variant in LNPEP that confers psoriasis risk. *J Invest Dermatol.* (2014) 134:359–65. doi: 10.1038/jid.2013.317
43. Zhen Q, Yang Z, Wang W, Li B, Bai M, Wu J et al. Genetic study on small insertions and deletions in psoriasis reveals a role in complex human diseases. *J Invest Dermatol.* (2019) 139:2302–12.e14. doi: 10.1016/j.jid.2019.03.1157
44. Saveanu L, Carroll O, Weimershaus M, Guermonprez P, Firat E, Lindo V, et al. IRAP identifies an endosomal compartment required for MHC class I cross-presentation. *Science.* (2009) 325:213–7. doi: 10.1126/science.1172845
45. Weger W, Hofer A, Wolf P, El-Shabrawi Y, Renner W, Kerl H, et al. The angiotensin converting enzyme insertion/deletion and the endothelin-1343A/4A gene polymorphisms in patients with chronic plaque psoriasis. *Exp Dermatol.* (2007) 16:993–8. doi: 10.1111/j.1600-0625.2007.00620.x
46. Veletza S, Karpouzis A, Giassakis G, Caridha R, Papaioakim M. Assessment of insertion/deletion polymorphism of the angiotensin converting enzyme gene in psoriasis. *J Dermatol Sci.* (2008) 49:85–7. doi: 10.1016/j.jdermsci.2007.08.005
47. Aleksiejczuk M, Gromotowicz-Poplawska A, Marcinczyk N, Przylipiak A, Chabielska E. The expression of the renin-angiotensin-aldosterone system in the skin and its effects on skin physiology and pathophysiology. *J Physiol Pharmacol.* (2019) 70:325–36. doi: 10.26402/jpp.2019.3.01
48. Nakada TA, Russell JA, Wellman H, Boyd JH, Nakada E, Thain KR, et al. Leucyl/cystinyl aminopeptidase gene variants in septic shock. *Chest.* (2011) 139:1042–9. doi: 10.1378/chest.10-2517
49. Hill LD, Hilliard DD, York TP, Srinivas S, Kusanovic JP, Gomez R, et al. Fetal ERAP2 variation is associated with preeclampsia in African Americans in a case-control study. *BMC Med Genet.* (2011) 12:64. doi: 10.1186/1471-2350-12-64
50. Johnson MP, Roten LT, Dyer TD, East CE, Forsmo S, Blangero J, et al. The ERAP2 gene is associated with preeclampsia in Australian and Norwegian populations. *Hum Genet.* (2009) 126:655–66. doi: 10.1007/s00439-009-0714-x
51. Andrés AM, Dennis MY, Kretzschmar WW, Cannons JL, Lee-Lin SQ, Hurle B, et al. Balancing selection maintains a form of ERAP2 that undergoes nonsense-mediated decay and affects antigen presentation. *PLoS Genet.* (2010) 6:e1001157. doi: 10.1371/journal.pgen.1001157
52. Goto Y, Ogawa Y, Tsumoto H, Miura Y, Nakamura TJ, Ogawa K, et al. Contribution of the exosome-associated form of secreted endoplasmic reticulum aminopeptidase 1 to exosomemediated macrophage activation. *Biochim Biophys Acta Mol Cell Res.* (2018) 1865:874888. doi: 10.1016/j.bbamcr.2018.03.009
53. Saulle I, Ibba SV, Torretta E, Vittori C, Fenizia C, Piancone F, et al. Endoplasmic reticulum associated aminopeptidase 2 (ERAP2) is released in the secretome of activated MDMs and reduces *in vitro* HIV-1 Infection. *Front Immunol.* (2019) 10:1648. doi: 10.3389/fimmu.2019.01648
54. Ranjit S, Wong JY, Tan JW, Sin Tay C, Lee JM, Yin Han Wong K, et al. Sex-specific differences in endoplasmic reticulum aminopeptidase 1 modulation influence blood pressure and renin-angiotensin system responses. *JCI Insight.* (2019) 4:e129615. doi: 10.1172/jci.insight.129615
55. Forni D, Cagliani R, Tresoldi C, Pozzoli U, De Gioia L, Filippi G, et al. An evolutionary analysis of antigen processing and presentation across different timescales reveals pervasive selection. *PLoS Genet.* (2014) 10:e1004189. doi: 10.1371/journal.pgen.1004189

Conflict of Interest: The authors declare that the research was conducted in the absence of any commercial or financial relationships that could be construed as a potential conflict of interest.

Copyright © 2020 Paladini, Fiorillo, Tedeschi, Mattorre and Sorrentino. This is an open-access article distributed under the terms of the Creative Commons Attribution License (CC BY). The use, distribution or reproduction in other forums is permitted, provided the original author(s) and the copyright owner(s) are credited and that the original publication in this journal is cited, in accordance with accepted academic practice. No use, distribution or reproduction is permitted which does not comply with these terms.

frontiers in Immunology

ORIGINAL RESEARCH
published: 23 July 2020
doi: 10.3389/fimmu.2020.01385

IL-15 and IL15RA in Osteoarthritis: Association With Symptoms and Protease Production, but Not Structural Severity

*Sophie C. Warner[1], Anjali Nair[2], Rahul Marpadga[2], Susan Chubinskaya[3], Michael Doherty[1,4], Ana M. Valdes[1,4] and Carla R. Scanzello[5,6]**

[1] Academic Rheumatology, Nottingham City Hospital, Nottingham, United Kingdom, [2] Section of Rheumatology, Rush University Medical Center, Chicago, IL, United States, [3] Division of Pediatrics, Rush University Medical Center, Chicago, IL, United States, [4] Arthritis Research UK Pain Centre and National Institutes for Health Research Nottingham Biomedical Research Centre, Nottingham, United Kingdom, [5] Translational Musculoskeletal Research Center & Section of Rheumatology, Corporal Michael J. Crescenz VA Medical Center, Philadelphia, PA, United States, [6] Division of Rheumatology, University of Pennsylvania Perelman School of Medicine, Philadelphia, PA, United States

Objective: Interleukin-15 (IL-15) is a pro-inflammatory cytokine that is increased in joint fluids of early-stage osteoarthritis (OA) patients, and has been associated with expression of proteases that can damage cartilage, and the development of neuropathic pain-like symptoms (NP) after nerve injury. The objective of this study was to further explore the role of IL-15 in the pathogenesis of OA cartilage degeneration and test genetic variation in the IL-15 receptor α gene (*IL15RA*) for an association with OA with radiographic severity and symptoms.

Methods: Cartilage samples from donors ($n = 10$) were analyzed for expression of the IL15 receptor α-chain using immunohistochemistry, and for responses to IL-15 *in vitro* using explant cultures. Data from two independent Nottinghamshire-based studies ($n = 795$ and $n = 613$) were used to test genetic variants in the *IL15RA* gene (rs2228059 and rs7097780) for an association with radiographic severity, symptomatic vs. asymptomatic OA and NP.

Results: IL-15Rα was expressed in chondrocytes from cartilage obtained from normal and degenerative knees. IL-15 significantly increased the release of matrix metalloproteinase-1 and -3 (MMP-1 and -3), but did not affect loss of proteoglycan from the articular matrix. Genetic variants in the *IL15RA* gene are associated with risk of symptomatic vs. asymptomatic OA (rs7097780 OR = 1.48 95% 1.10–1.98 $p < 0.01$) and with the risk of NP post-total joint replacement (rs2228059 OR = 0.76 95% 0.63–0.92 $p < 0.01$) but not with radiographic severity.

Conclusions: In two different cohorts of patients, we show an association between genetic variation at the IL15 receptor and pain. Although *ex vivo* cartilage explants could respond to IL-15 with increased protease production, we found no effect of IL-15 on cartilage matrix loss and no association between *IL15RA* variants and radiographic severity. Together, these results suggest that IL-15 signaling may be a target for pain, but may not impact structural progression, in OA.

Keywords: inflammation, pain, proteases, interleukins, interleukin-15, osteoarthritis, neuropathic pain, neuropathic pain-like symptoms

OPEN ACCESS

Edited by:
Erminia Mariani, University of Bologna, Italy

Reviewed by:
Erika H. Noss, University of Washington, United States
Deepika Sharma, University of Chicago, United States

***Correspondence:**
Carla R. Scanzello
carla.scanzello@va.gov;
cscanz@pennmedicine.upenn.edu

Specialty section:
This article was submitted to Autoimmune and Autoinflammatory Disorders, a section of the journal Frontiers in Immunology

Received: *14 February 2020*
Accepted: *29 May 2020*
Published: *23 July 2020*

Citation:
Warner SC, Nair A, Marpadga R, Chubinskaya S, Doherty M, Valdes AM and Scanzello CR (2020) IL-15 and IL15RA in Osteoarthritis: Association With Symptoms and Protease Production, but Not Structural Severity. Front. Immunol. 11:1385. doi: 10.3389/fimmu.2020.01385

INTRODUCTION

The inflammatory response has been shown to play an important role in osteoarthritis (OA) (1), both in symptomatic and structural manifestations, but the relative importance of specific inflammatory mediators in OA joints is yet to be fully elucidated. Previous work has evaluated common-gamma chain cytokines and specifically detected interleukin-15 (IL-15) in many synovial fluid (SF) specimens from people with knee OA (2, 3). IL-15 is a pro-inflammatory cytokine that is best characterized for its effects on T-lymphocyte and NK-cell activation, proliferation, and survival (4, 5). We previously found IL-15 levels in the SF to be elevated in early-stage disease compared with advanced disease and correlated with SF matrix metalloproteinases-1 and -3 (MMP-1 and MMP-3) levels (2). These two proteases are often elevated in the joints of OA patients and have been linked to extracellular matrix turnover. Using a proteomic approach to identify biomarkers of disease, other investigators found IL-15 detectable in serum samples from participants in the Baltimore Longitudinal Study of Aging (BLSA) (6). In this study, serum IL-15 was associated with radiographic OA changes in the knee and hands, and was elevated in individuals up to 10 years prior to observation of radiographic changes. Taken together, these studies suggest that IL-15 might play a role in early initiation events leading to joint degeneration in OA.

IL-15 has also been linked with pain in various rheumatologic diseases including rheumatoid arthritis (RA), lupus, and OA (2, 7–11). IL-15 inhibition has been tested in clinical trials for RA, and has been demonstrated to improve pain (12). In addition to nociceptive pain, IL-15 has been linked to the development of neuropathic pain-like symptoms (NP) after nerve injury, due to its role in neuroinflammation (13). In OA, multiple pain phenotypes have been described including NP (14, 15) and neuroinflammatory mechanisms have been implicated mechanistically [reviewed in (16)].

The association of IL-15 with the emergence of radiographic changes, protease production within the joint, and pain severity in OA, suggest that this cytokine may play multiple roles in OA disease pathogenesis. Importantly, IL-15 signaling is dependent on binding to the high specificity IL-15 receptor chain, interleukin-15 receptor α (IL-15Rα), encoded in humans by the *IL15RA* gene (17). The aims of this study therefore were to explore the potential effects of IL-15 on OA by examining both structural and symptomatic disease manifestations. Given the association with protease production in previous studies, we first evaluated whether chondrocytes express IL-15Rα, and whether IL-15 has a direct effect on protease production and matrix loss from human cartilage *in vitro*. We then investigated whether select *IL15RA* variants were associated with symptoms or radiographic severity in OA by examining two separate cohorts of patients.

MATERIALS AND METHODS

In vitro Cartilage Experiments

Cartilage Donors

Cartilage was collected within 24-h post-mortem from the knees of ten organ donors with no history of arthritis through the Gift of Hope Organ and Tissue Donor Network (Itasca, IL), through an IRB-approved bio-repository at Rush University Medical Center. Age and gender of the donors was recorded. Degenerative changes in the knee joint were evaluated by a pathologist at the time of dissection, according to the modified Collins grade (18). When degenerative changes were present, cartilage was taken from lesional areas. The characteristics of these donors are presented in **Table 1**, and representative gross morphology presented in **Figure 1**.

TABLE 1 | Characteristics of cartilage tissue specimens used for *in vitro* experiments.

Donor	Age range	Collins grade[#]	Cartilage characteristics
1	18–25	0	Normal
2	46–50	1	Minor fibrillation
3*	66–70	1	Minor fibrillation
4	71–75	1	Minor fibrillation
5	51–55	2	Fibrillation + fissures
6	61–65	2	Fibrillation + fissures
7	71–75	2	Fibrillation + fissures
8	66–70	3	≤30% full-thickness erosion
9	66–70	3	≤30% full-thickness erosion
10	56–60	4	≥30% full-thickness erosion

**Femoral cartilage was obtained from specimen #3. Tibial cartilage was obtained from all other donors.*

Immunohistochemistry

Tibial cartilage specimens from three organ donors were formalin-fixed and paraffin-embedded. Six-micron sections were prepared and stained for IL-15Rα using standard immunoperoxidase technique and a polyclonal antibody directed against the human IL-15Rα chain (goat anti-human IL-15Rα, Santa Cruz Biotechnology). Non-immune goat IgG was utilized as negative control for staining specificity.

Explant Culture

To test effects of IL-15 on cartilage, 4 mm cartilage punch biopsies were prepared from the tibial or femoral surfaces of organ donors ($n = 10$ donor experiments, each run in duplicate, **Table 1**). For each donor, 2 explants per well were placed in a 24 well plate with 1 ml DMEM (+100 U/ml Penicillin-Streptomycin). After 24 h, media was replaced with 1 ml of fresh media with or without recombinant human IL-15 (100 ng/ml, Peprotech, NJ). The concentration of IL-15 was chosen based on the range of concentrations required for *in vitro* stimulation of NK cell proliferation and activation (19). TNF-α + Oncostatin M (100 ng/ml each, R & D Systems, MN), a potent stimulus for MMP production and cartilage proteoglycan loss (20, 21) was used as a positive control. Every 2 days for up to 10 days, culture supernatants were collected and replaced with fresh media with or without cytokines. Consecutive 2-days supernatants were analyzed in duplicate from each well, and two wells per donor analyzed, for MMP-1, -3, and -9 using a human MMP 3-plex ultrasensitive electrically-activated chemiluminescence immunoassay (Meso Scale Discovery, Rockville MD) read on a Sector 6000 Imager. Total ng in each supernatant aliquot was

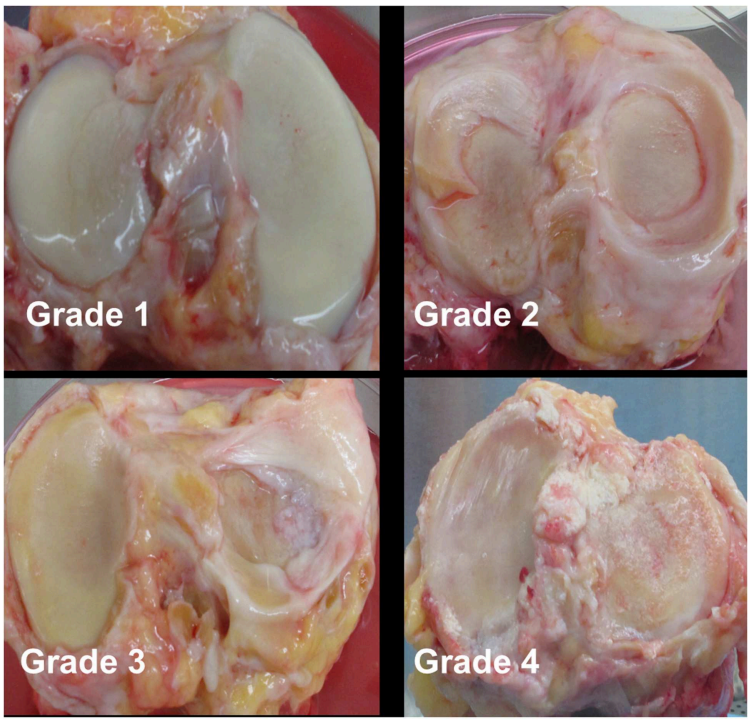

FIGURE 1 | Representative gross morphology of donor knees. Grade 1–4 represent modified Collins grade as follows: Grade 1 = limited disruption of the articular surface with only minor fibrillations; Grade 2 = fibrillation of cartilage with fissures ± small osteophytes; Grade 3 = osteophytes + cartilage fibrillation and fissuring with 30% or less of the cartilage surface eroded down to subchondral bone; Grade 4 = osteophytes and gross geometric bony change + >30% of the cartilage surface eroded down to the subchondral bone.

determined, cumulative amounts at each time point calculated, and results were expressed as the percentage of the total ng released in 10 days from the untreated control (=100%) to allow comparison between donors.

Explant supernatants (n = 7 donors) were processed for measurement of glycosaminoglycan (GAG) release using the Dimethyl Methylene Blue (DMMB) assay (22). For three donors, total GAG content (explants + supernatants) was measured as follows. Cartilage explants (fresh day 0 and those after 14 days of culture) were extracted and digested according to previously reported methods (23). Extractable GAG content of the explants was then determined, and total extractable GAG content (the sum of supernatants up to 14 days + explants after 14 days) was calculated and compared to unstimulated cultures. The percentage of the total GAG content released into the media was calculated as a measure of GAG breakdown.

Genetic Study of IL-15 Receptor Variants

Study Participants

A subset of knee OA cases from the Nottinghamshire-based Genetics of OA and Lifestyle (GOAL) study and from the Nottingham Genetics Case Control study [previously described (24)] were used in this analysis to assess the role of *IL15RA* variation on radiographic severity and symptoms in OA. All individuals from both cohorts had X-rays assessed at baseline. Analyses here are based on tibiofemoral (TF) Kellgren/Lawrence (K/L) grade. Symptomatic or asymptomatic status was available only for participants in the GOAL study. Additionally, hip OA cases are not included here because of a lack of asymptomatic hip OA cases. Individuals classified as asymptomatic OA cases were originally recruited as controls for OA and were later found to have radiographic evidence of knee OA, despite not reporting knee pain.

A postal questionnaire about joint pain, quality of life and medical history was sent on average 4.8 years later to individuals from both cohorts, including hip OA cases not included in the knee OA study, when most (91.4%) individuals had undergone a total joint replacement (TJR).

The North Nottinghamshire Research Ethics Committee gave approval for the ethics of the two studies. All participants gave written, informed consent (according to the Declaration of Helsinki).

Binary Trait Definitions for Statistical Analysis

The joint-specific version of the painDETECT questionnaire (PDQ) for NP symptoms of the joint was used (25), and included in the postal questionnaire administered after enrollment. Possible joint NP was classified as a score of >12 on the site-PDQ as described and validated previously (25). TF K/L scores were dichotomized as 0 = grade 2, 1 = grades 3 and 4 (in OA-affected individuals in both groups).

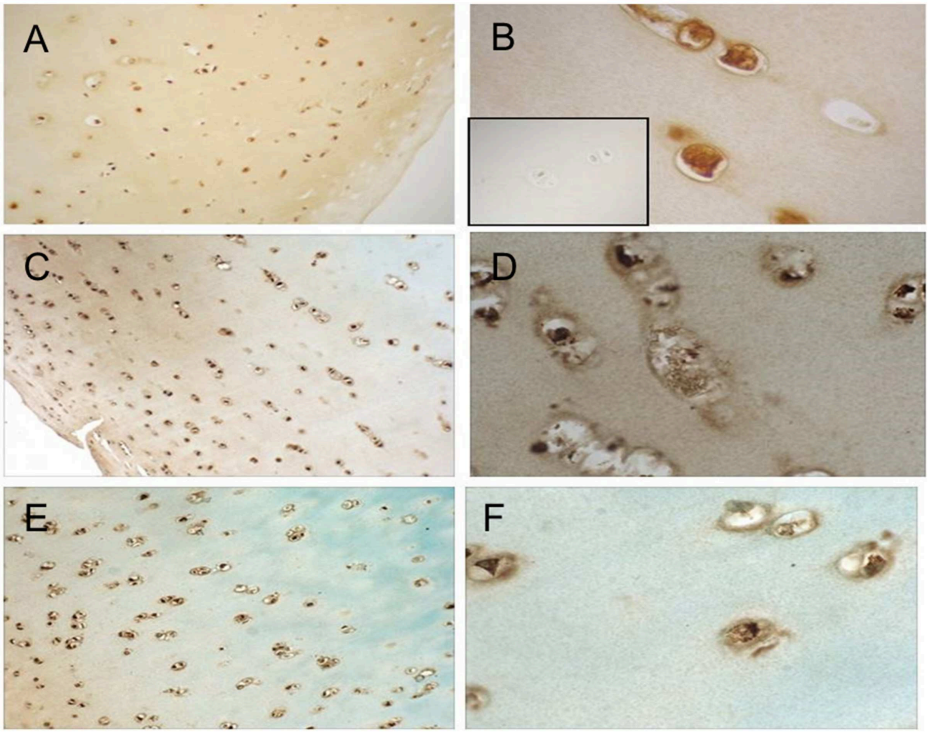

FIGURE 2 | IL-15Ra staining in human articular cartilage. Cartilage specimens were processed and immunostained as described. Representative photomicrographs of cartilage from a grade 0 donor **(A,B)**, grade 2 donor **(C,D)**, and grade 3 donor **(E,F)** at 10× **(A,C,E)** and 40× **(B,D,F)** are shown. Isotype-matched negative control staining is shown in inset of **(B)**.

Genetic Data

Blood samples from the participants in this study were processed to obtain genotype data as previously described (26). These data were available for all participants in this part of the study. Binary logistic regression analysis was used to test two genetic variants (SNPs) in the *IL15RA* gene, rs2228059 (mapping to chromosome 10 position 5960405, minor allele, C, with a frequency of 0.492) and rs7097780 (mapping to chromosome 10 position 5968264, minor allele G with a frequency of 0.323) for an association with TF K/L grade of radiographic severity and possible NP in both groups. These two SNPs together represent 67% of the variation in the *IL15RA* gene (https://snpinfo.niehs.nih.gov/snpinfo/snptag.htm).

Symptomatic vs. asymptomatic OA variables were also tested in the GOAL group only. The statistics package R (version 3.0.2) was used for these analyses. All analyses were adjusted for age, sex, and BMI. Meta-analysis was used to test the overall effect of *IL15RA* genotype across both groups where necessary.

RESULTS

Articular Chondrocytes Express the IL-15 Receptor α-Chain

Cellular responses to IL-15 are mediated by binding to the IL-15 receptor which is composed of three subunits: the IL-15Rα chain which confers binding specificity for IL-15, and a common β and γ chain shared by the IL-2 receptor (17). We therefore studied expression of IL-15Rα by articular chondrocytes. Formalin fixed, paraffin-embedded articular cartilage specimens from three donors (one each of grade 0, 2, and 3) were sectioned for immunohistochemical staining as described. As depicted in **Figure 2**, staining for IL-15Rα was observed in chondrocytes regardless of Collins grade. In addition, staining was observed throughout the thickness of the cartilage, from the superficial layer to the deep zone.

IL-15 Induces MMP-1 and MMP-3 Production From Articular Cartilage *in vitro*

Given the association of IL-15 with protease activity (3) we next tested whether IL-15 exposure could induce MMP production from articular chondrocytes using an *in vitro* explant system. MMP-1, -3, and -9 production was measured in explant supernatants collected every 2 days for 10 days. Levels were expressed as the percentage of the total released in 10 days without cytokine stimuli (100%). Release of MMP-1 in response to IL-15 was observed in cartilage explants from eight of 10 donors (mean ± SEM MMP-1 release: 843% ± 222 of control, **Figure 3A**), and MMP-3 in five of 10 donors (mean MMP-3: 206% ± 42 of control, **Figure 3B**). This release was delayed (observed at 4–6 days) compared to the positive control stimuli (TNF/OSM). IL-15 had no effect on MMP-9 release (mean 109% ± 17 of control, **Figures 3C,F**). When examined according to

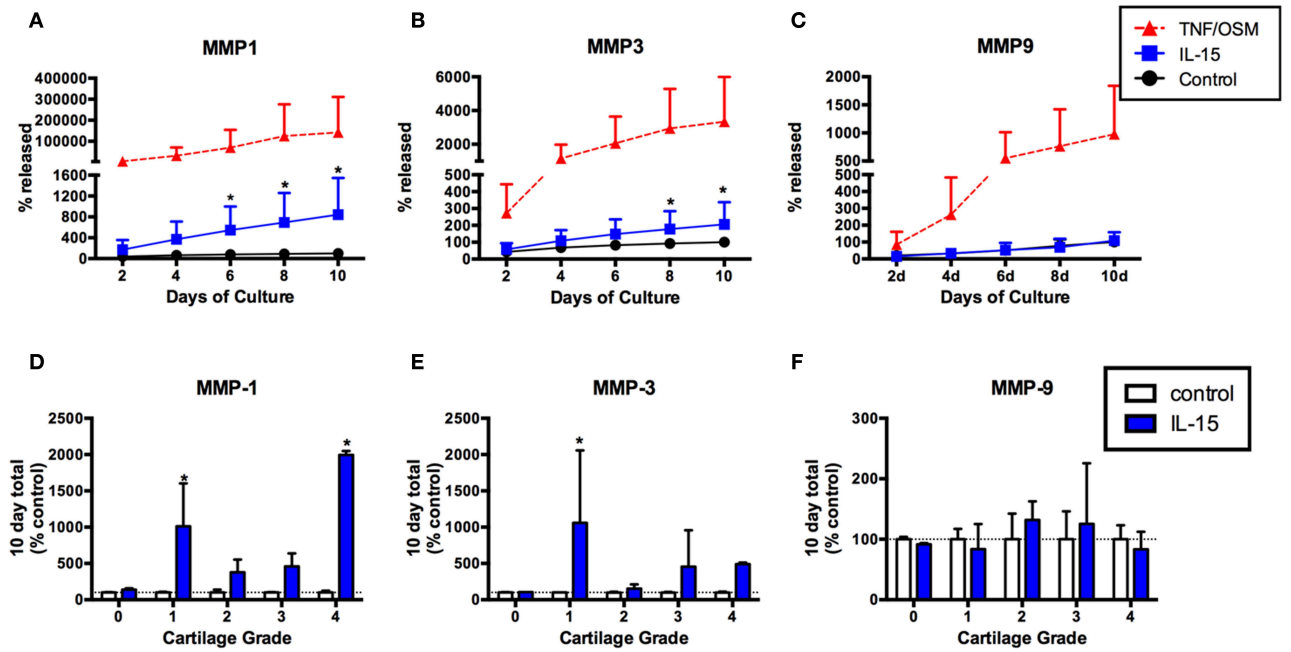

FIGURE 3 | IL-15 effect on MMP-1, -3, and -9 release from human cartilage explants over 10 days *in vitro*. Articular cartilage explants were exposed to IL-15 (100/ml) *in vitro* for 10 days as described, and supernatants collected and replaced every 2 days. Explants exposed to TNF + OSM served as a positive control. MMP-1, -3, and -9 were measured in explant supernatants at each time point, and levels expressed as the percent of the total amount produced in 10 days in unstimulated control cultures (mean ± SD of 10 experiments). IL-15 increased release of **(A)** MMP-1 and **(B)** MMP-3 compared to unstimulated control explants (*$p < 0.001$, 2-way ANOVA). **(C)** No effect of IL-15 on MMP-9 release was observed. **(D,E)** The effects of IL-15 on **(D)** MMP-1 and **(E)** MMP-3 release was highly variable, with the most significant differences observed in explants from donors with early (grade 1) degenerative changes. **(F)** There was no release of MMP-9 in response to IL-15, regardless of explant grade.

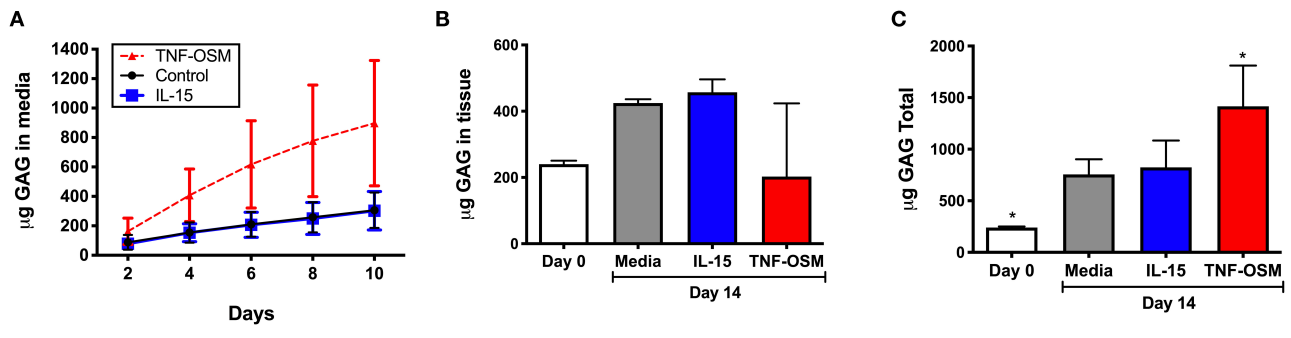

FIGURE 4 | Effect of IL-15 on GAG release and tissue GAG content *in vitro*. **(A)** Cartilage explants ($n = 7$ experiments) were exposed to 100 ng/ml rhIL-15 (blue squares) or left unstimulated (control black circles) as described. Exposure to TNFα and Oncostatin M (TNF-OSM, 100 ng/ml each, red triangles) served as a positive control for proteoglycan release. The cumulative GAG content of the media collected every 2 days for up to 10 days is depicted over 10 days in culture. IL-15 had no significant effect on GAG loss from explants compared to unstimulated control cultures. **(B)** GAG content of cartilage explants ($n = 3$ separate experiments) collected at day 0 (fresh) and after 14 days of culture was measured as described. IL-15 had no effect on cartilage tissue GAG content after 14 days compared to control unstimulated explants. TNF/OSM led to net loss (p = ns) of cartilage GAG content as expected. **(C)** The total GAG content of the culture system (explants + media aliquots) after 14 days *in vitro* was calculated to evaluate GAG synthesis and subsequent release. Total GAG content was increased at 14 days compared to baseline in unstimulated controls, indicating a net synthesis of GAGs in the explants. This was not further impacted by exposure to IL-15. *$p < 0.05$ compared to day 14 unstimulated explants.

Collins grade of the explant donor, MMP-1 release in response to IL-15 treatment was observed in explants with grade 1 through 4 cartilage degeneration, but not in the normal (grade 0) cartilage donor (**Figure 3D**). A similar pattern was observed with MMP-3 (**Figure 3E**).

As expected (20, 21), robust but variable MMP-1 and MMP-3 production was observed in response to the positive control stimuli TNF + OSM from all explants, whether from normal or degenerative donors (**Supplemental Figures 1A,B**). We found no significant differences in the TNF + OSM response when

comparing donors that responded to IL-15 vs. non-responders (**Supplemental Figures 1C,D**, Mann-Whitney $P > 0.05$), and no statistically significant correlation between the responses to IL-15 and TNF + OSM, for either MMP-1 (Spearman $r = 0.54$, $P = 0.11$) or MMP-3 ($r = 0.05$, $p = 0.89$) (**Supplemental Figures 1E,F**).

IL-15 Does Not Promote GAG Loss From Articular Cartilage

GAG content of culture supernatants was measured in seven experiments, to determine whether IL-15 impacted GAG loss from cartilage matrix. Over 10 days in culture there was an average loss of 306 (±46) μg GAG from the unstimulated explants that was not further enhanced by exposure to IL-15 (303 ± 50 μg, **Figure 4A**). Explants responded as expected to TNF/OSM with a loss of 897 (±161) μg in 10 days. Since cytokines can also modulate GAG synthesis by chondrocytes, we measured GAG content in explants from 3 of the donors as described in **Methods**. As shown in **Figure 4B**, over a 14 days culture period, GAG content increased slightly in unstimulated explants (240.0 ± 6.0 μg at day 0, to 424.8 ± 6.7 μg at day 14) suggesting some new synthesis. Exposure to IL-15 did not alter this increase (457.3 ± 22.4 μg). In contrast, in 2 of 3 experiments there appeared to be a decrease of GAG content of the tissue compared to day 0 explants in response to TNF/OSM exposure, although mean explant GAG was not different from unstimulated controls at day 14 (202.6 ± 127.6 μg, **Figure 4B**). When total GAG content of the system (14 days tissue + supernatants) was calculated there was no difference in unstimulated and IL-15 stimulated groups, while TNF/OSM exposure led to a net increase in total GAG content (media + explant) reflecting both enhanced synthesis and subsequent release into the media (**Figure 4C**).

Genetic Variation in the IL-15 Receptor Is Associated With Symptomatic OA and With Neuropathic Pain-Like Symptoms but Not With Radiographic Severity

The effects of IL-15 are dependent on binding to its highly specific receptor (17) which is encoded by the *IL15RA* gene. We next used a genetic approach to assess if there is a relation between *IL15RA* variation, radiographic severity and pain measures in people with OA. The descriptive characteristics of the participants with knee OA and post-TJR in this genetic study are shown in **Table 2**.

We found no significant association between either of the *IL15RA* variants and radiographic severity of knee OA (**Table 3**), although there was a trend between the G allele frequency at rs7097780 and TF K/L grade (K/L = 2: 30.2%, K/L = 3: 33.3%, K/L = 4: 36.2%, Armitage trend test $p = 0.07$). On the other hand, the frequency of the G allele was associated with risk of OA symptoms. A significant association was seen between the rs7097780 genotype and the risk of symptomatic vs. asymptomatic knee OA. The unadjusted analysis gave a result of: OR = 1.56 (1.18–2.07), $p = 0.0019$. After adjusting for age, sex and BMI the odds ratio remained significant, at 1.48 (1.10–1.98), $p = 0.0098$ (**Table 3**). Further adjustment for maximum TF knee OA grade gave a result of: OR = 1.43 (1.04–1.99), $p = 0.029$.

TABLE 2 | Descriptive statistics for the groups used in the genetic analysis.

	GOAL study	Nottingham genetics of OA study
Tibiofemoral OA cases *n* (%F)	551 (48.3%)	403 (54.8%)
Age (SD)	66.6 (6.7)	69.3 (8.8)
BMI (SD)	30.1 (5.0)	29.8 (5.1)
TF K/L grade (2/3/4)	116/295/140	30/261/112
Symptomatic/Asymptomatic TF OA	403/148	403/0
Post-TJR cases n	795	613
(F%, % post-total knee replacement)	(48.1%. 53.6%)	(56.8%, 64.9%)
painDETECT score mean (SD)	4.49 (6.3)	4.99 (7.6)
Possible neuropathic pain (%)	152 (13.8%)	109 (17.8%)
Unlikely neuropathic pain (%)	948 (86.2%)	504 (82.2%)
rs2228059 (C/A)	0.508/0.492	0.502/0.498
rs7097780 (G/A)	0.677/0.323	0.660/0.340

TABLE 3 | Association between knee OA and pain-related traits and two *IL15RA* SNPs.

Trait	*IL15RA* SNP	
	rs2228059 (effect allele = C)	rs7097780 (effect allele = G)
Radiographic severity: K/L grade 2 vs. grades 3 + 4	OR = 0.98 (0.75–1.27)	OR = 1.19 (0.90–1.57)
Symptomatic vs. asymptomatic knee OA	OR = 1.02 (0.76–1.36)	**OR = 1.48 (1.10–1.98), $p = 0.0098$**
Neuropathic pain post-TJR	**OR = 0.76 (0.63–0.92), $p = 0.005$**	OR = 0.94 (0.76–1.15)

Odds ratios (OR) are adjusted for age, sex, and BMI. Bold values indicate statistically significant results ($p < 0.01$).

To determine whether results could be driven by the subgroup of patients with NP, we re-ran the analysis removing participants with possible NP from the model. This reanalysis demonstrated an OR = 1.45 (1.05–2.01), $p = 0.025$.

The minor (C) allele in rs2228059 was associated with a lower risk of NP joint symptoms post-TJR. Before adjusting for covariates, the effect of rs2228059 genotype on the risk of NP in the GOAL cohort was: OR = 0.75 (0.58–0.96). A very similar effect size is seen in the Nottingham replication cohort: OR = 0.81 (0.60–1.09). After adjustment for covariates and meta-analysis of both cohorts, this achieves: OR = 0.76 (0.63–0.92), $p = 0.005$ (**Table 3**).

DISCUSSION

In this study, we explored the previously reported associations between IL-15, protease production, and pain in knee OA patients (3). Our results show associations of IL15RA variants with symptoms in knee OA, supporting a role for IL-15 signaling in symptomatic manifestations in patients with established OA. In contrast, we found no evidence to support a role for IL-15 in promoting structural damage, as there was no association

with radiographic severity in the cohort studies, and IL-15 did not stimulate cartilage degradation despite promoting MMP production in the explants.

Given our previous finding of an association between IL-15, MMP-1, and MMP-3 concentrations in patient synovial fluids (3), we began by testing whether IL-15 could directly impact cartilage protease production *in vitro* after confirming IL-15 receptor expression by human chondrocytes (**Figure 2**). Exposure of human articular cartilage to rhIL-15 led to cartilage secretion of MMP-1 and -3, but not MMP-9 (**Figure 3**), validating our previous results. These proteases are commonly observed to be upregulated in the setting of joint injury and arthritis (27). Although not as potent a stimulus as our positive control (TNFα + OSM), IL-15 induced measurable release of MMP-1 from 8 of 10, and MMP-3 secretion from 5 of 10 donors tested. Average (±SEM) MMP-1 release was 843 (±222)% and MMP-3 release 206 (±42)% greater than in unstimulated explants. The response to IL-15 was delayed compared to the positive control, raising the possibility that effects of IL-15 are indirect. IL-15 is known to induce production of other cytokines including TNFα (28) which could explain a delayed effect. Whether IL-15 could additionally synergize with TNFα to further promote MMP activity needs further exploration. In this study, we found no correlation between the responses of explants to TNF + OSM and IL-15 (**Supplemental Figure 1**), although it is possible we were underpowered to detect a subtle relationship. Still, to our knowledge this is the first report that this cytokine can directly activate human articular chondrocytes. Interestingly, protease production above control levels was not observed from the normal cartilage specimen, despite IL-15Rα expression. The small number of specimens utilized in this study precludes conclusions as to whether the impact of IL-15 on chondrocytes is dependent on age or the presence of degenerative changes, which will need to be tested in larger studies. But the response clearly requires additional factors beyond IL-15Rα expression. Moreover, these experiments demonstrate the importance of utilizing multiple tissue donors to assess human cartilage activity in explant culture systems, given the inherent variability of the response.

Despite our observation that IL-15 could induce MMP-1 and -3 production from cartilage explants *ex vivo*, this did not result in matrix loss and we found no association of *IL15RA* genetic variation with radiographic severity in the OA cohorts. This suggests that IL-15 likely does not play an important role in progression of cartilage degeneration in OA. Articular cartilage degradation in arthritic diseases involves a complex milieu of proteases that can cleave the proteoglycan and collagen networks of the articular matrix, leading to progressive matrix loss. Members of the MMP, cathepsin, and ADAMTS enzyme families cleave aggrecan (the main proteoglycan of the articular matrix) at multiple sites leading to an array of fragments or "neoepitopes" that are detectable in joint fluids and cartilage (29). In mice, evidence suggests that the aggrecanase ADAMTS5 is responsible for cleavage events leading to aggrecan loss from the matrix, but in humans multiple enzymes including ADAMTS-4,−5 and a variety of MMPs are thought to contribute (30). MMP-3 in particular is thought to play a role in progression of structural disease (31). Given our observed effect of IL-15 on protease production including MMP-3, we proceeded to test release of GAG fragments (as a measure of aggrecan breakdown) from the cartilage explants exposed to IL-15. We saw no release above unstimulated levels (**Figure 4**). In addition, no effect on aggrecan tissue content or net loss from the matrix was observed. We did not assess protease activity directly in this study, so it is possible that IL-15 increases enzyme production, but activity is controlled by molecular inhibitors (i.e., TIMPs, or tissue inhibitors of metalloproteinases) and other mechanisms. However, our results are consistent with recent evidence demonstrating that MMPs may be more involved in aggrecan turnover events within the matrix rather than aggrecan depletion from the matrix (32).

As we did not find that IL-15 on its own was directly pathogenic to articular cartilage, we proceeded to investigate a relationship with symptoms in OA, given reports of associations between IL-15 and pain in rheumatologic diseases (2, 7–11). Using genetic data available from the GOAL study we found that a variant in the *IL15RA* gene is associated with higher risk of symptomatic OA, but not with radiographic severity. Specifically, the presence of the G allele of the rs7097780 IL15RA variant was associated with a 1.48 (1.10–1.98)-fold higher risk of symptoms in patients with definite radiographic changes, and this risk was not affected by the severity of radiographic findings. In addition, removing the patients with possible NP from the analysis did not change the results significantly. Although it is unclear whether these results are related to the effect of IL-15 on protease production seen in the cartilage explants, it is possible that effects on pain may also be indirect. MMP mediated processing is implicated in the generation of a small peptide fragment of the aggrecan core protein (33) which can mediate inflammatory signaling in multiple cell types (34) and has been linked to pain-generation in OA models (35). Additionally, cartilage may be a source of molecular mediators of OA pain, such as nerve growth factor and tachykinin, as recently demonstrated in animal models (36). Independent of its effect on protease production, IL-15 may have direct effects on nociception. When injected into the footpads of mice (37), or intra-thecally in rats (38), IL-15 augmented pain-related outcomes. In this report, although we demonstrate that cartilage expresses the specific IL-15 receptor and can respond biologically to IL-15, whether cartilage itself is a source of IL-15 in the joint, or IL-15 induces other nociceptive mediators from cartilage, remains to be tested.

Another novel finding of this study is the relationship between the rs2228059 minor (C) allele and protection from NP post-TJR. This was demonstrated using data available from both cohorts of patients. However, this is unlikely to be related to the effect of IL-15 on cartilage as it was observed in individuals post-TJR, after native cartilage has been removed. It has been suggested that NP may be improved by inhibition of IL-15 (39). A proportion of individuals with OA suffer from NP (40, 41) so this cytokine may prove to have a relevant role in both nociceptive and neuropathic pain in OA. IL-15 can regulate inflammatory cell infiltration locally and in the peripheral nervous system after nerve injury, linking inflammation and pain generation (13, 39). Our data suggests here is a role to be investigated in more detail for IL-15 in joint NP pain that is not dependent on its effects on cartilage.

The link between IL-15 levels and radiographic severity is still unclear (2). A previous report demonstrated a relationship between serum IL-15 levels and emergence of radiographic changes (6). In the current genetic association study we found no consistent effects of *IL15RA* genotype on radiographic severity in two independent patient cohorts, after adjusting for common confounders. In both the GOAL and Nottingham study, only patients with K-L radiographic stage 2 or greater were examined, as opposed to the earlier study in which patients with no X-ray abnormalities at baseline were followed. Therefore, it is possible that we may have seen an effect of these genetic variants if patients with earlier stage disease were examined. However, current results together with our observation that IL-15 had no clear effect on cartilage GAG loss, suggest that the role of this cytokine in OA may be primarily on symptomatic manifestations of disease.

There are a number of limitations to the current study that need to be considered. For the *in vitro* studies we were only able to obtain normal cartilage from a single donor, limiting our ability to determine whether variability in the IL-15 response was related to the presence of degenerative changes. In addition, our assays did not distinguish between active and total MMP concentrations. With regards to the genetic study, we were able to see the same effect on NP in the two cohorts from the same recruitment area, but the lack of asymptomatic cases in the second cohort prevents us from validating our association with symptoms. Moreover, the lack of information on NP prior to joint replacement in the second cohort limits our analysis of NP at earlier stages of disease. Thus, these results require further replication. In addition, neither of the variants tested has a known functional role, e.g., in terms of ligand binding or expression, so we cannot directly link the genetic association seen to increased or decreased IL-15.

This is the first demonstration that cartilage is responsive to IL-15. Our data suggests a novel role for IL-15 in promoting protease release from cartilage, consistent with previous reports showing associations between IL-15 and protease levels in OA patients (3, 42), but the significance of this effect is as yet unclear as no effect on cartilage matrix loss was seen. As protease levels, particularly MMP-3 levels are commonly elevated in patient synovial fluids, it is possible that these proteases are a reflection of underlying inflammatory activity driven by cytokines, such as IL-15. IL-15Rα blockade can reduce acute inflammation (43), and joint inflammation specifically in an animal model of inflammatory arthritis (44). The association we found between specific *IL15RA* SNPs and symptoms in OA is particularly novel and interesting, as an association between IL-15 levels and OA pain has been reported (2). However, the impact of the specific *IL15RA* alleles studied on IL-15 signaling has not yet been well-studied. More research is needed to identify the effects of these genetic variations on IL-15 activity. But the results of this analysis support previous findings that IL-15 or IL-15 related activity may potentially be a biomarker to help assess disease severity in OA (2). Whether IL-15 activity or levels predict emergence of peripheral or central sensitization in the generation of neuropathic-type pain in OA is an important question that will also need to be addressed in future, longitudinal studies.

DATA AVAILABILITY STATEMENT

The raw data supporting the conclusions of this article will be made available by the authors, without undue reservation, to any qualified researcher.

ETHICS STATEMENT

The studies involving human participants were reviewed and approved by Rush University Medical Center Institutional Review Board and the North Nottinghamshire Research Ethics Committee. The patients/participants provided their written informed consent to participate in this study.

AUTHOR CONTRIBUTIONS

SW, AV, and CS: substantial contributions to the conception or design of the work. SW, AN, RM, SC, MD, AV, and CS: substantial contributions to the acquisition, analysis or interpretation of data, drafting the work or revising it critically for important intellectual content, approval for publication of the content, and agree to be accountable for all aspects of the work in ensuring that questions related to the accuracy or integrity of any part of the work are appropriately investigated and resolved.

FUNDING

This work was supported by a number of sources. SW was funded by a Ph.D. studentship awarded by the University of Nottingham. This study was supported by a EULAR project grant to AV (grant 108239), by the Arthritis Research UK Pain Centre (grant 18769), and by the Rush University Translational Science Consortium. CS was supported by National Institute of Arthritis, Musculoskeletal, and Skin Diseases 1K08AR057859 and services provided by the CTRC at the Children's Hospital of Philadelphia were supported by NIH grants UL1RR024134 (NCRR) and UL1TR000003 (NCATS), and instrumentation grant 1S10RR026853-01; donor acquisition and cartilage explant studies were supported by the Rush Ciba-Geigy Endowed Chair (SC).

None of the authors received fees, bonuses or other benefits for the work described in the manuscript. The funders had no role in the study design, in the collection, analysis or interpretation of the data, the writing of the manuscript or the decision to submit the manuscript for publication.

ACKNOWLEDGMENTS

The authors gratefully acknowledge the contributions of Sally Doherty and Maggie Wheeler to patient assessments at baseline, data collection and entry for the GOAL and Nottingham Genetics of OA studies. We would also like to thank the GOAL Study team. We thank Dr. Arkady Margulis for his assistance with collection of donor tissue and Arnavaz Hakimiyan, Michael Huvard, and Madeline Rollins for their contributions to data collection for the cartilage experiments. The authors would like to acknowledge the Gift of Hope Organ & Tissue Donor Network and the donor's family for providing human tissue for our research. Additionally, we would like to acknowledge

Vu T. Nguyen for coordination of explant assay data collection along with the services of the Clinical and Translational Research Center, Translational Core Lab of The Children's Hospital of Philadelphia for providing the instrumentation and expertise for the Electrochemiluminescent assays.

SUPPLEMENTARY MATERIAL

The Supplementary Material for this article can be found online at: https://www.frontiersin.org/articles/10.3389/fimmu.2020.01385/full#supplementary-material

REFERENCES

1. Kapoor M, Martel-Pelletier J, Lajeunesse D, Pelletier JP, Fahmi H. Role of proinflammatory cytokines in the pathophysiology of osteoarthritis. *Nat Rev Rheumatol*. (2011) 7:33–42. doi: 10.1038/nrrheum.2010.196
2. Sun JM, Sun LZ, Liu J, Su BH, Shi L. Serum interleukin-15 levels are associated with severity of pain in patients with knee osteoarthritis. *Dis Markers*. (2013) 35:203–6. doi: 10.1155/2013/176278
3. Scanzello CR, Umoh E, Pessler F, Diaz-Torne C, Miles T, Dicarlo E, et al. Local cytokine profiles in knee osteoarthritis: elevated synovial fluid interleukin-15 differentiates early from end-stage disease. *Osteoarthr Cartil*. (2009) 17:1040–8. doi: 10.1016/j.joca.2009.02.011
4. Kennedy MK, Glaccum M, Brown SN, Butz EA, Viney JL, Embers M, et al. Reversible defects in natural killer and memory CD8 T cell lineages in interleukin 15-deficient mice. *J Exp Med*. (2000) 191:771–80. doi: 10.1084/jem.191.5.771
5. Marks-Konczalik J, Dubois S, Losi JM, Sabzevari H, Yamada N, Feigenbaum L, et al. IL-2-induced activation-induced cell death is inhibited in IL-15 transgenic mice. *Proc Natl Acad Sci USA*. (2000) 97:11445–50. doi: 10.1073/pnas.200363097
6. Ling SM, Patel DD, Garnero P, Zhan M, Vaduganathan M, Muller D, et al. Serum protein signatures detect early radiographic osteoarthritis. *Osteoarthr Cartil*. (2009) 17:43–8. doi: 10.1016/j.joca.2008.05.004
7. Baslund B, Tvede N, Danneskiold-Samsoe B, Larsson P, Panayi G, Petersen J, et al. Targeting interleukin-15 in patients with rheumatoid arthritis: a proof-of-concept study. *Arthritis Rheum*. (2005) 52:2686–92. doi: 10.1002/art.21249
8. Waldmann TA. Targeting the interleukin-15/interleukin-15 receptor system in inflammatory autoimmune diseases. *Arthritis Rese Ther*. (2004) 6:174–7. doi: 10.1186/ar1202
9. Thurkow EW, van der Heijden IM, Breedveld FC, Smeets TJ, Daha MR, Kluin PM, et al. Increased expression of IL-15 in the synovium of patients with rheumatoid arthritis compared with patients with Yersinia-induced arthritis and osteoarthritis. *J Pathol*. (1997) 181:444–50. doi: 10.1002/(SICI)1096-9896(199704)181:4<444::AID-PATH778>3.0.CO;2-O
10. Aringer M, Stummvoll GH, Steiner G, Köller M, Steiner CW, Höfler E, et al. Serum interleukin-15 is elevated in systemic lupus erythematosus. *Rheumatology*. (2001) 40:876–81. doi: 10.1093/rheumatology/40.8.876
11. Baranda L, de la Fuente H, Layseca-Espinosa E, Portales-Prez D, Nio-Moreno P, Valencia-Pacheco G, et al. IL-15 and IL-15R in leucocytes from patients with systemic lupus erythematosus. *Rheumatology*. (2005) 44:1507–13. doi: 10.1093/rheumatology/kei083
12. Andersson AK, Li C, Brennan FM. Recent developments in the immunobiology of rheumatoid arthritis. *Arthritis Res Ther*. (2008) 10:204. doi: 10.1186/ar2370
13. Gómez-Nicola D, Valle-Argos B, Suardíaz M, Taylor JS, Nieto-Sampedro M. Role of IL-15 in spinal cord and sciatic nerve after chronic constriction injury: regulation of macrophage and T-cell infiltration. *J Neurochem*. (2008) 107:1741–1752. doi: 10.1111/j.1471-4159.2008.05746.x
14. Kittelson AJ, Stevens-Lapsley JE, Schmiege SJ. Determination of pain phenotypes in knee osteoarthritis: a latent class analysis using data from the osteoarthritis initiative. *Arthritis Care Res*. (2016) 68:612–20. doi: 10.1002/acr.22734
15. Arendt-Nielsen L, Nie H, Laursen MB, Laursen BS, Madeleine P, Simonsen OH, et al. Sensitization in patients with painful knee osteoarthritis. *Pain*. (2010) 149:573–81. doi: 10.1016/j.pain.2010.04.003
16. Cohen E, Lee YC. A mechanism-based approach to the management of osteoarthritis pain. *Curr Osteoporos Rep*. (2015) 13:399–406. doi: 10.1007/s11914-015-0291-y
17. O'Connell GC Pistilli EE. Interleukin-15 directly stimulates pro-oxidative gene expression in skeletal muscle *in-vitro* via a mechanism that requires interleukin-15 receptor alpha. *Biochem Biophys Res Commun*. (2015) 458:614–9. doi: 10.1016/j.bbrc.2015.02.015
18. Muehleman C, Bareither D, Huch K, Cole AA, Kuettner KE. Prevalence of degenerative morphological changes in the joints of the lower extremity. *Osteoarthr Cartil*. (1997) 5:23–37. doi: 10.1016/S1063-4584(97)80029-5
19. Satwani P, van de Ven C, Ayello J, Cairo D, Simpson LL, Baxi L, et al. Interleukin (IL)-15 in combination with IL-2, fms-like tyrosinekinase-3 ligand and anti-CD3 signifi cantly enhances umbilical cord blood natural killer (NK) cell and NK-cell subset expansion and NK function. *Cytotherapy*. (2011) 13:730–8. doi: 10.3109/14653249.2011.563292
20. Hui W, Rowan AD, Richards CD, Cawston TE. Oncostatin M in combination with tumor necrosis factor alpha induces cartilage damage and matrix metalloproteinase expression *in vitro* and *in vivo*. *Arthritis Rheum*. (2003) 48:3404–18. doi: 10.1002/art.11333
21. Sondergaard BC, Henriksen K, Wulf H, Oestergaard S, Schurigt U, Bräuer R, et al. Relative contribution of matrix metalloprotease and cysteine protease activities to cytokine-stimulated articular cartilage degradation. *Osteoarthr Cartil*. (2006) 14:738–48. doi: 10.1016/j.joca.2006.01.016
22. Hoemann CD. Molecular and biochemical assays of cartilage components. *Methods Mol Med*. (2004) 101:127–56. doi: 10.1385/1-59259-821-8:127
23. Sandy JD, Verscharen C. Analysis of aggrecan in human knee cartilage and synovial fluid indicates that aggrecanase (ADAMTS) activity is responsible for the catabolic turnover and loss of whole aggrecan whereas other protease activity is required for C-terminal processing *in vivo*. *Biochemical J*. (2001) 358:615–26. doi: 10.1042/bj3580615
24. Valdes AM, de Wilde G, Doherty SA, Lories RJ, Vaughn FL, Laslett LL, et al. The Ile585Val TRPV1 variant is involved in risk of painful knee osteoarthritis. *Ann Rheum Dis*. (2011) 70:1556–61. doi: 10.1136/ard.2010.148122
25. Freynhagen R, Baron R, Gockel U, Tölle TR. painDETECT: a new screening questionnaire to identify neuropathic components in patients with back pain. *Curr Med Res Opin*. (2006) 22:1911–20. doi: 10.1185/030079906X132488
26. Zeggini E, Panoutsopoulou K, Southam L, Rayner NW, et al. Identification of new susceptibility loci for osteoarthritis (arcOGEN): a genome-wide association study. *Lancet*. (2012) 680:815–23. doi: 10.1016/S0140-6736(12)60681-3
27. Tchetverikov I, Lohmander LS, Verzijl N, Huizinga TW, TeKoppele JM, Hanemaaijer R, et al. MMP protein and activity levels in synovial fluid from patients with joint injury, inflammatory arthritis, and osteoarthritis. *Ann Rheum Dis*. (2005) 64:694–8. doi: 10.1136/ard.2004.022434
28. Gupta U, Hira SK, Singh R, Paladhi A, Srivastava P, Pratim Manna P. Essential role of TNF-α in gamma c cytokine aided crosstalk between dendritic cells and natural killer cells in experimental murine lymphoma. *Int Immunopharmacol*. (2020) 78:106031. doi: 10.1016/j.intimp.2019.106031
29. Struglics A, Larsson S, Pratta MA, Kumar S, Lark MW, Lohmander LS. Human osteoarthritis synovial fluid and joint cartilage contain both aggrecanase-and matrix metalloproteinase-generated aggrecan fragments. *Osteoarthr Cartil*. (2006) 14:101–13. doi: 10.1016/j.joca.2005.07.018
30. Miller RE, Lu Y, Tortorella MD, Malfait AM. Genetically engineered mouse models reveal the importance of proteases as osteoarthritis drug targets. *Curr Rheumatol Rep*. (2013) 15:350. doi: 10.1007/s11926-013-0350-2
31. Lohmander LS, Brandt KD, Mazzuca SA, Katz BP, Larsson S, Struglics A, et al. Use of the plasma stromelysin (matrix metalloproteinase 3) concentration to

predict joint space narrowing in knee osteoarthritis. *Arthritis Rheum*. (2005) 52:3160–7. doi: 10.1002/art.21345
32. Struglics A, Hansson M. MMP proteolysis of the human extracellular matrix protein aggrecan is mainly a process of normal turnover. *Biochemical J*. (2012) 446:213–23. doi: 10.1042/BJ20120274
33. Fosang AJ, Neame PJ, Hardingham TE, Murphy G, Hamilton JA. Cleavage of cartilage proteoglycan between G1 and G2 domains by stromelysins. *J Biol Chem*. (1991) 266:15579–82.
34. Lees S, Golub SB, Last K, Zeng W, Jackson DC, Sutton P, et al. Bioactivity in an aggrecan 32-mer fragment is mediated via toll-like receptor 2. *Arthritis Rheumatol*. (2015) 67:1240–9. doi: 10.1002/art.39063
35. Miller RE, Ishihara S, Tran PB, Golub SB, Last K, Miller RJ, et al. An aggrecan fragment drives osteoarthritis pain through Toll-like receptor 2. *JCI Insight*. (2018) 3:95704. doi: 10.1172/jci.insight.95704
36. Driscoll C, Chanalaris A, Knights C, Ismail H, Sacitharan PK, Gentry C, et al. Nociceptive sensitizers are regulated in damaged joint tissues, including articular cartilage, when osteoarthritic mice display pain behavior. *Arthritis Rheumatol*. (2016) 68:857–67. doi: 10.1002/art.39523
37. Verri WA, Cunha TM, Parada CA, Wei XQ, Ferreira SH, Liew FY, et al. IL-15 mediates immune inflammatory hypernociception by triggering a sequential release of IFN-gamma, endothelin, and prostaglandin. *Proc Natl Acad Sci USA*. (2006) 103:9721–5. doi: 10.1073/pnas.06032 86103
38. Cata JP, Weng HR, Dougherty PM. Spinal injection of IL-2 or IL-15 alters mechanical and thermal withdrawal thresholds in rats. *Neurosci Lett*. (2008) 437:45–9. doi: 10.1016/j.neulet.2008.03.074
39. Austin PJ, Moalem-Taylor G. The neuro-immune balance in neuropathic pain: involvement of inflammatory immune cells, immune-like glial cells and cytokines. *J Neuroimmunol*. (2010) 229:26–50. doi: 10.1016/j.jneuroim.2010.08.013
40. Hochman JR, Gagliese L, Davis AM, Hawker GA. Neuropathic pain symptoms in a community knee OA cohort. *Osteoarthr Cartil*. (2011) 19:647–54. doi: 10.1016/j.joca.2011.03.007
41. Valdes AM, Suokas AK, Doherty SA, Jenkins W, Doherty M. History of knee surgery is associated with higher prevalence of neuropathic pain-like symptoms in patients with severe osteoarthritis of the knee. *Semin Arthritis Rheum*. (2013) 45:588–92. doi: 10.1016/j.semarthrit.2013.10.001
42. Tao Y, Qiu X, Xu C, Sun B, Shi C. Expression and correlation of matrix metalloproteinase-7 and interleukin-15 in human osteoarthritis. *Int J Clin Exp Pathol*. (2015) 8:9112–8.
43. Xq W, Orchardson M, Gracie JA, Leung BP, Bm G, Guan H, et al. The sushi domain of soluble IL-15 receptor α is essential for binding IL-15 and inhibiting inflammatory and allogenic responses *in vitro* and *in vivo*. *J Immunol*. (2001) 167:277–82. doi: 10.4049/jimmunol.167.1.277
44. Ruchatz H, Leung BP, Wei XQ, McInnes IB, Liew FY. Soluble IL-15 receptor α-chain administration prevents murine collagen-induced arthritis: a role for IL-15 in development of antigen-induced immunopathology. *J Immunol*. (1998) 160:5654–60.

Conflict of Interest: The authors declare that the research was conducted in the absence of any commercial or financial relationships that could be construed as a potential conflict of interest.

Copyright © 2020 Warner, Nair, Marpadga, Chubinskaya, Doherty, Valdes and Scanzello. This is an open-access article distributed under the terms of the Creative Commons Attribution License (CC BY). The use, distribution or reproduction in other forums is permitted, provided the original author(s) and the copyright owner(s) are credited and that the original publication in this journal is cited, in accordance with accepted academic practice. No use, distribution or reproduction is permitted which does not comply with these terms.

frontiers in Immunology

REVIEW
published: 02 September 2020
doi: 10.3389/fimmu.2020.01737

Microtopography of Immune Cells in Osteoporosis and Bone Lesions by Endocrine Disruptors

Roberto Toni[1,2,3,4], Giusy Di Conza[1], Fulvio Barbaro[1], Nicoletta Zini[5,6], Elia Consolini[1], Davide Dallatana[1], Manuela Antoniel[1,6], Enrico Quarantini[2], Marco Quarantini[2], Sara Maioli[1], Celeste Angela Bruni[1], Lisa Elviri[7], Silvia Panseri[8], Simone Sprio[8], Monica Sandri[8] and Anna Tampieri[8]*

[1] *Laboratory of Regenerative Morphology and Bioartificial Structures (Re.Mo.Bio.S.), Department of Medicine and Surgery - DIMEC, Unit of Biomedical, Biotechnological and Translational Sciences (S.BI.BI.T.), Museum and Historical Library of Biomedicine - BIOMED, University of Parma, Parma, Italy,* [2] *OSTEONET-CMG Unit (Osteoporosis, Nutrition, Endocrinology, and Innovative Therapies) at the Medical Center Galliera (CMG), San Venanzio, Italy,* [3] *Interdepartment Center for Law, Economics, and Medicine of Sport, University of Parma, Parma, Italy,* [4] *Division of Endocrinology, Diabetes, and Metabolism, Department of Medicine, Tufts Medical Center, Tufts University School of Medicine, Boston, MA, United States,* [5] *CNR-National Research Council of Italy, Institute of Molecular Genetics "Luigi Luca Cavalli-Sforza" - Unit of Bologna, Bologna, Italy,* [6] *IRCCS Istituto Ortopedico Rizzoli, Bologna, Italy,* [7] *Food and Drug Department, University of Parma, Parma, Italy,* [8] *ISTEC - CNR, Faenza, Italy*

OPEN ACCESS

Edited by:
Daniela Frasca, University of Miami, United States

Reviewed by:
Ivan Martin, University of Basel, Switzerland
Danka Grcevic, University of Zagreb School of Medicine, Croatia

***Correspondence:**
Roberto Toni
roberto.toni@unipr.it;
roberto.toni@unibo.it;
roberto.toni@tufts.edu

Specialty section:
This article was submitted to Autoimmune and Autoinflammatory Disorders, a section of the journal Frontiers in Immunology

Received: *25 March 2020*
Accepted: *29 June 2020*
Published: *02 September 2020*

Citation:
Toni R, Di Conza G, Barbaro F, Zini N, Consolini E, Dallatana D, Antoniel M, Quarantini E, Quarantini M, Maioli S, Bruni CA, Elviri L, Panseri S, Sprio S, Sandri M and Tampieri A (2020) Microtopography of Immune Cells in Osteoporosis and Bone Lesions by Endocrine Disruptors. Front. Immunol. 11:1737. doi: 10.3389/fimmu.2020.01737

Osteoporosis stems from an unbalance between bone mineral resorption and deposition. Among the numerous cellular players responsible for this unbalance bone marrow (BM) monocytes/macrophages, mast cells, T and B lymphocytes, and dendritic cells play a key role in regulating osteoclasts, osteoblasts, and their progenitor cells through interactions occurring in the context of the different bone compartments (cancellous and cortical). Therefore, the microtopography of immune cells inside trabecular and compact bone is expected to play a relevant role in setting initial sites of osteoporotic lesion. Indeed, in physiological conditions, each immune cell type preferentially occupies either endosteal, subendosteal, central, and/or perisinusoidal regions of the BM. However, in the presence of an activation, immune cells recirculate throughout these different microanatomical areas giving rise to a specific distribution. As a result, the trabeculae of the cancellous bone and endosteal free edge of the diaphyseal case emerge as the primary anatomical targets of their osteoporotic action. Immune cells may also transit from the BM to the depth of the compact bone, thanks to the efferent venous capillaries coursing in the Haversian and Volkmann canals. Consistently, the innermost parts of the osteons and the periosteum are later involved by their immunomodulatory action, becoming another site of mineral reabsorption in the course of an osteoporotic insult. The novelty of our updating is to highlight the microtopography of bone immune cells in the cancellous and cortical compartments in relation to the most consistent data on their action in bone remodeling, to offer a mechanist perspective useful to dissect their role in the osteoporotic process, including bone damage derived from the immunomodulatory effects of endocrine disrupting chemicals.

Keywords: osteoporosis, organoid, immunomodulation, bone remodeling, endocrine disrupting chemical, immunobiology

INTRODUCTION

Osteoporosis is a worldwide public health problem, primarily as a result of increasing survival in aging (1), involves an estimated 200 million people worldwide (2), and has a global economic impact estimated up to more than 20 billion euros per year during the next 5 years on the health care systems of Western countries (3). By definition, osteoporosis is a systemic skeletal disease characterized by decreasing bone mass and microarchitectural deterioration of bone tissue that leads to an increased risk of bone fragility and fracture (4). Osteoporotic changes worsen in postmenopausal females and can variably affect any bone, but more frequently the femoral neck, vertebrae, and distal radius where unique patterns of bone derangement emerge. This lesional microtopography is now gaining particular interest in bones traditionally considered less affected by osteoporosis such as the jaw (**Figures 1A,B**) because of the increased request of prosthetic implants (5) and as a unique site for chronic inflammation and aseptic osteonecrosis during antiresorptive therapy (6).

Different cellular and molecular mechanisms may lead to osteoporosis: however, the low-grade systemic inflammation associated with aging is emerging as a critical stimulus for diffuse bone loss and reduced bone regenerative potential. At the same time, it highlights the role of the immune cells to favor resorption and reduce deposition of mineral mass, as well as to hamper the action of bone progenitors (7). Immune cells residing in the bone may contribute to development of both primary (postmenopausal, senile) and secondary (autoimmune, infective, vascular, neurological, endocrine, and multiorgan failure) osteoporosis acting on the progenitors of osteoblasts (OBs) and osteoclasts (OCs) (8). Finally, beyond pharmacological treatments well-known to interfere with OBs and OCs, endocrine-disrupting chemicals (EDs) may affect the activity of the immune cells in bone, leading to bone weakness (9).

To shed light on the interplay between immune and other bone cells in early osteoporotic changes to the cancellous and/or cortical bone, we here analyze the selective segregation of immune cells in different bone compartments in basal and activated states. We also discuss this microtopography in relation to the best established views on the effect of immune cells in bone remodeling, both in physiological conditions and upon an either inflammatory or toxic trigger. Collectively, we offer a mechanistic and space-related perspective of the action of immune cells involved in the osteoporotic process.

MICROTOPOGRAPHY OF IMMUNE CELLS IN BONE COMPARTMENTS

Osteoporotic lesions exhibit a well-defined pattern in the different bone compartments, the topography of which is time-dependent: (1) resorption of cancellous trabeculae in the epiphysis of long bones, vertebrae, other short and flat bones, cranial diploe; (2) subendosteal and, later, subperiosteal resorption of the cortical lamellae, primarily in long bones; (3) intracortical resorption with thinning of the entire compact tissue, primarily in long bones (10). It is therefore clear that peculiar microanatomical conditions selectively expose specific bone sites to the osteoporotic damage following a temporal progression. The microtopography of the immune cells in the bone compartments reveals that their original location and triggered recirculation are consistent with the microanatomical specificities of the osteoporotic damage as described above.

Monocytes, Osteal Macrophages or Osteomacs, and Mast Cells

In the cancellous compartment of the epiphyses of long bones, and of flat and short bones, monocytes, and osteal macrophages or osteomacs (OMCs) are part of the mononuclear cells of the bone marrow (BM). Upon activation, monocytes migrate from the central to the perisinusoidal BM to enter the vascular sinuses and the venous capillaries *en route* to the cortical bone through the Haversian and Volkmann canals, up to the general circulation (11). This transfer pathway is supported by evidence that synthesis of interleukin 17 (IL-17) is increased both in BM cells and peripheral blood mononuclear cells during postmenopausal osteoporosis (12), suggesting a common BM source for both cell types.

In contrast, activated OMCs including proinflammatory M1 and anti-inflammatory M2 (13) may migrate from centers of erythropoiesis in the erythroblastic islands coincidental with the reticular niches of the central and perisinusoidal BM (14, 15) to the endosteal and subendosteal BM (i.e., tissue adjacent to main bulk of BM), to support myelopoiesis from hemopoietic stem cells (HSCs) and uncommitted progenitors (16). Therefore, an inflammatory trigger pushes monocytes and OMCs toward opposite directions inside the BM. Parts of the OMCs are present also in the connective periosteal layer of the compact bone (17). In this location, they are in a position to favor the shuttling of interstitial fluids from the extracellular matrix (ECM) of compact lamellae inside the periosteal lymphatics (18), thus preventing the detrimental mechanical effect of ECM fluid overloading on the cortical mineral mass (19).

Finally, mast cells are concentrated in the hematopoietic niche of the metaphyseal perisinusoidal BM, with some residing as flattened cells on the epiphyseal and diaphyseal endocortical surface. In osteoporotic bones, mast cells are found in close proximity to OCs, suggesting their massive migration to the endosteal BM (20).

T and B Lymphocytes and Dendritic Cells

T and B lymphocytes variably account for up to 20% of BM mononuclear cells (21, 22). In the spongy bone, the majority of T lymphocytes are distributed: (A) throughout the reticular argyrophilic stroma, contributed by the ramified processes of the adventitial reticular cells (so-called CAR cells in the mouse) enwrapping the vascular sinusoids in the perisinusoidal BM (23), and (B) in the hemopoietic parenchyma, condensed in lymphoid follicle-like structures (24) in the central BM (25). However, 1/3 T cells are $CD4^+$ $CD25^+$ regulatory T (Treg) lymphocytes

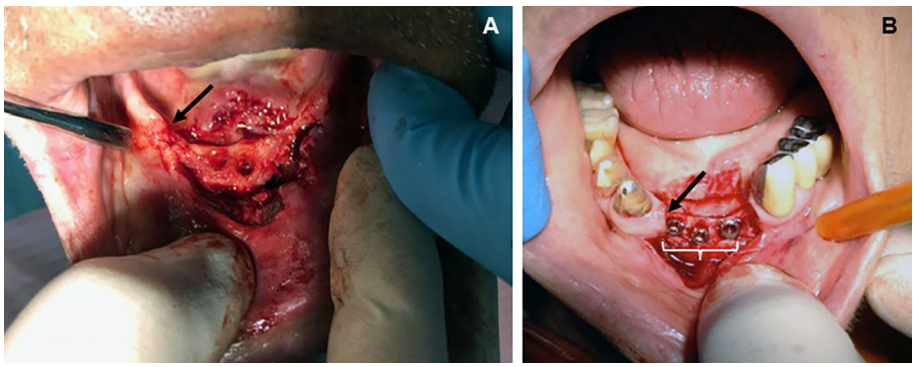

FIGURE 1 | Topographic distribution of bone lesions in the human jaw following classical osteoporotic processes (chronic bacterial inflammation and menopause). **(A)** Edentulous patient (male, age 74 years) showing osteoporotic vertical resorption (arrow) of the maxilla during severe periodontitis. Surgical displacement of the gum flap revealed consistent porosity of the vast majority of the exposed bone, including complete loss of the cortical bone but more limited destruction of the cancellous trabeculae; **(B)** loss of central and lateral, inferior incisors in a patient (female, age 74 years) with vertical resorption (arrow) of the jaw as a consequence of severe postmenopausal osteoporosis. Note the presence of bone implants (white bracket) becoming visible after exposing the resorbed bone through a gum flap. Osteoporosis led to a decreased rate of cancellous bone formation in both the implanted socket and interdental bone, thus increasing risk of trabecular microfractures and prosthetic instability (from the Odontostomatological Archive of CMG, San Venanzio di Galliera, BO, Italy, with permission).

that reside in both the perisinusoidal and endosteal BM (26). When T cells get activated, they are generally found condensed in the endosteal and subendosteal BM (also known as HSC area) to interact with endothelial capillary cells and sinusoid-derived pericytes (16).

Differently, both differentiation and activation of B cells seem to be constrained within the reticular niches of the central and perisinusoidal BM, as suggested by their obligatory interaction with IL-7–secreting cells selectively diffused to the same BM compartments (16, 27).

Finally dendritic cells are spread inside all four BM compartments, in perivascular locations including arterioles and venous sinuses, and in close contact to both endothelial and adventitial reticular cells (28).

KEY POINTS ON IMMUNOBIOLOGY OF BONE REMODELING RELEVANT TO THE MICROTOPOGRAPHY OF IMMUNE CELLS IN BONE COMPARTMENTS

In physiological conditions, all aforementioned immune cells contribute to bone growth and mineralization. However, in the vast majority of osteoporotic forms (primary and secondary), the immune cells induce overactivation of OCs coupled with a reduction in OB activity.

OMCs and Mast Cells

The OMCs mediate the transition between innate and adaptive immune responses. They have been found to be associated mainly with endosteal and, to a lesser extent, periosteal surfaces where they regulate maturation, function, and survival of OBs, collectively ensuring bone development, homeostasis, and repair (17, 29). Specifically, anti-inflammatory OMCs or M2 favor mineral deposition through formation of a canopy over mature matrix-producing OBs at sites of bone remodeling, and inhibit osteoclastogenesis through the action of IL-4 and IL-10 (30, 31). Differently, in a bone microenvironment characterized by chronic inflammation, proinflammatory OMCs or M1 stay close to endosteal OCs, and both cells respond to the lineage-specific growth factor macrophage colony-stimulating factor (CSF) released by mesenchymal stromal cells (MSCs) and OBs. As a result, OMCs secrete IL-1β, IL-6, and tumor necrosis factor (TNF) α catalizing differentiation of pre-OCs to functionally competent OCs, thus inducing bone resorption (30–32). A further level of OCs activation by M1 is provided through release of extracellular microvesicles containing histones (13). It is therefore expected that primary sites of lesion ensuing from action of OMCs are the trabecular subendosteal bone and internal free edge of the lamellae in the cortical case, only later involving the periosteal surface. Similarly, activated mast cells promote osteoclastogenesis by releasing histamine, TNF-α, and IL-6, and inhibit osteoblastogenesis primarily through secretion of IL-1 (20). Thus, it is expected that they initially induce resorption of the metaphyseal endosteum, only later involving the internal free edge of the cortical bone in both epiphysis and diaphysis.

T Cells

T cells represent a major player in the adaptive responses of bone to pathogens, accounting for the majority of resident lymphocytes. Upon activation, T cells strongly promote pre-OCs differentiation by secreting TNF-α and RANKL; consequently, they are involved in many forms of osteoporosis (33, 34). This action is boosted by TNF-α, IL-1, IL-17, and IL-18 secreted by surrounding cells (OMCs, OBs), which lead to upregulation of RANKL expression by T cells (7, 35). Then, T cell–dependent secretion of interferon γ (IFN-γ) enhances

formation of OCs and bone resorption, further favoring T cell–dependent cosecretion of TNF-α and RANKL under estrogen deficiency and infection (36). This explains the occurrence of osteoporosis in conjunction with chronic inflammatory disorders such as periodontitis in the postmenopausal female (37).

Among the various T-cell subpopulations, T helper 17 (T_H17) lymphocytes secrete IL-17 able to induce RANKL expression by OBs and synovial fibroblast, and TNF-α and IL-1 by synovial macrophages, promoting OC formation (38). In addition, IL-17 secreted by peripheral blood mononuclear cells directly stimulates human osteoclastogenesis, favoring formation of actin rings in mature OCs (39). Finally, T_H17 lymphocytes are downregulated by estrogens; thus, menopausal estrogen deficiency promotes local upregulation of T_H17 (40). Consistently, the number of T_H17 cells and levels of IL-17 in peripheral blood are increased in postmenopausal osteoporosis (12). Differentiation and expansion of T_H17 cells are also favored by a number of resident cells including (1) OBs, OMCs, and stromal cells of the osteogenic layer of the periosteum and endosteum, through local secretion of IL-1 and IL-6; (2) OBs and OCs via release of transforming growth factor α and bone morphogenetic proteins, the latter partly available in the bone ECM as latent stored proteins [so-called "crinopexic" molecules, a term originally proposed by the Nobel Laureate Roger Guillemin, see (41)]; (3) BM dendritic cells and OMCs by means of IL-23 (42, 43).

In contrast to a resorptive action, T cells may also exert an inhibitory regulation of osteoclastogenesis through the CD137–CD137L complex. Indeed, CD137 is a costimulatory member of the TNF receptor family induced by T-cell receptor activation on T cells, whereas CD137L is its ligand expressed on BM dendritic cells and OCs precursors. *In vitro*, the CD137–CD137L complex suppresses OCs activation by inhibiting the multinucleation process (44). Similar, T cell–dependent release of IFN-γ may *in vitro* block RANKL signaling and suppress OC formation (36). Finally, the anti-inflammatory subpopulation of Treg cells (45) may inhibit OC differentiation via intercellular contacts mediated by cytotoxic T-lymphocyte-associated protein 4 and release of IL-4 and IL-10 (46). For this reason, their stimulation ameliorates osteolytic bone destruction (24). Collectively, mice lacking T cells have osteoporotic bones, suggesting a contribution of T lymphocytes in maintaining bone homeostasis during basal physiology (47).

In summary, upon T-cell activation, primary expected sites of lesion are the subendosteal cancellous bone and the internal free edge of the cortical bone. However, thanks to their spread through veins efferent from the BM to the Haversian and Volkmann canals, T cells can then reach the inner part of osteons; here, pathological cortical porosity occurs as a result of local resorption, collapse and fusion of adjacent Haversian canals, and disappearance of osteocyte lacunae (10, 48). Only later, activated T lymphocytes may also trigger reabsorption of subperiosteal compact bone.

B Cells

B lymphocytes are a primary constituent of the hematopoietic niche of the BM (49), where recruitment and maturation of B-cell progenitors are controlled by adventitial reticular cells (positioned to enwrap the BM sinusoids) through release of CXCL12 (CXC chemokine ligand 12 or stromal cell–derived factor 1) (23, 47, 50). During an inflammatory state, B cells remaining attached to the central BM region may act as a source of RANKL to cause endosteal OC activation and bone resorption (51); equally, in postmenopausal osteoporotic patients, they release granulocyte-macrophage CSF to promote differentiation of OCs precursors (52).

In contrast, in physiological conditions the entire B lineage including multiple subsets of B-cell precursors, immature B cells, and plasma cells may act as inhibitory regulators of the RANK/RANKL system (53) by producing 64% of total BM osteoprotegerin (OPG). Thus, B cells basically favor synthesis of bone matrix and mineral deposition (47) that, conversely, are inhibited in the B cell–knockout mice resulting deficient in BM OPG and hence osteoporotic (51).

In conclusion, osteoporotic recruitment of B cells may lead to a double phase of catabolic and anabolic action in the bone: an initial resorption of the entire thickness of the cancellous lamellae followed by compensatory bone deposition, as reported to occur in the trabecular bone of the radius in postmenopausal osteoporosis (54).

Dendritic Cells

Dendritic cells are professional antigen-presenting cells that in the BM are better known as type 2 conventional dendritic cells (cDC2). They regulate memory of local T cells, promote survival of recirculating mature B cells, and by interacting with endothelial and adventitial reticular cells mobilize HSC, uncommitted progenitors, and OMCs in the hemopoietic niche (28). From the point of view of a local information system, they look like a multiplexer able to select numerous inputs toward a single output (either a prevalent immune or osteoregulatory response). Indeed, similarly to activated T cells, they may release RANKL to elicit osteoclastogenesis and bone resorption in response to an inflammatory osteoporotic insult (7); in contrast, similarly to B lymphocytes, cDC2 may participate in the regulation of physiological bone remodeling by secreting the RANKL decoy receptor OPG (53) and thus inhibit activation of OCs. As a result, during an osteoporotic trigger, cDC2 may act as a "buffer system" to counterbalance the prevailing osteocatabolic effects of each immune cell type toward an osteoanabolic one.

ROLE OF EDs AS INDUCERS OF OSTEOPOROSIS VIA IMMUNOMODULATION

Endocrine-disrupting chemicals are substances with an endocrine mode of action that adversely interfere with the activity of the endocrine system (55). Among the numerous ones contaminating our everyday environment, some have

been proved to interfere with bone remodeling leading to osteoporotic lesions including phthalates (present in plastics and cosmetics), alkylphenol ethoxylates or APE (added to detergents, additives for fuels and lubricants, perfume fragrances, chemical oils, and flame retardants), perfluoroalkyls (PFAs) (used in the industry of cookware, clothes, carpets, electronics, mechanics), bisphenol A or BPA (present in plastics, food containers, and materials for dental medicine), diethylstilbestrol (DES) (a synthetic estrogen considered in the treatment of selected prostate cancer cases), organotin compounds (used as industrial antifungal agents in textiles, agricultural fungicides, wood preservatives, and antibiofouling agents), and dioxin/dioxin-like compounds (primarily detected in pesticides, waste incineration, and different processes of combustion and paper fabrication) having high affinity for fat stores in animals and humans (9).

Among the few EDs studied for immunomodulatory activity, di(2-ethylhexyl)phthalate or DEHP and its metabolite mono(2-ethylhexyl)phthalate or MEHP act in the BM to inhibit proliferation and induce apoptosis of developing B lymphocytes while suppressing osteogenic MSC commitment in favor of adipogenesis (56, 57). Because increase in BM adipocytes elicits osteoclastogenesis through release of RANKL (58) and inhibits osteoblastogenesis via saturated fatty acids (59), a reduced number of B-cell precursors might contribute to an enhanced osteoclastogenesis reducing the available BM OPG (51, 53). A similar mechanism of bone loss is expected also with the organotin compound, tributyltin, which variably compromises

TABLE 1 | Effects of EDs on cells in bone compartments.

	OC	OB	HSC	MSC	BMC	BL
PFAs	Abnormal stimulation decreased viability	Increased differentiation decreased viability				
PFOS			Immunotoxicity, reduced differentiation	Immunotoxicity, reduced commitment		
BPA	Increased osteoclastogenesis	Suppressed function and activity		Metabolic alterations, enhanced proliferation, decreased reneval capacity, augmented adipogenic differentiation, alteration of the transcriptomic profile		
APE	Inhibited formation and differentiation	Reduced synthesis of osteocalcin and ALP				
DEHP		Decreased ALP		Decreased Runx2 expression		
MEHP				Suppressed osteogenic commitment, increased lipid accumulation		Inhibited proliferation and induced apoptosis
BBP		Mutagenesis	Reduced haematopoiesis		Reduced cellularity	
DBP		Mutagenesis				
DES	Decreased number and activity					
TBT		Suppressed expression of ALP and osteocalcin, inhibited calcium signaling, and deposition	Suppressed proliferation	Decreased osteogenic capacity, augmented adipogenic differentiation		Reduced progression from pro-B to pre-B
TPhT					Suppressed osteogenic lineage, increased proadipogenic markers	
TCDD	Reduced osteoclastogenesis	Suppressed maturation, reduced ALP and osteocalcin synthesis, reduced osteoblastogenesis	Decreased ability to complete normal differentiation, reduced BM retention and chemotaxis	Reduced Runx2 expression		
PCB	Reduced osteoclastogenesis	Reduced osteoblastogenesis	Reduced BM retention and chemotaxis			
BαP	Decreased activity	Abnormal proliferation				

B Ly, B lymphocytes; BMC, bone marrow cells; HSC, hematopoietic stem cells; MSC, mesenchymal stromal cells; OB, osteoblasts; OC, osteoclasts; ALP, alkaline phosphatase; APEs, alkylphenol ethoxylates; BαP, benzo[α]pyrene; BBP, benzyl-butyl-phthalate; BM, bone marrow; BPA, 4,4′-isopropylidenediphenol; DBP, di-n-butyl phthalate; DEHP, di(2-ethylhexyl)phthalate; DES, diethylstilbestrol; MEPH, mono(2-ethylhexyl)phthalate; PCB, polychlorinated biphenyls; PFAs, perfluoroalkyls; PFOS, perfluorooctane sulfonic acid; RunX2, Runt-related transcription factor 2; TBT, tributyltin; TCDD, 2,3,7,8-tetrachlorodibenzo-p-dioxin; TPhT, triphenyltin.

the morphological and functional aspects of all BM niches, and suppresses the proliferation of hematopoietic cells leading to reduced progression of B lymphocytes from the early pro-B to the pre-B stage (60).

Differently, the phthalate ester benzyl butyl phthalate downregulates expression of the histone deacetylases, sirtuins 1 and 3 (61), able to epigenetically inhibit subsets of T lymphocyte (T_H1 and T_H17), activate others (Treg), and ensure B lymphocytes survival (62). Thus, it may lead to cancellous bone resorption by a combined hyperactivation of T inflammatory cells and reduced B-cell OPG (7, 12, 35, 36, 40, 46, 51).

In addition, synthetic xenoestrogens such as APE, BPA, and DES may all variably damage survival, maturation, and activation of all immune BM cells (63) via still unknown immunomodulatory effects potentially relevant to the osteoporotic lesions. Finally, the PFA perfluorooctane sulfonic acid exhibits immunotoxicity and impairs MSC commitment (64, 65), supposedly leading to bone loss by reduced control of the BM immune cells on bone anabolism. A similar mechanism is possibly at work also with 2,3,7,8-tetrachlorodibenzo-*p*-dioxin, which blocks the ability of HSC and progenitors to complete a normal differentiation cycle (66). **Table 1** summarizes known effects of these and other EDs on cells residing in different bone compartments [from (9, 56, 57, 60, 62, 64–66)], whereas **Table 2** provides a tentative integrated view of primary sites of early bone involvement during an inflammatory and/or ED-dependent bone insult based on location and osteomodulatory effects of BM immune cells.

CONCLUSIONS

A peculiar *in vivo* feature of the bone immune cells is their quite selective segregation in specific BM regions and areas of the cortical bone, both in steady state and upon an inflammatory or ED-dependent insult. In physiological conditions, this cellular distribution is aimed at ensuring functional niches for hematopoiesis and myelopoiesis (23, 50). However, immune cells also regulate bone effector cells (OCs, OBs, MSC), leading to osteocatabolic and osteoanabolic responses selectively bonded to cancellous and/or compact bone. Knowledge of these patterns of response allows for recognition of presumable sites of early bone lesion in the course of an osteoporotic process, and we have here provided a tentative reference sketch integrating the microtopography of immune cells with their osteoinductive and osteolytic effects in basal state and after osteoporotic challenges. Indeed, both primary generalized forms of osteoporosis (postmenopausal and senile) and a number of secondary osteoporotic forms have in common a state of local bone inflammation leading to bone resorption (7, 8). In contrast, EDs may induce either increased bone resorption or inhibition of bone deposition. Collectively, we introduce a space-dependent innovative view of bone remodeling by immune cells in line with the most recent perspectives on the complex spatial logic underling BM function (67). We believe this approach may help to understand how different osteoporotic lesions develop, thus prompting the design of experimental tools for *in vitro* modeling of early phases of the osteoporotic process and related innovative treatments (68).

TABLE 2 | Microtopography of immune cells in the different bone compartments in basal state and in relation to either an inflammatory or an EDs insult.

Immune cells	Bone sites of residence	Bone sites of relocation following inflammation	Putative sites of early bone loss by inflammation	EDs effect on immune cells	Putative sites of early bone damage by EDs immunomodulation
Monocytes/ macrophages	Reticular niche of central and perisinusoidal BM regions; periosteum	Endosteal and subendosteal BM regions	Subendosteal trabecular bone; internal free surface of cortical bone; periosteal bone	[APE, BPA, DES, PFOS, TCDD] –	Full thickness of trabecular bone; subperiosteal cortical bone
Mast cells	Metaphyseal perisinusoidal BM; endosteum of epiphyseal and diaphyseal case	Metaphyseal endosteal BM; endosteum of epiphyseal and diaphyseal case	Subendosteal metaphyseal bone; internal free edge of epiphyseal and diaphyseal compact bone	?	?
T lymphocytes	Follicle-like structures of central and perisinusoidal BM regions	Endosteal and subendosteal BM regions	Subendosteal *trabecular bone; internal free surface of cortical bone*; periosteal bone ?	BBP++ [APE, BPA, DES, PFOS, TCDD] –	See * full thickness of trabecular bone
B lymphocytes and plasma cells	Reticular niche of central and perisinusoidal BM regions	Reticular niche of central and perisinusoidal BM regions	Full thickness of trabecular bone (coupled to compensatory trabecular deposition)	[DHEP, MEHP] –; TBT –; BBP –; [APE, BPA, DES, PFOS, TCDD] –	full thickness of trabecular bone (without compensatory trabecular deposition)
Dendritic cells	All BM regions	all BM regions	In dependance on prevailing effects of other immune cells	[APE, BPA, DES, PFOS, TCDD] –	?

APE, alkylphenols ethoxylates; BPA, bisphenol A; BBP, benzyl butyl phthalate; DES, diethylstilbestrol; DHEP, di(2-ethylhexyl)phthalate; MEHP, mono(2-ethylhexyl)phthalate; PFOS, perfluorooctane sulfonic acid; TCDD, 2,3,7,8-tetrachlorodibenzo-p-dioxin; ++, immunostimulatory action; –, immunoinhibitory action; ?, unknown. Squared brackets collect EDs with the same immunomodulatory action.

AUTHOR'S NOTE

RT is under the tenure of the DIMEC - CMG Collaboration Agreement signed on June 27, 2018. Part of these studies have been presented at the National Continuing Medical Education (CME) Program *"Osteoporosi: novità e prospettive"* held at CMG on January 18, 2020. SM and CAB are in training pre-doctoral fellows from the Course of Medical, Veterinary, and Pharmaceutical Biotechnologies at the University of Parma, Parma, Italy.

AUTHOR CONTRIBUTIONS

GD, FB, NZ, EC, DD, EQ, and MQ collected and studied the international literature on the topics detailed in the manuscript, and developed clinical studies on jaw osteoporosis. MA, LE, SM, CAB, SP, SS, MS, and AT provided support to analyze the biotechnological relevance of the functional microtopographical pattern ensued from the data acquisition. RT conceived all the ideas and design presented in the text leading the research team involved, wrote, and critically reviewed the entire manuscript. All authors gave the final approval to the manuscript.

FUNDING

This work has been possibile through Grant FIL UNIPR 2018-2019. Part of the ideas and technologies developed in this work have provided support to the current development of the European Project Horizon 2020 SCREENED Grant #825745. The authors are also grateful to the Emilia-Romagna Fund Sisma Ripopolamento 2/2019 at the Medical Center Galliera (CMG) in San Venanzio di Galliera (BO), Italy for providing technological resources useful to the studies on senile and inflammatory osteoporosis of the jaw in human subjects. EC is a recipient of an International Mobility Fellowship 2017-2018 at the University of Basel, CH, as fellow of the PhD program in Molecular Medicine at UNIPR, and a 2019-2020 Feliciani-Ferretti/co-sponsored EU Grant Horizon 2020 #825745 Fellowship at DIMEC - UNIPR by the title "*A preclinical model of browning of the adipose tissue for an innovative therapy of obesity*", Parma, Italy. DD is a recipient of a MEPA technical research contract under the tenure of the EU Grant Horizon 2020 #825745.

REFERENCES

1. Johnell O, Kanis JA. An estimate of the worldwide prevalence and disability associated with osteoporotic fractures. *Osteoporos Int*. (2006) 17:1726–33. doi: 10.1007/s00198-006-0172-4
2. Kanis JA. *On behalf of the World Health Organization Scientific Group. Assessment of Osteoporosis at the Primary Health-Care Level. Technical Report*. University of Sheffield, UK: World Health organization collaborating centre for metabolic bone diseases. University of Sheffield. (2007).
3. *National osteoporosis foundation. What is osteoporosis and what causes it?* (2014). Available online at http://nof.org/articles/7 (accessed July 22, 2014)
4. Raisz LG. Pathogenesis of osteoporosis: concepts, conflicts, and prospects. *J Clin Invest*. (2005) 115:3318–25. doi: 10.1172/JCI 27071
5. Giro G, Chambrone L, Goldstein A, Rodrigues JA, Zenóbio E, Feres M, et al. Impact of osteoporosis in dental implants: a systematic review. *World J Orthop*. (2015) 6:311–5. doi: 10.5312/wjo.v6.i2.311
6. Fassio A, Bertoldo F, Idolazzi L, Viapiana O, Rossini M, Gatti D. Drug-induced osteonecrosis of the jaw: the state of the art. *Reumatismo*. (2017) 69:9–15. doi: 10.4081/reumatismo.2017.983
7. Pietschmann P, Mechtcheriakova D, Meshcheryakova A, Föger-Samwald U, Ellinger I. Immunology of osteoporosis: a mini-review. *Gerontology*. (2016) 62:128–37. doi: 10.1159/000431091
8. Pagliari D, Tamburrelli FC, Zirio G, Newton EE, Cianci R. The role of bone immunological niche for a new pathogenetic paradigm of osteoporosis. *Anal Cell Pathol*. (2015) 2015:434389. doi: 10.1155/2015/434389
9. Agas D, Lacava G, Sabbieti MG. Bone and bone marrow disruption by endocrine-active substances. *J Cell Physiol*. (2019) 234:192–213. doi: 10.1002/jcp.26837
10. Osterhoff G, Morgan Elise F, Shefelbine SJ, Karim L, McNamara LM, Augat P. Bone mechanical properties and changes with osteoporosis. *Injury*. (2016) 47:116–20. doi: 10.1016/S0020-1383(16)47003-8
11. Sugiyama T, Nagasawa T. Bone marrow niches for hematopoietic stem cells and immune cells. *Inflamm Allergy Drug Targets*. (2012) 11:201–6. doi: 10.2174/187152812800392689
12. Zhang J, Fu Q, Ren Z, Wang Y, Wang C, Shen T, et al. Changes of serum cytokines-related Th1/Th2/Th17 concentration in patients with postmenopausal osteoporosis. *Gynecol Endocrinol*. (2015) 31:183–90. doi: 10.3109/09513590.2014.975683
13. Pieters BCH, Cappariello A, van den Bosch MHJ, van Lent PLEM, Teti A, van de Loo FAJ. Macrophage-derived extracellular vesicles as carriers of alarmins and their potential involvement in bone homeostasis. *Front Immunol*. (2019) 10:1901. doi: 10.3389/fimmu.2019.01901
14. Romaniuk A, Lyndina Y, Sikora V, Lyndin M, Karpenko L, Gladchenko O, et al. Structural features of bone marrow. *Interv Med Appl Sci*. (2016) 8:121–6. doi: 10.1556/1646.8.2016.3.3
15. Sugiyama T, Omatsu Y, Nagasawa T. Niches for hematopoietic stem cells and immune cell progenitors. *Int Immunol*. (2018) 31:5–11. doi: 10.1093/intimm/dxy058
16. Bonomo A, Monteiro Ana C, Gonçalves-Silva T, Cordeiro-Spinetti E, Gonçalves Galvani R, Balduino A. A T cell view of the bone marrow. *Front Immunol*. (2016) 7:184. doi: 10.3389/fimmu.2016.00184
17. Pettit AR, Chang MK, Hume DA, Raggatt LJ. Osteal macrophages: a new twist on coupling during bone dynamics. *Bone*. (2008) 43:976–82. doi: 10.1016/j.bone.2008.08.128
18. Edwards JR, Williams K, Kindblom LG, Meis-Kindblom JM, Hogendoorn Pancras CW, Hughes D, et al. Lymphatics and bone. *Hum Pathol*. (2008) 39:49–55. doi: 10.1016/j.humpath.2007.04.022
19. Pierce CS, Madhavan G, McLeod KJ. Emerging approaches in the prevention of osteoporosis. In: Gueldner SH, Grabo TN, Newman ED, Cooper DR editors. *Osteoporosis, Clinical guidelines for prevention, diagnosis and management*. New York, NY: Springer Publishing Company, LLC (2008) ch.15. p. 219–29.
20. Ragipoglu D, Dudeck A, Haffner-Luntzer M, Voss M, Kroner J, Ignatius A, et al. The role of mast cells in bone metabolism and bone disorders. *Front Immunol*. (2020) 11:163. doi: 10.3389/fimmu.2020.00163
21. Schirrmacher V, Feuerer M, Fournier P, Ahlert T, Umansky V, Beckhove P. T-cell priming in bone marrow: the potential for long-lasting protective anti-tumor immunity. *Trends Mol Med*. (2003) 9:526–34. doi: 10.1016/j.molmed.2003.10.001
22. Fauci AS. Human bone marrow lymphocytes. I. distribution of lymphocyte subpopulations in the bone marrow of normal individuals. *J Clin Invest*. (1975) 56:98–110. doi: 10.1172/JCI108085
23. Bianco P, Sacchetti B, Riminucci M. Osteoprogenitors and the hematopoietic microenvironment. *Best Pract Res Clin Haematol*. (2011) 24:37–47. doi: 10.1016/j.beha.2011.01.005

24. Zhao E, Huanbin Xu, Wang L, Kryczek I, Wu K, Hu Y, et al. Bone marrow and the control of immunity. *Cell Mol Immunol.* (2012) 9:11–9. doi: 10.1038/cmi.2011.47
25. Cordeiro-Spinetti E, Taichman Russell S, Balduino A. The bone marrow endosteal niche: how far from the surface? *J Cell Biochem.* (2015) 116:6–11. doi: 10.1002/jcb.24952
26. Zou L, Barnett B, Safah H, Larussa VF, Evdemon-Hogan M, Mottram P. Bone marrow is a reservoir for CD41CD251 regulatory T cells that traffic through CXCL12/CXCR4 signals. *Cancer Res.* (2004) 64:8451–5. doi: 10.1158/0008-5472.CAN-04-1987
27. Tokoyoda K, Egawa T, Sugiyama T, Choi B, Nagasawa T. Cellular niches controlling B lymphocyte behavior within bone marrow during development. *Immunity*. (2004) 20:707–18. doi: 10.1016/j.immuni.2004.05.001
28. Zhang J, Trinkaus K, Link DC. Bone marrow dendritic cells regulate hematopoietic stem/progenitor cell trafficking. *J Clin Invest.* (2019) 129:2920–31. doi: 10.1172/JCI124829
29. Hume DA. Differentiation and heterogeneity in the mononuclear phagocyte system. *Mucosal Immunol.* (2008) 1:432–41. doi: 10.1038/mi.2008.36
30. Takayanagi H. Osteoimmunology: shared mechanisms and crosstalk between the immune and bone systems. *Nat Rev Immunol.* (2007) 7:292. doi: 10.1038/nri2062
31. Nakashima T, Hayashi M, Takayanagi H. New insights into osteoclastogenic signaling mechanisms. *Trends Endocrinol Metab.* (2012) 23:582–90. doi: 10.1016/j.tem.2012.05.005
32. Chang MK, Raggatt LJ, Alexander KA, Kuliwaba JS, Fazzalari NL, Schroder K, et al. Osteal tissue macrophages are intercalated throughout human and mouse bone lining tissues and regulate osteoblast function *in vitro* and *in vivo*. *J Immunol.* (2008) 181:1232–44. doi: 10.4049/jimmunol.181.2.1232
33. Rauner M, Sipos W, Pietschmann P. Osteoimmunology. *Int Arch Allergy Immunol.* (2007) 143:31–48. doi: 10.1159/000098223
34. D'Amelio P, Grimaldi A, Di Bella S, Brianza SZ, Cristofaro MA, Tamone C, et al. Estrogen deficiency increases osteoclastogenesis up-regulating T cells activity: a key mechanism in osteoporosis. *Bone.* (2008) 43:92–100. doi: 10.1016/j.bone.2008.02.017
35. D'Amico L, Roato I. Cross-talk between T cells and osteoclasts in bone resorption. *Bonekey Rep.* (2008) 1:82. doi: 10.1038/bonekey.2012.82
36. Gao Y, Grassi F, Robbie RM, Terauchi M, Page K, Yang X, et al. IFN-γ stimulates osteoclast formation and bone loss *in vivo* via antigen-driven T cell activation. *J Clin Invest.* (2007) 117:122–32. doi: 10.1172/JCI30074
37. Taubman Martin A, Valverde P, Han X, Kawai T. Immune response: the key to bone resorption in periodontal disease. *J Periodontol.* (2005) 76:2033–41. doi: 10.1902/jop.2005.76.11-S.2033
38. Sato K, Suematsu A, Okamoto K, Yamaguchi A, Morishita Y, Kadono Y, et al. Th17 functions as an osteoclastogenic helper T cell subset that links T cell activation and bone destruction. *J Exp Med.* (2006) 203:2673–82. doi: 10.1084/jem.20061775
39. Korn T, Oukka M, Kuchroo V, Bettelli E. Th17 cells: effector T cells with inflammatory properties. *Semin Immunol.* (2007) 19:362–71. doi: 10.1016/j.smim.2007.10.007
40. Zhao R. Immune regulation of bone loss by Th17 cells in oestrogen-deficient osteoporosis. *Eur J Clin Invest.* (2013) 43:1195–202. doi: 10.1111/eci.12158
41. Feige JJ, Baird A. La crinopexie: un modèle décrivant les mécanismes qui régissent la biodisponibilité des facteurs de croissance. *Méd Sci.* (1992) 8:805–10. doi: 10.4267/10608/3231
42. Dong XN, Qin A, Xu J, Wang X. *In situ* accumulation of advanced glycation endproducts (AGEs) in bone matrix and its correlation with osteoclastic bone resorption. *Bone.* (2011) 49:174–83. doi: 10.1016/j.bone.2011.04.009
43. Cianci R, Cammarota G, Frisullo G, Pagliari D, Ianiro G, Martini M, et al. Tissue-infiltrating lymphocytes analysis reveals large modifications of the duodenal 'immunological niche' in coeliac disease after gluten-free diet. *Clin Transl Gastroenterol.* (2012) 3:28. doi: 10.1038/ctg.2012.22
44. Senthilkumar R, Lee HW. CD137L- and RANKL mediated reverse signals inhibit osteoclastogenesis and T lymphocyte proliferation. *Immunobiology.* (2009) 214:153–61. doi: 10.1016/j.imbio.2008.05.001
45. Pandolfi F, Cianci R, Pagliari D, Landolfi R, Kunkel S, Cammarota G. Cellular mediators of inflammation: tregs and T H 17 cells in gastrointestinal diseases. *Mediators Inflamm.* (2009) 2009:132028. doi: 10.1155/2009/132028
46. Zaiss MM, Axmann R, Zwerina J, Polzer K, Gücke E, Skapenko lA, et al. Treg cells suppress osteoclast formation: a new link between the immune system and bone. *Arthritis Rheum.* (2007) 56:4104–12. doi: 10.1002/art.23138
47. Li Y, Toraldo G, Li A, Yang X, Zhang H, Qian WP, et al. B cells and T cells are critical for the preservation of bone homeostasis and attainment of peak bone mass *in vivo*. *Blood.* (2007) 109:3839–48. doi: 10.1182/blood-2006-07-037994
48. Bernhard A, Milovanovic P, Zimmermann EA, Hahn M, Djonic D, Krause M, et al. Micro-morphological properties of osteons reveal changes in cortical bone stability during aging, osteoporosis, and bisphosphonate treatment in women. *Osteoporos Int.* (2013) 24:2671–80. doi: 10.1007/s00198-013-2374-x
49. Bianco P. Minireview: the stem cell next door: skeletal and hematopoietic stem cell "niches" in bone. *Endocrinology.* (2011) 152:2957–62. doi: 10.1210/en.2011-0217
50. Nagasawa T, Omatsu Y, Sugiyama T. Control of hematopoietic stem cells by the bone marrow stromal niche: the role of reticular cells. *Trends Immunol.* (2011) 32:315–20. doi: 10.1016/j.it.2011.03.009
51. Weitzmann MN. The role of inflammatory cytokines, the RANKL/OPG axis, and the immunoskeletal interface in physiological bone turnover and osteoporosis. *Scientifica.* (2013) 2013:125705. doi: 10.1155/2013/125705
52. Breuil V, Ticchioni M, Testa J, Roux CH, Ferrari P, Breittmayer JP, et al. Immune changes in post-menopausal osteoporosis: the immunos study. *Osteoporos Int.* (2010) 21:805–14. doi: 10.1007/s00198-009-1018-7
53. Walsh MC, Choi Y. Biology of the RANKL-RANK-OPG system in immunity, bone, and beyond, *Front Immunol.* (2014) 5:511. doi: 10.3389/fimmu.2014.00511
54. Kawalilak CE, Johnston JD, Olszynski WP, Kontulainen SA. Characterizing microarchitectural changes at the distal radius tibia in postmenopausal women using HR-pQCT. *Osteoporos Int.* (2014) 25:2057–66. doi: 10.1007/s00198-014-2719-0
55. Zoeller RT, Brown TR, Doan LL, Gore AC, Skakkebaek NE, Soto AM, et al. Endocrine-disrupting chemicals and public health protection: a statement of principles from the Endocrine Society. *Endocrinology.* (2012) 153:4097–110. doi: 10.1210/en.2012-1422
56. Schlezinger JJ, Howard GJ, Hurst CH, Emberley JK, Waxman DJ, Webster T, et al. Environmental and endogenous peroxisome proliferator-activated receptor gamma agonists induce bone marrow B cell growth arrest and apoptosis: interactions between mono(2-ethylhexyl) phthalate, 9-cis-retinoic acid, and 15-deoxy-Delta12,14-prostaglandin J2. *J Immunol.* (2004) 173:3165–77. doi: 10.4049/jimmunol.173.5.3165
57. Watt J, Schlezinger JJ. Structurally-diverse, PPARγ-activating environmental toxicants induce adipogenesis and suppress osteogenesis in bone marrow mesenchymal stromal cells. *Toxicology.* (2015) 331:66–77. doi: 10.1016/j.tox.2015.03.006
58. Veldhuis-Vlug AG, Rosen CJ. Clinical implications of bone marrow adiposity. *J Intern Med.* (2018) 283:121–39. doi: 10.1111/joim.12718
59. Rharass T, Lucas S. Bone marrow adiposity and bone, a bad romance? *Eur J Endocrinol.* (2018) 179:165–82. doi: 10.1530/EJE-18-0182
60. Baker AH, Wu TH, Bolt AM, Gerstenfeld LC, Mann KK, Schlezinger JJ. From the cover: tributyltin alters the bone marrow microenvironment and suppresses B cell development. *Toxicol Sci.* (2017) 158:63–75. doi: 10.1093/toxsci/kfx067
61. Agarwal DK, Maronpot RR, Lamb JC, Kluwe WM. Adverse effects of butyl benzyl phthalate on the reproductive and hematopoietic systems of male rats. *Toxicology.* (1985) 35:189–206. doi: 10.1016/0300-483X(85)90015-0
62. Warren JL, MacIver NJ. Regulation of adaptive immune cells by sirtuins. *Front Endocrinol.* (2019) 10:466. doi: 10.3389/fendo.2019.00466
63. Khan D, Ansar AS. The immune system is a natural target for estrogen action: opposing effects of estrogen in two prototypical autoimmune diseases. *Front Immunol.* (2016) 6:365. doi: 10.3389/fimmu.2015.00635
64. Bogdanska J, Borg D, Sundstro M, Bergstro U, Halldin K, Abedi-Valugerdi M, et al. Tissue distribution of 35Slabelled perfluorooctanoic sulfonate in adult mice after oral exposure to a low environmentally relevant dose or a high experimental dose. *Toxicology.* (2011) 284:54–62. doi: 10.1016/j.tox.2011.03.014

65. Bogdanska J, Sundstro M, Bergstro U, Borg D, Abedi-Valugerdi M, Bergman A, et al. Tissue distribution of 35S-labelled perfluorobutanesulfonic acid in adult mice following dietary exposure for 1-5 days. *Chemosphere*. (2014) 98:28–36. doi: 10.1016/j.chemosphere.2013.09.062
66. Stein SJ, Baldwin AS. Deletion of the NF-κB subunit p65/RelA in the hematopoietic compartment leads to defects in hematopoietic stem cell function. *Blood*. (2013) 121:5015–24. doi: 10.1182/blood-2013-02-486142
67. Sprio S, Sandri M, Iafisco M, Panseri I, Cunha C, Ruffini A, et al. Biomimetic biomaterials in regenerative medicine. In Ruys AJ, editor. *Biomimetic Biomaterials, Structure and Applications*. Cambride: Whoodhead Publishing (2013). p. 3–45. doi: 10.1533/9780857098887.1.3
68. Nombela-Arietta C, Manz MG. Quantification and three-dimensional microanatomical organization of the bone marrow. *Blood Adv*. (2017) 1:407–16. doi: 10.1182/bloodadvances.2016003194

Conflict of Interest: The authors declare that the research was conducted in the absence of any commercial or financial relationships that could be construed as a potential conflict of interest.

The reviewer IM declared a past co-authorship with one of the authors to the handling editor.

Copyright © 2020 Toni, Di Conza, Barbaro, Zini, Consolini, Dallatana, Antoniel, Quarantini, Quarantini, Maioli, Bruni, Elviri, Panseri, Sprio, Sandri and Tampieri. This is an open-access article distributed under the terms of the Creative Commons Attribution License (CC BY). The use, distribution or reproduction in other forums is permitted, provided the original author(s) and the copyright owner(s) are credited and that the original publication in this journal is cited, in accordance with accepted academic practice. No use, distribution or reproduction is permitted which does not comply with these terms.

frontiers in Immunology

ORIGINAL RESEARCH
published: 28 October 2020
doi: 10.3389/fimmu.2020.545980

CD147 Expressed on Memory CD4$^+$ T Cells Limits Th17 Responses in Patients With Rheumatoid Arthritis

Jinlin Miao[1,2†], Kui Zhang[1†], Zhaohui Zheng[1†], Rui Zhang[1†], Minghua Lv[1], Na Guo[1], Yingming Xu[1], Qing Han[1], Zhinan Chen[2] and Ping Zhu[1*]*

[1] Department of Clinical Immunology, PLA Specialized Research Institute of Rheumatology & Immunology, Xijing Hospital, The Fourth Military Medical University, Xi'an, China, [2] National Translational Science Center for Molecular Medicine & Department of Cell Biology, The Fourth Military Medical University, Xi'an, China

OPEN ACCESS

Edited by:
Erminia Mariani,
University of Bologna, Italy

Reviewed by:
Seung-Hyo Lee,
Korea Advanced Institute of Science and Technology, South Korea
Eddie A. James,
Benaroya Research Institute, United States

***Correspondence:**
Ping Zhu
zhuping@fmmu.edu.cn
Zhinan Chen
znchen@fmmu.edu.cn

[†]These authors have contributed equally to this work

Specialty section:
This article was submitted to Autoimmune and Autoinflammatory Disorders, a section of the journal Frontiers in Immunology

Received: 26 March 2020
Accepted: 06 October 2020
Published: 28 October 2020

Citation:
Miao J, Zhang K, Zheng Z, Zhang R, Lv M, Guo N, Xu Y, Han Q, Chen Z and Zhu P (2020) CD147 Expressed on Memory CD4$^+$ T Cells Limits Th17 Responses in Patients With Rheumatoid Arthritis. Front. Immunol. 11:545980. doi: 10.3389/fimmu.2020.545980

Rheumatoid arthritis (RA) is a common autoimmune disease in which T helper-type 17 (Th17) cells have been critically involved. CD147 is a T cell activation-associated molecule and is involved in T cell development. However, it remains unclear whether CD147 participates in Th17 responses in RA patients. In this study, we demonstrated that in both the RA and healthy controls (HC) groups, CD147 expression on CD4$^+$ T cells was increased in CCR6$^+$ and CD161$^+$ subsets, and was associated with IL-17 production. Ligation of CD147 with its monoclonal antibody (mAb) strongly inhibited Th17 responses, and knock down of CD147 expression on CD4$^+$ Tm cells specifically enhanced Th17 responses, triggered by coculture with *in vitro* activated monocytes from HC. Further functional studies showed that anti-CD147 mAb decreased the activation of AKT, mTORC1 and STAT3 signaling, which is known to enhance Th17 responses. Ligation of CD147 with its mAb on CD4$^+$ Tm cells specifically reduced Th17 responses induced by *in vitro* or *in vivo* activated monocytes from RA patients. In collagen-induced arthritis model, anti-CD147 mAb treatment reduced the Th17 levels and severity of arthritis *in vivo*. These data suggest that CD147 plays a negative role in regulating human Th17 responses. Anti-CD147 mAb can limit the extraordinary proliferation of Th17 cells and may be a new therapeutic option in RA.

Keywords: rheumatoid arthritis, inflammation, Th17 cells, CD147, STAT3

INTRODUCTION

Rheumatoid arthritis (RA) is a systemic inflammatory disease characterized by the infiltration of antigen-presenting cells (APCs) and T cells into the joints, synovial hyperplasia, and systemic inflammation. Th17 cells (T helper cells that produce interleukin 17 [IL-17]) are thought to promote the development and pathogenesis of RA (1–3). Investigations into the mechanisms that control Th17 responses in humans are essential for a greater understanding of RA pathogenesis and therapeutics. In this regard, much has been accomplished in the last decade.

In humans, Th17 cells express CCR6 (chemokine receptor 6) and CD161 (cluster of differentiation 161), which are useful as markers of Th17 cells (4, 5). Depending on signals from APCs, Th17 cells can not only be generated from CD4$^+$ naïve T cells, but also from CD4$^+$ memory T

(Tm) cells (6, 7). Evans et al. (6, 8) reported that *in vitro* activated monocytes, or *in vivo* activated monocytes from synovial fluid (SF) of RA patients, preferentially promoted Th17 responses in $CD4^+$ Tm cells. Further, Th17 responses in this process depended on cell-to-cell contact (6, 8), the blockade of costimulatory and adhesion pathway, including CD80/CD86, CD54, or CD40, did not affect the Th17 responses (8). As induced by APCs, membrane IL-1α may be involved in the conversion of $CD4^+$ Tm cells to Th17 cells (9). Further investigations are needed to assess whether any other cell membrane-derived signals are required for Th17 responses.

CD147 is a type I transmembrane glycoprotein that is broadly expressed on hemopoietic and nonhemopoietic cells (10), and is associated with a wide range of physiologic and pathologic functions, including lymphocyte development (11). CD147 has been linked to diverse pathological states in humans, including systemic lupus erythematosus and RA (12, 13). Interestingly, CD147 is strongly upregulated on T cells after activation (14) and has a critical role in thymocyte expansion and T-cell development (15, 16). Both antibody cross-linking and knockout mice assays indicated that CD147 may inhibit T cell receptor-mediated T cell activation and proliferation (14, 17). And CD147 is elevated on activated $CD4^+$ T cells and negatively regulates Th17 cell differentiation in mice (18). Evidence suggests substantial similarities and differences between murine and human Th17 cell development. Thus, the functions of CD147-regulating signal pathways in human Th17 cells, especially in a setting of inflammation, remain to be identified. Therefore, this study investigated whether CD147 is involved in human Th17 responses, and its potential mechanism in RA. In addition, the therapeutic effects of anti-CD147 mAb were evaluated, using a mouse model of collagen-induced arthritis (CIA).

MATERIALS AND METHODS

Patients and Healthy Controls

Peripheral blood (PB) samples were obtained from 31 patients with RA and 22 age- and gender-matched HC individuals (RA and HC groups, respectively; **Table 1**). Synovial fluid (SF) samples were collected from six patients with RA. All patients fulfilled the 1987 revised criteria of the American College of Rheumatology, and had never received disease-modifying drugs or corticosteroids. Disease activity was evaluated *via* the 28-joint disease activity score (DAS28). The study was approved by the Ethics Committee of Xijing Hospital, and all subjects provided written informed consent. The procedures were conducted in compliance with the Declaration of Helsinki.

TABLE 1 | Basic characteristics of HC and RA patients*.

Characteristics	HC	RA
Patients, n	22	31
Age, y	35.5 (28.75–44.25)	39.0 (29.0–44.0)
Female gender, n (%)	16 (72.7)	24 (77.4)
Disease duration, mo	NA	7.0 (3.0–12.0)
Rheumatoid factor positive, n (%)	NA	22(71.0%)
Anti-CCP positive, n (%)	NA	23 (74.2%)
ESR, mm/h	NA	32.0 (19.0–58.0)
CRP, mg/dL	NA	1.12 (0.33–4.12)
DAS28	NA	5.01(3.87–5.48)

Values are presented as median (interquartile range) unless indicated otherwise. CCP, cyclic citrullinated peptide antibodies; CRP, C-reactive protein; DAS28, 28-joints disease activity score; ESR, erythrocyte sedimentation rate; NA, not applicable.

Phenotypic Analysis

The following anti-human monoclonal antibodies were used for surface phenotype and intracellular cytokine staining: anti-CD4-fluorescein isothiocyanate (FITC); anti-CD4-phycoerythrin (PE); anti-CD161-PE; anti-CCR6-PE; anti-CD45RO-PE; anti-CD147-peridinin chlorophylla protein cyanine 5.5 dies (Percp–cy5.5); anti-interferon (IFN)-γ-FITC (all from BD Biosciences); and anti-IL-17A-allophycocyanin (APC; eBiosciences). Anti-mouse monoclonal antibodies included: anti-CD4-Percp; anti-IL-17A-APC; and anti-IFN-γ-FITC (all from BD Biosciences). Appropriately conjugated IgG antibodies were used as isotype controls. Cells were acquired on a FACSCalibur flow cytometer (BD Biosciences) and analyzed using Cell Quest software (BD Bioscience) and FlowJo 7.6.1 software (Tree Star).

Intracellular Cytokine Staining

For detection of intracellular cytokine production, cells were stimulated with 50 ng/ml of phorbol myristate acetate (Sigma-Aldrich) plus 1 μg/ml of ionomycin (Sigma-Aldrich) in the presence of 10 μg/ml GolgiStop (BD Bioscience) for 6 h at 37°C and 5% CO_2. After surface-staining of surface markers, cells were fixed and made permeable with BD Cytofix/Cytoperm solution and Perm/Wash solution in accordance with the manufacturer's instructions (BD Biosciences).

Cell Isolation

PB and SF mononuclear cells were isolated by Ficoll-Paque Plus density gradient centrifugation (Lymphocyte Separation Media; PAA Laboratories). For isolation of SF mononuclear cells, SF was incubated with 40 μg/ml of hyaluronidase (Sigma-Aldrich) for 30 min at 37°C, and then the pellet was dissolved in phosphate buffered saline and subjected to density gradient centrifugation. Purification of cell subsets was performed by magnetic cell sorting (Miltenyi Biotec) and confirmed by flow cytometry in accordance with the manufacturer's instructions. Briefly, $CD14^+$ monocytes (>94% pure) were isolated by positive selection using CD14 MicroBeads. The $CD14^-$ fraction was used for $CD4^+$ T cell isolation by using a negative depletion kit (>90% pure). Next, $CD4^+$ Tm cells were positively selected *via* CD45RO microbeads (>92% pure). The remaining $CD4^+$ naive T cells were further depleted of any remaining $CD45RO^+$ cells by a second depletion round (>90% pure).

Cell Coculture

Cells were cultured in RPMI medium 1640 (Gibco) supplemented with 1% penicillin/streptomycin, 1% glutamine, and 10% fetal calf serum (PAA Laboratories). For *in vitro* activation of monocytes, purified monocytes were pre-incubated with 100 ng/ml lipopolysaccharide (LPS, Sigma Aldrich) for 30 min at 37°C and 5% CO_2. Then cells were

washed twice with 10 ml of medium and recounted. For Th17 cell polarization, LPS-activated monocytes (1×10^5) were cocultured with 5×10^5 purified $CD4^+$ T cells and 100 ng/ml soluble anti-CD3 mAb (R&D Systems) for 3 days in 24-well plates. For CD147 ligation experiments, purified $CD4^+$ T cells were incubated with 10 μg/ml anti-CD147 mAb (HAb18, generated and identified in our lab) for 1 h, and then cells were washed and resuspended in medium. To determine the fold expansion, $CD4^+$ T cells were labeled with 2 mM carboxyfluorescein diacetate succinimidyl ester (CFSE; Invitrogen) before coculture.

Flow Cytometry Analysis of Phosphorylated Proteins

After being cocultured for 3 days or stimulated with immobilized anti-CD3mAb (plates coated with 5 μg/ml) and 1 μg/m soluble anti-CD28mAb for the indicate time, cells were fixed with 2% paraformaldehyde. Surface staining was followed by permeabilization with 90% methanol, and intracellular staining with antibodies including anti-Stat3-PE, anti-pStat3 (Y705)-Alexa Fluor 647, anti-pAkt (T308)-PE, anti-pAkt (S473)-Alexa Fluor 647 (all from BD Bioscience), anti-pS6 (Ser235/236)-Alexa Fluor 488 and anti-p70S6K (Thr421/Ser424) (all from Cell Signaling Technology). The anti-p70S6K staining was followed by secondary staining with anti-rabbit-IgG-Alexa Fluor 488 (Invitrogen).

Cytokine Analysis

The supernatants of cocultures were collected and stored at –80°C until cytokine testing was performed. The levels of IL-17 and IFN-γ were determined using Luminex technology in accordance with the manufacturer's instructions (EMD Millipore). The results were analyzed using BioPlex Manager 4 (Bio-Rad Laboratories).

Lentiviral Vector Transduction

As previously described (19), the Trans-Lentiviral pLKO System were used to produce lentiviral vectors expressing CD147-specific shRNA. Purified $CD4^+$ Tm cells were activated with immobilized anti-CD3 (1 μg/ml) and anti-CD28 (5 μg/ml) in the presence of human recombinant IL-2 (20 U/ml; R&D). After 24 h, the medium was carefully removed, cells were infected with viral supernatants and polybrene (6 μg/ml; Millipore) and centrifuged at 500*g* for 2 h at 4°C. Then cells were incubated for 48 h at 37°C and 5% CO_2. Next, transfected cells were selected by puromycin (Sigma Aldrich). After IL-2 withdrawal for 24 h, cells were collected to determine cell surface markers and coculture with monocytes.

Induction of CIA and Anti-CD147 mAb Treatment

The Animal Experiment Administration Committee of the University approved the animal care and experimental procedures. Male C57BL/6 mice were purchased from the Fourth Military Medical University, Laboratory Animal Center. All animals were 9 to 11 weeks old. CIA induction was performed as previously described (20). Briefly, C57BL/6 mice were immunized with type II collagen (CII; Chondrex) emulsified in complete Freund's adjuvant (CFA; Chondrex) on day 0 at the tail base. On day 21, a booster injection of CII emulsified with incomplete Freund's adjuvant (IFA; Chondrex) was administered. The mice were treated *via* intraperitoneal injection of anti-mouse CD147 mAb or isotype control mAb (5 mg/kg, n = 4; R&D Systems). Antibody was given every other day for 10 days starting on day 21. Thickness of both hind paws were measured by digital caliper. Signs of arthritis were scored for each paw on a scale of 0 to 4, as previously described (20). The mean arthritis index is the total arthritis score in all mice of each group divided by the number of mice in the group. The mice were killed on day 31 for experimental analysis.

Statistical Analysis

Differences between groups were determined using the nonparametric Mann-Whitney test. Paired samples were compared using a Wilcoxon matched-pairs signed rank sum test. Data analyses were performed using GraphPad Prism version 5.0 (GraphPad Software). For all tests, a two-sided *P* value less than 0.05 was considered significant.

RESULTS

Association Between CD147 Levels and IL-17 Production in $CD4^+$ T Cells

The main IL-17-secreting T (Th17) cells are $CD4^+CCR6^+$ and $CD4^+CD161^+$ (4, 5). In the present study, the CD147 levels of these Th17 cells were evaluated in both the RA and HC groups. In both groups but especially the RA, the CD147 levels in the $CD4^+CCR6^+$ and $CD4^+CD161^+$ cells were higher than that of the $CD4^+CCR6^-$ and $CD4^+CD161^-$ (**Figures 1A, B**). Further, in both the RA and HC groups, IL-17 production, but not IFN-γ, was mainly restricted to $CD147^{++}$ cells (**Figure 1C**). These results supported that CD147 expression maybe associated with Th17 cells in humans.

Effect of CD147 on Human Th17 Responses

To optimally induce Th17 response, purified bulk $CD4^+$ T cells, $CD4^+$ naive T cells, $CD4^+$ Tm cells and autologous $CD14^+$ monocytes from HC were isolated and cocultured under various conditions. The optimal condition for inducing Th17 cells is that $CD4^+$ Tm cells are stimulated with LPS-activated monocytes and anti-CD3 mAb for 3 days (see online **Supplementary Figure S1**). Subsequently, $CD4^+$ Tm cells, LPS-activated monocytes, and anti-CD3 mAb were cultured for 3 days, unless otherwise specified. Then to evaluate whether Th17 cells were induced from a non-committed $CD4^+$ Tm cell population or reflected simply a proliferation of preexisting Th17 cells, CFSE was used to determine the proliferation of IL-17 producing cells. Indeed, the $IL\text{-}17^+$ cell percentage in each generation increased with the proliferation of

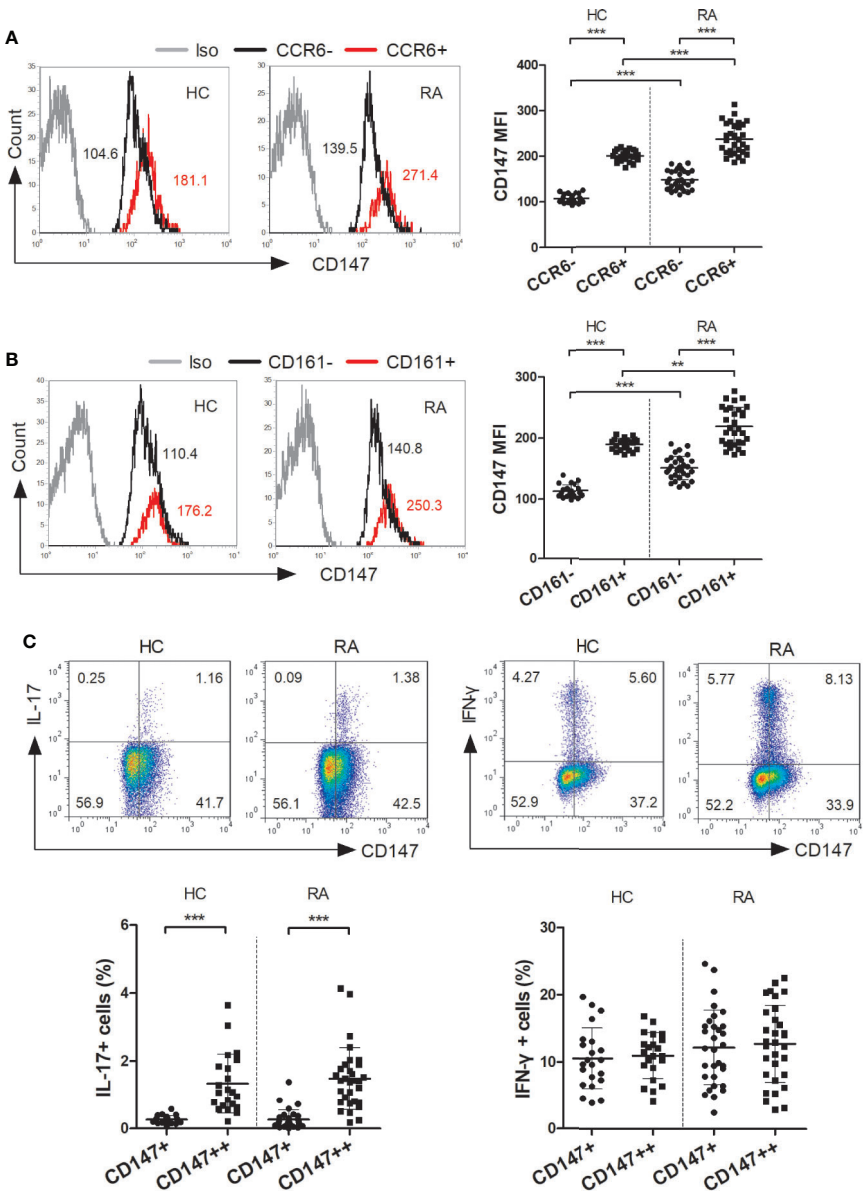

FIGURE 1 | CD147 expression was associated with IL-17 production. **(A, B)** Flow cytometry was used to assess CD147 expression on circulating $CD4^+$ T cell subsets, including $CCR6^{-/+}$ cells **(A)** and $CD161^{-/+}$ cells **(B)**, from healthy control (HC; n = 22) and rheumatoid arthritis (RA) patients (n = 31). **(C)** Flow cytometric dot-plots and cumulative data of intracellular IL-17 and IFN-γ production in $CD4^+$ T cells and stratified by their CD147 expression obtained from HC (n = 22) and RA patients (n = 31). Iso, isotype control mAb; $^{**}P < 0.01$; $^{***}P < 0.001$.

T cells (**Figure 2D**), indicating that LPS-activated monocytes switch non-committed Tm cells into Th17 cells.

Using the established coculture system, we investigated if CD147 ligation on $CD4^+$ Tm cells could modulate Th17 responses (**Figure 2**). When compared to isotype control mAb, anti-CD147 mAb strongly decreased the percentages of Th17 and Th17/Th1 cells, whereas Th1 cell percentage was not affected (**Figures 2A, B**). In support of this, the production of IL-17 from coculture supernatants was significantly decreased by the anti-CD147 mAb (**Figure 2C**). Furthermore, the percentage of $IL\text{-}17^+$ cells in the generation 0 to 2 was not affected by adding anti-CD147 mAb, but was decreased in generation 3 (**Figure 2D**). To confirm the potential role of CD147 in Th17 responses, lentiviral vectors expressing CD147-specific shRNA (LV-shCD147) were used to knock down CD147 expression in primary $CD4^+$ Tm cells (**Figure 2E**). Notably, compared with the negative control shRNA (LV-NC) transduced T cells, Th17 and Th17/Th1 cell percentage and IL-17 level were noticeably higher in LV-

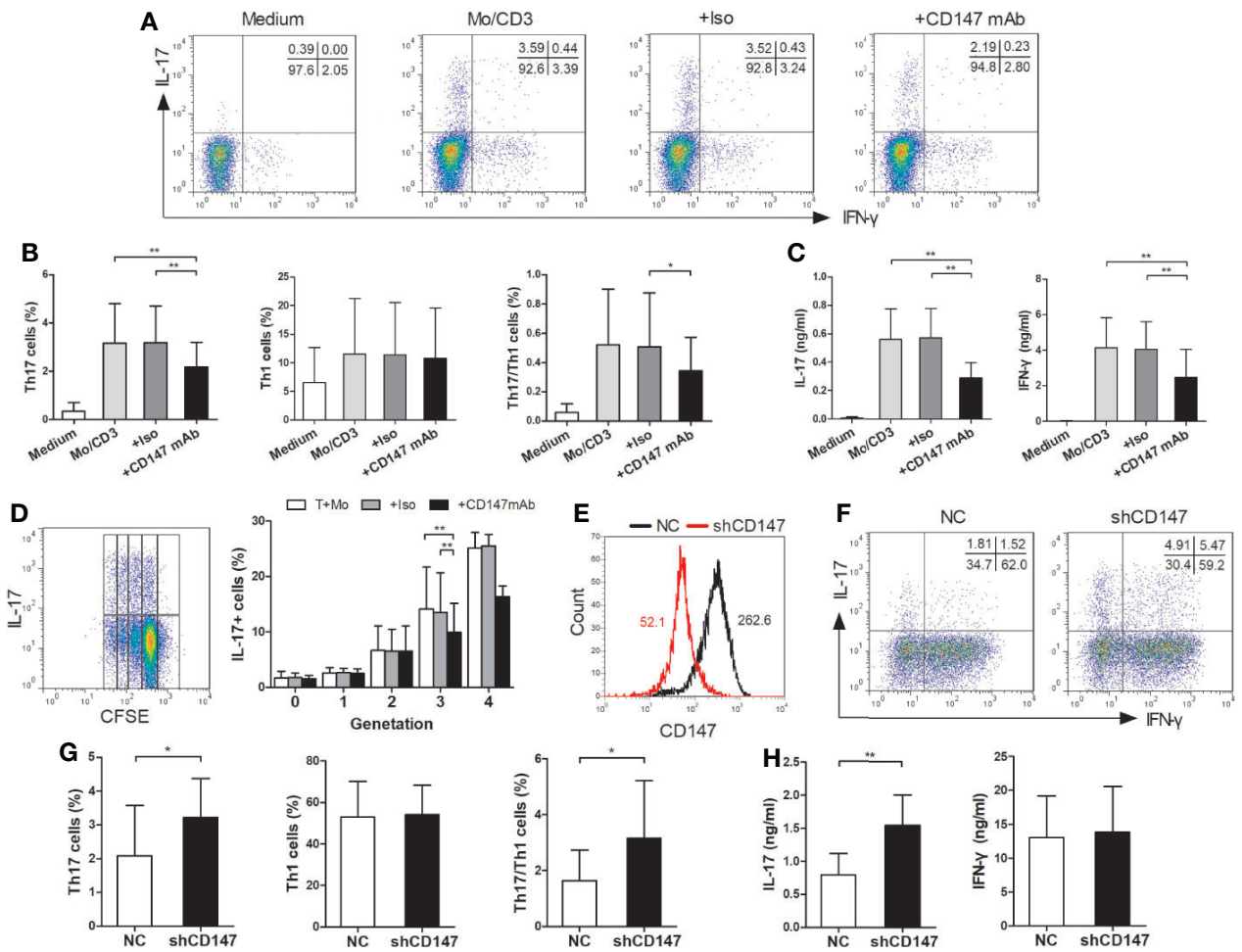

FIGURE 2 | CD147 suppresses human Th17 responses. **(A–C)** $CD4^+$ memory (Tm) cells from HC were cocultured with medium or LPS-activated monocytes (Mo) and anti-CD3 mAb, in absence or presence of isotype control mAb (Iso) or Anti-CD147 mAb for 3 days. Representative plots **(A)** and quantitative results of Th17, Th1 and Th17/Th1 cell percentages **(B)** in T cells, and IL-17 and IFN-γ production in cell culture supernatants **(C)** are shown (n = 9). **(D)** CFSE-labeled $CD4^+$ Tm cells were cocultured with LPS-activated Mo and anti-CD3 mAb in presence of Iso or anti-CD147 mAb for 3 days and then assessed the percentage of IL-17 producing cells in each generation (generation 0–3, n = 10; generation 4, n = 4). **(E)** Representative CD147 staining histogram in $CD4^+$ Tm cells from HC transduced with lentivirus expressing negative control shRNA (NC) or shRNA for CD147 (shCD147). **(F-H)** NC and shCD147 transduced $CD4^+$ Tm cells were cocultured with autologous LPS-activated Mo. Representative plots **(F)** and quantitative results of intracellular expression of IL-17 and/or IFN-γ **(G)** in T cells, and IL-17 and IFN-γ levels in cell culture supernatants **(H)** were shown (n = 9). $^*P < 0.05$; $^{**}P < 0.01$.

shCD147 transduced T cells, while Th1 cell and IFN-γ levels were not affected (**Figures 2F–H**). These data collectively suggest that CD147 plays a negative role in Th17 responses.

Effect of CD147 on AKT, mTORC1, and STAT3 Signaling

To evaluate the underlying mechanisms, we investigated the effect of CD147 on STAT3 (signal transducer and activator of transcription 3), a crucial regulator of Th17 lineage (21). Indeed, anti-CD147 mAb decreased STAT3 phosphorylation in $CD4^+$ Tm cells that induced by coculture with LPS-activated monocytes (**Figure 3A**). It has been reported that the signaling of PI3K, Akt, and mammalian target of rapamycin (mTOR) complexes positively regulates Th17 cell development (22). Further signal analysis showed that the levels of pAKT (T308), pS6K, and p70S6, but not of pAKT (S473), induced by CD3/CD28 ligation were partly inhibited in the presence of anti-CD147 mAb in comparison to isotype control mAb (**Figures 3B–D**). This suggests that CD147 may suppress Th17 responses by affecting AKT/mTOR signaling.

Effect of CD147 on Th17 Responses in RA Patients

We sought to assess whether the Th17 responses triggered by monocytes were suppressed by CD147 in patients with RA. First, CD147 expression on $CD4^+$ Tm cells from RA PB was higher than

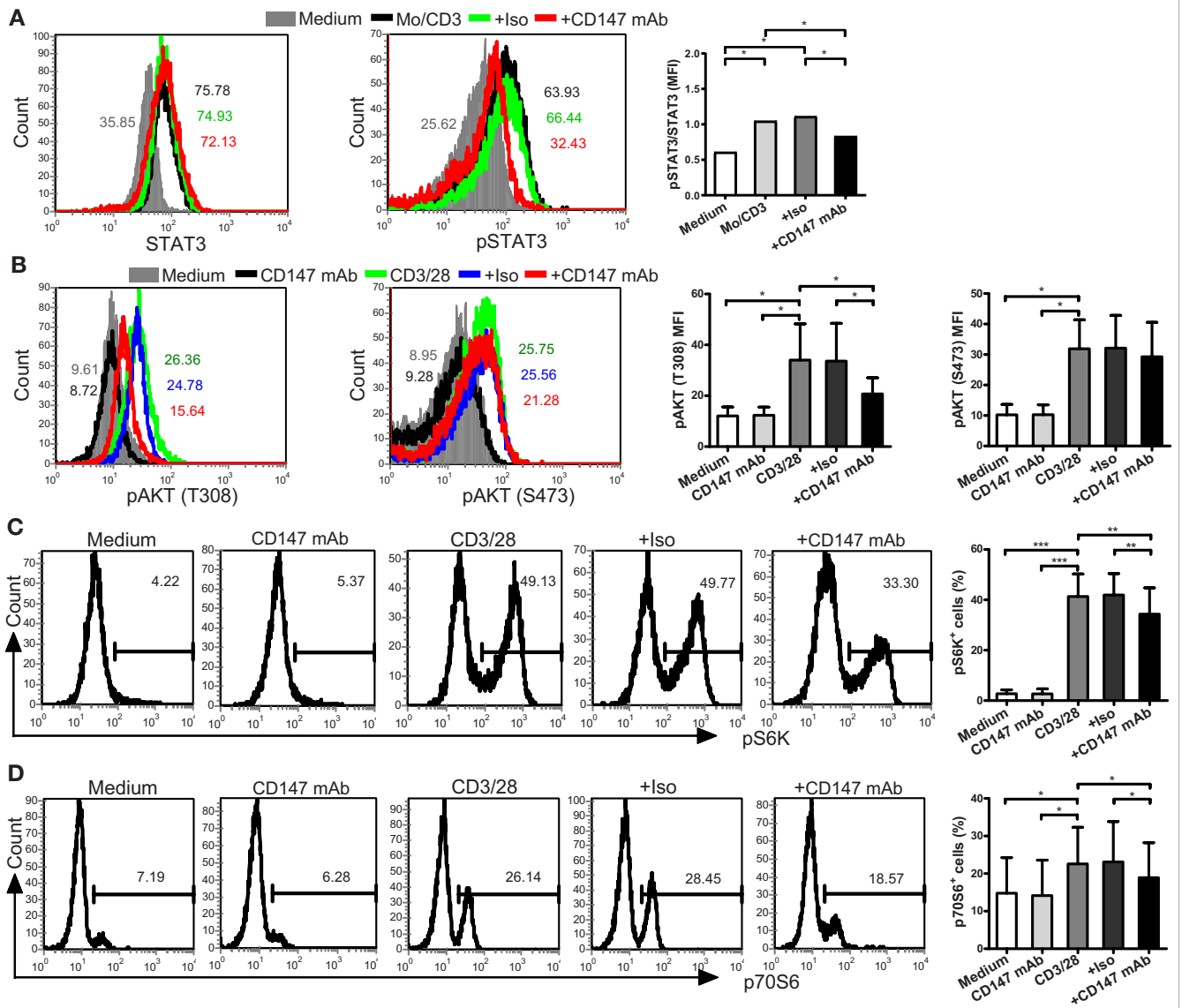

FIGURE 3 | Anti-CD147 mAb inhibits AKT, mTOR and STAT3 signaling. **(A)** $CD4^+$ Tm cells from HC were cocultured with medium or LPS-activated Mo and anti-CD3 mAb in presence of isotype control mAb (Iso) or anti-CD147 mAb for 3 days, then the expression of STAT3 and pSTAT3 were assessed by flow cytometry (n = 7). **(B)** Phospho-flow analysis of pAKT (T308) and pAKT (S473) in $CD4^+$ Tm cells from HC with medium or anti-CD147 mAb, with or without Iso or anti-CD147 mAb stimulated with anti-CD3 and anti-CD28 mAb for 5 min (n = 7). **(C, D)** Phospho-flow analysis of pS6K (n = 7; **(C)** and p70S6 (n = 6; **(D)** in $CD4^+$ Tm cells from HC with medium or anti-CD147 mAb, with or without Iso or anti-CD147 mAb stimulated with anti-CD3 and anti-CD28 mAb for 30 min. $^*P < 0.05$; $^{**}P < 0.01$; $^{***}P < 0.001$.

from HC PB, and its expression was further increased in RA SF (**Figure 4A**). Using $CD4^+$ Tm cells from HC PB, RA PB and RA SF, the magnitude of monocyte-driven Th17 and Th17/Th1 responses and IL-17 production were similarly in RA PB and HC PB, but strikingly decreased in RA SF (**Figures 4B, C**). In addition, similar to the data of HC, the increase in Th17, Th17/Th1 cells and IL-17 production in RA patients triggered by LPS-activated monocytes could be suppressed by adding anti-CD147 mAb (**Figures 4D, E**). There are numerous reports that $CD14^+$ monocytes from SF of RA patients were highly activated (23) and the activation status of the APCs played a crucial role in Th17 induction (6–8). To place these findings in a pathophysiological condition, we cocultured RA PB-derived $CD4^+$ Tm cells with autologous PB-derived monocytes, LPS-activated PB monocytes or SF-derived monocytes. As compared to PB-derived monocytes, SF-derived monocytes increased Th17 responses to a level comparable with that of LPS-activated PB monocytes (**Figure 4F**). Furthermore, anti-CD147 mAb also significantly decreased Th17 cell percentage and IL-17 production, but not Th1 cell percentage and IFN-γ production, that triggered by SF-derived monocytes (**Figures 4G–I**).

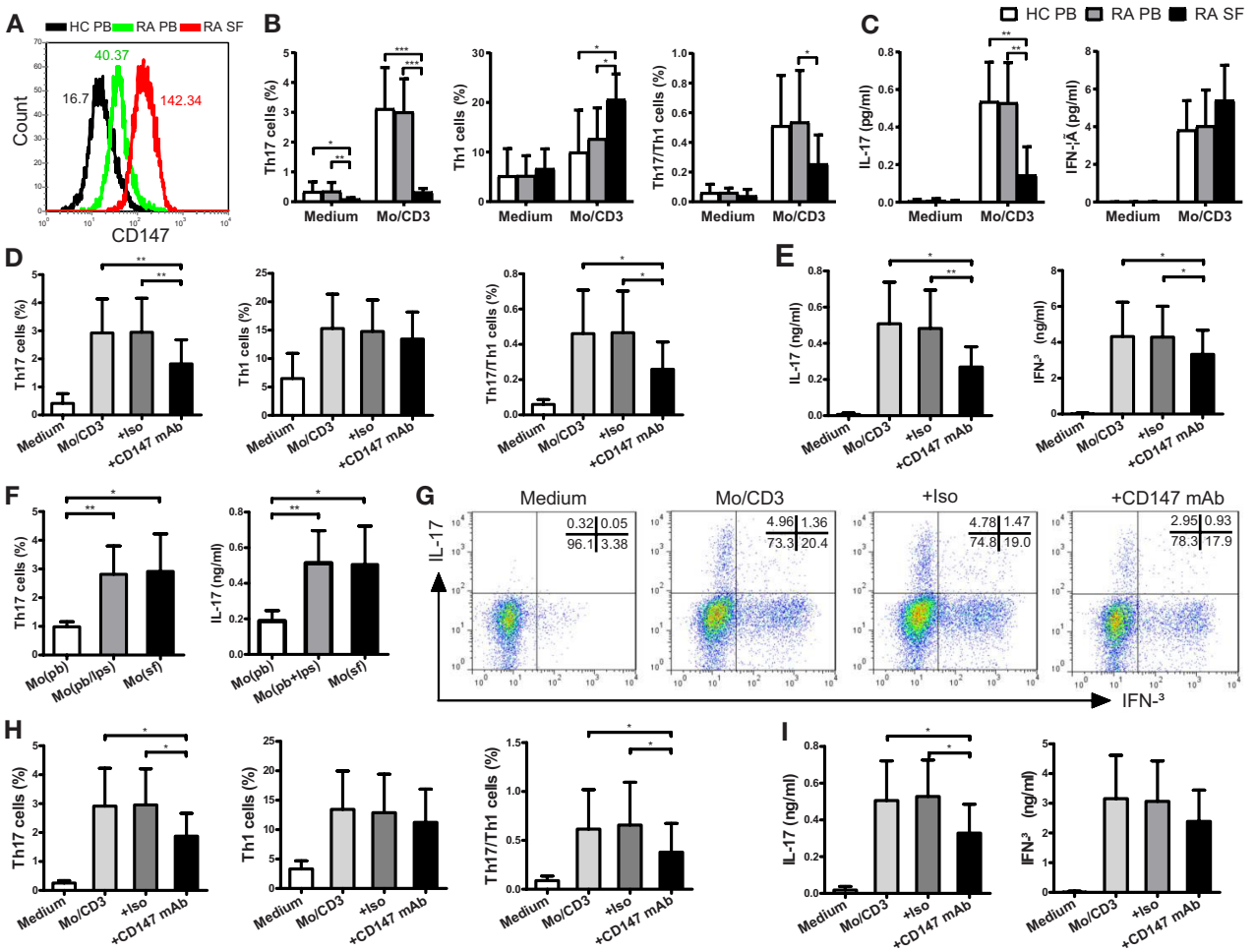

FIGURE 4 | CD147 suppresses Th17 responses in patients with RA. **(A)** Representative CD147 staining histogram in $CD4^+$ Tm cells from the peripheral blood of HC (HC PB), PB of RA (RA PB) and synovial fluid of RA (RA SF). **(B, C)** $CD4^+$ Tm cells from HC PB (n = 13), RA PB (n = 12) or RA SF (n = 6) were isolated and cocultured with medium or autologous PB LPS-activated Mo and anti-CD3 mAb. **(D, E)** $CD4^+$ Tm cells from RA PB were cocultured with medium or LPS-activated Mo in absence or presence of Iso or anti-CD147 mAb. Percentages of Th17, Th1 and Th17/Th1 cells **(B, D)** and levels of IL-17 and IFN-γ **(C, E)** are shown. **(F)** $CD4^+$ Tm cells from RA PB were cocultured with autologous Mo from PB (Mo (pb)), LPS-activated Mo from PB (Mo (pb/lps)) or Mo from SF (Mo (sf)), then Th17 cell percentage and IL-17 level are shown (n = 6). **(G–I)** $CD4^+$ Tm cells from RA PB were cocultured with medium or Mo from SF in absence or presence of Iso or anti-CD147 mAb. Representative plots **(G)** and quantitative results of intracellular expression of IL-17 and/or IFN-γ **(H)** in T cells, and IL-17 and IFN-γ levels in cell culture supernatants **(I)** were shown (n = 6). $^*P < 0.05$; $^{**}P < 0.01$; $^{***}P < 0.001$.

Anti-CD147mAb Treatment in RA Model

The *in vivo* effects of anti-mouse CD147mAb were studied using a mouse model of CIA (**Figure 5**). After first immunization, on day 21, mice were treated with anti-mouse CD147mAb or isotype control mAb every other day for 10 days (**Figure 5A**). In contrast to the isotype control mAb treatment, anti-CD147mAb treatment suppressed the increase in paw swelling (**Figure 5B**). The mean arthritis index of CIA mice was significantly reduced after 7 days of anti-CD147mAb treatment (**Figure 5C**). To observe the effect of anti-CD147mAb on Th17 responses, the peripheral blood, spleen and draining lymph node were collected and analyzed after anti-CD147mAb treatment. As shown in **Figure 5D**, the CIA mice expressed higher percentages of Th17 cells in the spleen and draining lymph nodes when compared with the normal mouse. Furthermore, Th17 cell levels in the spleen and draining lymph nodes were significantly decreased in anti-CD147mAb–treated CIA mice as compared to isotype mAb group (**Figure 5D**), whereas Th1 and Th17/Th1 cell levels were not significantly changed.

DISCUSSION

Numerous studies have suggested that Th17 cells and IL-17 play crucial roles in the chronic inflammatory response and subsequent tissue damage in RA (1–3). Indeed, targeting Th17 and IL-17 has been shown to ameliorate chronic inflammation in mouse RA models (24). In humans, anti-IL-17 therapy improved RA signs and symptoms (25). However, there are only limited data about

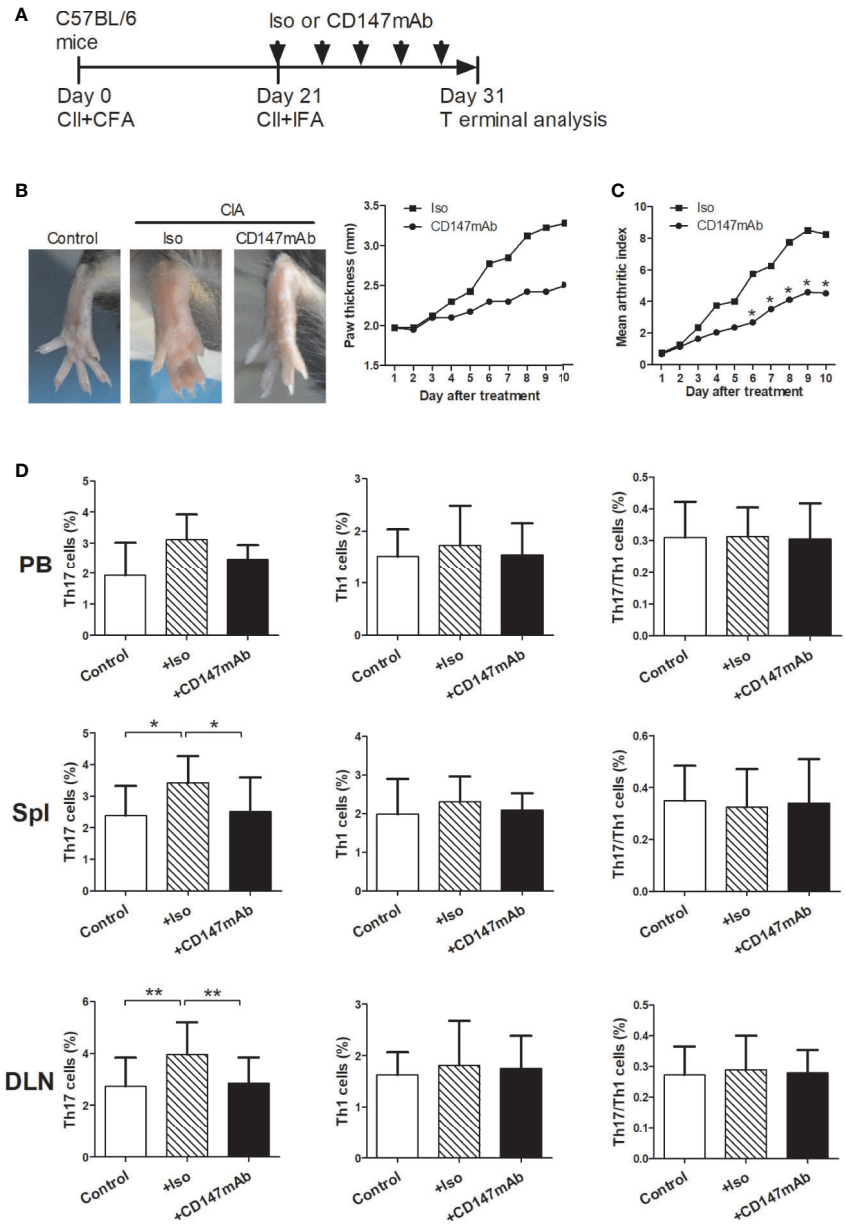

FIGURE 5 | Therapeutic effects of anti-CD147mAb in CIA model. **(A)** Experimental scheme for the analysis of CIA model. C57BL/6 mice were immunized on days 0 and 21, and treated with anti-mouse CD147 mAb (CD147 mAb) or isotype control mAb (Iso) at every other day for 10 days starting on day 21. **(B)** Representative hind paws from normal mice (Control), Iso and CD147 mAb treatment CIA mice (Day 31). The average thickness of both hind paws was measured (n = 4). **(C)** The mean arthritis index in CIA mice that were administrated Iso or CD147 mAb (n = 4). **(D)** Percentages of Th17, Th1 and Th17/Th1 cell in the PB, spleens (Spl) and draining lymph nodes (DLN) from Control and CIA mice treated with Iso or CD147 mAb (n = 4). $^{*}P < 0.05$; $^{**}P < 0.01$.

what drives human Th17 responses *in vivo*, particularly in human arthritic diseases. In this study, we provide evidence that CD147 expression was increased in IL-17–producing $CD4^+$ T cells, which in turn acts as a negative limitation loop to suppress human Th17 responses and inhibit the generation of Th17 cells in RA.

Firstly, we investigated the association between CD147 expression and Th17 cells in humans. In both HC and RA patients, CD147 expression on $CD4^+$ T cells was increased in $CCR6^+$ and $CD161^+$ fraction. Further, when $CD4^+$ T cells were split into two groups depending on their CD147 expression, IL-17 production was mainly restricted to $CD147^{++}$ subset in both the HC and RA patients. These phenotypic data suggest that CD147 expression on $CD4^+$ T cells closely correlated with Th17 cells in HC and RA groups. Therefore, similar to a study regarding mice (18), CD147 may suppress the extraordinary expansion of Th17 cells in human.

As previously reported (26), bulk $CD4^+$ T cells were cocultured with monocytes to induce Th17 responses. Our findings showed that Th17 cells were primarily induced by

cocultured $CD4^+$ Tm cells, but not $CD4^+$ naive T cells, with activated monocytes. As previously reported (8), activated monocytes relied on cell-contact with $CD4^+$ Tm cells to induce Th17 responses by performing transwell experiments (see online **Supplementary Figure S2**), suggesting membrane-derived signals are required in this process. Then we found that ligation of CD147 with its mAb in T cells impaired the Th17 responses induced from non-Th17-committed human Tm cells. Knocking down CD147 expression on $CD4^+$ Tm cells enhanced Th17 responses, but did not affect the Th1 responses. Therefore, these findings showed that anti-CD147 mAb is a stimulating Ab in this work, and CD147 probably plays a negative role in regulating human Th17 responses, but not Th1 responses.

The molecular mechanisms of Th17 responses have been intensively investigated, and numerous intracellular signaling pathways and transcriptional factors have been identified, including PI3K, Akt, mTOR, and STAT3. STAT3 plays a direct and crucial role in Th17 cell specification (27). Recent work has indicated that CD147 expressed in $CD4^+$ T cells inhibits Th17 cell differentiation by suppressing the IL-6/STAT3 pathway in mice (18). In humans, we demonstrated that ligation of CD147 with its mAb suppressed the STAT3 activation in $CD4^+$ Tm cells induced by coculture with LPS-activated monocytes. Further, mTOR plays an important role in STAT3 activation (28) and mTOR complex 1 (mTORC1) as a central regulator of Th17 lineage commitment by coordinating metabolic and transcriptional programs (22, 29, 30). There are mTOR complexes, including mTORC1 and mTORC2, working downstream and upstream of Akt (22). mTORC1 is activated by pAKT (T308) in a PI3K-dependent manner, whereas phosphorylation of AKT (S473) is mediated by the kinase mTORC2. Here, pS6K and p70S6 were used to assess mTORC1 and pAKT (S473) was used to assess mTORC2. Our data showed that ligation of CD147 with its mAb impairs the phosphorylation of pAKT (T308), pS6K, and p70S6, but not pAKT (S473). As previously reported, although CD147 may initiate proximal signaling molecules (such as LCK and CDK1) in T cells, the exact signaling pathway of CD147 is not fully clear in human (31). And the proximal signaling of CD147 in Th17 responses are still remain to be elucidated. What is more, augmenting the results reported in mice (18), our findings highlight the importance of metabolic activity in T cell fate decision, and indicate that the importance of the CD147-AKT-mTORC1-STAT3 pathway in the negative regulation of human Th17 responses.

Although Th17 cells play important roles in the pathogenesis of RA, Th17 responses are complex and incompletely understood in RA, particularly at the sites of inflammation. In this study, we examined the CD147 expression profile and monocyte-driven Th17 responses in patients with RA. Indeed, CD147 expression on $CD4^+$ Tm cells from RA SF was significantly higher than from HC PB and RA PB, which might partly explain why the monocyte-driven Th17 and Th17/Th1 responses were strongly decreased in $CD4^+$ Tm cells from RA SF. However, the monocyte-driven Th1 responses were significantly higher in RA SF than in RA PB and HC PB. These results are consistent with previous report (32), wherein Th17 cell percentage was decreased in the joints of patients with RA, but Th1 cells were more abundant in the joints. In agreement with the results of HC, anti-CD147 mAb inhibited the Th17 responses and IL-17 production induced by LPS-activated monocytes in patients with RA.

It was reported that *in vitro* LPS-activated monocytes exhibit a phenotype similar to that of *in vivo*-activated SF monocytes (1–3). As previous research reported (8), we found that *in vivo*-activated monocytes, from the local sites of inflammation, spontaneously induced Th17 responses in RA patients. Further, ligation of CD147 with its mAb specifically decreased *in vivo*-activated monocytes induced Th17 responses and IL-17 production, suggesting that CD147 is involved in the switch of Tm cells into Th17 cells at the site of inflammation in patients with RA. From another perspective, previous literatures reported by our and other teams suggested that CD147 has many ligands in tumor cells, erythrocytes or immunocytes, such as cyclophilin proteins, rhoptry-associated protein 2, integrins, and CD147 (33–35). However, the ligand of CD147 for inhibit Th17 responses in RA patients are still needed further investigations to explore. Consistent with our previous report (36), in the *in vivo* work, systemic administration of anti-CD147 mAb alleviated the severity of arthritis in CIA mice. Importantly, anti-CD147 mAb treatment simultaneously decreased the Th17 levels, but not Th1 and Th17/Th1, in the spleen and draining lymph node of CIA mice, supporting that anti-CD147mAb may improve CIA symptoms by specifically inhibiting Th17 responses. Therefore, it is reasonable to infer that in addition to Th17-cell depletion or IL-17 neutralization therapy, pharmacologic ligation of CD147 may be crucial for limiting the generation of pathogenic Th17 cells, and thus to attenuate the inflammatory response in patients with RA.

In summary, our data highlight the importance of CD147 in $CD4^+$ Tm cells and monocytes interactions in the shaping of Th17 responses. By suppressing STAT3 signaling, CD147 acts as a negative receptor on $CD4^+$ Tm cells to inhibit human Th17 responses. Ligation of CD147 with mAb may be a potential therapeutic approach in Th17-mediated diseases.

DATA AVAILABILITY STATEMENT

The raw data supporting the conclusions of this article will be made available by the authors, without undue reservation.

ETHICS STATEMENT

The studies involving human participants were reviewed and approved by Ethics Committee of Xijing Hospital. The patients/participants provided their written informed consent to participate in this study. The animal study was reviewed and approved by The Animal Experiment Administration Committee of the University.

AUTHOR CONTRIBUTIONS

JM, KZ, ZZ, and RZ performed most of the experiments and wrote the manuscript. PZ and ZC conceived the study and

revised manuscript. ML and NG participated in the experiments. YX and QH were in charge of patients' recruitment and clinical data collection. All authors contributed to the article and approved the submitted version.

FUNDING

This work was supported by the National Basic Research Program of China (No. 2015CB553704) and National Natural Science Foundation of China (No. 81801599).

ACKNOWLEDGMENTS

We thank Jia Li and Xianghui Fu for helping with the mouse model management.

SUPPLEMENTARY MATERIAL

The Supplementary Material for this article can be found online at: https://www.frontiersin.org/articles/10.3389/fimmu.2020.545980/full#supplementary-material

REFERENCES

1. van Hamburg JP, Tas SW. Molecular mechanisms underpinning T helper 17 cell heterogeneity and functions in rheumatoid arthritis. *J Autoimmun* (2018) 87:69–81. doi: 10.1016/j.jaut.2017.12.006
2. Furst DE, Emery P. Rheumatoid arthritis pathophysiology: update on emerging cytokine and cytokine-associated cell targets. *Rheumatol (Oxford)* (2014) 53:1560–9. doi: 10.1093/rheumatology/ket414
3. Lubberts E. The IL-23-IL-17 axis in inflammatory arthritis. *Nat Rev Rheumatol* (2015) 11:562. doi: 10.1038/nrrheum.2015.128
4. Singh SP, Zhang HH, Foley JF, Hedrick MN, Farber JM. Human T cells that are able to produce IL-17 express the chemokine receptor CCR6. *J Immunol* (2008) 180:214–21. doi: 10.4049/jimmunol.180.1.214
5. Maggi L, Santarlasci V, Capone M, Peired A, Frosali F, Crome SQ, et al. CD161 is a marker of all human IL-17-producing T-cell subsets and is induced by RORC. *Eur J Immunol* (2010) 40:2174–81. doi: 10.1002/eji.200940257
6. Evans HG, Suddason T, Jackson I, Taams LS, Lord GM. Optimal induction of T helper 17 cells in humans requires T cell receptor ligation in the context of Toll-like receptor-activated monocytes. *Proc Natl Acad Sci U S A* (2007) 104:17034–9. doi: 10.1073/pnas.0708426104
7. van Beelen AJ, Zelinkova Z, Taanman-Kueter EW, Muller FJ, Hommes DW, Zaat SA, et al. Stimulation of the intracellular bacterial sensor NOD2 programs dendritic cells to promote interleukin-17 production in human memory T cells. *Immunity* (2007) 27:660–9. doi: 10.1016/j.immuni.2007.08.013
8. Evans HG, Gullick NJ, Kelly S, Pitzalis C, Lord GM, Kirkham BW, et al. In vivo activated monocytes from the site of inflammation in humans specifically promote Th17 responses. *Proc Natl Acad Sci U S A* (2009) 106:6232–7. doi: 10.1073/pnas.0808144106
9. Foucher ED, Blanchard S, Preisser L, Descamps P, Ifrah N, Delneste Y, et al. IL-34- and M-CSF-induced macrophages switch memory T cells into Th17 cells via membrane IL-1alpha. *Eur J Immunol* (2015) 45:1092–102. doi: 10.1002/eji.201444606
10. DeCastro R, Zhang Y, Guo H, Kataoka H, Gordon MK, Toole B, et al. Human keratinocytes express EMMPRIN, an extracellular matrix metalloproteinase inducer. *J Invest Dermatol* (1996) 106:1260–5. doi: 10.1111/1523-1747.ep12348959
11. Muramatsu T. Basigin (CD147), a multifunctional transmembrane glycoprotein with various binding partners. *J Biochem* (2016) 159:481–90. doi: 10.1093/jb/mvv127
12. Pistol G, Matache C, Calugaru A, Stavaru C, Tanaseanu S, Ionescu R, et al. Roles of CD147 on T lymphocytes activation and MMP-9 secretion in systemic lupus erythematosus. *J Cell Mol Med* (2007) 11:339–48. doi: 10.1111/j.1582-4934.2007.00022.x
13. Wang CH, Yao H, Chen LN, Jia JF, Wang L, Dai JY, et al. CD147 induces angiogenesis through a vascular endothelial growth factor and hypoxia-inducible transcription factor 1alpha-mediated pathway in rheumatoid arthritis. *Arthritis Rheumatol* (2012) 64:1818–27. doi: 10.1002/art.34341
14. Koch C, Staffler G, Huttinger R, Hilgert I, Prager E, Cerny J, et al. T cell activation-associated epitopes of CD147 in regulation of the T cell response, and their definition by antibody affinity and antigen density. *Int Immunol* (1999) 11:777–86. doi: 10.1093/intimm/11.5.777
15. Chen R, Wang K, Feng Z, Zhang MY, Wu J, Geng JJ, et al. CD147 deficiency in T cells prevents thymic involution by inhibiting the EMT process in TECs in the presence of TGFbeta. *Cell Mol Immunol* (2020). doi: 10.1038/s41423-019-0353-7
16. Renno T, Wilson A, Dunkel C, Coste I, Maisnier-Patin K, Benoit DCA, et al. A role for CD147 in thymic development. *J Immunol* (2002) 168:4946–50. doi: 10.4049/jimmunol.168.10.4946
17. Staffler G, Szekeres A, Schutz GJ, Saemann MD, Prager E, Zeyda M, et al. Selective inhibition of T cell activation via CD147 through novel modulation of lipid rafts. *J Immunol* (2003) 171:1707–14. doi: 10.4049/jimmunol.171.4.1707
18. Maeda K, Kosugi T, Sato W, Kojima H, Sato Y, Kamimura D, et al. CD147/basigin limits lupus nephritis and Th17 cell differentiation in mice by inhibiting the interleukin-6/STAT-3 pathway. *Arthritis Rheumatol* (2015) 67:2185–95. doi: 10.1002/art.39155
19. Guo N, Zhang K, Lv M, Miao J, Chen Z, Zhu P. CD147 and CD98 complex-mediated homotypic aggregation attenuates the CypA-induced chemotactic effect on Jurkat T cells. *Mol Immunol* (2015) 63:253–63. doi: 10.1016/j.molimm.2014.07.005
20. Bevaart L, Vervoordeldonk MJ, Tak PP. Collagen-induced arthritis in mice. *Methods Mol Biol* (2010) 602:181–92. doi: 10.1007/978-1-60761-058-8_11
21. Tripathi SK, Chen Z, Larjo A, Kanduri K, Nousiainen K, Aijo T, et al. Genome-wide Analysis of STAT3-Mediated Transcription during Early Human Th17 Cell Differentiation. *Cell Rep* (2017) 19:1888–901. doi: 10.1016/j.celrep.2017.05.013
22. Nagai S, Kurebayashi Y, Koyasu S. Role of PI3K/Akt and mTOR complexes in Th17 cell differentiation. *Ann N Y Acad Sci* (2013) 1280:30–4. doi: 10.1111/nyas.12059
23. Walter GJ, Evans HG, Menon B, Gullick NJ, Kirkham BW, Cope AP, et al. Interaction with activated monocytes enhances cytokine expression and suppressive activity of human CD4+CD45ro+CD25+CD127(low) regulatory T cells. *Arthritis Rheumatol* (2013) 65:627–38. doi: 10.1002/art.37832
24. Lubberts E, Koenders MI, Oppers-Walgreen B, van den Bersselaar L, Coenen-de RC, Joosten LA, et al. Treatment with a neutralizing anti-murine interleukin-17 antibody after the onset of collagen-induced arthritis reduces joint inflammation, cartilage destruction, and bone erosion. *Arthritis Rheum* (2004) 50:650–9. doi: 10.1002/art.20001
25. Blanco FJ, Moricke R, Dokoupilova E, Codding C, Neal J, Andersson M, et al. Secukinumab in Active Rheumatoid Arthritis: A Phase III Randomized, Double-Blind, Active Comparator- and Placebo-Controlled Study. *Arthritis Rheumatol* (2017) 69:1144–53. doi: 10.1002/art.40070
26. Yang H, Wang J, Li Y, Yin ZJ, Lv TT, Zhu P, et al. CD147 modulates the differentiation of T-helper 17 cells in patients with rheumatoid arthritis. *Apmis* (2017) 125:24–31. doi: 10.1111/apm.12629
27. Hirahara K, Ghoreschi K, Laurence A, Yang XP, Kanno Y, O'Shea JJ. Signal transduction pathways and transcriptional regulation in Th17 cell differentiation. *Cytokine Growth Factor Rev* (2010) 21:425–34. doi: 10.1016/j.cytogfr.2010.10.006
28. Delgoffe GM, Kole TP, Zheng Y, Zarek PE, Matthews KL, Xiao B, et al. The mTOR kinase differentially regulates effector and regulatory T cell lineage

commitment. *Immunity* (2009) 30:832–44. doi: 10.1016/j.immuni.2009.04.014
29. Kurebayashi Y, Nagai S, Ikejiri A, Ohtani M, Ichiyama K, Baba Y, et al. PI3K-Akt-mTORC1-S6K1/2 axis controls Th17 differentiation by regulating Gfi1 expression and nuclear translocation of RORgamma. *Cell Rep* (2012) 1:360–73. doi: 10.1016/j.celrep.2012.02.007
30. Karmaus P, Chen X, Lim SA, Herrada AA, Nguyen TM, Xu B, et al. Metabolic heterogeneity underlies reciprocal fates of TH17 cell stemness and plasticity. *Nature* (2019) 565:101–5. doi: 10.1038/s41586-018-0806-7
31. Supper V, Hartl I, Boulegue C, Ohradanova-Repic A, Stockinger H. Dynamic Interaction- and Phospho-Proteomics Reveal Lck as a Major Signaling Hub of CD147 in T Cells. *J Immunol* (2017) 198:2468–78. doi: 10.4049/jimmunol.1600355
32. Takeshita M, Suzuki K, Kondo Y, Morita R, Okuzono Y, Koga K, et al. Multi-dimensional analysis identified rheumatoid arthritis-driving pathway in human T cell. *Ann Rheum Dis* (2019) 78:1346–56. doi: 10.1136/annrheumdis-2018-214885
33. Schmidt R, Bultmann A, Fischel S, Gillitzer A, Cullen P, Walch A, et al. Extracellular matrix metalloproteinase inducer (CD147) is a novel receptor on platelets, activates platelets, and augments nuclear factor kappaB-dependent inflammation in monocytes. *Circ Res* (2008) 102:302–9. doi: 10.1161/CIRCRESAHA.107.157990
34. Zhu X, Wang S, Shao M, Yan J, Liu F. The origin and evolution of Basigin (BSG) gene: A comparative genomic and phylogenetic analysis. *Dev Comp Immunol* (2017) 72:79–88. doi: 10.1016/j.dci.2017.02.007
35. Zhang MY, Zhang Y, Wu XD, Zhang K, Lin P, Bian HJ, et al. Disrupting CD147-RAP2 interaction abrogates erythrocyte invasion by Plasmodium falciparum. *Blood* (2018) 131:1111–21. doi: 10.1182/blood-2017-08-802918
36. Luan J, Zhang K, Yang P, Zhang Y, Feng F, Zhu YM, et al. The combination of FK506 and an anti-CD147 mAb exerts potential therapeutic effects on a mouse model of collagen-induced arthritis. *Mol Immunol* (2018) 101:1–9. doi: 10.1016/j.molimm.2018.05.013

Conflict of Interest: The authors declare that the research was conducted in the absence of any commercial or financial relationships that could be construed as a potential conflict of interest.

Copyright © 2020 Miao, Zhang, Zheng, Zhang, Lv, Guo, Xu, Han, Chen and Zhu. This is an open-access article distributed under the terms of the Creative Commons Attribution License (CC BY). The use, distribution or reproduction in other forums is permitted, provided the original author(s) and the copyright owner(s) are credited and that the original publication in this journal is cited, in accordance with accepted academic practice. No use, distribution or reproduction is permitted which does not comply with these terms.

frontiers in Immunology

ORIGINAL RESEARCH
published: 29 October 2020
doi: 10.3389/fimmu.2020.535010

Complement Expression and Activation in Osteoarthritis Joint Compartments

Elisa Assirelli[1]*, *Lia Pulsatelli*[1], *Paolo Dolzani*[1], *Erminia Mariani*[1,2], *Gina Lisignoli*[1], *Olga Addimanda*[3,4†] and *Riccardo Meliconi*[3,4]

[1] Laboratory of Immunorheumatology and Tissue Regeneration, Istituto di Ricovero e Cura a Carattere Scientifico (IRCCS) Istituto Ortopedico Rizzoli, Bologna, Italy, [2] Department of Medical and Surgical Sciences, Alma Mater Studiorum—University of Bologna, Bologna, Italy, [3] Medicine and Rheumatology Unit, IRCCS Istituto Ortopedico Rizzoli, Bologna, Italy, [4] Department of Biomedical and Neuromotor Sciences, Alma Mater Studiorum—University of Bologna, Bologna, Italy

Objective: To investigate complement(C) factors(F) and their activation fragments expression in OA joint tissues.

Design: Immunohistochemistry and quantitative imaging were performed to analyze C3, C4, and CF (factor) B expression on osteochondral biopsies (43 patients) collected during arthroplasty. Isolated chondrocytes and synoviocytes, cartilage and synovial tissues obtained from surgical specimens of OA patients (15 patients) were cultured with or without IL-1β. Real time PCR for CFB, C3, and C4 was performed. Culture supernatants were analyzed for C3a, C5a, CFBa, and terminal complement complex (TCC) production.

Results: In osteochondral biopsies, C factor expression was located in bone marrow, in a few subchondral bone cells and chondrocytes. C3 was the most expressed while factor C4 was the least expressed factor. Gene expression showed that all C factors analyzed were expressed both in chondrocytes and synoviocytes. In chondrocyte cultures and cartilage explants, CFB expression was significantly higher than C3 and C4. Furthermore, CFB, but not C3 and C4 expression was significantly induced by IL-1β. As to C activation factors, C3a was the most produced and CFBa was induced by IL-1β in synovial tissue. TCC production was undetectable in isolated chondrocytes and synoviocytes cell culture supernatants, whereas it was significantly augmented in cartilage explants.

Conclusion: C factors were locally produced and activated in OA joint with the contribution of all tissues (cartilage, bone, and synovium). Our results support the involvement of innate immunity in OA and suggest an association between some C alternative pathway component and joint inflammation.

Keywords: osteoarthritis, complement system, cartilage, synovium, joint tissue

OPEN ACCESS

Edited by:
Daniela Frasca,
University of Miami, United States

Reviewed by:
Jillian M. Richmond,
University of Massachusetts Medical School, United States
Natasa Strbo,
University of Miami, United States

****Correspondence:***
Elisa Assirelli
elisa.assirelli@ior.it

†Present address:
Olga Addimanda,
Programma Dipartimentale di Reumatologia, Dipartimento Medico, Azienda Unità Sanitaria Locale (AUSL) Bologna, Bologna, Italy

Specialty section:
This article was submitted to Autoimmune and Autoinflammatory Disorders, a section of the journal Frontiers in Immunology

Received: *14 February 2020*
Accepted: *05 October 2020*
Published: *29 October 2020*

Citation:
Assirelli E, Pulsatelli L, Dolzani P, Mariani E, Lisignoli G, Addimanda O and Meliconi R (2020) Complement Expression and Activation in Osteoarthritis Joint Compartments. Front. Immunol. 11:535010. doi: 10.3389/fimmu.2020.535010

INTRODUCTION

Local and systemic low-grade inflammation is recognized as one of the major triggering factors in Osteoarthritis (OA) pathogenesis in combination with age, biomechanical stress, and metabolic derangement (1–3). While systemic inflammation is strictly associated with ageing ("inflammaging") (4) and metabolic alterations, local inflammation is more related to biomechanical stress and traumatic events (5).

Inflammation in OA joints is mainly the result of the activation of the innate immunity response which involves different cells such as macrophages, synoviocytes, chondrocytes, bone cells, and various soluble molecules (6). One of the main molecular pathways in innate immunity is the Complement system, which intervenes in several responses such as leukocyte chemotaxis, microorganism opsonization, phagocytosis, and cell lysis (7).

Complement proteins are synthetized in the liver and by immune cells, but other cell lineages (eg, skin cells, astrocytes, and glia cells, muscles cells) (8) are also involved in physiological and pathological production and activation of complement factors. Complement activation proceeds through three distinct pathways: the classical, the lectin (mannose-activated) and the alternative pathway which converge in the cleavage of C3 component by C3 convertase. This cleavage results in the formation of C5 convertase which in turn activates C5 with the formation of C5b, the first component of C5b-9 complex, known as Terminal Complement Complex (TCC) or Membrane Attack Complex (MAC), responsible for cell lysis (9). However, a large number of non-lytic functions (such as the release of pro-inflammatory cytokines and chemokines or the expression of Platelet-derived or b-Fibroblast growth factors) can result by the generation of C5b-9. During this process, the production of potent inflammatory fragments (C3a and C5a) amplify the inflammatory response by binding to the cognate receptors on several target cells (10).

In addition to its physiological role in infection defense and in removal of tissue damage derived debris, Complement exerts pathological functions in several diseases characterized by chronic inflammation. It is well known its role in inflammatory arthritides and connective tissue disorders, while more recently complement activation has been involved in OA pathomechanisms (5, 10–13).

In this study we aimed at elucidating the different contributions of OA patient joint tissues in the production of alternative and classical Complement pathway factors and at evaluating any local activation of Complement. Thereof, the central molecule C3, the classical pathway molecule C4 and the alternative pathway molecule Factor B (CFB) were assessed in different tissue compartments of OA patient joints. Then the activation fragments generated in the same tissues as well as C5b-C9 complex and the role of IL-1β in these processes were also evaluated.

We found that CFB was the most expressed component followed by C3, that the activation fragments C3a, C5a, and CFBa were produced *in vitro* mainly by isolated chondrocytes and that TCC was mainly produced by cartilage tissue and to a lesser extent by synovial tissue.

MATERIALS AND METHODS

This study was approved by the ethical committee of the Rizzoli Orthopaedic Institute and written informed consent was obtained from the patients. The procedures were in accordance with the ethical standards of the responsible committee on human experimentation (institutional and national) and with the Helsinki Declaration of 1975, as revised in 2013.

Osteochondral Biopsies: Histologic Score and Immunohistochemistry Analysis of C3, C4, and CFB

Full-thickness osteochondral biopsies were collected (14) from 43 patients, 16 with OA (9 males, 7 females; mean age, 67 years; range, 59–75 years), 12 with Rheumatoid Arthritis (RA) (12 females; mean age, 65 years; range, 22–85 years) and 15 Post-traumatic patients (PT) (7 males, 8 females; mean age, 64 years; range, 24–82 years), undergoing knee, hip or shoulder arthroplasty.

Briefly, osteochondral biopsies were fixed, embedded in paraffin, sliced in serial sections (5 μm thick) by a microtome and stained with hematoxylin-eosin and Safranin O fast green, as previously described (15).

The severity of cartilage damage was assessed using Mankin score evaluation (16) and immunohistochemistry analysis was used to evaluate C3, C4 and CFB positive cells across cartilage and bone. Sections were heated overnight at 56°C, rehydrated, and incubated with primary antibodies (Santa Cruz biotech, Dallas, USA) against C3 (at a concentration of 2.5 μg/ml), C4 (at a concentration of 0.5 μg/ml) and CFB (at a concentration of 12.5 μg/ml). Signals were developed with a biotin/streptavidin amplified, alkaline phosphatase-based detection system (Biocare Medical, Pacheco, CA, USA) with fuchsin as a substrate. After nuclear counterstaining with hematoxylin, sections were mounted in glycerol gel and stored for subsequent analysis. Sections of each biopsy were processed as negative controls, according to the above-described procedure, omitting the primary antibody. Specificity was assessed by appropriate isotypic control at the concentration of the corresponding primary antibody.

Semi-quantitative image analysis of immunohistochemistry stained slides was performed on optical microscope fields (20× objective lens) for each section. The analysis was performed using Red/Green/Blue (RGB) with Software NIS-Elements and Eclipse 90i microscope (Nikon Instruments Europe BV) equipped with a CCD camera (dimension of the sensor 2/3 inches) 104 mounted on 0.7× C-mount. Imaging analysis results were expressed as percentages of positive area in the section analyzed.

Tissue Explants

Ex vivo cartilage and synovium tissue explants were obtained from 15 patients with knee OA (6 males, 9 females; mean age, 72 years; range, 60–83 years) undergoing joint replacement surgery. Cartilage and synovium tissues were weighted and seeded in 24-well plates, one specimen per well.

Chondrocyte Isolation

Chondrocytes were isolated by sequential enzyme digestion after cartilage fragmentation as previously detailed (17) and incubated

in DMEM medium (SIGMA, Sigma Aldrich, St. Louis, USA) supplemented with 100 U/ml penicillin, 100 µg/ml streptomycin (Invitrogen, Carlsbad, CA, USA) 10% FBS (GIBCO, Thermo Fisher Scientific, NY, USA) for 24 h at 37°C with 5% CO2 in a humidified atmosphere. High-density chondrocyte cultures were seeded at 250,000 cells per well in 24-well plates.

Synoviocyte Isolation

Synovial membrane specimens were finely minced. Tissue fragments were seeded in petri dishes and maintained with OPTIMEM (GIBCO, Thermo Fisher Scientific, NY, USA) culture medium supplemented with 100 U/ml penicillin, 100 µg/ml streptomycin (Invitrogen, Carlsbad, CA, USA), 10% FBS (GIBCO, Thermo Fisher Scientific, NY, USA) for about 10 days at 37°C with 5% CO2 in a humidified atmosphere (18). The cells were then maintained into culture flasks and all experiments were performed on cells obtained between the third and fifth passage. Synoviocytes were seeded at 200,000 cells per well in 24-well plates.

In Vitro Stimulation

Tissue explants and isolated cells were all maintained with appropriate culture medium prepared as described above, but without serum (starvation conditions) for 24 h and then they were stimulated with 2 ng/ml of rhIL-1β (R&D Systems, Minneapolis, USA). Optimal IL-1β concentration and incubation time for detecting complement factor production were previously determined by dose-dependent and kinetic experiments (not shown). After 24 h of incubation, culture supernatants (both unstimulated and stimulated) were collected and maintained at −80°C until analysis. Cartilage tissue explants and isolated chondrocytes were analyzed to elucidate the role of cartilage matrix components and the ability of isolated chondrocytes to produce complement factors. Synovial tissue (comprising both synovial macrophages and fibroblast like synoviocytes-FLS) and isolated FLS alone were analyzed to discriminate the contribution of both cell type to complement production. RNA was extracted from isolated cells by a direct lysis in the culture plates. Tissue explants were frozen and maintained in liquid nitrogen until RNA extraction. For this purpose, frozen samples were pulverized with the grinding mill Mikro-Dismembrator S (Sartorius Stedim Italy SpA, Italy) in 5 ml PFTE shaking flasks with a stainless-steel grinding ball.

Real-Time, Quantitative Reverse Transcriptase Polymerase Chain Reaction (RT-PCR)

Total cellular RNA was extracted using TRIZOL reagent (INVITROGEN, Life Technologies, NY, USA) following the protocol recommended by the manufacturer. RNA was reverse transcribed using SuperScript VILO cDNA Synthesis kit (INVITROGEN, Life Technologies, NY, USA), following manufacturer's instructions. RNA specific primers for PCR amplification (**Table 1**) were generated from GeneBank sequences using the NCBI primer-Blast tool. Real-time PCR was run on the LightCycler Instrument (Roche S.p.A, Monza, Italy) using the SYBR Premix Ex Taq (TAKARA Biomedicals; Tokyo, Japan) with the following protocol: 95°C for 10 s, followed by 45 cycles at 95°C for 5 s and 60°C for 20 s and the increase in PCR product was monitored for each amplification cycle by measuring the increase in fluorescence due to the binding of SYBR Green I Dye to dsDNA. The crossing point values were determined for each sample and specificity of the amplicons was confirmed by melting curve analysis. Amplification efficiency of each amplicon was evaluated using 10-fold serial dilutions of positive control cDNAs and calculated from the slopes of log input amounts plotted versus crossing point values. They were all confirmed to be high (>92%) and comparable; mRNA levels for each target gene were calculated normalized (ratio) to glyceraldehyde-3 phosphate dehydrogenase (GAPDH, reference gene), according to the ΔΔCt method and expressed as "Number of molecules per 100,000 GAPDH".

TABLE 1 | List of primers used in Real-Time PCR.

Gene		Primer Sequence	Ta (°C)
Gapdh	Forward	CCTGGCCAAGGTCATCCATG	60
	Reverse	CGGCCATCACGCCACAGTT	
C3	Forward	TCAACCACAAGCTGCTACCC	60
	Reverse	CTGGCCCATGTTGACGAGTT	
CFB	Forward	GGGGTAGAGATCAAAGGCGG	60
	Reverse	TGGATTGCTCTGCACTCTGC	
C4	Forward	GGGTTTGGTGGGCAATGATG	60
	Reverse	GAGGCTTCCACTCTCTGCTT	

Complement Activation Fragment Concentrations

Complement fragment C3a, C5a, CFBa, and complex C5b-9 concentrations were evaluated in culture supernatants obtained both from tissues and isolated chondrocytes and synoviocytes by using commercial kits (C3a and C5b-9 Elabscience E.L.I.S.A. kit, Houston, TX, USA; C5a Origene E.L.I.S.A. kit, Rockville, MD, USA; CFBa Quidel E.L.I.S.A. kit, San Diego, CA, USA) following the manufacturer's instructions. Factor concentration was normalized for milligram (mg) of tissue or for 100,000 cell number as appropriate.

Statistical Analysis

Data were expressed as medians, interquartile ranges and minimum to maximum values. The Kolmogorov Smirnov test was performed to test normality of continuous variables. The Friedman ANOVA test with Dunn's correction was used to compare Complement factor staining positivity within each disease and Kruskal-Wallis test with Dunns correction was performed to compare a single Complement factor among diseases. The Spearman Correlation test was used to assess the correlation between the staining positivity of each complement factor and the Mankin score. The General Linear Mixed Models analysis with Complement factors as dependent variables, articular tissue types and IL-1β stimulus as fixed effects and age as covariate were used to assess the influence of articular tissue type and IL-1β stimulus alone or combined on modifications of the analyzed factors. Wilcoxon matched paired test with Bonferroni correction for multiple

comparisons was used to compare the production of complement factor activation fragments. A p value <0.05 was considered significant. Statistical analysis was performed using SPSSv.19.0 (IBM Corp., Armonk, NY, USA) and GraphPad prism for Windows, version 5.01 (Nashville, TN, USA).

RESULTS

C3, C4, and CFB Staining on Osteochondral Biopsies

Complement factors staining was mainly located in the bone marrow, with positive areas widespread among bone trabeculae and adipose tissue, whereas cartilage positivity was found only in few samples (**Figure 1**). Semi-quantitative image analysis of immunohistochemical staining showed that C3 was more expressed than C4 in OA and PT patients (C3 vs C4 p<0.0001 either in OA and PT). In PT patients also CFB was more expressed than C4 (p<0.0001). No difference was observed between C3 and CFB staining in OA and PT. In RA patients, even if the expression trend of C3, C4 and CFB appeared similar to that observed in OA and PT groups, no difference among these factors was observed.

Both C3 and CFB expressions were significantly augmented in PT compared to OA patients (p< 0.05), furthermore CFB was also more expressed in PT than in RA patients (p<0.05) (**Figure 1**). C3 and CFB were similar in both OA and RA, whereas C3 was similar in RA and PT.

C4 expression appeared almost negligible, except some sporadic cases, and similarly expressed in all patient groups. Complement factors expression did not correlate with Mankin score, as determined by Spearman Correlation test and no differences were found among different joints (data not shown).

Complement Factor Gene Expression in Cartilage Tissue, Chondrocytes, and Synoviocytes

Cartilage tissue as well as isolated chondrocytes and synoviocytes spontaneously expressed complement factor genes of both the classical and alternative ways, even if in different amounts (**Figure 2**).

IL-1β pro-inflammatory stimulus enhanced only CFB gene expression, either in cartilage tissue (p=0.021) and in isolated chondrocytes and synoviocytes (p=0.038 and p=0.030 respectively). On the contrary, C3 and C4 basal gene expression was not up-modulated by IL-1β stimulation (**Figure 2**).

Furthermore, the influence of tissue type on gene expression of the three analyzed factors in both unstimulated and IL-1β–stimulated conditions was observed.

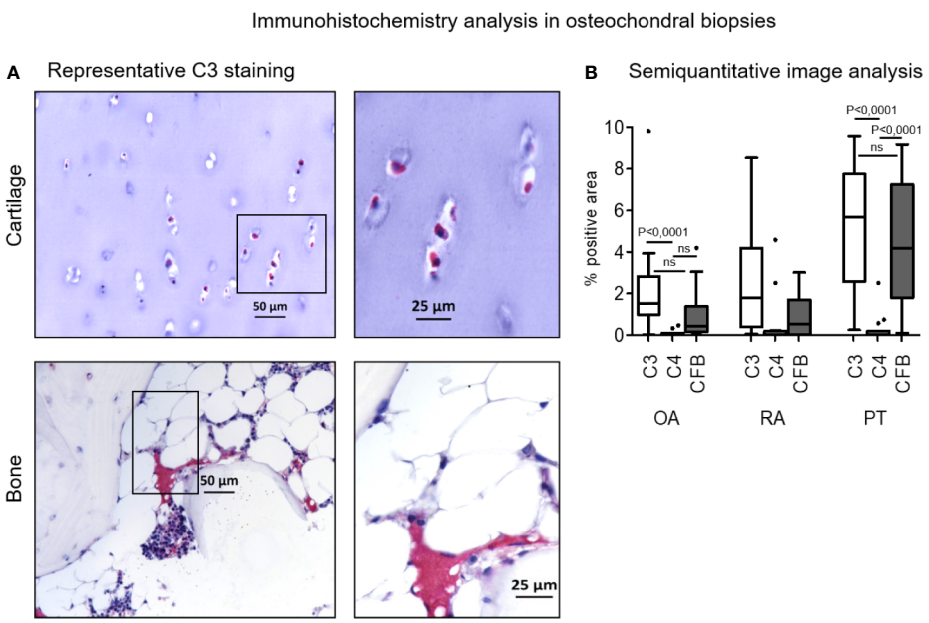

FIGURE 1 | Immunohistochemistry analysis of C3, C4, CFB in osteochondral biopsies. **(A)** Bone and cartilage C3 representative staining positivity (original magnification, 10× scale bar, 50 µm and 20×; scale bar, 25 µm). Red staining for positive cells, counterstaining with hematoxylin in purple. **(B)** Image analysis of C3, C4 and CFB in osteochondral biopsies: Osteoarthritis (OA), Rheumatoid Arthritis (RA), Post Traumatic cases (PT). Results are expressed as median (bars), interquartile ranges (boxes), minimum to maximum values (whiskers) and outliers (solid circles). Comparison among C factors within patient groups showed statistical significance in OA patients (C3 vs C4, p<0.0001) and PT patients (C3 vs C4 and C4 vs CFB, p<0.0001). Comparison among patient groups within C factors. C3 factor: OA vs RA and RA vs PT, not significant; OA vs PT, p<0.05. C4 factor: OA vs RA, RA vs PT and OA vs PT, not significant. CFB factor: OA vs RA, not significant; RA vs PT and OA vs PT, p<0.05.

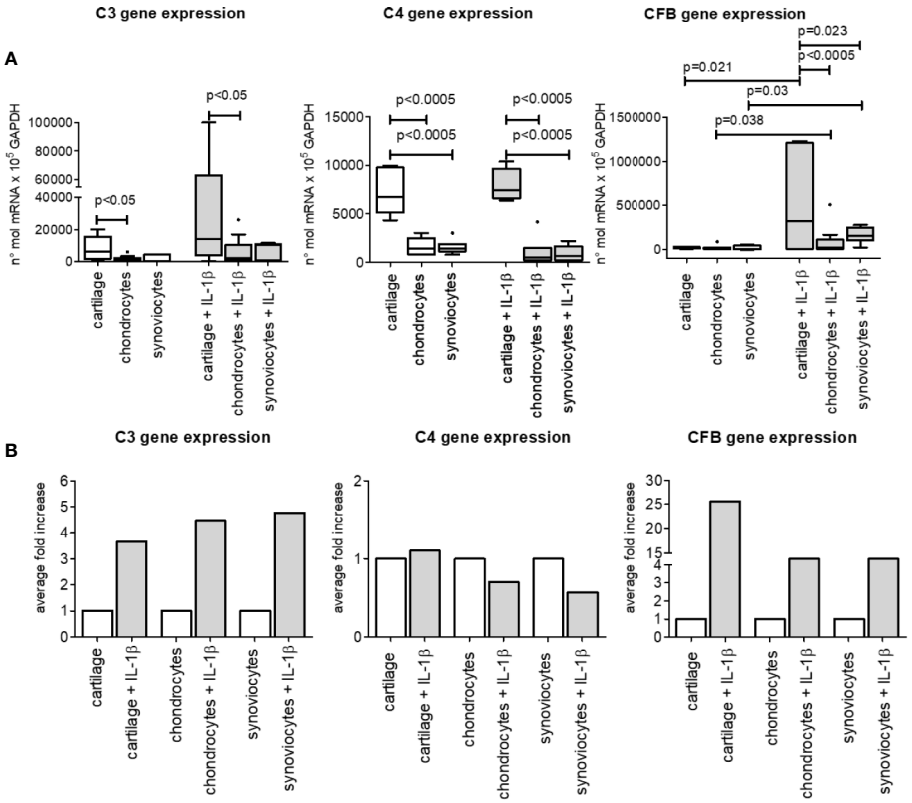

FIGURE 2 | C3, C4, and CFB gene expression in OA cartilage tissue, isolated chondrocytes and isolated synoviocytes. **(A)** Relative amount of gene expression. Results are expressed as median (bars), interquartile ranges (boxes), minimum to maximum values 542 (whiskers) and outliers (solid circles). Only statistically different comparisons where indicated. **(B)** Average fold increase in respect to unstimulated samples. Bars indicates average mean.

Indeed, C3 gene basal expression as well IL-1β–stimulated one was higher in cartilage tissue than in isolated chondrocytes ($p<0.05$), whereas no difference was found between cartilage tissue and isolated synoviocytes both in basal and stimulated conditions (**Figure 2**).

As to C4 gene, besides its different expression between cartilage and isolated chondrocytes ($p<0.0005$, both in unstimulated and stimulated conditions), it also showed a greater expression in cartilage than in isolated synoviocytes ($p<0.0005$, both in unstimulated and stimulated conditions).

No difference in C3 and C4 gene expression was observed between isolated chondrocytes and synoviocytes, whatever unstimulated or stimulated.

CFB gene expression was similar in all types of unstimulated samples analyzed (**Figure 2**), on the contrary under the IL-1β–stimulated conditions, CFB gene was more expressed in cartilage tissue than in isolated chondrocytes ($p<0.0005$) and synoviocytes ($p=0.023$). No CFB gene differences were observed between isolated chondrocytes and synoviocytes stimulated with IL-1β (**Figure 2**).

The comparison among C3, C4 CFB gene expressions to evaluate the most expressed factor independently of articular compartment, as determined by General Linear Model analysis, evidenced that CFB was the most expressed factor, followed by C3 and by C4 (CFB vs C3 and vs C4, $p<0.0005$; C3 vs C4, $p<0.02$), (data not shown).

Release of Activation Fragments in Culture Supernatants of Cartilage and Synovium Tissues and of Isolated Chondrocytes and Synoviocytes

Cartilage and synovium tissues (**Figure 3A**), isolated chondrocytes and synoviocytes (**Figure 3B**) were all able to spontaneously release complement activation fragments (C3a, C5a, CFBa) in culture supernatants, even if at very variable concentrations.

C3a was the most produced among activation factors independently of the sample type (**Figures 3A, B**) followed by CFBa, whereas C5a release was the lowest.

On the contrary, C5b-9 complex release was only detectable in culture supernatants of cartilage and synovium tissues (**Figure 3A**) but was below the detection limit when evaluated in culture supernatants obtained from isolated chondrocytes and synoviocytes (**Figure 3B**).

IL-1β did not influence activation fragment release but the CFBa up-modulation in synovium tissue ($p=0.002$) (**Figure 3A**)

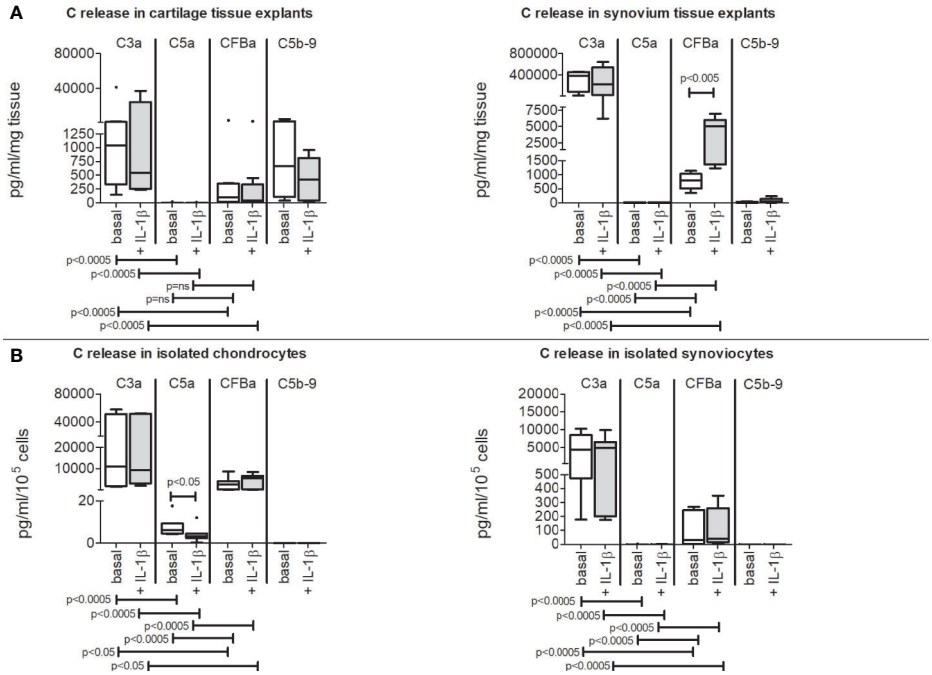

FIGURE 3 | Release of C3a, C5a, CFBa activation fragments and C5b-9 complex from OA patients. Results are expressed as median (bars), interquartile ranges (boxes), minimum to maximum values (whiskers) and outliers (solid circles). Where not indicated, the comparisons are not significant. **(A)** Cartilage and synovium tissue culture supernatants. **(B)** Isolated chondrocyte and synoviocyte culture supernatants.

and for C5a down-modulation in isolated chondrocytes (p=0.038) (**Figure 3B**).

The comparison of the release of C3a, C5a, CFBa fragments between cartilage and synovium tissues, as determined by General Linear Model analysis, showed that all these factors were more concentrated in synovium tissue supernatants (p<0.0002 at least) (**Figure 4A**). Conversely, the results obtained by comparing isolated cells showed higher release of activation fragments by isolated chondrocytes (p<0.05) (**Figure 4B**).

DISCUSSION

In this study, the contribution of the different joint tissues (cartilage, synovium and bone) in producing components of the Complement system was evaluated. We found that C3, C4, and CFB complement factors were expressed by all joint tissues.

Immunohistochemical staining in osteochondral biopsies from OA, RA and PT patients showed a similar pattern, with C3 and CFB more expressed than C4. This expression was mainly located in the bone marrow portion of the osteochondral biopsies, where it could contribute to sustain bone inflammation and bone marrow edema, that is one of the pathological hallmark of OA (19).

A newly found potential trigger of innate immunity in OA is Gut Microbioma (GM). In a very recent study, Dunn and colleagues provided the first evidence of microbial nucleic acid signatures in human and mouse cartilage tissue. Interestingly they found an increase in gram-negative constituents in OA cartilage compared to control cartilage (20) GM was firstly detected in synovial fluid of OA patients, but it is hypothesized that it could reach subchondral cartilage through blood vessels located in subchondral bone tide mark, at the interface between bone and cartilage. In fact, osteochondral plate angiogenesis occurring early in OA could facilitate transient migration of still living bacteria or some of their products up to the deeper layers of cartilage (21). Bacterial DNA is strongly immunogenic and together with lipopolysaccharide produced by gram-negative constituents can prime the proinflammatory innate immune response in joints, activating innate immunity both through Toll Like Receptors (which are up-regulated in OA) and complement system activation. Complement factors were more expressed in osteochondral biopsies from PT patients, in agreement with described trauma-related activation of complement cascade due to the release of damage-associated molecular patterns (DAMPs) by injured tissues (22). Since trauma is an event potentially leading to OA development, it would be interesting, in light of these results, to analyze post-traumatic patients that have actually developed OA, also in relation to the expression level of complement factors.

Gene expression in cartilage tissue and isolated chondrocytes and synoviocytes from OA knees, confirmed the immunohistochemical results: C3 and in particular CFB were more expressed than C4, thus demonstrating a major *in situ* generation of the main molecules involved in alternative complement activation pathway.

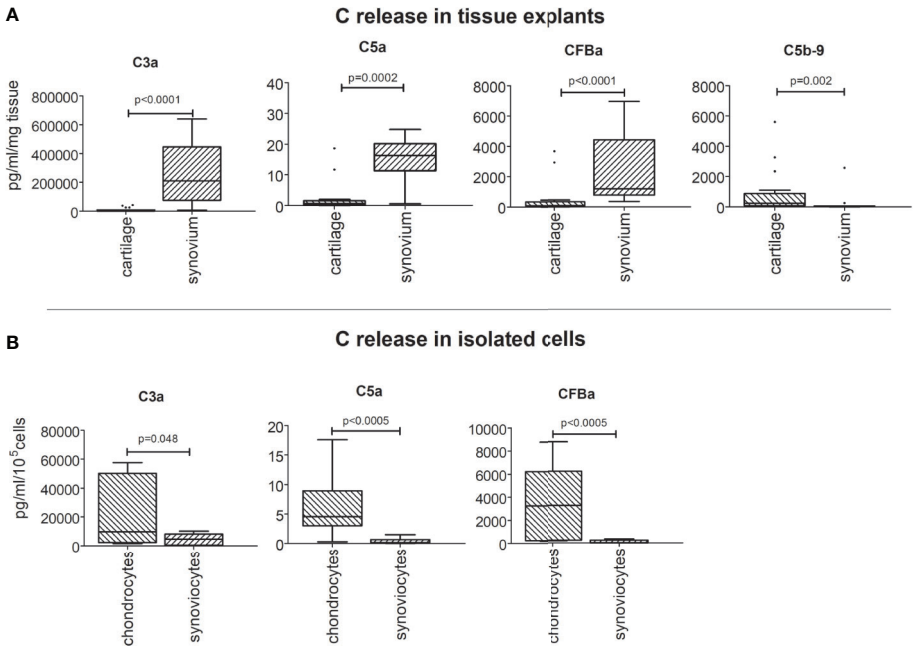

FIGURE 4 | Comparison of C3a, C5a, CFBa fragment release between cartilage and synovium tissues **(A)**, and between isolated chondrocytes and synoviocytes **(B)**. Results are expressed as median (bars), interquartile ranges (boxes), minimum to maximum values (whiskers) and outliers (solid circles).

In addition, the prevalent expression of C3 and CFB genes in cartilage tissue compared to isolated chondrocytes and synoviocytes, supports the hypothesis that endogenous extracellular matrix (ECM) components are able to stimulate Complement factor expression.

Cartilage oligomeric matrix protein (COMP), a family of extracellular matrix proteins, also known as thrombospondin-5 (TSP-5), is recognized as particularly relevant in OA pathogenesis. Indeed, COMP serum concentrations were found increased in patients with early signs of cartilage damage (23) and correlated with synovial fluid concentrations (24). In addition, COMP serum levels were associated with the development of pain and radiographic knee signs of OA (25). Interestingly, COMP exerts a dual effect on the complement cascade as it can inhibit both the classical and lectin pathways by binding C1q and, at the same time, it can activate the alternative pathway by binding C3 and properdin. Finally, elevated levels of COMP-C3b complex has been found in OA synovial fluid (26, 27).

Besides COMP, other cartilage ECM components can interact with complement factors or activate complement cascade such as: Collagen II-containing immune-complexes (28), Hyaluronan intra-articular therapeutic injections (29) and DAMPs derived from OA tissue debris (30).

The different amounts of C3a, C5a, CFBa activation fragments detected in cartilage and synovium tissues as well as in isolated chondrocyte and synoviocyte cultures evidenced that Complement activation may take place without the need for parent molecules coming from blood stream.

We found higher production of activation fragments in culture supernatants of synovium tissue compared to cartilage one, whereas the opposite was observed in culture supernatants of isolated chondrocytes and synoviocytes. In these conditions higher concentration of complement activation fragments was produced by isolated chondrocytes, in agreement with previous observations demonstrating that complement proteins were synthesized locally by chondrocytes and upregulated in OA joint (12).As to the conflicting results on synovium when analyzed as a whole tissue or as isolated synoviocytes, it must be considered that synovium tissue comprises specialized resident Fibroblast-Like Synoviocytes (FLSs) that are interspersed with macrophages (31).

Accordingly, we can speculate that the difference in complement activation fragment production may due to the progressive loss of the macrophage component in cultures of isolated synoviocytes and the resulting FLS enrichment, due to *in vitro* passages (32). If, on the one hand, macrophages, as part of the innate immune system arm, were already known to produce complement factors (33) on the other, to the best of our knowledge, this study first showed that human primary fibroblast-like synoviocytes from OA patients also contributed to C activation factors production, in line with their known role in synovitis (34). However, it cannot be excluded that the normalization of the results by weight of tissue, not taking in account the cellularity characteristics between cartilage and synovium, may have caused an overestimation in the whole synovium.

In addition, C3a and C5a are also involved in the onset of pain (10) and in our model a greater release of C3a than C5a was observed, suggesting a major C3a responsibility in the development of pain. If antagonists for the respective receptors are possible candidates for the treatment of this symptom, the blockade of the C3a fragment receptor could probably be more promising,

considering also C3 key position at the crossing between classical and alternative Complement pathways (35, 36). However, since C3a and C5a are also chemotactic for bone marrow–derived hematopoietic stem cells and mesenchymal stem cells (MSC) (37–39), the inhibition of specific receptors could prevent MSC trafficking, thus negatively influencing OA cartilage repair and bone remodeling (40, 41).

Similarly to single activation factors, also C5b-9 complex displayed paradoxical results being present only in tissue cultures (both cartilage and synovium), suggesting that extracellular matrix components are also able to influence the Terminal-Complement Complex formation as evidenced for the initial steps of the Complement cascade.

TCC is important in mediating chondrocyte death in OA or (in sub-lytic amount) in activating signaling pathways that drive the expression of catabolic and pro-inflammatory molecules (10). In particular, it increases the chondrocytes' expression of multiple genes encoding cartilage-degrading enzymes (MMPs- and ADAMTSs), inflammatory cytokines and chemokines as well as the expression of other complement effectors. Therefore, both cartilage and synovium tissues can synergistically produce Complement activation factors, thus amplifying pathogenic complement signaling in osteoarthritis (42).

As concerning the effect of IL-1β stimulation, we noted that its action favored the alternative way of Complement by up-modulating both CFB gene expression in all experimental settings and CFBa fragment release in synovium tissue.

Concurrently, IL-1β decreased C5a fragment production in isolated chondrocytes cultures but was totally irrelevant for the other Complement activation fragments analyzed. IL-1β is a pleiotropic cytokine involved in many inflammatory pathways and it is considered an important player in cartilage degradation although the exact contribution of IL-1β to joint destruction *in vivo* remains controversial. Indeed, a recent study showed the non-involvement of IL-1β in synovial inflammation and cartilage destruction during collagenase-induced OA and it was suggested that other inflammatory mediators (possibly the alarmins, IL-6 and IL-17) could be responsible for the joint damage (43, 44). In agreement, in a recent study performed in a translational model, complement factor B was upregulated in IL-17A–treated cartilage explant (45).

Finally, Osteoarthritis treatment with IL-1β inhibitors was not fully satisfactory, thus resizing the role of this interleukin in OA pathogenesis (46–48). Lastly, we cannot exclude that the different response to stimulation with IL-1β in the analyzed tissues may also in part depend on the various distribution of IL-1 receptors in cartilage, synovium and isolated chondrocytes and synoviocytes (49).

Overall the results of this study indicate a higher expression of factors belonging to alternative Complement Pathway. A pivotal role of the alternative way was suggested in chondrocyte transformation and terminal differentiation during endochondral ossification (a fundamental step in OA progression, leading to osteophyte formation), based on the localization of C3, CFB and properdin (a positive regulator of complement alternative pathway) in resting and in hypertrophic zone of cartilage (50).

Furthermore C3f, a fragment released by catabolic degradation of C3b by Factor H, a regulator of alternative pathway of complement (51) has been identified as specific biomarker for OA, pointing out the prevailing involvement of the Complement alternative way in Osteoarthritis.

Recently, the role of the alternative pathway was validated by the demonstration of a local expression of adipsin (a component of the alternative complement way) in OA joint tissues and by the association between adipsin and synovial membrane inflammation and cartilage damage through the activation of complement (52). In conclusion, this study concurs to the accumulating evidences concerning the involvement of the innate immune response in the pathogenesis and progression of OA and suggests an association between some C alternative pathway component and joint inflammation, possibly suggesting complement as a future therapeutic target for patients with Osteoarthritis.

DATA AVAILABILITY STATEMENT

The datasets generated for this study are available on request to the corresponding author.

ETHICS STATEMENT

The studies involving human participants were reviewed and approved by Rizzoli Orthopedic Institute ethic committee, IRCCS Istituto Ortopedico Rizzoli, Bologna, Italy. The patients/participants provided their written informed consent to participate in this study.

AUTHOR CONTRIBUTIONS

All authors contributed to the article and approved the submitted version. EA, LP, and RM conceived and designed the study. EA, PD, and OA performed the experiments. LP, EA, EM, and RM drafting of the article. GL and EM critically revised the article for important intellectual content.

FUNDING

This research was funded by Italian Health Ministry "5 per mille funds" and by Bologna University RFO funds.

ACKNOWLEDGMENTS

The authors thank Elettra Pignotti for performing statistical analysis.

REFERENCES

1. Felson DT. Obesity and Knee Osteoarthritis. *Ann Intern Med* (1988) 109:18. doi: 10.7326/0003-4819-109-1-18
2. Guilak F. Biomechanical factors in osteoarthritis. *Best Pract Res Clin Rheumatol* (2011) 25:815–23. doi: 10.1016/j.berh.2011.11.013
3. Sokolove J, Lepus CM. Role of inflammation in the pathogenesis of osteoarthritis: latest findings and interpretations. *Ther Adv Musculoskelet Dis* (2013) 5:77–94. doi: 10.1177/1759720X12467868
4. Millerand M, Berenbaum F, Jacques C. Danger signals and inflammaging in osteoarthritis. *Clin Exp Rheumatol* (2019) 37:48–56.
5. Robinson WH, Lepus CM, Wang Q, Raghu H, Mao R, Lindstrom TM, et al. Low-grade inflammation as a key mediator of the pathogenesis of osteoarthritis. *Nat Rev Rhematol* (2016) 12:580–92. doi: 10.1038/nrrheum.2016.136
6. Haseeb A, Haqqi TM. Immunopathogenesis of osteoarthritis. *Clin Immunol* (2013) 146(3):185–96. doi: 10.1016/j.clim.2012.12.011
7. Sarma JV, Ward PA. The complement system. *Cell Tissue Res* (2011) 343:227–35. doi: 10.1007/s00441-010-1034-0
8. Morgan BP, Gasque P. Extrahepatic complement biosynthesis: Where, when and why? *Clin Exp Immunol* (1997) 107:1–7. doi: 10.1046/j.1365-2249.1997.d01-890.x
9. Nesargikar P, Spiller B, Chavez R. The complement system: History, pathways, cascade and inhibitors. *Eur J Microbiol Immunol* (2012) 2:103–11. doi: 10.1556/eujmi.2.2012.2.2
10. Silawal S, Triebel J, Bertsch T, Schulze-Tanzil G. Osteoarthritis and the complement cascade. *Clin Med Insights Arthritis Musculoskelet Disord* (2018) 3:11. doi: 10.1177/1179544117751430
11. Ritter SY, Subbaiah R, Bebek G, Crish J, Scanzello CR, Krastins B, et al. Proteomic analysis of synovial fluid from the osteoarthritic knee: Comparison with transcriptome analyses of joint tissues. *Arthritis Rheum* (2013) 65:981–92. doi: 10.1002/art.37823
12. Bradley K, North J, Saunders D, Schwaeble W, Whaley K, Jeziorska M, et al. Synthesis of classical pathway complement components by chondrocytes. *Immunology* (1996) 88:648–56.
13. Struglics A, Okroj M, Swärd P, Frobell R, Saxne T, Lohmander LS, et al. The complement system is activated in synovial fluid from subjects with knee injury and from patients with osteoarthritis. *Arthritis Res Ther* (2016) 18:1–11. doi: 10.1186/s13075-016-1123-x
14. Lisignoli G, Toneguzzi S, Grassi F, Piacentini A, Tschon M, Cristino S, et al. Different chemokines are expressed in human arthritic bone biopsies: IFN-γ and IL-6 differently modulate IL-8, MCP-1 and rantes production by arthritic osteoblasts. *Cytokine* (2002) 20(5):231–8. doi: 10.1006/cyto.2002.2006
15. Gabusi E, Manferdini C, Paolella F, Gambari L, Kon E, Filardo G, et al. Focal Defects of the Knee Articular Surface: Evidence of a Regenerative Potential Pattern in Osteochondritis Dissecans and Degenerative Lesions. *BioMed Res Int* (2017) 2017:9036305. doi: 10.1155/2017/9036305
16. Mankin HJ. Biochemical and metabolic aspects of osteoarthritis. *Orthop Clin North Am* (1971) 2(1):19–31.
17. Pulsatelli L, Dolzani P, Piacentini A, Silvestri T, Ruggeri R, Gualtieri G, et al. Chemokine production by human chondrocytes. *J Rheumatol* (1999) 26 (9):1992–2001.
18. Assirelli E, Filardo G, Mariani E, Kon E, Roffi A, Vaccaro F, et al. Effect of two different preparations of platelet-rich plasma on synoviocytes. *Knee Surg Sport Traumatol Arthrosc* (2015) 23(9):2690–703. doi: 10.1007/s00167-014-3113-3
19. Collins JA, Beutel BG, Strauss E, Youm T, Jazrawi L. Bone marrow edema chronic bone marrow lesions of the knee and the association with osteoarthritis. *Bull Hosp Joint Dis* (2016) 74(1):24–36.
20. Dunn CM, Velasco C, Rivas A, Andrews M, Garman C, Jacob PB, et al. Identification of Cartilage Microbial DNA Signatures and Associations With Knee and Hip Osteoarthritis. *Arthritis Rheumatol* (2020) 72:1111–22. doi: 10.1002/art.41210
21. Berthelot JM, Sellam J, Maugars Y, Berenbaum F. Cartilage-gut-microbiome axis: A new paradigm for novel therapeutic opportunities in osteoarthritis. *RMD Open* (2019) 5:1–7. doi: 10.1136/rmdopen-2019-001037
22. Huber-Lang M, Kovtun A, Ignatius A. The role of complement in trauma and fracture healing. *Semin Immunol* (2013) 25(1):73–8. doi: 10.1016/j.smim.2013.05.006
23. Jiao Q, Wei L, Chen C, Li P, Wang X, Li Y, et al. Cartilage oligomeric matrix protein and hyaluronic acid are sensitive serum biomarkers for early cartilage lesions in the knee joint. *Biomarkers* (2016) 21(2):146–51. doi: 10.3109/1354750X.2015.1118547
24. Addison S, Coleman RE, Feng S, McDaniel G, Kraus VB. Whole-body bone scintigraphy provides a measure of the total-body burden of osteoarthritis for the purpose of systemic biomarker validation. *Arthritis Rheum* (2009). doi: 10.1002/art.24856
25. Kluzek S, Bay-Jensen AC, Judge A, Karsdal MA, Shorthose M, Spector T, et al. Serum cartilage oligomeric matrix protein and development of radiographic and painful knee osteoarthritis. A community-based cohort of middle-aged women. *Biomarkers* (2015) 20(8):557–64. doi: 10.3109/1354750X.2015.1105498
26. Happonen KE, Saxne T, Aspberg A, Mörgelin M, Heinegård D, Blom AM. Regulation of complement by cartilage oligomeric matrix protein allows for a novel molecular diagnostic principle in rheumatoid arthritis. *Arthritis Care Res* (2010) 62(12):3574–83. doi: 10.1002/art.27720
27. Gialeli C, Gungor B, Blom AM. Novel potential inhibitors of complement system and their roles in complement regulation and beyond. *Mol Immunol* (2018) 102:73–83. doi: 10.1016/j.molimm.2018.05.023
28. Koobkokkruad T, Kadotani T, Hutamekalin P, Mizutani N, Yoshino S. Arthrogenicity of type II collagen monoclonal antibodies associated with complement activation and antigen affinity. *J Inflammation* (2011) 8:31. doi: 10.1186/1476-9255-8-31
29. Dragomir CL, Scott JL, Perino G, Adler R, Fealy S, Goldring MB. Acute inflammation with induction of anaphylatoxin C5a and terminal complement complex C5b-9 associated with multiple intra-articular injections of hylan G-F 20: A case report. *Osteoarthr Cartil* (2012) 20:791–5. doi: 10.1016/j.joca.2012.03.020
30. Land WG. Emerging role of innate immunity in organ transplantation Part II: Potential of damage-associated molecular patterns to generate immunostimulatory dendritic cells. *Transplant Rev* (2012) 26(2):73–87. doi: 10.1016/j.trre.2011.02.003
31. Smith MD, Barg E, Weedon H, Papengelis V, Smeets T, Tak PP, et al. Microarchitecture and protective mechanisms in synovial tissue from clinically and arthroscopically normal knee joints. *Ann Rheum Dis* (2003) 62:303–7. doi: 10.1136/ard.62.4.303
32. Zimmermann T, Kunisch E, Pfeiffer R, Hirth A, Stahl HD, Sack U, et al. Isolation and characterization of rheumatoid arthritis synovial fibroblasts from primary culture - Primary culture cells markedly differ from fourth-passage cells. *Arthritis Res* (2001) 3(1):72–6. doi: 10.1186/ar142
33. Lubbers R, van Essen MF, van Kooten C, Trouw LA. Production of complement components by cells of the immune system. *Clin Exp Immunol* (2017) 188:183–94. doi: 10.1111/cei.12952
34. Sellam J, Berenbaum F. The role of synovitis in pathophysiology and clinical symptoms of osteoarthritis. *Nat Rev Rheumatol* (2010) 6(11):25–35. doi: 10.1038/nrrheum.2010.159
35. Quadros AU, Cunha TM. C5a and pain development: An old molecule, a new target. *Pharmacol Res* (2016) 112:58–67. doi: 10.1016/j.phrs.2016.02.004
36. Jang JH, Clark JD, Li X, Yorek MS, Usachev YM, Brennan TJ. Nociceptive sensitization by complement C5a and C3a in mouse. *Pain* (2010). doi: 10.1016/j.pain.2009.11.021
37. Ratajczak MZ, Reca R, Wysoczynski M, Yan J, Ratajczak J. Modulation of the SDF-1-CXCR4 axis by the third complement component (C3)-Implications for trafficking of CXCR4+ stem cells. *Exp Hematol* (2006) 34(8):986–95. doi: 10.1016/j.exphem.2006.03.015
38. Ratajczak MZ, Kim C, Ratajczak J, Janowska-Wieczorek A. Innate immunity as orchestrator of bone marrow homing for hematopoietic stem/progenitor cells. in. *Adv Exp Med Biol* (2013) 735:219–32. doi: 10.1007/978-1-4614-4118-2_15
39. Schraufstatter IU. Complement activation in the context of stem cells and tissue repair. *World J Stem Cells* (2015) 7(8):1090–108. doi: 10.4252/wjsc.v7.i8.1090
40. Diekman BO, Rowland CR, Lennon DP, Caplan AI, Guilak F. Chondrogenesis of adult stem cells from adipose tissue and bone marrow: Induction by growth factors and cartilage-derived matrix. *Tissue Eng Part A* (2010) 16(2):523–33. doi: 10.1089/ten.tea.2009.0398
41. Hengartner NE, Fiedler J, Schrezenmeier H, Huber-Lang M, Brenner RE. Crucial role of IL1beta and C3a in the in vitro-response of multipotent mesenchymal stromal cells to inflammatory mediators of polytrauma. *PloS One* (2015) 10(1):e0116772. doi: 10.1371/journal.pone.0116772

42. Wang Q, Rozelle AL, Lepus CM, Scanzello CR, Song JJ, Larsen DM, et al. Identification of a central role for complement in osteoarthritis. *Nat Med* (2011) 17:1674–9. doi: 10.1038/nm.2543
43. van Dalen SCM, Blom AB, Slöetjes AW, Helsen MMA, Roth J, Vogl T, et al. Interleukin-1 is not involved in synovial inflammation and cartilage destruction in collagenase-induced osteoarthritis. *Osteoarthr Cartil* (2017) 25(3):385–396. doi: 10.1016/j.joca.2016.09.009
44. Kapoor M, Martel-Pelletier J, Lajeunesse D, Pelletier JP, Fahmi H. Role of proinflammatory cytokines in the pathophysiology of osteoarthritis. *Nat Rev Rheumatol* (2011) 7:33–42. doi: 10.1038/nrrheum.2010.196
45. Sinkeviciute D, Porcelli C, Aspberg A, Onnerfjord P, Bay-Jensen A-C. Characterization of the IL-17 effect on articular cartilage in a translational model. An explorative study. *Osteoarthr Cartil* (2019) 27:S292–3. doi: 10.1016/j.joca.2019.02.682
46. Jotanovic Z, Mihelic R, Sestan B, Dembic Z. Role of interleukin-1 inhibitors in osteoarthritis: An evidence-based review. *Drugs Aging* (2012) 29(5):3437–58. doi: 10.2165/11599350-000000000-00000
47. Calich ALG, Domiciano DS, Fuller R. Osteoarthritis: Can anti-cytokine therapy play a role in treatment? *Clin Rheumatol* (2010) 29(5):451–5 doi: 10.1007/s10067-009-1352-3
48. Cohen SB, Proudman S, Kivitz AJ, Burch FX, Donohue JP, Burstein D, et al. A randomized, double-blind study of AMG 108 (a fully human monoclonal antibody to IL-1R1) in patients with osteoarthritis of the knee. *Arthritis Res Ther* (2011) 13(4):R125. doi: 10.1186/ar3430
49. Silvestri T, Pulsatelli L, Dolzani P, Frizziero L, Facchini A, Meliconi R. In vivo expression of inflammatory cytokine receptors in the joint compartments of patients with arthritis. *Rheumatol Int* (2006) 26:360–8. doi: 10.1007/s00296-005-0586-x
50. Andrades JA, Nimni ME, Becerra J, Eisenstein R, Davis M, Sorgente N. Complement proteins are present in developing endochondral bone and may mediate cartilage cell death and vascularization. *Exp Cell Res* (1996) 227 (2):208–13. doi: 10.1006/excr.1996.0269
51. Józsi M, Tortajada A, Uzonyi B, Goicoechea de Jorge E, Rodríguez de Córdoba S. Factor H-related proteins determine complement-activating surfaces. *Trends Immunol* (2015) 36(6):74–84. doi: 10.1016/j.it.2015.04.008
52. Valverde-Franco G, Tardif G, Mineau F, Paré F, Lussier B, Fahmi H, et al. High in vivo levels of adipsin lead to increased knee tissue degradation in osteoarthritis: Data from humans and animal models. *Rheumatol (U K)* (2018) 57:1851–60. doi: 10.1093/rheumatology/key181

Conflict of Interest: The authors declare that the research was conducted in the absence of any commercial or financial relationships that could be construed as a potential conflict of interest.

Copyright © 2020 Assirelli, Pulsatelli, Dolzani, Mariani, Lisignoli, Addimanda and Meliconi. This is an open-access article distributed under the terms of the Creative Commons Attribution License (CC BY). The use, distribution or reproduction in other forums is permitted, provided the original author(s) and the copyright owner(s) are credited and that the original publication in this journal is cited, in accordance with accepted academic practice. No use, distribution or reproduction is permitted which does not comply with these terms.

Advantages of publishing in Frontiers

OPEN ACCESS
Articles are free to read for greatest visibility and readership

FAST PUBLICATION
Around 90 days from submission to decision

HIGH QUALITY PEER-REVIEW
Rigorous, collaborative, and constructive peer-review

TRANSPARENT PEER-REVIEW
Editors and reviewers acknowledged by name on published articles

Frontiers
Avenue du Tribunal-Fédéral 34
1005 Lausanne | Switzerland

Visit us: www.frontiersin.org
Contact us: frontiersin.org/about/contact

REPRODUCIBILITY OF RESEARCH
Support open data and methods to enhance research reproducibility

DIGITAL PUBLISHING
Articles designed for optimal readership across devices

FOLLOW US
@frontiersin

IMPACT METRICS
Advanced article metrics track visibility across digital media

EXTENSIVE PROMOTION
Marketing and promotion of impactful research

LOOP RESEARCH NETWORK
Our network increases your article's readership